Sheffield Hallam University

A Sheffield Hallam University thesis

ProQuest Number: 10701059

ProQuest 10701059

FACTORS INFLUENCING THE SECONDARY

HARDENING OF VANADIUM STEELS

A thesis submitted to the Council for National Academic

Awards for the degree of

DOCTOR OF PHILOSOPHY

AT

SHEFFIELD CITY POLYTECHNIC

BY

JOHN ROGER SWINDELL B.Sc.

JULY 1979

FACTORS INFLUENCING THE SECONDARY HARDENING OF VANADIUM STEELS

This thesis is based on an investigation undertaken during
the period April 1973 to July 1977 at Sheffield City Polytechnic.
During this period, frequent meetings were held to discuss the
progress of the research project.

Furthermore, the following lecture modules were attended from
the part-time M.Sc. course in Industrial Metallurgy, at
Sheffield City Polytechnic:-

    1.   Tool Materials

    2.   High Strength Alloys

The results obtained in this investigation and the theories
developed are, to the best of my knowledge, original except
where reference has been made to other authors.   No part of
this thesis has been submitted for a degree at any other
University or College.

July 1979

Synopsis.

Research over the last twenty years has conclusively shown that the secondary hardening of high speed steels is due to precipitation hardening by carbides formed on tempering. Vanadium carbide offers the major contribution to this phenomenon, and primarily for this reason, vanadium is present in all grades of high speed steel.

The object of this research was to attempt to improve the secondary hardening response of high speed steels, due to V_4C_3 precipitation. There were two important aspects, these being the effects of varying elements on the nucleation rate of this carbide on tempering and to attempt to improve the dissolution rate of V_4C_3 during austenitisation. A considerable amount of research has been carried out on the orientation relationship between precipitating V_4C_3 particles in a ferrite matrix, but little work has been undertaken on the effect of other elements on this precipitation mechanism.

Simple ternary and quaternary alloys were melted, containing in each instance, iron, carbon and vanadium and in the latter case an additional alloying element. A number of commercial purity steels were also employed, these being carburised to give a range of carbon contents in the cases.

True secondary hardening did not occur in the high purity steels which only contained vanadium as an alloying addition, but this did take place in the high purity steels in which a second alloying addition was present. All the commercial purity steels showed secondary hardening peaks, over a wide range of carbon contents, with the exception of those with

very low vanadium levels (0.05 and 0.06 wt. %). Optimum secondary hardening occurred at or close to the stoichiometric vanadium : carbon ratios for V_4C_3 formation in these steels.

The nucleation of V_4C_3 took place on dislocations surrounded by solute atoms. This meant that the greater distortion and higher free energy associated with the presence of solute atoms in the matrix, the higher the nucleation rate of V_4C_3. Silicon and manganese had the greatest effects in increasing the nucleation rate of V_4C_3 , as the lattice parameters of these elements differed quite appreciably with that of ferrite.

Non-carbide forming elements, with the exception of silicon, increased the dissolution rate of V_4C_3 during austenitisation. These elements decreased the interatomic bond strength between vanadium and carbon atoms in the V_4C_3 lattice. Silicon had the effect of retarding the diffusion of vanadium atoms away from the carbide and into the austenite lattice.

A very surprising aspect of this research was that some of the high purity steels graphitised during long term tempering at 560°C. This was due to V_4C_3 decomposing into graphite, but the addition of molybdenum, manganese, chromium or tungsten prevented this phenomenon.

The results of this work allowed a suggestion to be made of the composition of a low alloy tool steel. This steel was a compromise composition between optimum secondary hardening response due to V_4C_3 precipitation and maximum dissolution rate of primary V_4C_3 on austenitisation. Such a steel would have a much lower cost than high speed steels.

CONTENTS

CHAPTER 1

1.   Introduction

The metallurgy of high speed tool steels has rarely been carried out in a basic manner.   Usually the work has consisted of altering the alloy composition in an attempt to obtain better cutting properties, without a full understanding of the metallurgical principles involved.

In this research it was decided to make a detailed study of the effect of one of the most important alloying elements present in high speed steel, namely vanadium.   This element is known to be a very strong carbide former, its carbide having a high hardness and hence aiding the wear resistance properties of the tool.   In addition, the precipitation of vanadium carbide on tempering is vitally important in giving the property of secondary hardening to high speed steel.

Therefore, on this theme, the object of the work is to endeavour to obtain improved secondary hardening response from vanadium carbide precipitation.   Only by having the vanadium and carbon dissolved in the martensitic matrix after hardening can the possibility exist of obtaining secondary hardening by vanadium carbide precipitation.   The effect of individual alloying elements on vanadium carbide solution during austenitisation is thus an integral part of this research.   Similarly, whether these elements enhance vanadium carbide precipitation is another vital factor.

From this simplified approach it is hoped to understand better the role of vanadium in high speed steels, and to be able to achieve optimum secondary hardening response from the precipitation of vanadium carbide.

2. Literature Survey

2.1 The Partitioning of Alloying Elements Between the Matrix and Carbide Phases in High Speed Tool Steels.

2.1.1 Primary Carbides Present in High Speed Steels.

The carbide most commonly found in high speed steel is η (M_6C), where M stands for metal atoms. This was firstly identified by Goldschmidt [1], who described the carbide as "high speed steel carbide". The reason for this was that he found this carbide present in very large proportions in a range of high speed steels. He found the same type of carbide in both tungsten and molybdenum based steels, and so deduced that the tungsten and molybdenum atoms were interchangeable. The crystal structure of the carbide was found to be face-centred cubic.

In later work, Goldschmidt [2] carried out an X-ray investigation on electrolytic carbide extracts from T1 high speed steel (TABLE 1). This showed that the composition of the carbide could vary between Fe_4W_2C and Fe_3W_3C. He found that chromium and vanadium were both very soluble in the carbide, being capable of interchanging with either the iron or tungsten atoms. This ambiguity in positioning was he thought in accordance with the transitional character of chromium and vanadium. The atomic sizes would be favourable for chromium and vanadium to replace iron (as they do in ferrite when carbon is absent), whilst valencies and the character of chromium and vanadium as carbide-formers would tend to place them in a carbon environment, in a similar manner to tungsten.

The second carbide that Goldschmidt [1] found present was K ($M_{23}C_6$). Most of the metal atoms he [2] found to be chromium, but iron, tungsten, molybdenum and vanadium were all found to be capable of replacing some of the chromium. The

crystal structure of this carbide was also found to be face centred cubic.

The third primary carbide that Goldschmidt[1] identified in high speed steel was vanadium carbide (V_4C_3), which he found to have a face-centred cubic, sodium-chloride type structure. Goldschmidt[2] had great difficulty in identifying this carbide in T1 high speed steel in the as-hardened condition. This was due to the tungsten content of the steel being much higher than the vanadium, so that most of the carbide present was M_6C. However, by X-ray analysis he readily identified V_4C_3 in high speed steels with higher vanadium contents than T1.

Vanadium carbide has often been quoted as VC or classed as being of the MC type. Goldschmidt[1] undertook X-ray analysis of vanadium carbide and found it could exist over a range of composition between VC and V_4C_3. He pointed out that discrepancies in lattice parameter measurement of the carbide between Becker[3] and Maurer, Döring and Pulewka[4] were due to analysis of the two different compounds, VC and V_4C_3.

The carbide V_4C_3 has a defect lattice with respect to the carbon sites and can exist with VC in steels over a solid solution range. Lattice parameter measurements for vanadium carbide of 4.13 and 4.30 Å by Osawa and Oya,[5] were in the opinion of Goldschmidt, obtained from carbides at the two extreme ends of the solid solution range. His conclusion was that V_4C_3 was the most likely vanadium carbide to appear in steels, thus confirming earlier work by Wever, Rose and Eggers.[6]

The three carbides which have been mentioned are the normal primary carbides present in high speed steels.

However, there are another three primary carbides which may be present in these alloys. One of these carbides is M_7C_3, which is quite often present in high speed steels, whilst M_2C and M_3C may form in these alloys with very high carbon contents.

Steven, Nehrenberg and Philip [7] carried out a detailed study of the chromium carbides that were present in M2 (TABLE 1) high speed steel, in the annealed condition, over a whole range of carbon contents. Their results showed that, with carbon levels of 1.1 wt. % and above, the chromium carbide present was M_7C_3 and not $M_{23}C_6$.

Mukherjee [8] undertook a detailed study of the chromium carbides present in a range of commercial high speed steels. In general, he found that for alloys containing more than 1.0 wt. % carbon, the chromium carbide M_7C_3 was formed instead of $M_{23}C_6$. The particular steels in which he determined that M_7C_3 was present were M41, M42, M46 and high carbon versions of M2 and M35 (TABLE 1).

The carbide M_2C (where M represents tungsten or molybdenum atoms) had been known, for a considerable length of time, to be precipitated during the tempering of high speed steels. [9] However, it is only in latter years that research has shown that M_2C can be present in these alloys as a primary carbide. Gedberg, Sidelkovsky, Melnikov, Kazak and Loktyushin [10] identified the carbide phases present in some high speed steels with high carbon contents, in the as-cast condition. They detected the carbide M_2C, but stated that this phase was metastable. The tendency of M_2C was to dissolve in either the eutectic phase or in inclusions formed along grain boundaries.

Steven, Hauser, Neumeyer and Capenos [11] carried out a

detailed study of the carbides present in high-carbon high speed steels. They claim that M_2C starts to replace M_6C in steels with carbon contents in excess of 1.20 wt. %. However, most high speed steels have carbon levels below this value (usually between 0.75 and 1.0 wt. %).

Bungardt, Haberling, Rose and Weigand, [12] Preis and Lennartz [13] and Horn [14] all detected M_2C in high-carbon M2 high speed steel. Preis and Lennartz were not able to determine the presence of any of this carbide in the alloy at carbon contents less than 1.26 wt. %, but above this value, M_2C started to replace M_6C. Their results also showed that even in this high-carbon steel, quantities of silicon in excess of 0.70 wt. % caused M_6C to form, rather than M_2C.

Horn found that the elements molybdenum, chromium and vanadium promoted the formation of the carbide M_2C, whilst nitrogen and silicon that of M_6C. Part of her work consisted of assessing the stabilities of the various carbides at temperatures in excess of those used for solution treatment. The results exhibit M_2C to be unstable, reacting with the surrounding austenite to form M_6C and MC.

Haberling and Kiesheyer [15] undertook a detailed study of the effects of silicon on the carbides formed in M7 high speed steel with a high carbon content. They varied the silicon level between 0.34 and 2.20 wt. %, and found that increasing amounts of this element favoured the decomposition of the carbide M_2C, with formation of M_6C and MC. Therefore, their results in this respect were in agreement with those of Preis and Lennartz, [13] Horn [14] and also Schlatter and Stepanic [16].

Fischer and Kohlhaas [17] are also in agreement that high carbon and low silicon contents are required for M_2C to

form as a primary carbide in high speed steels.   However,
they point out that other factors are necessary for this
carbide to be present.   Their results on a range of high
speed steels, showed that M_2C was only present in steels
with high molybdenum and low to medium vanadium contents.
When the vanadium level was in excess of 2 wt. %, M_6C tended
to form rather than M_2C, and in this respect their results
were contrary to those of Horn. [14]

A further factor which they found to be important in
controlling the type of carbide present, was the cooling rate
after casting.   Rates of cooling greater than 4^oC/min. tended
to cause M_6C to form in M36 (TABLE 1) high speed steel with a
high carbon level, whilst the converse meant M_2C was present.
Their theory for this was that with slow cooling rates,
localised enrichment in alloying elements occurred during
solidification, allowing the alloy carbide M_2C to form rather
than M_6C, which has a very high iron content.   Optical
microscopy exhibited M_2C to have a needle-like shape, whilst
M_6C had a fishbone or skeleton form.   Long term annealing
(24 hrs) of this steel at 1050^oC caused all the M_2C to dissolve.

The final primary carbide which has been found to be
present in high speed steels is the iron-base carbide M_3C.
Goldschmidt [2] found small amounts of M_3C when determining
the carbides that were present in a range of high speed steels.
The most precise research on the presence of this carbide,
however, has been undertaken by Haberling, Rose and Weigand, [18]
and once again the importance of the carbon content in controll-
ing the types of carbide present is clearly illustrated.

These workers investigated the carbides present in M2
high speed steel over a range of carbon levels from 0.4 to 3.4

wt. %. The results showed that when the carbon content of this steel was above the stoichiometric value (i.e. 1.15 wt.%), the remaining amount of this element reacted with iron to form Fe_3C. The maximum carbon level that they employed gave a volume fraction of primary carbide for this steel, in the annealed condition, of almost 50%; the majority of which was M_3C.

2.1.2   Detailed Compositions of the Primary Carbides

The electron microprobe was used to analyse the carbides present in as-cast T1 high speed steel by Jones and Mukherjee.[19] Their results indicated the presence of the normal high speed steel carbides M_6C, $M_{23}C_6$ and V_4C_3. The M_6C was shown to contain 26.7 iron, 3.6 chromium, 2.3 vanadium, 65.8 tungsten and 1.6 wt. % carbon. Results from the analysis of V_4C_3 showed the carbide to consist of 7.1 iron, 7.0 chromium, 47.5 vanadium, 14.4 tungsten and 24.0 wt. % carbon. Finally the analysis of $M_{23}C_6$ showed that this carbide was richer in iron than chromium. The iron level was 46.7 as against 27.8 wt. % chromium; the contents of the other alloying elements in this carbide were 3.4 vanadium, 15.1 tungsten and 7.0 wt. % carbon.

The carbon figures in each case were obtained by adding the weight percentages of all the other alloying elements present and subtracting the total from 100 wt. %. Accurate analysis for carbon by means of the microprobe is difficult to achieve, owing to the low atomic number of this element.

The low chromium and high iron contents that Jones and Mukherjee found in the carbide $M_{23}C_6$ were not surprising as Goldschmidt [20] showed that this carbide could exist over a composition range of $(Cr\ Fe)_{23}C_6$ to $(Fe\ Cr)_{21}W_2C_6$. Similarly,

the quite high tungsten level that these workers found in this carbide is explained by the above composition range.

In high chromium steels (14.0 wt. % chromium), containing no other carbide forming elements, $M_{23}C_6$ contains between 60.0 and 67.3 wt. % of chromium. This was found by Gullberg,[21] who analysed this carbide both by means of the microprobe and by chemical analysis of extracted residue. Correlation of the results from the two analysis techniques was very good.

Baikov, Baranova, Kupalova and Aleksandrova[22] used X-ray techniques to study the carbide deposits of the MC type that were obtained by electrolytic extraction from four grades of high speed steels, in the annealed condition. These steels had compositions ranging as follows:- carbon 0.89 - 0.98, chromium 3.52 - 4.18, vanadium 1.7 - 2.25, molybdenum 0 - 6.0 and tungsten 0 - 12.0 wt. %. Their results showed that these changes in composition were accompanied by alterations in the analysis of the vanadium carbide present in the steels. In this carbide lattice, up to 35% of the vanadium atoms could be replaced by tungsten, molybdenum or chromium.

The vanadium carbide which was extracted from the steel containing 12.0 wt. % of tungsten, contained almost the limiting quantity of this element that could be dissolved. However, analysis of the vanadium carbide from the two alloys containing both tungsten and molybdenum, showed that molybdenum replaced vanadium to a greater extent than did tungsten.

Further research was carried out on a similar range of steels for the analysis of vanadium carbide by Baikov, Baranova and Kupalova.[23] The only exception to the steels on which they had previously carried out research[22] was an alloy containing 0.90 carbon, 3.35 chromium, 3.36 vanadium and 6.42

wt. % molybdenum, there being no tungsten present. They again used the technique of electrolytic extraction and X-ray analysis to show that the vanadium carbide in this range of steels contained between 42.8 and 46.5 wt. % of vanadium.

This highest vanadium content was, as expected, in the carbide from the steel with 3.36 wt. % vanadium, whilst the lowest level was from the alloy containing only 1.7 wt. % of the element. Their results again showed that molybdenum could replace vanadium atoms in the vanadium carbide to a greater extent than could tungsten. On a weight percentage basis the tungsten and molybdenum contents of the vanadium carbide over the range of steels varied, in both cases from 0 to 36.2.

The chromium and carbon contents of the steels varied very little and hence the concentrations of these elements in the vanadium carbide were fairly constant over the range of alloys. The carbon levels varied from 13.4 to 17.1 and the chromium from 3.5 to 4.1 wt. %. Their analysis results showed that no iron was present in the vanadium carbide, and in this respect their results differed from those of Jones and Mukherjee. [19]

Lennartz and Preis [24] used the technique of electrolytic extraction and chemical analysis to determine the compositions of the carbides MC and M_6C present in the high speed steel Komo 310 (TABLE 1), in the as-hardened condition. This is one of the high-cobalt high speed steels, containing 10 wt. % of this element. Their results showed the metal atoms in the carbide MC to have a composition of 0.8 iron, 4.1 chromium, 43.5 vanadium, 39.3 tungsten, 12.2 molybdenum and 0.1 wt. % cobalt. The metal atoms in the carbide M_6C consisted of 28.9 iron, 3.3 chromium, 4.6 vanadium, 45.0 tungsten, 14.7 molybdenum and 3.5 wt. % cobalt.

These results clearly show that tungsten and molybdenum can replace a considerable number of vanadium atoms in the carbide MC, and are thus in agreement with those of Baikov, Baranova and Kupalova.[23] Cobalt was shown to be able to replace a small amount of the iron which was present in M_6C.

Further research was carried out by Lennartz and Preis [13] on the analysis of the metal atoms present in the carbides MC and M_6C in a range of high speed steels after hardening. The composition ranges of these steels were generally not very wide, and can be listed as follows:- carbon 0.8 to 1.0, chromium 3.75 to 4.25, vanadium 2.0 to 3.0, molybdenum 3.0 to 5.0, tungsten 3.0 to 10.0 and cobalt 0 to 10.0 wt. %. Over this range of alloys, the carbide MC contained between 0.8 and 1.4 iron, 4.1 and 6.7 chromium, 43.5 and 54.3 vanadium, 24.2 and 39.9 tungsten, 12.2 and 19.7 molybdenum and 0 to 0.5 wt. % cobalt. The carbide M_6C contained 21.2 to 31.7 iron, 3.3 to 4.1 chromium, 3.4 to 23.3 vanadium, 30.3 to 45.0 tungsten, 14.7 to 23.9 molybdenum and 0 to 3.5 wt. % cobalt.

The carbide MC was shown to vary quite considerably in composition over the range of steels. Increases in both the tungsten and molybdenum contents of the alloy caused further solution of these elements in this carbide. The highest tungsten level found in the MC was in the high speed steel Komo 310, which contained 10.0 wt. % of this element. Very little cobalt was present in the MC and the iron and chromium contents of this phase were quite stable over the range of alloys.

Analysis results of M_6C showed that this carbide could dissolve more cobalt than was the case for MC. The composition of M_6C in the steels was reasonably consistent with one exception. This was the high speed steel Mo 325 (TABLE 1), which contained

2 wt. % vanadium and only 3 wt. % of both tungsten and molybdenum. The M_6C extracted from this alloy had metal atoms consisting of 23.3 wt. % vanadium, whilst in the other materials this figure did not exceed 5.4 wt. %. This clearly showed that in relatively low-alloy content high speed steels, vanadium could replace both tungsten and molybdenum in M_6C.

Lennartz and Preis [13] also extracted and analysed the M_6C and MC carbides from M2 high speed steel with a range of carbon contents from 0.85 to 1.51 wt. %, in the as-hardened condition. These variations in the carbon level only slightly altered the compositions of both of the carbides. The analysis of the metal atoms in MC, for these carbon levels, varied between 0.7 to 1.2 iron, 6.0 to 6.7 chromium, 38.0 to 46.8 vanadium, 26.8 to 31.2 tungsten and 19.6 to 22.9 wt. % molybdenum; whilst those present in M_6C ranged from 30.9 to 31.8 iron, 3.7 to 4.2 chromium, 3.0 to 6.3 vanadium, 35.9 to 37.5 tungsten and 22.7 to 24.3 wt. % molybdenum.

Fischer and Kohlhaas [17] analysed the primary carbides present in certain high speed steels in the as-hardened condition by means of the electron microprobe. Their results are presented in the form of the weight percentages of elements present in the metal atoms of the carbides. They divided the alloys into three groups, with the first of these being based on the T1 (18 wt. % tungsten) high speed steel. The second series had relatively high vanadium contents (up to 5 wt. %), whilst the last had high molybdenum levels.

They detected the carbides MC and M_6C in all of these steels and the compositions of these phases were in good agreement when analysed in the same alloys as those employed by Lennartz and Preis. [13] This suggests that the techniques

of electron probe microanalysis and electrolytic extraction followed by chemical analysis are both accurate when assessing the metal content of primary carbides in high speed steels.

A major difference in the work by Fisher and Kohlhaas compared to that of Lennartz and Preis was in the maximum tungsten and molybdenum contents that they employed in their steels. Lennartz and Preis did not exceed 10.0 tungsten and 5.0 wt. % molybdenum, whilst the former had maximums of 18 and 9 wt. % respectively. Fisher and Kohlhaas showed that the extra amount of these two elements was present in the M_6C carbide in these steels. Two illustrations of this fact are given in the analyses of metal atoms in M_6C in T1 and M1 high speed steels. The former contained 54.8 wt. % tungsten whilst the latter 45.5 wt. % molybdenum.

2.1.3 The Stoichiometric Ratio in High Speed Steels

The significance of stoichiometric metal : carbon ratio to form carbides in high speed steels is emphasised by Hoyle.[25] He listed the weight percentage of carbon for 1 wt. : of an alloying element to form the normal primary carbides present in high speed steels (TABLE 2). In the case of the carbide M_6C, he gave this as having a formula of W_2C or Mo_2C. The reason for this is, although the carbide has a formula of $Fe_4 (W, Mo)_2C$, this does not affect the proportion of carbon to alloying element for carbide formation. It can be clearly seen from these stoichiometric carbon values that considerably higher weight (or atomic) percentage carbon is required to form vanadium carbide than either M_6C or $M_{23}C_6$.

Mukherjee [8] pointed out that the stoichiometric ratio for high speed steels is somewhat misleading in the sense that

the primary carbides present tend to dissolve other alloying elements. He mentioned that because of this point, little attempt is made to produce high speed steels to exact stoichiometric ratios, but generally alloys are reasonably close to this ideal value.

An exception to this failure to take into account the dissolution of elements in the primary carbides present in high speed steels was made by Baikov, Baranova and Kupalova.[23] They determined formulae for vanadium carbide that took this fact into account in these alloys, and also calculated ideal stoichiometric ratios for the formation of this phase.

Their results showed that this carbide could have a formula ranging from $(V_{0.77} W_{0.17} Cr_{0.06}) C_x$ in high-tungsten molybdenum-free high speed steels to $(V_{0.67} Mo_{0.28} Cr_{0.05}) C_x$ in these steels with high molybdenum contents, but free of tungsten. This clearly illustrates the greater capacity of molybdenum than tungsten in replacing the vanadium present in vanadium carbide. In this formula x represents the number of carbon atoms.

For ideal stoichiometry, over this range of carbide compositions, they found that 1 wt. % vanadium combined with 0.8 $\pm$ 0.03 wt. % (tungsten and molybdenum), 0.1 $\pm$ 0.01 wt. % chromium and 0.28 $\pm$ 0.1 wt. % carbon. This is to form a carbide of formula $MC_{0.88}$, this being intermediate between MC and M_4C_3.

2.1.4   The Free Energies of Formation of Carbides

Richardson [26] undertook a detailed study of the chemical affinity between differing metal atoms and carbon. The equations that he developed were for metal atoms reacting with

one atom of carbon and also took into account the effect of temperature. His results have been slightly modified to show the free energies of formation of carbides on a basis of one atom of each of the particular metals reacting with carbon at 25°C (TABLE 3).

In this work he includes two of the important primary carbides that are present in high speed steels, namely VC and $Cr_{23}C_6$. Vanadium carbide is shown to be very stable, having a high negative free energy of formation. The carbide $Cr_{23}C_6$ is considerably less stable than vanadium carbide, as is another carbide that can be present in these steels, Cr_7C_3.

There is no free energy value given for the formation of M_6C, the other important carbide present in high speed steels, although a value is given for WC. However, the carbide M_6C has effectively a formula of Mo_2C or W_2C, and in fact Richardson determined the free energy of formation of the former carbide over the temperature range 0 to 1000°C.

Unfortunately, due to experimental problems, the free energy equation for the formation of Mo_2C was not accurate. Nevertheless, sufficient information was gained to show that Mo_2C was in fact a very stable carbide.

2.1.5 The Partitioning of Elements in High Speed Steels in the Annealed condition

In high speed steels, the analyses of various elements as weight percentages can be very misleading. This fact was firstly recognised by Gill, [27] who pointed out that one of the elements present, namely tungsten, had a high atomic weight. Tungsten is present in large amounts in many high speed steels, so it

is also useful to think in terms of atomic percentages when comparing this element with others in the steel. Molybdenum in high speed steels behaves in a very similar manner to tungsten and so a direct comparison of weight percentages of these two elements is relevant. This shows that 1 wt. % molybdenum has the same effect as between 1.6 and 2.0 wt. % tungsten. Gill presented histograms comparing atomic and weight percentages of tungsten and other alloying elements occurring in T1 and M2 high speed steels (Fig. 1).

Kayser and Cohen [28] found that, in the annealed condition, high speed steels consisted of between 26 and 32% by volume of carbides, with the remainder of the structure ferrite. The exact quantity of carbide within this range depended on both the carbon content of the particular alloy and the amount of carbide forming elements present. Their results are shown in FIG. 2 for the weight and atomic percentages of the principal elements found in the overall carbide as electrolytically extracted from types T1, M10 and M2 (TABLE 1) high speed steels, and analysed by chemical means.

These authors noticed that the overall carbide from each steel contained similar amounts of tungsten, molybdenum and chromium, whilst the vanadium and carbon levels were somewhat higher in that extracted from M10 and M2. Both of these steels contain 0.15 wt. % more carbon and 1.0 wt. % more vanadium than T1 high speed steel. This tendency for additional vanadium and carbon to concentrate in the carbide phase was found to be considerably more marked in the high-carbon/high-vanadium steels T15 and M4 (TABLE 1). These alloys gave overall carbide having an analysis of 20 to 25 vanadium and 29 to 32 wt % carbon, along with a carbide volume fraction of 32%.

The analysis that they conducted on the ferrite matrix in annealed high speed steel revealed that this phase generally consisted of less than 1.5 tungsten, 1.0 molybdenum, 0.4 wt. % vanadium and little or no carbon. However, over one half of the chromium content remained in solution in the ferrite, and any cobalt present in the steel was dissolved to a large extent.

Chodorowski, Jurczak and Lampe [29] investigated the effect of increased carbon content on the phase analysis of the high speed steels SW9 and SW12, in the annealed condition. The only difference in the analyses of these two alloys lies in their tungsten contents, with SW12 containing 3 wt. % more of this element. The high-carbon alloys were classified as SW9C and SW12C, and contained between 0.27 and 0.33 wt. % more of carbon than SW9 and SW12 (TABLE 1).

They employed a technique of electrolytic extraction of the carbides and subsequent analysis of the residue. From these analysis figures, and with a knowledge of the volume fraction of carbides present, these authors were able to calculate the matrix composition of the alloys.

Their results showed the high speed steel SW9 to have a carbide volume fraction of 18.9%, with a matrix analysis of 0.95 tungsten, 2.43 chromium, 0.11 vanadium and 96.51 wt.% iron. However, increasing the carbon content of this alloy by 0.27 wt. % (SW9C) caused the carbide volume fraction to rise to 23.0%. This created a depletion in the matrix of tungsten, chromium and vanadium of 0.95, 1.07 and 0.06 wt. % respectively, with a subsequent increase in iron of 2.08 wt. %. In fact no tungsten at all was present in the matrix of SW9C in the annealed condition.

The calculated analysis of the matrix of the high speed steel SW12C, yielded a composition of 0.99 tungsten, 2.17 chromium, 0.15 vanadium and 96.69 wt. % iron. The carbide volume fraction of the steel was 24.0%. They did not undertake the matrix analysis of the alloy SW12, but instead averaged out the matrix compositions obtained on this steel by Koshiba, Kimura and Horado [30] and Sato, Nishizawa and Murai. [31] These results gave a matrix composition of 0.25 tungsten, 0.54 chromium and 0.13 wt. % vanadium in excess, and 0.92 wt. % iron in depletion, of the contents of these elements in the matrix of the high-carbon alloy, SW12 C. The volume fraction of carbide present was 20.0%.

Chodorowski, Jurczak and Lampe concluded that increasing the carbon content of both SW9 and SW12 high speed steels caused a depletion in the matrix of the carbide forming elements. This was due to the presence of extra carbon, with which they could react to form carbides. An increase in either the carbon or tungsten content of the steel caused a greater volume fraction of carbides to be present.

They worked on different steels to those used by Kayser and Cohen, [28] but nevertheless their matrix analysis results are in good agreement. Generally the results correspond with earlier matrix analysis work conducted on SW9 high speed steel by Arkharov, Kvater and Kiselev, [32] Ivanov, [33], Nikanorov, [34] Malkiewicz, Bojarski and Foryst [35] and Gulyaev, Kupalova and Landa [36]. These workers determined volume fractions of carbide present in this steel, in the annealed condition, as ranging from 16.2 to 19.0 %.

Popandopulo [37] determined the ratio of the carbides MC and M_6C in a range of tungsten-molybdenum and tungsten-molybdenum-

cobalt high speed steels. The carbides were anodically separated and subjected to chemical and X-ray structural analysis. His results showed that, in tungsten-molybdenum high speed steels, the MC/M_6C ratio was raised with an increase in the molybdenum content of the alloy.

This was in agreement with the findings of Baikov, Baranova and Kupalova, [23] who determined that molybdenum replaced a greater quantity of the vanadium atoms present in vanadium carbide, than did tungsten. Therefore, more vanadium would be free to form a greater volume fraction of its own carbide in high speed steels with high molybdenum contents. The other conclusion that Popandopulo drew was that in high speed steels containing tungsten, molybdenum and cobalt, the MC/M_6C ratio was decreased with increased concentrations of carbon and cobalt. However, this effect was only very slight with respect to cobalt.

An intermetallic compound may be present in certain high speed steels in the annealed condition. This fact was firstly recognised by Goldschmidt, [1] and he termed the phase ε'. Unfortunately, he only found very small quantities of this phase and so was unable to determine its formula.

The formula of this same intermetallic compound in iron-tungsten and iron-molybdenum alloys had earlier caused considerable disagreement. Original research on these alloy systems by Arnfelt [38] showed that the compound had the general formula M_3R_2. This corresponded to Fe_3W_2 and Fe_3Mo_2 in iron-tungsten and iron-molybdenum alloys respectively. He also verified that the phase had a close packed hexagonal structure.

Sykes and Van Horn [39] determined the presence of Fe_3W_2 in a series of iron-tungsten binary alloys. They also pointed out the presence of another intermetallic compound in this system, namely Fe_2W. In later work, Arnfelt and Westgren [40] and Westgren [41] verified the existence of compounds of formulae Fe_7W_6 in iron-tungsten alloys and Fe_7Mo_6 in iron-molybdenum alloys. Their findings were that both of these compounds had rhombohedral structures and were isomorphous with the cobalt-tungsten compound, Co_7W_6.

Prior to undertaking this research, these authors did not think that Fe_2W existed in iron-tungsten alloys. However, they then found both Fe_7W_6 and Fe_2W in these materials, but did not determine the presence of any Fe_3W_2. The compound Fe_2W was shown to have a rhombohedral structure and they concluded that the phase Arnfelt [38] himself had thought was Fe_3W_2, with this same crystal structure, was in fact Fe_2W. Sykes and Van Horn [39] had actually found the existence of Fe_2W but the second intermetallic phase, that they thought to be Fe_3W_2 in this system, was Fe_7W_6.

In more recent work, Goldschmidt [42] determined that the intermetallic compound present in some high speed steels, in the annealed condition, was in fact Fe_7W_6 (or Fe_7Mo_6). The precipitation of a phase of this type, at tempering temperatures between 600 and $700^{\circ}C$ has been utilised in a new range of tool materials. Actually the precipitated compound is $(Co\ Fe)_7W_6$, with the cobalt and iron atoms being interchangeable.

In these recently developed alloys, the carbon content can be as low as 0.06 wt. %, whilst the cobalt level is of the order of 25 wt. %. Tungsten is also present, in the range

17 to 26 wt. %, but these materials are generally free of chromium and vanadium.

Kupalova, Landa, Malinkina and Fadyushina, [43] Brostrem and Geller [44] and Kupalova and Stepnov [45] all attempted to develop these alloys to have strength and red hardness properties intermediate between normal high speed steels and sintered metal carbides. Some Co_7W_6 is present in the iron-tungsten-cobalt alloys in the annealed condition, but this is completely taken into solution on austenitisation at $1150^{\circ}C$. The very low carbon content of these alloys means that they are considerably softer in the as-hardened condition than high speed steels.

However, after tempering, the hardness values of the two materials are very similar, owing to the considerable quantity of precipitation of Co_7W_6 in the iron-tungsten-cobalt alloys. In fact, these authors claim that iron-tungsten-cobalt alloys are superior with respect to red hardness, to high speed steels. They claim that hardness commences to decline in hardened and tempered high speed steels at temperatures between 620 and $650^{\circ}C$, whilst temperatures in excess of $700^{\circ}C$ are required before this phenomenon occurs in iron-tungsten-cobalt alloys. The field of application of these alloys is in the machining of titanium alloys, cavitation-resistant austenitic chromium-manganese steels and heat resistant alloys based on nickel. All of these materials are particularly difficult to machine.

2.1.6   The Solubility of the Primary Carbides during Austenit-
       isation

High speed steels are very complex materials and no single equilibrium diagram can completely represent their behaviour and show all the reactions taking place. Many attempts to compromise have been made, the most successful of which is

shown in FIG. 3 for T1. This diagram was proposed by Murakami and Hatta [46] and modified slightly in the high temperature region by Kuo [47] and at lower temperatures by Goldschmidt [42]. The diagram shows a binary section at 18 tungsten and 4 wt. % chromium through the quaternary iron-tungsten-chromium-carbon system.

This simplified equilibrium diagram for T1 high speed steel is very useful in explaining both the reactions taking place on cooling this alloy after casting and the temperatures required for austenitisation. The temperature range of austenitisation for this steel is illustrated in FIG. 3, the upper limit being almost at $1300^{\circ}C$. High austenitisation temperatures are required for high speed steels to take into solution as much of the primary carbide as possible. The upper level of the austenitisation temperature range for high speed steels is restricted by a safety margin of approximately $50^{\circ}C$ before liquid phase starts to form in the particular system. Even temperatures intermediate between this upper limit and that at which liquid phase is formed, cause a marked coarsening of the martensite along with grain growth.

However, this simplified equilibrium diagram has two major drawbacks. The first of these is that it takes no account of vanadium, which is one of the most important alloying elements present in high speed steels. Vanadium is a strong carbide former, so it would have the effect of moving this diagram to the right. The other factor is that the carbide cementite (Θ) is included in the diagram rather than $M_{23}C_6$.

A considerable amount of research has been undertaken on the solubility during austenitisation of the primary carbides present in high speed steels. Carbides were identified in

differing alloys, in both the annealed and as-hardened conditions. The austenitisation treatments during hardening varied considerably in the different research projects.

These results clearly show the high degree of stability of MC, and to a slightly lesser extent of M_6C. Tungsten favours the formation of M_6C rather than MC in high speed steels, whilst molybdenum has the opposite effect. Both these were important conclusions to be gleaned from the results. In fact the results are most conveniently expressed in tabular form, and this is presented in Table 4.

2.2   The Secondary Hardening of High Speed Steels

In the as-hardened condition, high speed steels contain considerable quantities of retained austenite (20 to 30% by volume).   This high value led early researchers to think that the presence of austenite in these alloys was responsible for the phenomenon of secondary hardening during tempering. The feeling was that hardening was caused by the conversion of austenite to bainite at the tempering temperature, or to martensite on cooling from this temperature.   In addition, the precipitation of alloy carbides in austenite during tempering was thought to contribute towards the hardening.

An example of this thinking was the classic work of Cohen and Koh, [65] although some of their findings were incorrect the research was still a basis for further work on the tempering of high speed steels.   They stated that four stages occurred during the tempering of these alloys.   The first stage involved precipitation of cementite from the martensite, followed by carbide precipitation from austenite in the second stage. Austenite transformation took place in stage three with the redissolution of cementite in the ferrite in the final stage and subsequent precipitation of complex carbide.   These researchers postulated that the second and third stages were responsible for secondary hardening, but more recent work has disproved these theories.

White and Honeycombe [66] undertook an electron diffraction study of extracted carbon replicas from T1 high speed steel, in the hardened and tempered condition.   Their results showed that precipitation of $M_{23}C_6$ from austenite was complete at $400^{\circ}C$, which was well below the temperature for the secondary hardening

peak.   In addition, double tempering of this alloy yielded
almost the same hardness results as the single treatment.
This again proved that transformation of the retained austenite,
this time to martensite on cooling, was not responsible for
the.occurrence of secondary hardening.

Payson [67] offered the additional evidence that the
master tempering curve (FIG. 9) for high speed steel, derived
according to the method of Hollomon and Jaffe, [68] showed
no discontinuity.   He claimed that if secondary hardening
was dependent on austenite decomposition there would be a sharp
change in slope of the curve at a point just beyond the hardness
peak.

The final proof that secondary hardening was not due to
either precipitation in retained austenite or transformation
of this phase to bainite or martensite, was given by Kuo. [69]
He found pronounced secondary hardening in a low-carbon steel,
which contained only molybdenum as an alloy addition.   The
steel contained no detectable austenite in the as-hardened
condition.

Kuo was also the first person to determine beyond doubt,
that the secondary hardening of high speed steels was actually
due to precipitation hardening, and that this precipitation
occurred within the martensite.   He employed a technique of
electrolytic extraction of carbides followed by X-ray powder
analysis, to find which carbides were present in a range of
these alloys, in the hardened and tempered condition.   The
tempering temperatures used were between 500 and 800°C, and
in each case the time was 1 hr.

At tempering temperatures up to, and including 650°C,
the only carbides detected were the two stable primary carbides

M_6C and VC.   However, after tempering at $675^{\circ}C$, the carbide M_2C was found to have been precipitated.   Kuo determined that this carbide existed as a solid solution, with a composition between W_2C and Mo_2C in high speed steels containing both tungsten and molybdenum.

Tempering at $750^{\circ}C$ caused the precipitation of either of the chromium-based carbides, $M_{23}C_6$ or M_7C_3, the latter being present in alloys with high carbon contents.   In all the alloys, M_2C was still precipitated at this temperature.   However, after tempering at $800^{\circ}C$, the carbide M_2C had completely dissolved in each alloy and the only precipitated carbide which remained was either $M_{23}C_6$ or M_7C_3.   There was one exception, and this was the alloy T4, which contained some VC after being tempered at this temperature.

Kuo also conducted a long-term temper of 500 hrs. at $700^{\circ}C$ for these steels.   The only precipitated carbide present after tempering for 1 hr. at this temperature was M_2C, but after 500 hrs. this carbide had completely dissolved in each alloy, whilst M_6C, VC and either $M_{23}C_6$ or M_7C_3 had been precipitated. This phenomenon was accompanied by a marked softening of the steels.

The secondary hardening peaks were found to be between 560 and $580^{\circ}C$ in all these high speed steels.   No X-ray lines were obtained from precipitated particles which had been extracted from samples tempered within this temperature range. This was undoubtedly due to the extremely fine size of these particles.

However, the fact that M_2C was the only precipitate detected at a temperature just beyond that required for peak hardness, caused Kuo to conclude that this carbide was responsible

for secondary hardening in high speed steels. He also determined that the precipitation and coagulation of W_2C in tungsten-type high speed steels was greatly retarded by the addition of either chromium or cobalt.

Hobson and Tyas [70] agreed with the findings of Kuo on the tempering of high speed steels. They claimed that secondary hardening in these alloys was due to precipitation of M_2C at 560°C. Tempering in excess of 620°C caused the resolution of M_2C and Fe_3C, followed by precipitation and coalescence of the alloy carbides M_6C and $M_{23}C_6$. This caused drastic softening within the temperature range 620 to 650°C.

These workers also mention the possibility of MC contributing towards the secondary hardening mechanism of high speed steels. They felt that the great resistance to coalescence of this carbide could account for a proportion of the hardening reaction, although secondary to that caused by M_2C precipitation.

Tekin and Richman [71] employed the technique of electron diffraction to identify the carbides which were present during the tempering of T1 high speed steel. They extracted plastic replicas from samples of this alloy which were in the hardened and tempered condition. The tempering temperatures used were between 450 and 700°C and times from 1 to 50 hrs.

Their results showed that the maximum secondary hardening effect was obtained after tempering for 8 hrs. at 500°C or 4 hrs. at 550°C. Tempering at temperatures in excess of 600°C caused a very marked softening of this alloy.

The first precipitate to form was cementite, but this carbide was not present in samples which had been tempered at 550°C, or above. Tempering at 500°C caused the precipitation of W_2C, which appeared to form from cementite laths by means of

an in situ transformation. They felt that secondary hardening was mainly due to W_2C precipitation.

They determined that precipitation of $M_{23}C_6$ commenced at a tempering temperature of 550°C, and this occurred within the retained austenite as well as in the martensite. This was well above the temperature which White and Honeycombe [66] found for the precipitation of $M_{23}C_6$ in austenite. However, Tekin and Richman stated that precipitation of this carbide in austenite only contributed very slightly towards the secondary hardening of this alloy.

Tempering at 650°C gave a very overaged structure, with the additional precipitation of V_4C_3 and M_6C. These authors did not consider that precipitation of either of these carbides had much effect on the secondary hardening of T1 high speed steel.

Cope [72] electrolytically extracted carbides from samples of T1 and M2 high speed steels, in the hardened and tempered condition. In order to detect the precipitated carbides which were present, he employed the high tempering temperatures of 700, 750 and 800°C, thereby overaging the precipitated particles. He also varied the tempering times from 15 minutes to 50 hours.

His results showed that M_2C was readily precipitated in both these alloys after tempering for 15 minutes at 700°C. Increasing the time at this temperature to 5 hrs. caused $M_{23}C_6$ to precipitate in both steels and MC to do likewise in M2. Further tempering of both alloys at 750 and 800°C caused no further precipitates to form.

The fact that M_2C was always the predominant precipitate in these two high speed steels supported the findings of Kuo, [69] Hobson and Tyas [70] and Tekin and Richman. [71] All these

workers claimed that the precipitation of this carbide was responsible for secondary hardening in high speed steels.

White and Honeycombe [66] employed the techniques of electron diffraction and X-ray powder analysis in an attempt to determine the secondary hardening precipitate in T1 high speed steel. Carbon replicas were extracted from samples which had been tempered at temperatures between 300 and $700^{o}C$, and so allowed diffraction patterns to be obtained from precipitated particles.

The results showed that the carbide $M_{23}C_6$ was precipitated at temperatures between 550 and $600^{o}C$. This precipitate coarsened appreciably on tempering at $700^{o}C$. Furthermore, X-ray diffraction of extracted carbide residues also revealed that $M_{23}C_6$ was precipitated during tempering. It was not possible to detect the presence of precipitated VC or M_2C in any of the extracted residues, and neither could diffraction patterns be obtained from these carbides.

These workers concluded that the precipitation of $M_{23}C_6$ on tempering was responsible for the secondary hardening of high speed steels. They could find no evidence to agree with Goldschmidt's [2] postulation that $M_{23}C_6$ precipitated within M_6C particles. However, because the diffraction patterns of the two carbides are so similar, a selective carbide extraction method would be required to verify this fact.

Mukherjee [73] refuted the suggestion of Hobson and Tyas [70] that the precipitation of M_2C was responsible for the secondary hardening of high speed steels. He used electron and X-ray diffraction techniques to determine that $M_{23}C_6$ was precipitated in specimens of T1 high speed steel, which had been tempered at $560^{o}C$. The hexagonal carbide, M_2C, was

absent in samples which had been tempered at this temperature. Therefore, this author was in complete agreement with White and Honeycombe [66] that the precipitation of $M_{23}C_6$ was the crucial factor in the secondary hardening of T1 high speed steel.

However, in more recent work Mukherjee, Stumpf, Sellars and McGtegart [74] found that the precipitation of $M_{23}C_6$ was unlikely to produce marked secondary hardening in ferrite. These two cubic phases have quite differing lattice parameters and this was responsible for precipitated $M_{23}C_6$ coarsening rapidly in ferrite during tempering.

Research that has been carried out in the last few years has confirmed an opinion held by Payson. [67]   He felt that in high speed steels which contained in excess of 0.5 wt. % vanadium, the secondary hardening precipitate was V_4C_3.   The hardening effect due to Mo_2C or W_2C precipitation was much less than that of V_4C_3.

A further point of interest from this research was that he found cementite present in high speed steels which had been tempered at $540^{\circ}C$.   However, tempering at temperatures in excess of $540^{\circ}C$ caused all this phase to redissolve.   This is in good agreement with the earlier findings of Michel and Papier [75] and Johnson. [76]

After finding that his earlier work [73] on the nature of the secondary hardening precipitate in high speed steels was incorrect, Mukherjee [18] undertook transmission electron microscopy on carbon replicas which had been extracted from samples of T1, M2 and M50 high speed steels, in the hardened and tempered condition.   These samples had been tempered for varying times at $560^{\circ}C$.   The electron diffraction results

exhibited that V_4C_3 was the major secondary hardening
precipitate in all three alloys, although some contribution
in this respect was obtained from M_2C precipitation. He
found no precipitates to be present in the retained austenite
at any stage of tempering, and this was contrary to the finding
of Tekin and Richman. [71]

The advent of the thin foil technique for the preparation
of samples for transmission electron microscopy has been a
vital factor in the identification of V_4C_3 as the secondary
hardening precipitate in high speed steels. This preparation
technique allows electron diffraction patterns to be taken
from very fine precipitated particles, so allowing these to be
identified.

Lévêque and Condylis [77] used samples in the form of
thin foils to study the precipitates which formed during the
tempering of T1 high speed steel. They hoped that this would
allow the determination of the precipitate which was responsible
for causing secondary hardening in this alloy.

Their results showed that cementite was the first carbide
to precipitate out during tempering. Eventually this phase
decomposed in the following manner:-

$$Fe_3C \xrightarrow{600^{\circ}C} W_2C + V_4C_3 + Cr_7C_3 \xrightarrow{700^{\circ}C} M_6C, V_4C_3, M_{23}C_6$$
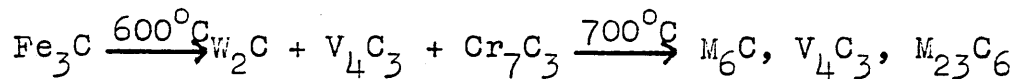
It was interesting to note that the first chromium carbide
that these authors found to be precipitated during tempering
was Cr_7C_3, and not $M_{23}C_6$. The latter was shown to form after
tempering at $700^{\circ}C$. They reached the conclusion that secondary
hardening of this alloy was mainly attributable to V_4C_3
precipitation, with W_2C also offering some contribution.

Horn [78] employed the technique of electron diffraction in an attempt to identify the carbides which were precipitated during the tempering of M2, high-carbon M2, vanadium-free M2 and M1 high speed steels. Her results showed that in all the steels which contained vanadium, the partly coherent carbide MC, which precipitated from the martensite at a temperature of approximately $550^{\circ}C$, was responsible for secondary hardening. The precipitated MC particles caused a lattice strain which was diminished at higher tempering temperatures by their loss of coherence.

In these alloys there was a considerable amount of precipitation of $M_{23}C_6$ and M_6C at tempering temperatures between 600 and $650^{\circ}C$. Both these carbides tended to coagulate rapidly and thus caused a marked deterioration in hardness. The hexagonal carbide, M_2C, was present as a fine precipitate in steels which had been tempered at $650^{\circ}C$. This carbide was found to be unstable in ferrite and probably formed in areas of retained austenite.

The secondary hardening precipitate was also MC in the steels with high carbon contents (1.26 and 1.51 wt. %). Increasing the carbon level of M2 had the effect of extending the temperature range over which $M_{23}C_6$ and M_6C precipitation occurred. As a result of this, the precipitation temperature range of MC was narrowed and thereby caused more marked softening of these two alloys with increasing tempering temperature than was the case for normal M2 high speed steel. The carbide M_2C could not be identified in the temperature range where secondary hardening took place in these alloys.

The steel which was free of vanadium did exhibit a small amount of secondary hardening. Somewhat surprisingly the

secondary hardening precipitate was found to be $M_{23}C_6$ and not M_2C. Colombier and Lévêque [79] had obtained electron diffraction patterns from W_2C particles which had precipitated in the temperature range 550 to 600°C, in a sample of T1 high speed steel which was free of vanadium. They attributed secondary hardening to the precipitation of this carbide. Horn, however, could find no evidence of M_2C precipitation in the secondary hardening temperature range, in all the alloys that she investigated.

Further evidence that V_4C_3 is the secondary hardening precipitate in high speed steels has been presented by Bungardt, Haberling, Rose and Weigand [12] and Kunze. [80] The former felt that to obtain the optimum secondary hardening response, the tempering treatment should be stepped. Kunze showed that tempering at temperatures beyond 600°C caused the carbides M_2C and M_6C to precipitate, with a marked decrease in hardness of the alloy.

A very interesting theory was presented by Kupalova, Baykov and Kabayev [81] concerning the mechanism of vanadium carbide precipitation during the tempering of high speed steels. Their research concerned two alloys which had compositions identical with the martensitic matrix phases of SW9 and M2 high speed steels, in the as-hardened condition. The analyses were as follows:- 0.50 and 0.41 carbon, 7.12 and 3.36 tungsten, 3.88 and 3.25 chromium, 0 and 2.35 molybdenum and 1.0 and 1.11 wt. % vanadium for SW9 and M2 respectively.

The steels were austenisised at 1240°C for 15 minutes in order to dissolve all the carbides that were present. Samples were then tempered at temperatures between 380 and 860°C, for times varying from 5 minutes to 8 hours. Precipitated carbide

particles were electrolytically extracted and the resultant residue subjected to X-ray diffraction analysis.

The first carbide to precipitate on tempering was M_3C, with M_2C, MC, M_7C_3 ($M_{23}C_6$) and M_6C forming at temperatures up to $700^{\circ}C$. This is in good agreement with the precipitated phases found by Sato, Nishizava and Murai [82] when working on similar alloys. However, these workers identified the carbide M_2C as being W_2C, whilst Kupalova, Baykov and Kabayev [81] were of the opinion that this was actually V_2C.

Only very weak lines were obtained for this carbide on X-ray powder photographs. Chemical analysis, however, of the total carbide precipitate, which had been extracted from samples tempered at temperatures where M_2C was known to precipitate, revealed that this phase was richer in vanadium than tungsten.

Shönberg [83] had determined the phases present in the binary vanadium-carbon system. He found the following transformations taking place with increasing carbon content.

$$V \longrightarrow V + V_2C \longrightarrow V_2C \longrightarrow V_2C + VC \longrightarrow VC.$$
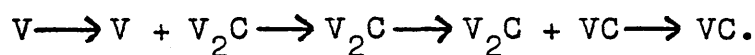
Kupalova, Baykov and Kabayev were of the opinion that the vanadium atoms dissolved in the martensitic matrix of high speed steels, undergo these reactions during tempering. They developed the following equations for carbide precipitation during the tempering of high speed steels between 550 and $800^{\circ}C$:-

$$V_2C \longrightarrow V_2C + VC + Cr_7C_3 \longrightarrow V_2C + VC + Cr_7C_3 + M_6C \longrightarrow Cr_7C_3 + M_6C + VC \longrightarrow VC + M_6C.$$
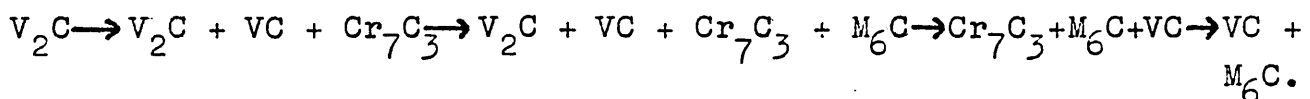
Their opinion was that secondary hardening in these alloys was due to vanadium carbide precipitation. The major hardening contribution was from the formation of the relatively unstable carbide V_2C, which later transformed to VC.

There has been no subsequent research to support the
interesting theory of these workers.   The X-ray powder
technique for the identification of fine precipitated particles
is not as sensitive as electron diffraction from thin foil
samples.   Precipitated carbides are only detected by X-ray
means after tempering at temperatures well in excess of those
at which they are originally formed.

2.2.1   The Influence of Cobalt on the Secondary Hardening
         of High Speed Steels

Ever since the early work of French and Digges, [84]
there has been a considerable amount of interest shown in
the effect of cobalt in high speed steels.   Their results
showed that addition of cobalt improved the cutting properties
of these alloys, allowing increased speeds to be employed
during machining.

Gudtsov and Gelfand [85] and Zmihorski [86] found that
additions of cobalt improved the secondary hardening response
and hot hardness of high speed steels.   Cobalt appeared to
have the effect of moving the eutectic reaction to higher
temperatures in these steels.   This allowed increased auste-
nitisation temperatures to be used with resultant improvement
in the degree of carbide solution.   They felt that this
increase in the alloy content of the matrix gave a marked
improvement in the amount of precipitation taking place during
the tempering of high speed steels, thereby resulting in
superior secondary hardening response and hot hardness.

More recent research, however, has shown the theories of
Gudtsov and Gelfand to be incorrect.   Gulyaev and Kupalova [87]
and Mazur, Krawiarz and Kaliszewski [88] demonstrated that
the effect of cobalt in improving the secondary hardening and

hot hardness of high speed steels was due to three factors.
This element reinforced interatomic bonds within the
martensitic matrix and also reduced grain boundary energy.
Finally cobalt was shown to reduce the diffusional mobility
of atoms in the martensite solid solution.   This last factor
had the major effect in improving the hot hardness of these
alloys.   Cobalt created a retardation in the rate of softening
of martensite and caused precipitates to both form, and not
overage except at higher temperatures.

Popandopulo [89] stated that cobalt gave an intensifica-
tion to precipitation hardening mechanisms in high speed steels.
The resultant improvement in secondary hardness, caused by
the addition of 15 wt. % cobalt, increased two to threefold
the wear resistance, thermal conductivity and cutting ability
of these steels.

The other important effect cobalt has in high speed steels
is the introduction of a fifth stage of tempering.   Chandok,
Hirth and Dulis, [90] Williams [91] and Rousseau [92] all
showed that precipitation of the intermetallic compound,
Co_7W_6, took place on tempering these alloys at temperatures
of approximately $650^{\circ}C$.   This precipitation greatly retarded
the softening of these steels at high tempering temperatures.
Rousseau, however, only found that the fifth stage of tempering
took place in high speed steels containing above 10 wt. %
cobalt.

2.3   The Importance of the Carbon :Vanadium Ratio in High Speed Steels

The classical research on the significance of the carbon : vanadium ratio in high speed steels was undertaken by Blickwede, Cohen and Roberts. [93]   They used the base composition of M2 high speed steel (i.e. 6 tungsten, 5 molybdenum and 4 wt. % chromium), and altered the vanadium contents incrementally from 0 to 10 wt. % at carbon levels which ranged from 0.1 to 2.5 wt.%. A differential etching technique was developed to allow the various carbides to be identified.   Carbides were also electrolytically extracted and the resultant residue subjected to X-ray powder analysis.

Their results showed that five different phase fields existed over the range of carbon : vanadium ratios employed in these alloys, in the annealed condition.   These are shown in FIG. 10 and can be listed as follows:-

1. $MC + M_3R_2$.   (M_3R_2 is an intermetallic compound

2. $M_6C + MC + M_3R_2$.

3. $M_6C + M_3R_2$.

4. $M_6C + MC + M_{23}C_6$.

5. $M_6C + M_{23}C_6$.

These phase regions are listed in order of increasing carbon : vanadium ratios of the steels.   The phase field $M_6C + M_3R_2$ is difficult to classify, as this only occurs in those alloys with very low carbon and vanadium contents. Their results showed that the primary carbide M_6C was present in all the alloys, whilst MC was only absent in those with very low vanadium levels.   It should be mentioned here that the carbon : vanadium ratio which is generally employed in high speed steels is such as to produce the fourth phase region

(i.e. $M_6C + MC + M_{23}C_6$) listed above.

The intermetallic compound, which was found to be present in some of the steels, was given the formula M_3R_2. However, subsequent research by Goldschmidt [42] has shown this compound to have a formula M_7R_6. The presence of the intermetallic compound or the carbide, $M_{23}C_6$, in high speed steels in the annealed condition, was governed by the carbon : vanadium ratio of the particular alloy. Formation of $M_{23}C_6$ in preference to the intermetallic compound was favoured by a high carbon : vanadium ratio , whilst the converse held for the existence of M_3R_2. Blickwede, Cohen and Roberts make no mention of the carbide, M_7C_3, being present rather than $M_{23}C_6$, in these steels with high carbon contents, and Steven, Nehrenberg and Philip [7] and Mukherjee [8] are very critical of this fact.

The five constitutional zones present in the annealed steels split into eight regions after austenitisation at temperatures between 930 and $1260^{\circ}C$, as illustrated in FIG. 11. Four of these fields corresponded to compositions which remained ferritic even up to $1260^{\circ}C$, but differed in the nature of the excess phases as follows:-

1. α + M_6C (+ M_3R_2 below $1090^{\circ}C$)

2. α + M_6C + MC (+ M_3R_2 below $1090^{\circ}C$)

3. α + MC (+ M_3R_2 below $1090^{\circ}C$)

4. α + M_6C + MC

On the low vanadium, high carbon side of the last phase field above (i.e. α + M_6C + MC), the matrix of the alloys became partially austenitic:-

5. α + M_6C + MC (+ γ above $1150^{\circ}C$)

The remaining three regions contained compositions whose matrices were fully austenitic at temperatures above $930^{\circ}C$, but in two of the cases δ- ferrite appeared during austenitisation:-

6. γ + M_6C + MC (+ $M_{23}C_6$ below $1090^{\circ}C$)

7. γ + M_6C + MC (+ $M_{23}C_6$ below $1150^{\circ}C$ + δ above $1090^{\circ}C$)

8. γ + M_6C (+ $M_{23}C_6$ below $1150^{\circ}C$ + δ above $1035^{\circ}C$)

From these results Blickwede, Cohen and Roberts determined that the compositions of high speed steels should be such that the phases in region 6 above were present during austenitisation. Alloys of this composition could be readily austenitised and were capable of attaining high hardness values after subsequent quenching.

The full importance of the carbon : vanadium ratio in high speed steels was shown by these authors in FIG. 12. Within the triangle exist ratios which given potentially useful high speed steels. Compositions to the right of the triangle (i.e. low ratios) give alloys which are not quench hardenable, owing to ferrite being present, even at high temperatures. This is due to the strong ferrite stabilising effect of vanadium.

Therefore, the necessity of raising the carbon content by approximately 0.25 wt. % for each 1 wt. % additional vanadium, over a base composition of 0.55 carbon and 1.0 wt. % vanadium in M2 high speed steel is clearly illustrated. Higher ratios gave increasing amounts of retained austenite. Carbon levels in excess of 1.7 wt. % meant the steel was impossible to forge.

As a result of this important work by Blickwede, Cohen and Roberts, the super high speed steels were developed.

These can be classed as having carbon and vanadium contents
in excess of 1.25 and 3.0 wt. % respectively (M4, T15 and
M15).   The super high speed steels have excellent wear
resistance owing to the large quantity of vanadium carbide
present and are very difficult to grind in the hardened and
tempered condition.   A good deal of research has been carried
out on the development of these alloys, the most important of
which was by Mortier, [94] Elsen E., Elsen G. and Markworth, [95]
Zaitsev, Rogovtsev and Doronin [96] and Mortier. [97]

Kinzel and Burgess [98] also showed that increased
vanadium levels in high speed steels must be accompanied by
rises in carbon contents if the alloys were to remain quench
hardenable.   They used steels of base composition 0.80 carbon,
17.3 tungsten and 4.1 wt. % chromium, with variations in
vanadium levels between 0 and 10 wt. %.   Results showed that
vanadium contents in excess of 2.5 wt. % caused a marked dete-
rioration in as-quenched hardness of the alloys (FIG. 13).
In fact, the high-vanadium steels, which contained appreciable
quantities of ferrite, forged in a manner similar to plain
carbon steels.

Roberts [99] determined the relationship between the
volume fraction of the carbide MC and vanadium content of
M2-base high speed steel, in the as-hardened condition.
Increasing the vanadium level of this alloy from 2.0 to 6.0
wt. % gave a fourfold rise in the volume fraction of MC remain-
ing undissolved after austenitisation at $1205^{\circ}C$.   He stated
the importance of the undissolved MC particles giving high
speed steels excellent wear resistance.   This is a fact which
was very much endorsed by Fischer and Kohlhaas, [17] who found

that MC was the hardest carbide present in high speed steels (TABLE 5), and hence was instrumental in providing their wear resistance.

Roberts also deduced the importance of dissolving quite a high proportion of the primary MC carbides during austenitisation, in order to give the steel a high degree of precipitation hardening during tempering, and hence good hot hardness. The balance between the proportion of dissolved and undissolved MC carbides, was therefore, very critical.

The importance of hot hardness of high speed steels was illustrated by Harder and Grove. [100] They showed that the increased cutting ability of high speed steels with high carbon and vanadium contents was not only due to their improved wear resistance. These steels have good hot hardness and this is a vital factor in their superior cutting ability when compared with other high speed steels. This fact is clearly illustrated in FIG. 14, with the alloy T15, which contains 5 wt. % of both vanadium and cobalt having higher hot hardness than other high speed steels, including T6, which has a cobalt content of 12 wt.% but only 2 wt. % vanadium.

Weigand and Haberling [101] attempted to find the ideal carbon : vanadium ratio to give optimum secondary hardening in M2-base high speed steel. They employed narrow composition ranges, with carbon contents between 0.84 and 1.04 wt. % and vanadium levels from 1.53 to 2.18 wt. %. Their results showed that increased carbon:vanadium ratios led to higher secondary hardness and better tempering resistance, due to the increased carbon content of the steel matrix.

However, a reduction in the vanadium level of the alloy is connected with a depletion in volume fraction of vanadium carbide.

This means that steels with the same carbon : vanadium ratios do not necessarily possess identical properties. Thus, a higher secondary hardness, gained by a reduction in the vanadium content is accompanied by a lower wear resistance.

Geller, Ivanov and Kremnev [102] determined the effect of increased vanadium content on the secondary hardening response of a high speed steel with basic classification SW12C. The vanadium levels ranged between 2.57 and 4.9 wt. %, and the alloy with the highest concentration of this element was most resistant to softening at tempering temperatures up to $500^{\circ}C$. However, at temperatures beyond $500^{\circ}C$, this steel softened more rapidly than normal high speed steels. In fact, this steel only gave a low degree of secondary hardening, owing to the small amount of carbide precipitation that occurred on tempering between 550 and $600^{\circ}C$. The reason for this was that the matrix was impoverished in carbon, this element having reacted with the extra vanadium atoms to form a greater volume fraction of primary MC, a considerable proportion of which was not taken into solution during subsequent austenitisation.

Oertel and Grutzner [103] carried out lathe tool cutting tests with tools of composition 19 tungsten, 4 chromium and 4 wt. % vanadium, but with carbon contents varying from 0.93 to 1.48 wt. %. The results showed that the maximum tool life was obtained at a carbon level of 1.25 to 1.30 wt. % (FIG. 15). This carbon content is in fact used in both T9 and M4 high speed steels, both of which contain 4 wt. % vanadium.

An interesting piece of research was undertaken by Wadell, [104] who set out to develop a low-alloy version of M2 high speed steel which could be used for the manufacture

of twist drills. The basis of his idea was cost saving in alloy additions. He thought that maximum secondary hardening response was not being obtained in many high speed steels, owing to the large amount of carbon which was out of solution. This element had reacted with vanadium to form carbides.

Wadell termed his new high speed steel as D950, the full analysis of which is given in TABLE 1. He found that the carbon : vanadium ratio of the new alloy was very sensitive and thought this was probably the case for all high speed steels. The optimum ratio for D950 was 0.86. Reduction of the ratio to 0.77 caused a marked deterioration in secondary hardeningand twist drill performance.

Drilling tests showed that D950 gave a similar performance to M2 high speed steel. The biggest drawback with the new steel was the low volume fraction of primary vanadium carbides that were present after hardening and tempering. This rendered the alloy unsuitable for tool applications which were subject to excessive wear.

Berry [105] made the point that high carbon : vanadium ratios in high speed steels could lead to chromium depletion of the matrix and ensuing deterioration in oxidation resistance. The surplus carbon would react with more chromium to form carbides. This fact only applies to steels in the annealed condition, as both the chromium carbides, $M_{23}C_6$ and M_7C_3, are readily dissolved during austenitisation.

2.4   The Secondary Hardening of Vanadium Steels

The original work on the tempering of vanadium steels was undertaken by Houdremont, Bennek and Schrader [106] and Houdremont, Neumann and Schrader. [107]   They felt that the secondary hardening phenomenon observed in these alloys was due mainly, if not entirely, to the precipitation of the carbide VC.   Their results also showed that vanadium carbide had a strong resistance to solution treatment, and high austenitisation temperatures were required to obtain the maximum secondary hardening effect.

Koch and Wiester [108] employed the technique of chemical analysis of electrolytically extracted carbide residues from vanadium steels in the hardened and tempered condition. Cementite was the only carbide precipitated at temperatures up to, and including $500^{\circ}C$.   Secondary hardening took place in the alloys tempered between 500 and $550^{\circ}C$, and this was associated with vanadium carbide precipitation.   Analysis of the extracted residue from a steel tempered at $550^{\circ}C$ compared with another at $500^{\circ}C$, showed a decrease in iron content from 73 to 21 wt. %, with a corresponding increase in vanadium from 9 to 67 wt. %.   However, cementite did not disappear completely until a tempering temperature of $700^{\circ}C$ was employed.

Kuo [109] found very pronounced secondary hardening on tempering a steel of composition 0.32 carbon and 1.36 wt. % vanadium at temperatures of between 500 and $600^{\circ}C$.   He carried out transmission electron microscopy on extracted carbon replicas from the tempered alloys.   The only carbide which had precipitated at temperatures up to $450^{\circ}C$ was cementite, and this was of approximately the same shape and

size as that which would have formed in a plain carbon steel after a corresponding treatment. Therefore, he concluded that the pronounced resistance to softening imparted to steels by vanadium was not due to the effect of this element on the growth rate of cementite.

Tempering this alloy at $525^{\circ}C$ caused minute threads of VC to appear, and the quantity of these increased without any appreciable growth up to a temperature of $600^{\circ}C$. Within this temperature range the volume fraction of cementite diminished, until this phase went completely into solution after tempering at $650^{\circ}C$. This is in good agreement with the finding of Koch and Wiester. [108] Further increase in tempering temperature from 650 to $750^{\circ}C$ caused the VC threads to grow into needles, discs and spheroids respectively. Even after tempering the steel at $750^{\circ}C$ for 1 hour, the VC particles were still smaller than $500\overset{\circ}{A}$.

Seal and Honeycombe [110] compared the secondary hardening response between a steel containing chromium and another with vanadium. The carbon content of both these commercial purity steels was 0.22 wt. %, whilst one contained 9.1 wt. % chromium and the other 1.0 wt. % vanadium. Samples of the two alloys were hardened and then tempered at temperatures between 100 and $700^{\circ}C$ for varying times.

The steel which contained chromium resisted softening very well at temperatures up to $500^{\circ}C$ (FIG. 16). However, tempering at temperatures beyond this caused a rapid reduction in hardness of the alloy. Hardness readings on the vanadium steel revealed that this was softer at low tempering temperatures than its counterpart containing chromium. Tempering the vanadium steel between 550 and $600^{\circ}C$ caused a marked

secondary hardening peak to occur (FIG. 17), and this alloy resisted softening at temperatures in excess of 600°C to a far greater extent than that containing chromium.

The only precipitate obtained on tempering the vanadium steel at temperatures between 250 and 500°C was cementite. Electron microscopic examination showed that the marked . softening of the alloy in this temperature range coincided with an increase in the size of the cementite particles. Tempering at 550°C for 1 hour caused much of the cementite to redissolve and to be replaced by a nebulous precipitate, which was identified by electron diffraction as being V_4C_3. This corresponded with a sharp rise in hardness of the alloy. The precipitated vanadium carbide particles were in the form of rodlets, approximately $20\overset{\text{o}}{\text{A}}$ wide and 50 to $100 \overset{\text{o}}{\text{A}}$ long, after tempering for 100 hrs. at 550°C. These particles became spheroidal (100 to $200 \overset{\text{o}}{\text{A}}$ diameter) when the hardness peak was exceeded. This is in good agreement with the results of Kuo. [109]

In a slightly more recent piece of research, Seal and Honeycombe [111] demonstrated that a steel which contained 0.23 carbon and 0.97 wt. % vanadium gave appreciably more secondary hardening than an alloy with this same carbon content but with 0.99 wt. % molybdenum. Tempering the vanadium steel at 600°C caused an increase in hardness of 90 HV/20 compared with that obtained after tempering at 500°C, whilst the corresponding value was only 15 HV/20 for the alloy which contained molybdenum.

The original work on the determination of the orientation relationship between precipitated V_4C_3 particles and the

ferrite matrix was undertaken by Baker and Nutting. [112]
Their results showed the following relationship:-

$$\{100\}_{V_4C_3} // \{100\}_\alpha$$

$$\langle 100 \rangle_{V_4C_3} // \langle 110 \rangle_\alpha$$

Electron diffraction patterns of the precipitated particles showed arcing, and this suggested Widmanstätten precipitation of the carbides.

Smith [113] confirmed the orientation relationship determined by Baker and Nutting. [112] He also found by electron microscopy the presence of small parallel streaks within the grains of thin foils of a vanadium (1 wt. %) steel with low carbon content (0.2 wt. %), after tempering at 600°C for 30 minutes. These were similar to the zones found in aluminium - 4 wt. % copper alloys by Nicholson and Nutting, [114] with the exception that the streaks in the steel were connected by the network of dislocations.

Nicholson and Nutting found that, as a result of the formation of Guinier - Preston [2] zones on ageing an aluminium - 4 wt. % copper alloy, coherent straining of the lattice could occur for a distance of approximately 200 $\overset{o}{\text{A}}$ around the precipitates. Baker and Nutting [112] noticed an unusual etching effect at the interface of coherent precipitates of V_4C_3 during early stages of precipitation. The size of these etched regions was 300 to 500 $\overset{o}{\text{A}}$, and appeared to represent the strain fields around the precipitated particles.

More recent research by Hornbogen [115] [116] [117] has proved beyond all doubt that Guinier - Preston zones can form in body centred cubic α-iron. He found the presence of these zones in high purity iron-molybdenum, iron-copper and iron-

gold alloys.   The other aspect of this work was to determine whether there was a relationship between the number of vacancies in the iron lattice and the rate of formation of the zones.

In earlier work on an aluminium - 4 wt. % copper alloy, the rate of clustering of copper atoms was compared with the estimated supersaturation of vacancies by Sorbo, Treaftis and Turnbull, [118] Silcock [119] and Chiou, Herman and Fine. [120]   A relationship was found to exist between the supersaturation of vacancies and the rate of formation of the zones.   It was assumed that, after quenching from a temperature T_2, the diffusion coefficient D_c at the temperature of ageing T_1 could be derived by multiplication of the normal diffusion coefficient D_{T_1} by the ratio of the actual number of vacancies to the equilibrium number:-

$$D_c = D_o \; \exp\left(\frac{-U_m}{RT_1}\right) \; \exp\left(\frac{-U_f}{RT_2}\right) = D_o \; \exp\left(\frac{-Q}{RT_1}\right) \frac{C_{T_2}}{C_{T_1}} \quad ..EQN. \; 2$$

where Q = Activation energy for diffusion.

U_f = Energy of formation of a vacancy.

U_m = Energy of motion of an atom.

C = Concentration of vacancies, and is calculated approximately from:-

$$C_T = \frac{n_v}{N} = \exp\left(\frac{-U_f}{RT}\right) \quad ....EQUATION \; 3.$$

n_v = Number of vacancies.

N = Total number of atoms.

The results of the work by Hornbogen [115] on iron - 20 wt. % molybdenum showed there was definitely a relationship between the quantity of vacancies in the parent metal and

the rate of formation of solute zones. He employed the theory of thermal vacancies and the assumption that:-

$$U_f \simeq \frac{Q}{2} = 30,000 \text{ cal./mole} \quad \ldots\ldots\text{EQUATION } 4$$

The supersaturation of vacancies was, therefore:-

$$\frac{CT_2}{CT_1} = 10^{4.7} \quad \ldots\ldots\ldots\text{EQUATION } 5$$

Where T_1 = Ageing temperature = $500^{\circ}C$.

T_2 = Solution treating temperature = $1440^{\circ}C$.

Vacancies created sites for zone formation and supersaturation of vacancies enhanced the diffusion rates of the atoms. Hornbogen considered the case of a molybdenum atom migrating to the dislocation ring to form a ring-shaped zone. The diffusion coefficient for this was determined from the equation:-

$$D_{exp} \simeq \left(\frac{x^2}{t}\right) \quad \ldots\ldots\ldots\text{EQUATION } 6$$

Where x = Average distance travelled by a molybdenum atom.

t = Time for half completion of zone formation.

He determined that, for an ageing temperature of $500^{\circ}C$, D_{exp} = 0.3 x 10^{-16} cm^2/sec. This value was well within the expected range for normal diffusion of substitutional solutes in alpha iron at $500^{\circ}C$. From an estimation of the supersaturation of vacancies and substitution in EQUATION 2, the diffusion coefficient of molybdenum atoms in alpha iron (D_c) was found to be 10^{-11} cm^2/ sec.

Therefore, the overall process of clustering in an alpha iron-molybdenum solid solution could be described as taking place over four definite steps. The first of these was the segregation of vacancies, that ultimately collapsed

into dislocation rings on (100) planes. This was followed by the diffusion of solute atoms to these dislocation rings. The formation of ring-shaped clusters of molybdenum atoms then took place on dislocations, and these grew into discs. Zone growth was mainly by normal diffusion. Finally the zones lost partial coherency with the matrix, thereby causing two body centred cubic lattices to coexist.

Smith and Nutting [121] suggested the possibility of vanadium enriched zones forming prior to the precipitation of V_4C_3 during the tempering of vanadium steels. They likened these to the Guinier - Preston [1] zones formed in the ageing of aluminium - 4 wt. % copper alloys. However, although they felt that the presence of the zones helped to reduce the rate of softening of these steels at temperatures up to $500^{\circ}C$, secondary hardening was due to the precipitation of V_4C_3 in the ferrite matrix.

In more recent research, definite confirmation was given by Irani and Honeycombe, [122] [123] Honeycombe [124] and Speirs, Roberts, Grieveson and Jack [125] of the presence of solute-rich zones in vanadium steels, the zones being rich in vanadium and carbon atoms. Irani and Honeycombe [123] compared the nature of zone formation in two steels, both containing 0.2 wt. % carbon, but one having 4 wt. % molybdenum and the other 1 wt. % vanadium. The alloys were solution treated at $1250^{\circ}C$, subsequently quenched and then tempered at temperatures between 500 and $700^{\circ}C$.

Zones formed in both alloys prior to the precipitation of either Mo_2C or V_4C_3. Diffraction patterns taken from

solute-rich zones in the molybdenum steel contained spots
which were distorted into 'streaks'. These two-dimensional
zones had the effect of expanding the iron lattice locally
along the $\langle 100 \rangle$ directions.

However, the zones which formed in the vanadium steel
were spherical in shape. These could not be detected from
electron diffraction patterns, as their three-dimensional
form ruled out the diffraction 'streaks' observed in the
molybdenum steel. The contrast in the shapes of the
molybdenum and vanadium zones could be explained from a
consideration of the relative misfit of the two atoms in the
iron lattice. Molybdenum has a larger atomic diameter than
vanadium, and so atoms of the former cause a greater misfit
(10.2%) in the iron lattice than those of the latter (6.7%).
This meant that molybdenum atoms created a more pronounced
local expansion of the iron matrix lattice and so were
capable of forming only two-dimensional zones, whilst vanadium
was able to form three-dimensional spherical zones.

The determination of the presence of solute-rich zones
in molybdenum and vanadium steels offered enlightenment on
the secondary hardening mechanism taking place. Correlation
of hardness results and structures obtained by electron
microscopy revealed that the initial rise to peak hardness
coincided with the formation of solute-rich zones in the
iron matrix, and was not due to precipitation of alloy
carbides as suggested by Seal and Honeycombe [111] and Smith
and Nutting. [121].

Irani and Honeycombe, therefore, were of the opinion
that secondary hardening of molybdenum and vanadium steels
was due to the preprecipitation process of solute zone

formation, and the effects due to coherent carbide preci-
pitation were prevalent at higher tempering temperatures.
They observed that when coherent precipitation of either
Mo_2C or V_4C_3 took place the hardness deteriorated, although
still remaining well in excess of the corresponding value
of the as-quenched alloy.

This confirmed that the precipitated carbides strengthened
the matrix, but were not as effective in this respect as
the solute-rich zones. Tempering between 650 and $700^{\circ}C$
caused a further decrease in hardness of both steels, due
to the precipitated carbides coarsening and eventually
becoming incoherent with the iron matrix.

Ustinovshchikov, Kovenskiy and Vlasov [126] undertook
research on the precipitation of certain carbides in alloy
steels using X-ray diffraction and electron microscopy
techniques. The steels employed contained in each case
only one alloying addition, namely chromium, molybdenum or
vanadium, and had carbon contents ranging between 0.14 and
0.33 wt. %.

These authors found that prior to alloy carbide
precipitation on tempering, short range ordering or separa-
tion of substitutional solid solutions occurred. Regions
enriched with the alloying element, which result from ordering
slowly change into mixed zones of carbide and substitutional
atoms of the G.P. - zone type. Cementite is formed in
regions denuded of alloying element, and later in the
tempering cycle this phase is either completely or partially
dissolved, with the carbon atoms diffusing through the solid
solution to the G.P. zones. This results in saturation of
the zones and transformation into alloy carbides.

From these findings, three reasons were presented for the secondary hardening of alloy steels. The first was the presence of carbon in the solid solution, particularly during dissolution of cementite. Other factors were the formation of a band structure and increase in coherent stresses at the carbide/matrix interface.

Tekin and Kelly, [127] however, could find no evidence of solute zone formation during the tempering of two vanadium steels. The full analyses of these alloys were not given, but one was of high purity, containing 0.1 carbon and 0.5 wt% vanadium, whilst the other was a commercial steel with 0.2 carbon and 1.0 wt. % vanadium. These alloys both exhibited marked secondary hardening on tempering between 540 and 600°C. This was particularly the case for the steel with higher vanadium content, which had a secondary hardening peak of 80 HV/10.

At low tempering temperatures, the two vanadium steels tempered in a manner very similar to plain carbon steels. Cementite was observed to persist as laths on $\{110\}_\alpha$ in the vanadium steels at temperatures up to 500°C. However, precipitation of V_4C_3 occurred on dislocations at tempering temperatures well below that required for peak hardness. There was a spread in the orientation of the precipitates of 3 to 5°, giving rise to arced V_4C_3 reflections on electron diffraction patterns. Long term tempering was required for V_4C_3 precipitation to occur at low temperatures, an example of this being 15 hours at 450°C.

Higher tempering temperatures caused the V_4C_3 particles to grow as plates on $\{100\}_\alpha$ planes out into the matrix, thereby

losing their variation in orientation and closely obeying
the relationship proposed by Baker and Nutting. [112]
Tempering at a temperature close to that necessary to give
peak hardness caused V_4C_3 particles to nucleate homogeneously
in the matrix as well as on dislocations. These precipitates
again formed on $\{100\}_\alpha$.

At no stage of the tempering process were vanadium-
rich zones observed, as suggested by Irani and Honeycombe [123]
and Honeycombe. [124] Tekin and Kelly were of the opinion
that secondary hardening in vanadium steels was due to the
lattice straining of the matrix caused by V_4C_3 precipitation
and also to the locking of dislocations by these particles.
They claimed that the rapid softening which took place at
tempering temperatures in excess of $620^\circ C$ was a result of
the precipitated V_4C_3 becoming less effective in locking
dislocations.

The microstructural changes which took place at various
tempering temperatures were virtually identical for both the
commercial and high purity vanadium steels. However, as
would be expected, a greater quantity of V_4C_3 was precipitated
between 540 and $600^\circ C$ in the alloy with higher carbon and
vanadium contents, thereby causing this steel to secondary
harden to a greater degree. It was very surprising that
these authors used alloys of differing composition to compare
secondary hardening in commercial and high purity vanadium
steels. They did employ the same carbon : vanadium ratio,
but this does not guarantee identical properties, as Livshits
and Shcherbakova [128] determined for vanadium steels, whilst
Weigand and Haberling [101] did likewise for high speed steels.

Nishida and Tanino [129] showed that secondary hardening occurred in vanadium steels with a carbon content of 0.17 wt.%, when in excess of 0.1 wt. % vanadium was present. Beyond this content, the amount of secondary hardening was approximately proportional to the vanadium level of the alloy. The onset of secondary hardening coincided with the precipitation of fine particles of V_4C_3 along dislocation lines and on tangled dislocation nodes within the matrix.

Isizuka [130] evaluated the secondary hardening response in a series of vanadium steels, with carbon contents ranging from 0.30 to 1.0 wt. % and vanadium between 0.4 and 2.9 wt.%. The alloys were of commercial purity, and contained small amounts of chromium, nickel, copper and molybdenum. He employed very high solution treatment temperatures for the high-vanadium steels (eg. 1350°C) in order to take into solution a high proportion of the primary vanadium carbide. Hardness tests on the alloys in the as-quenched condition revealed that hardness rose slightly with increase in vanadium content, due to solid solution hardening.

All the steels exhibited secondary hardening on tempering between 550 and 600°C, this being most marked in those which contained in excess of 1 wt. % vanadium. However, this peak was moved to slightly lower tempering temperatures in the alloys with highest vanadium content (i.e. 2.9 wt. %). Some of the high-vanadium steels had hardness values in excess of 60 HRC after being tempered at temperatures necessary to give optimum secondary hardening.

Aoki and Tanino [131] found that the addition of 0.1 wt.% vanadium to a low-carbon steel caused secondary hardening to

occur on tempering. The maximum effect was obtained after tempering at $625^{\circ}C$ for 1 hour. Extremely fine particles of V_4C_3 (less than 50 $\overset{\text{o}}{A}$ in diameter) were precipitated along dislocation lines and on tangled dislocation nodes at the temperature necessary to give the onset of secondary hardening. The increase in internal stress due to the precipitation of these fine coherent V_4C_3 particles was thought to be the reason for secondary hardening.

Goldshteyn [132] also determined that only very small amounts of vanadium were required to give secondary hardening in steels. This hardening was due to the precipitation of VC, which in turn was not associated with the formation and dissociation of cementite. Very little vanadium was found to be dissolved in the cementite.

Goldshteyn and Farber [133] showed that the formation of precipitates of VC was proceeded by the segregation of vanadium and carbon atoms at crystal structure defects, as a result of tempering between 350 and $450^{\circ}C$. The first precipitates of VC were observed by transmission electron microscopy on thin foils which had been tempered at $500^{\circ}C$ for 2 hours. These were formed mainly on dislocations and were in the form of plates, 15 to 30 $\overset{\text{o}}{A}$ thick, and 100 to 200 $\overset{\text{o}}{A}$ long. The particles were formed independently of cementite, and this is in agreement with the earlier work of Goldshteyn. [132] This was confirmed by observing that VC had been readily precipitated in a steel with a very low carbon : vanadium ratio, whilst very little cementite had formed on tempering.

These workers found that secondary hardening occurred

during the tempering of a range of vanadium steels, and they attempted to relate this with the mutual arrangement of vanadium carbide and ferritic iron lattices (FIG. 18). This allowed a calculation to be made of the incompatibility between these two phases from a knowledge of the condition of conservation of coherence. The latter condition was at a minimum in the directions $\langle 110 \rangle_{VC}$ and $\langle 100 \rangle_{\alpha-Fe}$, whereby:-

$$d_{\langle 110 \rangle VC} - d_{\langle 100 \rangle \alpha-Fe} = 2.95\overset{o}{A} - 2.86\overset{o}{A} = 0.09\overset{o}{A} \quad ..EQN.7$$

The maximum condition for the conservation of coherence was in the directions $\langle 100 \rangle_{VC}$ and $\langle 100 \rangle_{\alpha-Fe}$, whereby:-

$$d_{\langle 100 \rangle VC} - d_{\langle 100 \rangle \alpha-Fe} = 4.17\overset{o}{A} - 2.86\overset{o}{A} = 1.31\overset{o}{A} \quad ..EQN\ 8$$

This was from employing the accepted values of $a_{\alpha-Fe} = 2.86\overset{o}{A}$ and $a_{VC} = 4.17\overset{o}{A}$.

Therefore, it can be taken that if there is a lattice incompatibility of up to 1 interplanar distance, the precipitated particles will be coherent with the matrix and no dislocations will form on their interface. Such a lattice incompatibility would occur in $\langle 110 \rangle_{VC}$ directions with a particle size of $\frac{2.86}{0.09} = 31.77$ unit cells or $2.95\overset{o}{A} \times 31.77 = 93.72\ \overset{o}{A}$, and in $\langle 100 \rangle_{VC}$ directions for $\frac{2.86}{1.31} = 2.18$ unit cells or $4.17\ \overset{o}{A} \times 2.18 = 9.09\overset{o}{A}$. The conclusion from this is that coherent precipitates of vanadium carbide in ferritic iron will be in the form of plates, with a length : thickness ratio of approximately 10:1. This was close to the ratio that Goldshteyn and Farber determined practically, by means of transmission electron microscopy for the size of the first vanadium carbide particles to precipitate on tempering.

Friedel [134] attempted to ascertain the conditions under which a precipitated particle loses coherency with the matrix. He assumed that the originally coherent precipitate became non-coherent when it had grown to a size necessary to make the elastic energy, that arose from the difference in the atomic volumes of matrix and precipitate, exceed the value of the surface energy γ. This allowed him to derive the following relationship:-

$$r_c = \frac{4\gamma}{\delta^2 \mu} \quad \ldots\ldots \text{EQUATION 9}$$

Where r_c = Critical radius of the particle necessary to retain coherency with the matrix.

γ = Surface energy at the interface between the precipitate and matrix.

δ = Difference in lattice parameters of the precipitate and matrix.

μ = Modulus of elasticity in shear of the matrix.

The value of the surface energy at the interface between the precipitate and matrix can be determined from the relationship:-

$$\gamma = 0.03 \mu' \; b' \quad \ldots\ldots \text{EQUATION 10}$$

Where μ' = Modulus of elasticity in shear of the precipitate.

b' = Burgers vector of the particle.

Kelly and Nicholson [135] showed that the stress necessary for the deformation of a particle could be determined approximately by a comparison of the work done by the applied stress during the movement of the particle over a distance equal to its diameter with the work equal to the surface energy. From a basis of this assumption, they derived an equation involving the maximum radius of a particle (r_c) about to be deformed:-

$$r_c = \frac{2\mu b^2}{\pi \gamma} \quad \ldots\ldots \text{EQUATION 11.}$$

Where μ = Modulus of elasticity in shear of the matrix.

b = Burgers vector of the matrix.

γ = Surface energy at the interface between the precipitate and matrix.

Prnka [136] substituted practically determined values into these equations in order to calculate the coherency requirement for V_4C_3 particles in a ferrite matrix. He obtained values of $r_c = 70\overset{o}{A}$ using Equations 9 and 10 as derived by Fridel, [134] and $106\overset{o}{A}$ from Equation 11 by Kelly and Nicholson, [135] and clearly these results are in quite good agreement. This meant that when V_4C_3 precipitated particles exceed between 70 and $106\overset{o}{A}$ in diameter they lose coherency with the ferrite matrix.

He also employed the orientation relationships determined by Baker and Nutting [112] and verified by Tekin and Kelly [127] and Raynor, Whiteman and Honeycombe [137] to ascertain the size that V_4C_3 particles could grow in certain directions to retain coherency with the ferrite matrix. The V_4C_3 particles precipitated on $(100)_\alpha$ and he assumed that loss of coherency in any arbitrary direction occurred when the inconsistency of the lattice exceeded 50% of the interatomic spacing. On this basis the V_4C_3 particles can only grow to 1 to 2 elementary units of the V_4C_3 lattice (4 to $8\overset{o}{A}$) in the direction $[100]_{V_4C_3}$, whereupon the energy of deformation produced must be reduced by the extra plane of iron atoms, or in other words by a surface dislocation. Thus, V_4C_3 particles may reach a maximum thickness of 10 to $20\overset{o}{A}$ to retain coherency with the ferrite matrix.

However, in the direction $[110]_{V_4C_3}$, the particles can grow as much as 25 interatomic spacings (i.e. 73Å). This means that V_4C_3 particles, in excess of 146Å in diameter, will be incoherent with the iron matrix. These results clearly show the cause of the precipitated V_4C_3 particles being plate-shaped, and are in excellent agreement with those of Goldshteyn and Farber.[133] Practically determined dimensions by Tekin and Kelly[127] and Raynor, Whiteman and Honeycombe[137] of V_4C_3 particles which had precipitated at a temperature required to give optimum secondary hardening, exhibited good correlation with the calculated values of Prnka.

Smith[138] found that the peak secondary hardness in a vanadium steel was obtained after tempering at $600^{\circ}C$ for 1 hour. The microstructure of the alloy at this stage consisted of a fine dispersion of platelets of vanadium carbide, approximately 100 to 150Å long and 10Å thick and numbering about $10^{17}/cm^3$. These platelets were lying in $\{100\}$ planes of the ferrite and obeyed the orientation relationship as determined by Baker and Nutting.[112]

He was of the opinion that at peak hardness, the precipitated particles were at the size limit at which they could retain coherency with the matrix, and the formation of interfacial dislocations was just commencing. This would result in maximum interfacial strain. Tempering at $600^{\circ}C$ for 100 hours caused the particles to grow and become too large to be coherent and no dislocations were observed at the interfaces between the matrix and precipitate. These particles were spherical, and approximately 500 Å in diameter.

In fact the dislocations were held stable by the V_4C_3 particles for 50 hours at $600^\circ C$, but beyond this time the number of particles fell below $10^{16}/cm^3$, thereby allowing the dislocations to anneal out.

Smith although not completely ruling out nucleation on dislocations, held the view that vanadium carbide nucleated homogeneously in the matrix. This was contrary to the finding of Tekin and Kelly [127] and Goldshteyn and Farber [133] that the nucleation was on dislocations. Smith found some precipitated particles lined up along dislocations after tempering the alloy at $600^\circ C$, but at this temperature the dislocations would be mobile. Therefore, in attempting to move to form sub-boundaries or to anneal out, the dislocations would be held by the growing particles, and the latter would give the appearance that they had nucleated on dislocations. Particles nucleated in the matrix would rapidly be connected by dislocations, which in turn could act as paths of easy diffusion for vanadium and carbon atoms. However, both Tekin and Kelly and Smith were in agreement that vanadium carbide nucleation at high tempering temperatures ($650^\circ C$ and above) was homogeneous within the ferrite matrix.

Nishida and Tanino, [139] Goldshteyn, [140] Honeycombe [141] and Darbyshire and Barford [142] all determined that V_4C_3 particles were nucleated on dislocations at a tempering temperature which corresponded with that required to give the secondary hardening peak in vanadium steels. The last-mentioned authors could not accept the view of Tekin and Kelly [127] and Smith [134] that homogeneous nucleation occurred at a late stage of a precipitation reaction in a

system which exhibited a marked preference for heterogeneous nucleation in the early stages.

Darbyshire and Barford considered that, at high tempering temperatures, recovery in a matrix of high dislocation density would be expected to take place. This process would be hampered by the vanadium carbide particles during the early stages of precipitation, but as these particles coarsened at later stages, would become easier. Therefore, the dislocations in their new configuration could nucleate vanadium carbide particles again. This meant that the measured rate of precipitation was the sum of that due to the continued growth of the original particles (which at this stage may not be associated with dislocations), and new growth on dislocations in their new configuration.

Whiteman and Keown [143] were of the opinion that alloy carbides (including V_4C_3) nucleated on interface dislocations at boundaries between cementite and ferrite, as well as on matrix dislocations, during tempering. The carbides nucleated at these boundaries tended to coarsen more rapidly than those nucleated on matrix dislocations.

Farber and Belenky [144] and Goldshteyn [145] both showed that vanadium additions caused structural steels to secondary harden markedly. The strengthening effect of these alloys was due to the interaction of slip dislocations with the precipitated vanadium carbide particles, which pinned the dislocations inherited from the martensite. The latter author found that adding 0.1 wt. % vanadium to these steels increased their strength by 10 to 20% without impairing ductility and toughness.

Davenport [146] undertook research to determine the cause of the 'arced' reflections of constant d-spacing in electron diffraction patterns obtained from hardened and tempered vanadium steels by Tekin and Kelly [127] and Smith. [134] The former authors deduced that these reflections came from fine V_4C_3 particles which had nucleated on dislocations. Explanation of the 'arcing' was given as being due to a misorientation of the precipitate particles associated with the region near the core of the dislocation.

Davenport showed that the 'arcing' was in fact due to diffraction from an epitaxial oxide (Fe_3O_4) layer on the foil surface. He obtained 'arced' reflections in diffraction patterns taken from vanadium steels which had been tempered at a temperature below that required for vanadium carbide precipitation. Final verification was given by a dark field taken using an 'arced' diffraction spot, and this revealed fine oxide particles.

Tanino and Sato [147] employed the slip trace method to determine the volume fraction of precipitated V_4C_3 particles as 0.184% in a vanadium steel with low carbon content, which had been tempered at a temperature necessary to give the secondary hardening peak. However, they were of the opinion that errors could be incurred in this technique by inaccurate identification of the shape of precipitates and in measurement of their size; in addition the inclination of the foil surface was very critical. Another factor was that the volume fraction or precipitated particles tended to be overestimated by the existence of strain fields and dislocations around those particles.

A good deal of interest has been shown in the secondary

hardening responses of chromium/molybdenum/vanadium steels,

as these are employed in many applications where good creep

properties are required.   Research on these alloys has

often involved the assessment of the effect of one of these

carbide-forming elements on the degree of secondary hardening

of a steel which contained another carbide-forming element.

One such piece of work was by Smith and Nutting, [121] who

determined the effect of chromium and molybdenum on the

secondary hardening response of a vanadium steel.

They used a base composition of 0.2 carbon and 0.7 wt. %

vanadium, and added in one case 0.5 wt. % molybdenum and in

the other 3.0 wt. % chromium.   The addition of molybdenum

caused an increase in as-quenched hardness of 36 V.P.N. when

compared with the steel which only had vanadium as an alloying

addition.   Furthermore, the tempered hardness of the

vanadium/molybdenum steel was between 20 and 40 V.P.N.

higher than that of the vanadium steel, after a corresponding

treatment.

This caused Smith and Nutting to draw the conclusion

that the effect of molybdenum was in strengthening the

ferrite rather than precipitation hardening.   In fact there

was no evidence of precipitated molybdenum carbide in any

of the samples, even after tempering at 700 and 750°C.

Vanadium carbide was precipitated in the vanadium/molybdenum

steel and the microstructural changes of this alloy on

tempering were the same as for the vanadium steel.   The

addition of molybdenum, however, meant that the maximum secondary hardness was attained at a slightly shorter tempering time, thereby suggesting that this element raised the diffusion rate of vanadium in ferrite.

Hardness tests on samples of the vanadium/chromium steel which had been tempered at differing temperatures revealed very interesting results. This alloy did not exhibit secondary hardening, unlike the vanadium steel, but was more resistant to softening on tempering than a chromium steel.

Tempering the vanadium/chromium steel at 600°C caused vanadium carbide to precipitate more rapidly than in the vanadium steel. Some larger precipitated carbides were present in the vanadium/chromium steel and these were presumed to be Cr_7C_3. In fact Shaw and Quarrell [148] had found that both these carbides could co-exist in this type of steel.

Seal and Honeycombe [110] found that a vanadium/chromium steel with the same carbon content as employed by Smith and Nutting, [121] but with higher chromium (9.0 wt. %) and vanadium levels (0.97 wt. %), did exhibit a small degree of secondary hardening at 560°C. However, reducing the vanadium content of this steel to 0.38 wt. % meant that the hardness peak was eliminated.

Crafts and Lamont [149] also carried out research on a series of vanadium/chromium steels, with carbon contents ranging from 0.16 to 0.28 wt.%. Three levels of chromium were used, namely 1.0, 3.0 and 5.0 wt. % whilst the vanadium ranged from 0 to 1.05 wt. %. The alloys which contained 3.0 and 5.0 wt. % chromium did not exhibit secondary hardening on tempering, irrespective of their vanadium contents.

However, those with a chromium content of 1.0 wt. % showed secondary hardening peaks at all of the vanadium levels employed (i.e. 0.29, 0.52 and 1.04 wt. %).

Baker and Nutting [112] investigated the effect on secondary hardening of a vanadium/molybdenum steel of increased molybdenum content, compared to that employed by Smith and Nutting. [121] They used the same base composition as the latter authors (i.e. 0.2 carbon and 0.7 wt.% vanadium) but increased the molybdenum level to 2.70 wt. %.

This steel had an as-quenched hardness of 415 V.P.N. and exhibited secondary hardening on tempering. The peak hardness was 506 V.P.N. and this occurred after tempering at $600^{\circ}C$ for 1 hour. This value was slightly higher than the peak hardness determined by Smith and Nutting [121] for the steel with lower molybdenum content (0.5 wt. %).

Tempering the high-molybdenum steel at $600^{\circ}C$ for 1 hour caused the cementite to re-dissolve and vanadium carbide precipitated out. Long tempering treatments (100 hours) at $650^{\circ}C$ caused large M_6C carbides to form at ferrite boundaries. These persisted along with V_4C_3, even after tempering for 100 hours at $730^{\circ}C$, as clearly shown in FIG. 19.

The addition of molybdenum to a vanadium steel did not, therefore, cause the disappearance of the secondary hardening peak as was the effect, found by Smith and Nutting, [121] of chromium addition. At low tempering temperatures, molybdenum caused solid solution hardening of the ferrite. However, molybdenum like chromium, increased the rate of softening of a vanadium steel at high tempering temperatures.

This could be explained by molybdenum causing an increase in the diffusion rate of vanadium atoms or by this element

replacing vanadium in the precipitated carbides, thereby altering the energy at the interface between the precipitated particles and ferrite.   The carbide M_6C was precipitated at high temperatures in the high-molybdenum steel and this grew rapidly, leading to the dissolution of small V_4C_3 particles and subsequent rapid softening.

Irvine and Pickering [150] found that the carbon : vanadium ratio to give optimum secondary hardening in a steel which also contained 0.5 wt. % molybdenum, was 1 : 3. Lattice parameter measurements of V_4C_3 formed in vanadium/ molybdenum steels of varying vanadium content showed considerable fluctuations with change in vanadium : molybdenum ratio.   They determined that at low vanadium levels, up to 40 at. % molybdenum was present in the V_4C_3 particles.

The importance of the carbon : vanadium ratio on the degree of secondary hardening in low alloy vanadium/ molybdenum steels was also mentioned by Crafts and Lamont [151] and Pickering. [152]   The latter author found that the time to give maximum secondary hardening was reduced by increased vanadium content in these steels.   He also determined that the addition of 0.5 wt. % molybdenum to a series of vanadium steels, with low carbon contents, caused in some cases, precipitation of $M_{23}C_6$ (i.e. in this case $Fe_{21}Mo_2C_6$) at high tempering temperatures.   This precipitate only formed in steels with vanadium contents of 0.3 wt. %, or less.   Alloys which had in excess of this vanadium level did not contain any precipitated $M_{23}C_6$, even after tempering at $700^{\circ}C$ for 100 hours.

Geller, Moiseev and Aranovich [153] carried out research to determine the secondary hardening responses in

a series of vanadium/chromium die steels. These alloys
had high carbon contents ranging from 1.07 to 1.90 wt. %,
with chromium levels between 3.2 and 13.1 wt. % and vanadium
from 0.8 to 4.3 wt. %. Secondary hardening was only obtained
in one alloy, and this had the highest carbon, chromium and
vanadium contents, whilst the other steels were very resis-
tant to softening on tempering, but not giving a hardness
peak.

Colombier and Lévêque [154] also found that the
addition of chromium reduced the secondary hardening response
of a steel which contained vanadium. They obtained marked
secondary hardening in a series of vanadium steels, with
carbon contents ranging from 0.25 to 0.91 wt. % and vanadium
levels from 1.43 to 1.96 wt. %. Peak hardness occurred
after tempering at $600^{\circ}C$ for 1 hour, and this corresponded
with the dissolution of cementite and precipitation of fine
particles of vanadium carbide. The degree of secondary
hardening was directly related to the vanadium content of
the matrix.

The addition of 4.3 wt. % chromium to a steel containing
0.41 carbon and 1.93 wt. % vanadium gave a very slight
secondary hardening peak at a reduced temperature of $560^{\circ}C$.
This steel, however, was more resistant to softening over
a wide range of tempering temperatures than a steel with
coresponding carbon and vanadium levels, but without chromium.

These authors also determined that small additions of
nickel and manganese had little effect on the secondary
hardening response of a vanadium steel. However, Suzucki,
Sato and Tanino [155] found that these elements did improve

the degree of secondary hardening in this type of steel, with nickel being the more effective.

Biswas and Seal [156] determined the effects of cobalt additions on the tempering characteristics of certain vanadium steels. These steels were of commercial purity and had carbon contents from 0.45 to 0.52 wt. %, vanadium levels between 0.12 and 0.95 wt. % and cobalt from 0 to 7.70 wt. %. The addition of cobalt to vanadium steels improved the amount of secondary hardening, this being particularly the case in alloys which contained in excess of 0.8 wt. % vanadium. In such a steel, the addition of 2.60 wt. % cobalt gave an increase in the secondary hardening peak of 2.5 HRC, but further additon of this element to 7.70 wt. % gave no more improvement in this phenomenon.

There was a difference in the mode of precipitation of V_4C_3 in the vanadium/cobalt and vanadium steels. Tempering the vanadium steel at 600°C caused V_4C_3 to precipitate in 'cloud like' clusters but these were absent in the vanadium/cobalt steel. In the latter alloy, the V_4C_3 particles appeared to nucleate homogeneously in the matrix.

Cobalt had the very useful effect of increasing the nucleation rate and retarding the growth rate of both cementite and vanadium carbide in the tempering of vanadium steels. This accounted for the excellent resistance to softening that these steels had at high tempering temperature Cementite was still present in these alloys, even after tempering for 1 hour at 650°C.

The addition of small amounts of tantalum and niobium (0.05 to 0.25 wt. %) to a 1 wt. % vanadium steel with carbon content of 0.2 wt. %, was shown to improve secondary hardening reponse by Seal and Honeycombe.[157]   These additions also had the effects of raising the temperature of attainment of peak hardness to 650°C and reducing the rate of softening at high tempering temperatures.

These authors found that tantalum and niobium entered into solid solution in the vanadium carbide and so caused lattice expansion and increased coherency stresses, the result of which was higher peak hardness on tempering. Explanation of the displacement of the hardness peak to higher temperatures was given by the fact that tantalum and niobium atoms, in both the ferrite and carbide phases, retarded the diffusion rate of vanadium atoms in and into the ferrite.   This meant that vanadium carbide nucleated at higher tempering temperatures and had a reduced growth rate, so remaining coherent with the ferrite matrix at higher temperatures than would be the case for a vanadium steel.

Transmission electron microscopy revealed that tantalum and niobium carbides both precipitated in steels which had been tempered at 700°C.   This was at too high a temperature to contribute towards the secondary hardening peak, but these carbides did help to reduce the rate of softening of these steels at high tempering temperatures.

Viswanathan and Beck [158] determined that the addition of aluminium to a low alloy steel which contained chromium, vanadium and molybdenum gave an improvement in rupture

strength at 593°C.   They were of the opinion that the
presence of aluminium in solid solution in this steel had
the effect of causing increased precipitation of vanadium
carbide during stress rupture tests at 593°C.

2.6 The Partitioning of Elements in Low Alloy Steels Containing Vanadium

2.6.1 The Composition of Primary Carbides in Low Alloy Steels Containing Vanadium

Cochnar and Cadek [159] determined the compositions of the primary carbides present in a steel of composition 0.3 carbon, 1.5 chromium and 0.15 wt. % vanadium. They electrolytically extracted the carbides and subjected the residue to chemical and X-ray analysis. Cementite was one of the carbides present and this contained small amounts of chromium and vanadium. Vanadium carbide contained 7.0 wt. % chromium and 5.7 wt. % iron, whilst the chromium carbide, M_7C_3, had a vanadium content of 6.5 wt. %.

Staska, Block and Kulmburg [160] used the electron microprobe to analyse the carbides present in a steel of composition 0.45 carbon, 5.5 chromium and 1.8 wt. % vanadium. The carbide, M_7C_3, had an analysis of 43.1 chromium, 9.8 vanadium, 40.8 iron and 6.3 wt. % carbon, whilst the corresponding figures for V_4C_3, were 4.5, 70.3, 11.2 and 14.0 wt. %. The carbon contents were determined by totalling the weight percentages of the other elements and subtracting this value from 100 wt. %.

Cochnar, Zemcikova, Freiwillig and Cadek [161] extracted and analysed vanadium carbides in equilibrium with ferrite. The steels they used had carbon contents of 0.30 wt. % and contained additions of chromium. These samples were annealed for long periods to attain an equilibrium state, this being fixed by quenching. The carbide, V_4C_3, which was in equilibrium with ferrite, contained 79 vanadium, 6 iron and up to 7 wt. % chromium. They also determined that the

distribution coefficient of vanadium (i.e. ratio of the
vanadium concentration in the carbide to that in the ferrite
matrix) decreased with increased vanadium content of the
steel. Similarly the chromium distribution coefficient
decreased with higher levels of vanadium and chromium in
the steel.

2.6.2 The Solubility of Vanadium Carbide During the Austenitisation of Low Alloy Steels Containing Vanadium

Rakhshtadt, Lanskaya, Suleimanov and Katkova [162]
determined the optimum austenitisation conditions to obtain
complete solution of vanadium carbide in a series of
vanadium steels. These alloys were of commercial purity,
with carbon contents ranging from 0.22 to 0.35 and vanadium
levels 1.20 to 1.74 wt. %. Electrical restivity and micro-
hardness measurements were made along with the employment of
optical microscopy in determining that an austenitisation
temperature of between 1130 and 1220°C, for a soaking time
of 10 minutes, was required to give complete solution of
vanadium carbide in these steels. These conditions are
very similar to those obtained by Gervasev, Vinitskii and
Goldshteyn [163] for complete solution of this carbide in
vanadium steels.

Guterman and Goldshteyn [164] attempted to determine
the effect on manganese and chromium on the solubility of
vanadium carbide during the austenitisation of commercial
purity vanadium steels. The compositions of these steels
ranged from 0.39 to 0.42 carbon, 0.23 to 1.91 manganese,
0.31 to 0.48 silicon, 0.18 to 1.87 chromium and 0.85 to

2.60 wt. % vanadium.   These alloys were austenitised at temperatures between 900 and 1250°C, followed by quenching into water.

The carbides were electrolytically extracted and the residue was subsequently analysed by chemical means. Comparison of the analysis of the extracted carbide phase with the full analysis of the particular steel allowed these authors to calculate the content of the matrix.

Vanadium carbide was shown to be very resistant to solution during austenitisation, and even soaking for 30 minutes at 1200°C did not give complete solubility of this carbide in steels which contained in excess of 2.0 wt. % vanadium.   However, the presence of manganese and chromium in the steels considerably raised the solubility of vanadium carbide in austenite, this being particularly the case with the latter element.   This effect was most marked in an austenitisation temperature range of 900 to 1000°C.   Taking as an example the austenitisation of steels with vanadium contents of 0.95 wt. %, the matrix of the vanadium steel contained 0.11 wt. % vanadium, that of the vanadium/manganese steel 0.18 wt. % whilst that of the vanadium/chromium steel 0.40 wt. % of this element.

Their results on the effect of manganese were in agreement with those of Kogan and Entin, [165] who also determined that the addition of manganese increased the solubility of vanadium carbide during the austenitisation of a steel of commercial purity.   Kogan and Entin were of the opinion that manganese weakened the bonds between vanadium and carbon atoms present in vanadium carbide. This would have the effect of making the carbide

less stable and so easier to take into solution on austenitising.

Guterman and Goldshteyn thought that chromium was having the same effect as manganese. However, chromium is a stronger carbide former than manganese, so on this basis would not be expected to weaken the interatomic forces between vanadium and carbon atoms, present in vanadium carbide, to as large an extent as would manganese. Therefore, the very marked effect of chromium in increasing the solubility of vanadium carbide during austenitisation was somewhat surprising.

These authors found that the vanadium content of the matrix was very much a function of the vanadium level of the alloy. Increasing the vanadium content of the steel from 0.9 to 2.0 wt. % caused a doubling of the vanadium matrix level after austenitising the alloys at all the temperatures employed, and subsequent quenching.

Gervasyev, Goldshteyn, Panfilova and Rudenko [166] also deduced that the addition of chromium to vanadium steels had the effect of increasing the dissolution rate of V_4C_3 during austenitisation. The reason which they presented for this phenomenon was that chromium reduced the thermodynamic activity of carbon in austenite, thereby assisting the transfer of carbon from V_4C_3 to the solid solution. This, therefore, increased both the dissociation rate of the carbide and the diffusion rate of vanadium atoms from the carbide to austenite.

3. Experimental Procedure

3.1 Manufacture of the Alloys

3.1.1 Melting of the High Purity Steels

The alloys were melted in a high frequency induction furnace under vacuum. A pre-formed magnesia crucible was used, and this was washed out with high-purity molten iron before the melting was commenced. This was to avoid contamination of the alloys from previous melts which had been made in the crucible.

All these alloys contained iron, carbon and vanadium. but seven of them also had a fourth element present. When these steels were melted, a wash-out melt with molten iron was carried out between each melt, to prevent any contamination of the following melt by the additional element present in the preceding alloy.

The materials used in the melting were all of high purity, and can be listed as follows:-

1. Japanese Iron (low oxygen content).

2. Carbon (as Graphite).

3. Vanadium.

4. Silicon.

5. Manganese.

6. Nickel.

7. Cobalt.

8. Molybdenum.

9. Chromium.

10. Tungsten.

The vanadium was of 99.97% purity. which is a very high level for this metal. This was achieved by triple electron beam refinement of the metal. The impurities present were aluminium and silicon, and these can be as high as 2 to 3 wt. %

in ferro-vanadium, which is the normal source of vanadium in alloy steelmaking.

The additions to the melt were calculated on the basis of 100% yield, using a charge weight of 4 kg. Melting down was carried out under an argon atmosphere, at a pressure of 33 KN/m^2. All the additions to the melts were made during this period, with the exception of manganese. When each charge was molten, the pressure was reduced to 40-70 N/m^2 and held at this value for approximately 10 minutes.

The pressure was then increased to 33 KN/m^2 and it was at this stage that manganese was added to the melt. This metal has a high vapour pressure, and so addition of it, along with the other elements in the early stages of melting would cause considerable manganese loss due to evaporation.

Each charge was cast at 1550°C, at a reduced pressure, into a cast iron ingot mould of cross section 6.0 cm square. These ingots were allowed to remain under vacuum until they had completely cooled. The full analyses of these alloys are given in TABLE 6.

3.1.2 Melting of the Commercial Purity Steels

Commercial purity vanadium steels are the vanadium steels which are produced by normal industrial steelmaking practice. Alloying additions employed in the commercial purity steels melted in this research were the same as would be employed in industrial steelmaking. The elements silicon, manganese, sulphur and phosphorus were at levels which would approximate to those generally expected in industrially melted steel. Aluminium and nitrogen were present in some

of the steels as alloying additions, but the presence of chromium and molybdenum were only as impurities.

These alloys were air melted in a high frequency induction furnace. The furnace lining was Thermax G10, which consisted of magnesite 84.6, CaO 2.0, Al_2O_3 10.0, FeO 1.4 and SiO_2 2.0 wt. %. The materials used in the melting were as follows:-

1. Swedish Iron.
2. High Carbon Ferro-Manganese.
3. Low Carbon Ferro-Manganese.
4. High Nitrogen Ferro-Manganese.
5. Ferro-Silicon.
6. Ferro-Vanadium.
7. Aluminium.

The iron was melted in the furnace and then aluminium, ferro-silicon, ferro-manganese and ferro-vanadium were added to make up a charge weight of 15kg. Each charge was cast at $1580^{\circ}C$ into a cast iron ingot mould of cross section 7.6 cm square. The full analyses of the air melted steels are given in TABLE 7.

All the steels had low carbon contents and the levels of this element and manganese were controlled by adjusting additions of high and low carbon ferro-manganese to give desired values. Some of the steels had high nitrogen contents and these were achieved by additions of high nitrogen ferro-manganese, which contained 5.81 wt. % of this element. In these cases, the additions of high and low carbon ferro-manganese were adjusted to take into account the increased manganese level of the melt due to addition of high nitrogen ferro-manganese.

Aluminium was used for deoxidation but additional amounts of this element were required in some of the alloys. In such

cases, calculation of the aluminium addition had to take into account the relatively high aluminium content of the ferro-vanadium (2.2 wt. %). The ferro-vanadium also contained 1.2 wt. % silicon, so additions of ferro-silicon had to be modified to accommodate this extra silicon addition.

3.2   Processing of the Ingots

The ingots were given a stress-relieving anneal at 800°C
for 6 hours to remove any stresses inherent from casting.
In order to prevent decarburisation, the ingots were coated
with Berkatekt (hydrocarbon based solution) prior to annealing.
The surfaces of the ingots were then planed, so as to remove
any surface defects.   Furthermore, the piping formed during
solidification was cut from the top of each ingot.

The high purity steels were forged from 6.0 cm. square
section size to 1.9 cm. square bar, a reduction in area of
90%.   These alloys were heated to 1050°C in a controlled
atmosphere furnace prior to forging.   This furnace atmosphere
had a very low oxidising potential in order to prevent de-
carburisation.   Each ingot required at least one reheat before
the desired section size was obtained.   In fact the vanadium/
chromium steel was very resistant to deformation and needed
four reheats to produce 1.9 cm^2 bar.

Steels of commercial purity were given the same amount
of reduction (90%) on those of high purity.   These alloys,
therefore were forged from 7.6 cm. square section size to 2.4 cm.
square bar.   Forging was carried out at 1100°C after heating
the ingots in a controlled atmosphere furnace.   Only one
reheat was necessary for each ingot in order to obtain the
desired section size.

All the bars were given a sub-critical anneal at 700°C
for 8 hours after forging.   The bars were coated with
Berkatekt and packed in steel tubes to prevent any decarburi-
sation.   The ends of these tubes were sealed with fireclay.
At this temperature, decarburisation would only be very slight,
even without taking any precautions against its occurrence.

However, in this research, the losses of small amounts of surface carbon could be detrimental to accurate hardness measurements.

The high purity steel bars were cut by mechanical saws into pieces of 3mm. thickness. This sample thickness was ideal for X-ray diffraction and allowed easy cutting of hardened samples for optical microscopy and electron probe microanalysis. Several samples of 1mm. thickness were cut from each bar. These were to be used to make thin foils for transmission electron microscopy.

3.3 Carburisation of the Commercial Purity Steels

The commercial purity steels had low carbon contents of between 0.08 and 0.09 wt. %. Carburising these alloys would give a carbon gradient from edge to centre of each bar. This would allow the determination of secondary hardening responses over a range of vanadium : carbon ratios. A carbon content of between 1.2 and 1.3 wt. % at the surface of each bar was the objective for the carburisation treatment.

Bar samples were cut to suitable lengths in order to fit inside the steel boxes, which were to be used for pack carburising. A layer of activated charcoal was laid in the bottom of each box, under four pieces of bar, which were separated from each other and the sides of the boxes. The two boxes were then completely filled with activated charcoal. Lids were placed on top of the boxes and each box was made airtight by sealing the lid in position by means of high temperature cement. All gaps between the lids and sides of the boxes were completely filled with cement.

The samples were carburised at 920°C for 24 hours, with all the boxes being loaded together in one large furnace. This long carburisation time was employed in order to obtain an appreciable carbon gradient from edge to centre of each sample. After the required time at the carburising temperature the samples were allowed to furnace cool. Carbon contents are given in TABLE 8, from edge to centre, of one of the steels after carburisation. The carburised bars were then cut by mechanical saws into pieces of 3mm. thickness.

3.4 Hardening and Tempering

3.4.1 Hardening

Samples of both the high and commercial purity steels were hardened. A range of austenitisation temperatures and times were employed for the high purity alloys, and these are presented in TABLES 9 and 10, the times quoted being actual times at the austenitisation temperature. The vertical sections through the iron-carbon-vanadium system, as shown in FIG. 20, were used as a basis for deciding the minimum austenitisation temperatures to be used for the vanadium steels.

Differing austenitisation temperatures were employed for the various commercial purity steels as shown in TABLE 11 but only one austenitisation treatment was employed for each alloy. This was because these steels were only to be used for hardness determinations and metallographic examination . Deciding on the optimum austenitisation conditions for each alloy was difficult owing to the considerable carbon gradient from edge to centre of these samples. However, the ideal austenitisation conditions which were determined for the high purity vanadium steels were used as a basis for deciding the most suitable treatments for the commercial purity alloys.

Austenitisation of all the alloys was carried out in an electrically heated furnace, using an inert atmosphere of argon to prevent decarburisation. The furnace was purged with argon for 15 minutes prior to the samples being inserted and this gas was passed through the furnace for the entire duration of austenitisation.

Four samples were loaded into a small steel tray, care being taken that these samples did not overlap each other,

as this could affect the quenching rate in localised areas.
The furnace was allowed to stabilise at the desired tempera-
ture for at least 30 minutes before the samples were inserted.
Furnace temperature control was by means of thyristors and
this resulted in only small temperature fluctuations ($\pm$ 4°C)
once the furnace had sufficient time to stabilise at the
desired temperature.

Temperature measurements were obtained by means of a
chromel-alumel thermocouple connected to a potentiometer, with
cold junction compensation being taken into account.   The end
of the thermocouple was placed inside the tray containing the
specimens, so that the actual temperature of the latter was
measured.   The specimens were water quenched after the required
time at the particular austenitising temperature.   This
procedure was the same for the hardening of all the alloys.

3.4.2   Tempering

The hardened alloys were all given identical tempering
treatments.   With the exception of those to be given long-
term treatments, each sample was given a single temper for
1 hour, the following temperatures being employed:-

100, 150, 200, 300, 400, 500, 550, 560, 580, 600 and
700°C.

High purity steels, in the as-hardened condition, had
been subjected to optical metallographic examination, in order
to determine the optimum austenitisation conditions for each
alloy.   Only samples which had been given ideal austenitising
treatments were tempered, for steels which contained vanadium
and a second alloying addition.

However, samples of the high purity vanadium steels, which

had been austenitised at temperatures either below or above that ideally required for each particular alloy, were tempered along with those which had been austenitised under optimum conditions. This was in order to determine the secondary hardening responses of vanadium steels which were either underhardened or overheated, and also to assess the effect of vanadium matrix content on these responses.

The high and commercial purity steels were also given long-term tempering treatments at the temperature where secondary hardening was expected to commence in these alloys (i.e. 560°C). This was in order to determine the variation in hardness and microstructure with time at this tempering temperature. Tempering times employed ranged from 2 to 220 hours. Only samples which had been austenitised under ideal conditions were used for long-term tempering.

Samples of high purity alloys, which were to be used to make thin foils for examination by transmission electron microscopy, were tempered at temperatures ranging from 560 to 700°C, for times varying from 1 to 100 hours. Generally, only specimens which had received optimum austenitisation treatments were employed.

Low temperature tempering (i.e. 100 and 150°C) was carried out in an oil bath. The samples were loaded inside small wire baskets, which were immersed into the oil bath when this had stabilised for 15 minutes at the desired temperature. Temperature readings were taken by means of a thermometer immersed in the bath, and these were found to vary by $\pm$ 2°C during the treatments.

Salt baths were employed for all the other tempering treatments. Samples were tied onto lengths of stainless steel wire, and these were immersed into a salt bath, which had been allowed to stabilise for 1 hour at the required temperature. The tempering temperatures fluctuated by $\pm 2^\circ C$ during these treatments.

Temperature measurements were obtained by means of a chromel-alumel thermocouple connected to a potentiometer. This thermocouple had an alloy steel sheathing, to prevent corrosive attack from the molten salt. The end of the thermocouple was immersed inside the salt bath, care being taken that the thermocouple did not touch the sides of the bath, as this could affect the temperature reading. Cold junction compensation for the thermocouple was taken into account for each potentiometer reading.

The tempering at 200 and $300^\circ C$ was carried out in a salt bath consisting of a mixture of sodium nitrite and sodium nitrate. For the higher tempering temperatures of 400 to $600^\circ C$ a bath containing sodium chloride and sodium sulphate was used, whilst at $700^\circ C$ a bath consisting of a mixture of sodium chloride and sodium carbonate was employed.

3.5 Specimen Preparation for Optical Metallography

Samples of each high purity alloy in the as-cast, forged, annealed, as-hardened and hardened and tempered conditions were prepared for metallographic examination. Similarly, specimens of the commercial purity steels in the annealed, carburised, as-hardened and hardened and tempered states were prepared.

Longitudinal and transverse sections were cut from each specimen by means of a water cooled cutting off wheel. Only very low cutting rates were employed for samples which were either in the as-hardened condition or had been tempered at low temperatures. This was in order to keep the temperature of these specimens to a minimum (the water cooling aided this), as softening due to over tempering could occur if care was not taken during cutting.

The samples were hot mounted in bakelite, with the exception of those which either had been tempered at 100 or 150°C or were in the as-hardened condition. These specimens were cold mounted, to ensure that no slight degree of softening due to the temperature of hot mounting, took place.

The mounted specimens were prepared on a series of emery grinding papers, from 150 to 600 mesh. Final preparation was carried out on diamond impregnated polishing wheels, graded from 6 to $\frac{1}{4}$ micron. All the polished samples were etched in 2% nital solution.

3.6 Optical Metallography

The whole series of samples was examined by means of an optical microscope. Metallographic examination was carried out at magnifications ranging from x150 to x320. Photographs of the microstructures were taken using a Zeiss Ultraphot Microscope.

3.7 Grain Size Determination

Assessment of the prior austenite grain sizes of the high purity steels was made by comparison with standard A.S.T.M. grain size charts. This technique was suitable because the grains were quite uniform in size for each alloy.

Some difficulty was experienced in detecting the grain boundaries in these steels, in the as-hardened condition. Only in samples which had been austenitised at very high temperatures, and hence in which some grain growth had occurred, could the prior austenite grain boundaries be observed after etching. However, tempering the alloys revealed the prior austenite grain boundaries more readily, and so some of the grain size assessments were made after this treatment.

3.8 Quantitative Metallography

3.8.1 Determination of the Volume Fraction of Graphite

Very surprisingly, graphite formed in some of the high purity steels during long term tempering at $560^{\circ}C$. Point counting was carried out to determine the volume fraction of this phase in each specimen. An optical microscope was employed for this, with a magnification of X600 being used for all the counts. The grid consisted of two very fine wires, mounted at right angles to each other in the eyepiece of the microscope.

The sizes of the graphite rosettes ranged from 2 to 10 μm diameter in the various alloys. A stage traverse of 20 μm was employed for each count, as it was important that this value exceeded the largest size of the graphite rosettes, if maximum accuracy was to be attained. A total of 1200 point counts were taken on each specimen in order to obtain the desired accuracy and confidence level from the results.

3.8.2 Determination of the Volume Fraction of Primary Carbides

The primary carbides had diameters ranging from 0.5 to 5 μm in the various high purity steels. Determination of the volume fraction of this phase by means of an optical microscope was difficult, owing to the very fine nature of some of the carbides. It was, therefore, decided to use an electron microscope for this work.

Samples of the high purity steels, in the as-hardened condition, were prepared in exactly the same manner as those for optical metallographic examination, with one additional process. These specimens were etched in 2% nital solution,

followed by the extra operation of coating with carbon.
This latter operation was achieved by arcing between two
graphite electrodes, which were situated directly above the
samples (three samples were coated at one particular time).
A total coating time of 4 seconds, achieved by two bursts of
2 seconds duration, was found to give an ideal thickness of
deposit. The operation was carried out under vaccuum.

A grid was inscribed on the surface of each of the coated
samples by means of a scalpel. The sample was then immersed
in 6% nital solution. Two electrodes, which were connected
to a Polaron power supply source, were also immersed in this
solution, with the end of the anode being in contact with the
specimen. The extraction of the replicas was carried out at
a voltage of 25 volts and a current of 15 milliamps.

Extraction of the replicas was completed by immersing the
sample in methanol and water respectively. The effect of
surface tension caused the replicas to open out fully in the
water. These replicas were then caught on copper grids and
allowed to dry before being inserted in the specimen holder.

The microscope used was a J.E.M. 50 Superscope. This is
a small electron microscope, which is capable of attaining a
magnification of x4000. A grid was made, with the same
diameter as the microscope screen, from thin, transparent
plastic sheet. On this grid were drawn lines at right angles
to each other, giving a total of 45 points of intersection.

Point counts were carried out on 89 different fields,
giving a total number of 4000 points actually counted, thereby
giving the required accuracy and confidence level. A magnifica-
tion of x2000 was employed, this being adequate to readily
resolve the fine primary carbides which were present in these
alloys.

3.9   Hardness Testing

All the samples were hardness tested by means of a Vickers Pyramid Hardness Machine.   These tests were carried out on mounted polished specimens.   The load employed was 30kg., the only exception being for samples which had been carburised, in which case the load was 5kg.   This lighter load was utilised in order that accurate hardness tests could be attained at specific carbon contents within the carburised cases.

The load of 30 kg. was selected, as being the heaviest load (with resultant greatest accuracy) which could be employed for the softer samples, whilst maintaining the requirements of British Standard Number 427:   Part 1 for this type of hardness test.   These stipulations were that the thickness of the test piece should be at least 1.5 times the diagonal of the indentation and that the distance between the centre of any indentation and any edge of the test piece, or edge of any other indentation, should be not less than 2.5 times the diagonal of the indentation.

These requirements must be met if maximum accuracy is to be achieved, that is, if impression distortion and hence inaccuracies in the measurements of the lengths of the diagonals are to be avoided.   The hardness values were calculated by taking the average of five impressions on each specimen.

3.10   The Determination of Retained Austenite

The X-ray diffraction technique was employed for the determination of retained austenite, being the most suitable for this purpose.   Basically, this is due to there being a direct relationship between the amount of each phase present and the intensity of its X-ray diffraction pattern, for a steel consisting of martensite and austenite.   Austenite and martensite have different crystal structures (face centred cubic and very slightly distorted body centred tetragonal respectively) and these have high symmetry, so the X-ray patterns consist of relatively few lines.   The majority of these lines are widely separated and can be measured without interference with each other.

The decision was to use a molybdenum tube for this work as this had more suitable overall properties than chromium, cobalt or copper.   The molybdenum tube gives a high output, low absorption and fluorescence, relatively deep sample penetration and permits the use of several martensite and austenite peaks.

Retained austenite determinations were carried out on samples of the high purity alloys, in the as-hardened condition. The specimens were all 1.9 cm. square by 3mm. thickness, and were wet ground to remove any very slight amounts of scale or decurburisation.   These samples were then etched in 6% nital solution to remove any surface stress effects incurred from grinding.

A Siemens Kristalloflex 4 X-ray diffractometer was employed for this work.   The main scans were carried out using a specimen rotation speed of 1°/min. and a chart speed of 1cm./ min., the radiation being molybdenum K_{α}.   Other conditions employed were a voltage of 50 kilovolts, current 18 milliamps,

sensitivity 400 impulses/sec., along with an aperture of $\frac{1}{2}^{O}$ divergence and a 0.4mm receiving slit. Monochromatic radiation could be approached by the use of pulse height analysis and appropriate filters.

Higher sensitivity conditions were used to scan through angles where austenite peaks should occur. For these scans the sensitivity was 1×10^{2} impulses/sec., with zero suppression being necessary in some cases. A specimen rotation speed of 0.25^{O}/min. was employed, but the chart speed, aperture, receiving slit, voltage and current were the same as for the main scans. Both the main and high sensitivity scans were carried out with the specimen spinning.

3.11   Phase Analysis by Means of the Electron Microprobe

The electron microprobe was ideal for the phase analysis of these alloys.   Some of the primary carbides were of a sufficiently large size to be analysed with a high degree of accuracy.   In addition, a considerable number of matrix areas could be analysed in each specimen, thereby appreciably reducing the errors which could be incurred.

Phase analysis was carried out on samples of the high purity steels, in both the annealed and as-hardened conditions. These latter samples had been austenitised over a range of temperatures, and in some cases, for differing times. Specimens 6mm long by 3mm thickness, were cut for microanalysis by means of a water cooled cut-off wheel.

All the specimens were hot mounted in bakelite at a temperature of $130^{o}C$ and a pressure of 0.25 kg/mm^{2}.   Using both a low mounting temperature and pressure meant that the bakelite did not fully cure, but was sufficiently strong to hold the samples during preparation.   The method of preparation was exactly the same as for samples required for optical metallography, with a $\frac{1}{4}$ micron finish being produced.   The specimens could be easily removed from the soft bakelite mounts and were then washed and dried.   A brass specimen holder was used, as these alloys did not contain copper or zinc.

In order to obtain the greatest accuracy in the micro-analysis results, the pure metal standards required were removed from the specimen table and polished on the $\frac{1}{4}$ micron wheel.   This was to ensure that the standards had good surface finishes, as the presence of fine scratches could cause in-accuracies in the results.

The analysis was carried out by means of a Cambridge X-ray Scanning Microanalyser, Mark 2A. This instrument employs the Castaing technique of microanalysis, which consists essentially of spectrographic analysis of the X-ray emission excited from a small point on the surface of a specimen by a finely focussed beam of electrons. A tungsten filament, heated in a vacuum, acts as a source of electrons, which emerge from a triode electron gun as a divergent beam.

The basic operational conditions of the microprobe were the same for each specimen. These consisted of a gun potential of 25 kilovolts, beam current 5×10^{-5} amps, take-off angle 20°, and probe current 1.6×10^{-7} amps, with a beryllium window being used. The coolant gas employed consisted of a mixture of 97% argon and 3% carbon dioxide. It was essential to maintain the probe current constant at the stated value when counts were being taken, as variations in this could lead to inaccuracies in the results. After each specimen change, the divergent beam was accurately re-focussed into a spot, of approximately 1μm in diameter at the surface of the specimen.

Microanalyses for vanadium, iron, manganese, nickel, chromium, cobalt and tungsten were carried out using a lithium fluoride crystal in the spectrometer. In each instance first order $K\alpha_1$ radiation was selected by the crystal, with the exception of tungsten, in which case the radiation was first order $L\alpha_1$.

The atomic numbers of silicon and molybdenum were such that these elements were not suitable for analysis by means of a lithium fluoride crystal. Silicon radiation could not be selected by this crystal and only second order $K\alpha_1$ radiation

could be selected for molybdenum. Therefore, a P.E.T. crystal was employed for the analysis of these two elements, as this was capable of selecting first order radiation ($K\alpha_1$ for silicon and $L\alpha_1$ for molybdenum), thereby allowing a higher degree of accuracy to be attained in the results.

Analysis for carbon could not be carried out on this microprobe. Carbon has a low atomic number and hence a high Bragg Angle. These characteristics mean that carbon radiation has a low intensity and is very difficult to detect. A considerable amount of this radiation would be absorbed by the specimen, with a small quantity being absorbed even by the beryllium window.

Only carbides with diameters in excess of 3μm were analysed, otherwise errors would be incurred, as determined in the early stages of this research. This was because the beam either overlapped or penetrated beneath small carbide particles, (the depth of penetration of the electron beam was $\frac{1}{2}\mu$m). Both these phenomena would lead to counts being obtained from the area surrounding the carbide, as well as from the carbide itself.

The carbides were readily detected on the X-ray image, when the analysing crystal in the spectrometer was aligned to the required angle to select the radiation from the particular carbide forming element. In addition, the carbides could be observed on the electron image, which was formed from back-scattered electrons.

Photographs were taken of carbides on the electron image and of the distribution of each element between the matrix

and carbides on the X-ray image.   The magnifications of the

photographs ranged from x 1100 to x 3000.   Pulse height

analysis was employed for the X-ray image photographs, in

order to eliminate the background radiation.

Twenty matrix areas were analysed in each specimen.

The object of this large number of analyses was to achieve

a high degree of accuracy in the results.   Counts were only

taken on areas where there was no interference radiation from

carbides.   Such areas were ascertained by observing the number

of radiation pulses for vanadium whilst very slowly moving

the specimen.   The minimum values shown on the pulse monitor

were counts from true matrix areas where the electron beam

was not in contact with any carbide particles.   For the alloys

which contained molybdenum, chromium and tungsten, care was

also taken that the electron beam was not in contact with the

carbides of these elements when matrix analyses were carried

out.

The analysing crystal was not just set at the Bragg Angle

of a particular element, the analysis for which was required.

Instead, for each analysis, the crystal was slowly rotated

through the Bragg Angle until the maximum level of radiation

was observed on the pulse monitor for the desired element.

This meant that optimum selection of the required radiation

was being made by the analysing crystal.   Counts were then

carried out with the crystal set at this angle.

For the analysis of every element, two counts were taken

of duration 10 seconds each, this being also the case for

the standards.   Average values between the two count rates

were then calculated.   Counts were always made on the required

standards after all the analyses had been completed on each
specimen.   This was in order to ensure the highest degree
of accuracy, as the amount of radiation from the standards
can vary fractionally over a period of time, due to very slight
variations in operating conditions.

The background radiation was measured for each element
in the steel and also for the standards.   These counts were
taken at angles approximately 2° from either side of the
angle where peak radiation was being selected by the analysing
crystal for the particular element.   For alloys which contained
two elements with similar Bragg Angles (e.g. iron and cobalt),
only one background count was made for each of these elements,
as the second count would be very close to the Bragg Angle
of the other.

Two corrections were made to the results obtained from
the microprobe.   The first of these was to the count rates,
as the dead time correction of the counter must be taken into
account.   Standard tables were used to obtain this correction,
which was quite appreciable at high count rates.   This
statistical value was added to the measured count rate.

The other correction was to the actual calculated analysis
results.   This took into account the absorption of X-ray
emission of an element by the specimen itself.   Standard
graphs were employed to determine the effect that other elements
present in each steel, had on the absorption of X-ray emission
of the element for which analysis was required.   The elements
with high densities absorbed some of the radiation of those
with lower values of this physical property.

3.12   Transmission Electron Microscopy

Samples of the high purity alloys, which were to be used to make thin foils for transmission electron microscopy, had a thickness of 1mm.   Most of these specimens were in the hardened and tempered condition, but some were also in the as-hardened and hot worked states.

The thickness of each of these samples was reduced to 0.5mm by grinding on emery papers.   Discs of 3mm diameter were then punched from every sample.   The punch employed for this purpose had a tungsten carbide tip.   These discs were further ground on 400 mesh emery paper to a thickness of 0.25mm.   For this purpose, the discs were held in a special clamp, which had an orifice 3mm in diameter, and so was ideal for keeping the samples flat during grinding.

During both grinding operations, it was ensured that equal amounts were removed from both ground faces, by checking dimensions with a micrometer.   This was done to remove any very slight amounts of scale or decarburisation from the surfaces of the discs.

Thin foils were produced by means of a Struers Automatic Foil Unit, which allowed thin foils of good quality to be obtained due to the current cutting out as soon as the disc perforated.   The electrolyte employed consisted of a mixture of 940ml acetic acid and 60ml perchloric acid, this being maintained at 15°C by means of water cooling.   In addition, the voltage used was 65 volts, along with a current of 14 milliamps and a low electrolyte flow rate.

These conditions gave excellent polishing of the discs and caused performation in approximately 5 minutes.   This

was a sufficiently long time to allow a considerable amount
of uniform thinning in the area adjacent to the hole, thereby
giving a large region to be examined by means of the electron
microscope.

Precautions had to be taken to prevent the thin foils
oxidising if these were being kept in excess of 1 day. The
thin foils were placed in small, sealed sample bottles, which
contained anhydrous methanol, and were refrigerated at $-75^{\circ}C$.

Examination of the thin foils was carried out by means
of a J.E.M. 100B transmission electron microscope. All the
thin foils were examined under bright field conditions and
photographs taken of interesting features in the structures.
The magnifications employed ranged from x30,000 to x100,000.
A small number of bright field photographs were also taken
from extracted carbon replicas, prepared from high purity
alloys in the hardened and tempered condition.

Diffraction patterns were taken from primary and precipi-
tated carbides, and from matrix areas. The camera length
employed in each case was 40cm. Periodically, a diffraction
pattern was taken from a pure aluminium sample, in order to
allow the camera constant to be accurately calculated.

Dark field electron microscopy was also carried out,
using reflections from precipitated carbide particles. This
allowed the other precipitated particles, of the same composi-
tion and orientation as the carbide which was giving the
reflection on the diffraction pattern, to be shown in the dark
field. The distribution of these precipitated particles
could then be readily observed.

Photographs were taken of some of the dark fields, showing the distribution of precipitate particles, and in each case a bright field photograph was taken, at the same magnification, of the corresponding area. This readily illustrated which particles were showing on the dark field.

3.13   Scanning Electron Microscopy

The object of employing this technique was to confirm whether the phase which formed during long term tempering some of the high purity steels, was in fact graphite.   A sample (Alloy 1 after tempering for 220 hours at $560^{\circ}C$) in which this phase was observed by means of optical metallography was used for E.D.A.X. (energy dispersive analysis of X-rays) analysis on a FSEM 500 electron microscope.   The specimen had been hot mounted and prepared in the normal manner as for subsequent optical metallography, with the etchant used being 2% nital solution.

X-ray maps were obtained for iron and vanadium on fields showing the particles in question.   This allowed confirmation to be attained as to the identity of the dark phase, which could be observed in some of the steels, during optical metallography in the unetched condition.

CHAPTER 4

4. Experimental Results

4.1 Optical Metallography

4.1.1 Examination in the as-Cast Condition

4.1.1.1 The High Purity Steels Containing Only Vanadium as an Alloying Addition

Each of these alloys had a structure consisting of ferrite, pearlite and vanadium carbides. In Alloy 1 (0.39 wt. % vanadium) the carbides were present as a grain boundary network (FIG. 21). The ferrite grain size was quite coarse and the pearlite was difficult to resolve at low magnifications.

The ferrite grain size of Alloy 2 (0.79 wt. % vanadium) was finer than that of Alloy 1. In addition, the former alloy contained more vanadium carbide but less pearlite than the latter. These factors were even more pronounced in Alloy 3 (1.62 wt. % vanadium), the microstructure of which is shown in FIG. 22. This alloy had a very slightly dendritic structure, and once again the pearlite was difficult to resolve at low magnifications.

4.1.1.2 The High Purity Steels Containing Vanadium and a Second Alloying Addition

The microstructures of these steels all comprised of ferrite, pearlite and a carbide phase. This primary carbide was entirely vanadium carbide in the alloys which did not contain another carbide forming element apart from vanadium. However, in the steels which contained molybdenum, chromium or tungsten, the carbides of these elements were also present along with vanadium carbide. A point which should be made here, is that designation of steels in this series is by the

second alloying addition, which is given in brackets after the alloy number.

There were two major differences in the structures of these alloys. The first of these concerned the amount of pearlite which was present, this being lower in the steels where the additional element was a carbide former (Alloys 5(Mo), 8(Cr) and 10(W)). This is clearly illustrated for Alloy 10(W) in FIG. 23. However, Alloys 4(Si), 6(Mn), 7(Ni) and 9(Co) had structures consisting of quite appreciable quantities of pearlite, as shown in FIG. 24 for Alloy 9(Co).

The second difference was in the shape of the carbide phase present in these alloys. In the steels which contained tungsten and molybdenum, the carbide phase was in the form of a skeleton type of network, as shown for Alloys 10(W) and 5(Mo) in FIGS. 23 and 25 respectively. This was a much less pronounced form of the skeleton (or Chinese script) type of eutectic carbide which is present in high speed steels, in the as-cast condition. However, this factor was less marked in the other steels, although some irregular shaped carbides were present in these, as illustrated in FIGS. 24 and 26 for Alloys 9(Co) and 6(Mn) respectively.

Three of the steels (Alloys 4(Si), 6(Mn) and 9(Co)) had markedly dendritic structures. These are shown for Alloys 9(Co) and 6(Mn) in FIGS. 24 and 26. For all the steels, the ferrite grains were not as coarse as those in Alloy 1. The pearlite had a small inter-lamellar spacing in some of the alloys, but could be resolved at reasonably low magnifications in Alloys 5(Mo), 8(Cr) and 10(W) (i.e. the steels where the additional element was a carbide former).

4.1.2   Examination in the as-Cast and Annealed Condition

4.1.2.1 The High Purity Steels

Stress relieving some of these alloys at 800°C for 6 hours caused very little difference in their microstructures. This is clearly illustrated for Alloy 10(W) in FIG. 27, with the structure being virtually identical with that in the as-cast condition.

The exceptions to this were the four steels which had dendritic structures in the as-cast state.   Annealing these alloys caused this dendritic structure to break down.   In addition, the slow cooling rate employed during this treatment resulted in quite coarse pearlite being formed, as is shown for Alloy 9(Co) in FIG. 28.

4.1.3   Examination in the Forged Condition

4.1.3.1 The High Purity Steels

The microstructures revealed that each of the alloys had partially recrystallised on hot working.   This is shown for Alloys 9(Co) and 10(W) in FIGS. 29 and 30 respectively, where recrystallisation had clearly commenced in some of the grains. Two factors were basically responsible for the degree of re-crystallisation not being higher in these steels.   The first of these was the quite rapid cooling rate of the bars after hot working, whilst in addition, the amount of reduction had been quite low.

Longitudinal sections of these steels showed the carbides strung out in the direction of working, as illustrated in FIGS. 29 and 30.   The skeleton type of carbide network which was present in Alloys 5(Mo) and 10(W) in the as-cast condition,

had been broken up by hot working.

4.1.4   Examination in the Annealed Condition

4.1.4.1 The High Purity Steels

In the annealed condition, the steels all had structures consisting of primary carbides, spheoridised cementite particles and ferrite.   The pearlite which was present in these alloys prior to annealing, had transformed into very fine cementite particles and ferrite.   This is illustrated for Alloys 9(Co) and 10(W) in FIGS. 31 and 32 respectively.

4.1.4.2 The Commercial Purity Steels

These alloys had structures consisting of ferrite grains and vanadium carbides, pearlite not being present owing to the very low carbon contents involved.   Very marked grain growth had occurred during the annealing of Alloys 11 and 15 (0.06 and 0.05 wt. % vanadium respectively), as shown for the former steel in FIG. 33.

However, this was not the case for the other alloys, which all had quite fine ferrite grain sizes, as illustrated for Alloy 14 (1.11 wt. % vanadium) in FIG. 34.   These other steels all contained more vanadium than Alloys 11 and 15 and hence greater quantities of vanadium carbide.   The presence of this stable carbide would pin the ferrite grains during annealing and thereby prevent grain growth.

4.1.5   Examination in the Carburised Condition

4.1.5.1 The Commercial Purity Steels

The microstructures of these alloys after carburisation comprised of appreciable quantities of pearlite.   This is

illustrated for Alloy 14 in FIG. 35, this being the structure at a distance of 2mm. from the outer surface of the sample. Ferrite and vanadium carbides were also present in the microstructure.

With increased distance from the outer surface of each specimen, the amount of pearlite diminished. This is shown for Alloy 14 in FIG. 36, at a depth of 3mm. from the outer surface of the sample. In all cases, the pearlite was very fine and difficult to resolve. The case depths of all the alloys were quite consistent at a value of 4mm., the core structures being ferritic.

4.1.6 Examination in the as-Hardened Condition
4.1.6.1 The High Purity Steels Containing Only Vanadium as an Alloying Addition

Each of the alloys, in the as-hardened condition, had a martensitic structure. Even austenitising at the lowest temperature employed (i.e. 850°C) and subsequent water quenching, produced this type of structure in these steels. This is illustrated in FIG. 37 for Alloy 2. The martensite which formed after a low temperature austenitisation treatment was very fine.

The optimum austenitisation condition for each alloy was ascertained by the coarseness of the martensite which formed and the grain size of this phase, this being classed as a commercially ideal structure. In the case of Alloy 1, the ideal treatment was soaking for 20 minutes at 920°C, the microstructure being produced after water quenching is shown in FIG. 38. Higher austenitising temperatures than this caused a marked coarsening of the martensite in the steel,

and at temperatures in excess of $1040^{\circ}C$, very appreciable grain growth occurred. The structure of this alloy, after austenitisation at $1150^{\circ}C$ for 20 minutes, is illustrated in FIG. 39.

The other steels, which both had higher vanadium contents than Alloy 1, required higher austenitisation temperatures to produce ideal as-hardened microstructures. A temperature of $1000^{\circ}C$ was needed for Alloy 2 and $1120^{\circ}C$ for Alloy 3 (in each case the soaking time was 20 minutes) to give these optimum microstructures, as shown in FIGS. 40 and 41 respectively.

Austenitisation of Alloy 2 at temperatures in excess of $1000^{\circ}C$ resulted in an appreciable coarsening of the martensite, and a considerable increase in the prior austenite grain size occurred at above $1080^{\circ}C$. The as-hardened structure of this alloy, after austenitisation at $1150^{\circ}C$ for 20 minutes is shown in FIG. 42.

However, the martensite in Alloy 3 was considerably more resistant to coarsening than that present in the other two steels. This is illustrated in FIG. 43, which shows that the structure of this alloy in the as-hardened condition, after austenitisation at $1150^{\circ}C$ for 20 minutes, was only slightly overheated. An austenitisation temperature of between 1160 and $1180^{\circ}C$ was required before appreciable martensite coarsening and grain growth took place in Alloy 3.

The primary carbides present in these steels were fine, and longitudinal sections revealed the directionality of these due to hot working. As would be expected, the volume fraction of carbides in these alloys in the as-hardened condition, increased with a rise in vanadium content of the steel. This

is illustrated in FIGS. 37 to 43, with the volume fraction of carbides being greatest in Alloy 3, and least in Alloy 1, after corresponding austenitisation treatments.

Increasing the soaking time from 20 to either 30 or 45 minutes made virtually no difference to the microstructure, except in the cases of specimens which had been austenitised at temperatures in excess of $1100^{\circ}C$. However, even at these high austenitisation temperatures, the increased soaking times only caused slight changes in the structures. This is illustrated for Alloy 3 in FIGS. 43 and 44, which are the structures after austenitising at $1150^{\circ}C$ for 20 and 45 minutes respectively, and subsequent quenching. The longer time caused slightly more pronounced overheating than the shorter treatment, this being shown by an increase in both grain growth and martensite coarseness.

4.1.6.2   The High Purity Steels Containing Vanadium and a Second Alloying Addition

These steels had very similar microstructures to Alloy 3 after corresponding austenitisation and quenching treatments. In addition, any differences in the structures within this series of alloys were small, after similar hardening treatments.

Austenitisation at $850^{\circ}C$ for 20 minutes and subsequent water quenching resulted in a fine martensitic structure being formed in each steel. High austenitising temperatures caused considerable increases in both the coarseness of the martensite and the prior austenite grain size. These two factors were the major considerations in deciding the optimum austenitisation treatments for these alloys.

The controlling feature for the ideal heat treatment of these steels was whether the additional alloying element was a carbide former. When this was the case, the optimum austenitisation treatment was a soak for 20 minutes at 1150°C, but where the extra element was not a carbide former this temperature was reduced to 1120°C, again for the same time.

In actual fact the overriding factor was the coarseness of the martensite, for although the steel containing silicon was resistant to grain growth at temperatures below 1170°C, the martensite was coarsening at a temperature of 1120°C, whilst the situation was reversed for the steel in which chromium was present. The structures of Alloys 4(Si) and 8(Cr) after austenitisation at 1120 and 1150°C and subsequent water quenching, are shown in FIGS. 45 and 46 respectively.

Very marked grain growth occurred in the steels containing chromium, manganese, nickel and cobalt after austenitisation at temperatures in excess of 1150°C. This was also the case for those with molybdenum, silicon and tungsten present after austenitising at above 1170°C. The structures are shown for Alloys 6(Mn) and 10(W) after austenitisation at 1200°C for 20 minutes and subsequent quenching, in FIGS. 47 and 48.

The volume fractions of carbides present in these steels were greatest for Alloys 5(Mo) and 10(W). This is illustrated for Alloys 5(Mo) and 7(Ni) in FIGS. 49 and 50 respectively, which are the as-hardened structures of these steels after austenitisation at 1100°C for 20 minutes.

4.1.6.3   <u>The Commercial Purity Steels</u>

These eight alloys consisted basically of four different vanadium levels. The only difference between each pair of steels with the same vanadium content was in their nitrogen

levels.   Microstructures of these alloys, in the as-hardened condition, were controlled by the vanadium contents, as was the case for the high purity steels which only contained vanadium as an alloying addition.

The optimum austenitisation conditions for these steels were 860°C for Alloys 11 and 15, 900°C for Alloys 12 and 16, 940°C for Alloys 13 and 17 and 1040°C for Alloys 14 and 18, in every case the soaking time being 20 minutes.   Deciding on the ideal austenitising treatments was difficult, owing to the range of carbon contents within the carburised case of each specimen.   However, the conditions quoted above are a compromise, and represent those required to ideally harden every steel at the carbon level 2mm. from the outer surface of the specimen.

There was some structural variation across the carburised case in these steels, in the as-hardened condition.   This was due to both the carbon content of the martensite and to the various degrees of hardening (i.e. whether the steel was over-heated or underhardened) at different areas within the case. These resulted in differing rates of chemical attack by the etchant, as illustrated for Alloy 17 in FIG. 51.   The darker zone is nearest to the outside surface of the specimen, being 2mm. from the edge.

4.1.7   Examination in the Hardened and Tempered Condition

4.1.7.1 The High Purity Steels Containing Only Vanadium as an Alloying Addition

Tempering of these alloys at temperatures up to 200°C caused no change in the optical microstructures, compared with

those obtained in the as-hardened condition. However, at the higher temperatures of between 200 and 400°C there was an alteration in the form of the martensite, which had a less acicular nature than that formed during hardening. This is illustrated for Alloys 1 and 3 in FIGS. 52 and 53 respectively.

For tempering temperatures up to 400°C there was very little difference between the structures of the three steels, after corresponding treatments. Increased temperatures, however, from 400 to 600°C resulted in differences in the form of the martensite, with these being very much a function of the vanadium content of each steel.

The martensite which was formed in Alloy 1, after tempering for 1 hour at 500°C, etched very rapidly and was indicative of being over tempered, as illustrated in FIG. 54. However, this phase in Alloy 3, after tempering under these same conditions, was still quite resistant to etching, and resembled somewhat the martensite present in the steel in the as-hardened condition. The structure of this alloy is shown in FIG. 55.

Tempering at 600°C for 1 hour resulted in a narrowing of the difference in microstructure, with respect to the degree of martensite tempering, between Alloys 1 and 3. In fact after tempering at 700°C, for this same time, there was very little variation in the structures of all three steels, as illustrated for Alloys 2 and 3 in FIGS. 56 and 57 respectively.

4.1.7.2   The High Purity Steels Containing Vanadium and a
          Second Alloying Addition

As was the case in the as-hardened condition, these steels all had very similar microstructures to Alloy 3 after corresponding tempering treatments. The martensite present in each

alloy was very resistant to tempering at temperatures up to, and including 500°C. This is illustrated in FIGS. 58 and 59 for Alloys 6(Mn) and 7(Ni), which had been tempered for 1 hour at 300 and 500°C respectively.

The higher temperature of 600°C resulted in the formation of a well tempered martensite, which etched quite rapidly. This is illustrated for Alloys 5(Mo) and 7(Ni) in FIGS. 60 and 61 respectively, both these steels having been tempered at this temperature for 1 hour, and is taken a stage further after treatment at 700°C for each steel, as shown for the same time at this temperature for Alloy 9(Co) in FIG. 62.

4.1.7.3   The Commercial Purity Steels

The degree of martensite tempering in these steels was difficult to ascertain, owing to the differential etching rates, caused by variation in carbon content across the carburised case. However, the variation of etching rate in this layer was less pronounced than for these alloys in the as-hardened condition. The martensite which was present in steels with the highest vanadium levels (i.e. Alloys 14 and 18), and to a lesser extent in Alloys 13 and 17, was more temper resistant than that in the other alloys.

Tempering Alloys 14 and 18 at temperatures of 600°C, and above, resulted in a considerably overtempered martensite being formed. The microstructure of Alloy 18, after tempering for 1 hour at 700°C, is shown in FIG. 63, this being at a point 1mm. from the surface of the sample.

This same phenomenon occurred on tempering the other steels at 500°C, although to a reduced extent in the cases of Alloys 13 and 17, which had moderately high vanadium contents

of 0.55 and 0.53 wt. % respectively. Illustrated in FIGS. 64 and 65 are the structures of Alloys 15 and 13 respectively, the former after tempering at 550°C for 1 hour and the latter as a result of this same time at 600°C. Both these structures are at a position 1mm. from the edge of the specimen.

4.1.8. Examination After Long Term Tempering Treatments

4.1.8.1 The High Purity Steels Containing Only Vanadium as an Alloying Addition

Long term tempering of these alloys at 560°C caused some very interesting changes in the microstructures. Tempering Alloy 1 at this temperature, for times up to 12 hours, resulted in an overtempered martensite being formed. However, increasing the time to 16 hours caused graphite to be present in the structure, as illustrated in FIG. 66. The volume fraction of graphite particles was low and these were also quite small in size, with an average diameter of 5μm.

Tempering Alloy 1 for 60 hours at 560°C resulted in a completely ferritic matrix being formed. In addition, longer times caused increases in both the volume fraction and size of the graphite particles. These three phenomena are illustrated for Alloy 1, after tempering at the longer times of 120 and 160 hours, in FIGS. 67 and 68 respectively. The graphite particles present after these two longer term tempering treatments were of the rosette form, with the average size of these after tempering for 160 hours at 560°C being 10μm in diameter.

Increasing the tempering time for Alloy 1 to 190 hours caused further growth of the graphite rosettes, as shown in FIG. 69, their average size after this treatment being 12μm.

Microscopical examination in the unetched condition also allowed the graphite rosettes to be observed, as illustrated for this steel after tempering at 560°C for 190 hours in FIG. 70.

The structures of Alloy 2, after corresponding tempering treatments, were quite similar to those of Alloy 1 with two major exceptions. In the first place, a purely ferritic matrix was not formed until a longer tempering time of 100 hours at 560°C, as shown in FIG. 71.

The second factor was the minimum time required for graphite to form during the tempering of Alloy 2 at 560°C. This was 40 hours, as illustrated in FIG. 72, and was thus considerably longer than was the case for Alloy 1. The average diameter of the graphite particles after tempering under these conditions was 3μm.

Raising the tempering times to 70 and 100 hours caused respective increases in both the volume fraction and size of the graphite rosettes, as illustrated in FIGS. 73 and 71 respectively. The average diameter of the rosettes after tempering for 100 hours at 560°C was 5μm.

Further increases in tempering time to 160 and 220 hours resulted in only marginal increases in the size of the rosettes as shown in FIGS. 74 and 75 respectively. The average diameter of the graphite rosettes after tempering for 220 hours was 6μm. There appeared to be only slight changes in the volume fraction of this phase after tempering for these longer periods.

Many of the graphite particles had formed from the stringers of primary vanadium carbides, and so had marked directionality. This indicated that some of these carbides

had transformed to graphite during long term tempering.
Growth had occurred by further diffusion of carbon into the particles.

Considerably longer tempering times were required to produce a completely ferritic matrix and for graphite to form in Alloy 3 at 560°C, than was the case for Alloys 1 and 2. The time necessary to satisfy the former requirement was 190 hours, and the structure of Alloy 3 after tempering under these conditions is shown in FIG. 76.

The minimum time needed for graphite to form in Alloy 3 was 100 hours, as illustrated in FIG. 77. These particles were quite fine, with an average diameter of 3μm. Once again some of the particles could be clearly observed to have formed from the vanadium carbides, although a number of carbides were still present in the structure.

Increased tempering times caused very little further growth of the graphite particles in Alloy 3. The microstructure of this steel, after tempering for 160 hours and 190 hours is shown in FIGS. 78 and 76 respectively. Even after the longer of these two treatments, the graphite particles had only an average diameter of 4μm.

4.1.8.2   The High Purity Steels Containing Vanadium and a
            Second Alloying Addition

Graphite did not form in Alloys 5(Mo), 6(Mn), 8(Cr) and 10(W) during any of the long term tempering treatments. This is illustrated in the cases of Alloys 8(Cr) and 10(W), after tempering at 560°C for the longest time employed (i.e. 220 hours), in FIGS. 79 and 80 respectively.

However, in the other three steels (i.e. Alloys 4(Si), 7(Ni) and 9(Co))graphite did form during tempering. The minimum tempering times, at 560°C required for this phase to form, were 120 hours for Alloys 4(Si) and 7(Ni) and 100 hours for Alloy 9(Co). Tempering these steels for longer periods resulted in increases in the size of the graphite particles. The microstructures of Alloys 4(Si), 7(Ni) and 9(Co), after tempering for 220 hours, are shown in FIGS. 81, 82 and 83 respectively. After this long term treatment, the largest graphite particles were present in Alloy 9(Co), with the average diameter of these being 5μm.

A considerable proportion of the graphite particles present in these three steels had formed from primary vanadium carbides, as illustrated in FIGS. 81, 82 and 83. This effect was particularly marked in the case of Alloy 9(Co), where the graphite particles clearly had the directionality of the pre-existing vanadium carbides. However, some primary carbides were still present in these three steels after long term tempering.

The martensitic matrices in Alloys 5(Mo), 8(Cr) and 10(W) were more resistant to tempering than those present in the other steels. Even tempering Alloys 8(Cr) and 10(W) for 220 hours at 560°C did not produce ferritic structures, as illustrated in FIGS. 79 and 80 respectively.

In the cases of the other four steels, Alloys 4(Si) and 6(Mn) contained a more temper resistant martensite than Alloys 7(Ni) and 9(Co). The microstructure of Alloy 4(Si) after tempering for 220 hours, is shown in FIG. 81, and even after this long term treatment, the matrix did not appear to be completely ferritic.

However, ferrite was formed in Alloys 7(Ni) and 9(Co) after tempering for this period at 560°C, as illustrated in FIGS. 82 and 83 respectively.

4.1.8.3   The Commercial Purity Steels

Graphite was not present in any regions of the carburised case in each of the commercial purity steels, after long term tempering treatments.   Even after tempering these steels for 220 hours, this phase had not formed, as illustrated for Alloy 18 in FIG. 84.   This microstructure was obtained at a point 1mm. from the outer surface of the specimen.

Ferrite was formed in the carburised cases of these steels, with the exception of Alloys 14 and 18, after very long term tempering treatments.   In the cases of Alloys 14 and 18, the matrix phase was still over tempered martensite, even after tempering at 560°C for 220 hours.   The microstructure of Alloy 14, after tempering under these conditions, is shown in FIG. 85, this being at a distance of 1mm. from the outer surface of the sample.

A point, however, which must be made here is that no conclusive means exists of differentiating between over tempered martensite and ferrite, by means of optical metallography, for alloy steels which have been tempered at high temperatures.   Very often, a considerable degree of over-tempering is required to determine that the matrix phase is in fact ferrite, and not a slightly tetragonal martensite.

For the sake of comparisons between the steels in this work, the etching rates in 2% nital and the acicular nature of the matrix have been employed as differentiating criteria. Results are presented later from transmission electron microscopy which clearly show the nature of the matrix phases of some of the alloys.

4.2 Grain Size Determination

4.2.1 The High Purity Steels Containing Only Vanadium as an Alloying Addition

The most marked variations in grain size, after a range of differing austenitisation treatments, was in the case of Alloy 1. Austenitising this steel at temperatures up to, and including $1000^{\circ}C$, resulted in quite a fine grain size being produced (e.g. A.S.T.M. 7 after austenitisation at $1000^{\circ}C$ for 20 minutes). However, austenitisation treatments at temperatures in excess of $1000^{\circ}C$ caused considerable grain growth in Alloy 1, with the grain size, after austenitising for 20 minutes at $1150^{\circ}C$, being A.S.T.M. 1.

Closely following Alloy 1 for the highest variations in grain size, over the various austenitisation temperatures employed, was Alloy 2. The finest grain size of this steel was after austenitising at $850^{\circ}C$ for 20 minutes (A.S.T.M.9), whilst the coarsest was A.S.T.M. 1, which was produced after a treatment for the same time, but at a temperature of $1200^{\circ}C$. Very marked grain growth occurred in Alloy 2 after austenitisation at temperatures in excess of $1050^{\circ}C$.

As a result of each corresponding austenitisation treatment, Alloy 3 had always the finest grain size of these three steels. This alloy had a very fine grain size of A.S.T.M. 11 after austenitising at $850^{\circ}C$ for 20 minutes, while even as a result of treatment at $1150^{\circ}C$ for this same time, the value was only A.S.T.M. 6. However, increasing the austenitisation temperature of Alloy 3 to $1200^{\circ}C$, did result in very marked grain growth taking place.

The effect of changes in austenitisation time on the grain sizes of these alloys was very slight. In the cases of Alloys 2 and 3, increasing the austenitising time to 30 and 45 minutes at 1000 and 1120°C respectively caused no alterations in grain sizes compared with those obtained after soaking for 20 minutes at these corresponding temperatures. Raising the austenitisation time of Alloy 1 from 20 to 45 minutes at 920°C did result in a slight increase in grain size from A.S.T.M. 8 to 7. All the grain sizes of these steels after the various austenitisation treatments, are given in TABLE 12.

4.2.2   The High Purity Steels Containing Vanadium and a Second Alloying Addition

Each of these steels had a grain size of A.S.T.M. 11 as a result of austenitisation at 850°C for 20 minutes. This was also the case, for increased austenitisation temperatures up to, and including 1000°C, with one slight exception. A very slight amount of grain growth did occur on austenitising Alloy 8(Cr) at 1000°C for 20 minutes.

Increasing the austenitisation temperature to 1050°C did cause slight grain growth in all the steels, apart from Alloys 5(Mo) and 10(W). Grain growth, however, did occur in these two steels on austenitising at 1100°C, as was also the case for the other alloys. As a result of treatment at this temperature, the grain sizes of the steels ranged from A.S.T.M. 9 to 8.

Austenitisation of Alloys 6(Mn), 7(Ni), 8(Cr) and 9(Co) at temperatures in excess of 1120°C resulted in quite appreciable

grain growth occurring, whereas this phenomenon did not take place until temperatures above $1150^{\circ}C$ were employed for Alloys 4(Si), 5(Mo) and 10(W).   All the steels had coarse grain sizes after austenitising at $1200^{\circ}C$, the value in each case being A.S.T.M. 4.   The grain sizes of all these steels are presented in TABLE 13, with the soaking time in each case being 20 minutes.

4.3. Quantitative Metallography

4.3.1 The Volume Fraction of Graphite

4.3.1.1 The High Purity Steels Containing Only Vanadium as an Alloying Addition

The graphs of volume fraction of graphite against tempering time at $560^{\circ}C$ were basically of the same form for Alloys 1 and 2, as shown in FIG. 86. Minimum times for graphite formation were 16 and 40 hours for Alloys 1 and 2 respectively. However, although there was a difference in the times required for this phase to form, the graphs for both these steels were virtually linear up to, and including, a tempering time of 120 hours. In this region the gradient of the graph for Alloy 2 was greater than that for Alloy 1.

There were considerable decreases in the gradients of both these graphs on tempering for times in excess of 120 hours. This was particularly the case between 190 and 220 hours, where the differences in volume fractions of graphite present, after these two times, were only 0.2 and 0.1% for Alloys 1 and 2 respectively. Both these steels had a volume fraction of graphite of 5.2%, after tempering for 220 hours.

The form of the graph for Alloy 3 was quite similar to those for Alloys 1 and 2, except that this was linear over the whole range of times employed, as shown in FIG. 87. A minimum time of 100 hours was needed for graphite formation to occur in Alloy 3.

In the case of this steel, there was an approximately linear relationship between the volume fraction of graphite and tempering time, for times between 100 and 220 hours. There was no decrease in gradient of the graph at very long tempering times, as was the case for Alloys 1 and 2. The

gradient of the graph for Alloy 3 was less than in the linear regions for Alloys 1 and 2.

4.3.1.2 The High Purity Steels Containing Vanadium and a Second Alloying Addition

The relationships between the volume fraction of graphite and tempering time were linear for Alloys 4(Si), 7(Ni) and 9(Co), as shown in FIG. 87. Only differences in the graphs for these steels were the gradients and minimum times required for graphite to form.

In the cases of Alloys 4(Si) and 7(Ni), the minimum time necessary for graphite formation was the same, this being 120 hours. The volume fraction of this phase, after tempering under these conditions, was 0.9% for the former alloy and 0.7% for the latter. In addition, the gradient of the graph for Alloy 4(Si) was very slightly greater than that for Alloy 7(Ni).

Graphite, however, formed in Alloy 9(Co) after a minimum tempering time of 100 hours, with the volume fraction being 1.5%. The gradient of the graph for this alloy was very similar to those for Alloys 4(Si) and 7(Ni). In fact the gradients of all these three graphs were very close to that for Alloy 3, but less than for the linear portions of Alloys 1 and 2.

4.3.2 The Volume Fraction of Primary Carbides

4.3.2.1 The High Purity Steels Containing Only Vanadium as an Alloying Addition

The relationships between volume fraction of primary carbides and austenitisation temperature for these steels are

presented in FIG. 88, with in each case the soaking time being
20 minutes.   There were some similarities between the forms
of the graphs, but also some significant differences.

In the annealed condition, the volume fraction of carbides
was greatest for Alloy 3 and least for Alloy 1.   This was
also the case after each corresponding austenitisation treat-
ment, with subsequent water quenching.

Austenitisation of these alloys at 850°C resulted in
marked decreases in the volume fractions of primary carbides
present.   This effect was most marked for Alloy 1 and least
for Alloy 3.   Increasing the austenitising temperature up to,
and including 1100°C, caused very little further decrease in
the volume fraction of this phase in each steel.   Austeniti-
sation, however, at temperatures between 1100 and 1150°C did
result in more appreciable carbide solubility, particularly
in the case of Alloy 3.

A very considerable decrease in the volume fraction of
carbides present in Alloy 3 occurred as a result of austeniti-
sation at 1200°C.   This effect was less marked for Alloy 2
and considerably less so for Alloy 1.

Increasing the soaking time for Alloy 3 to 45 minutes,
as opposed to 20 minutes, made very little difference to the
carbide content, as a result of austenitisation at any
temperature in the range 850 to 1200°C.   The relationship
between the volume fraction of carbides and austenitisation
temperature, employing the longer soaking time, is presented
in FIG. 89.

4.3.2.2   The High Purity Steels Containing Vanadium and a
          Second Alloying Addition

The forms of the graphs of volume fraction of carbides
against austenitisation temperature for these steels could
be divided into four different types.   All the graphs are
presented in FIGS. 90, 91, and 92, with in each case the soaking
time being 20 minutes.

In the first classification were Alloys 6(Mn), 7(Ni) and
9(Co).   The forms of the graphs for these steels were very
similar to that for Alloy 3.   There was an appreciable reduc-
tion in the carbide content of each of these steels on
austenitisation at 850°C, as opposed to the volume fraction
present in the annealed condition.   Increasing the austenitising
temperature, however, up to, and including 1100°C, caused
virtually no further decreases in the carbide contents of these
steels.

The solubility of the carbides did increase for each of
these steels as a result of austenitisation at 1150°C.   In
fact this effect became considerably more pronounced at the
higher temperature of 1200°C.

In the second category was Alloy 4(Si).   The relationship
between carbide content and austenitisation temperature for
this steel was very similar to those for Alloys 3, 6(Mn), 7(Ni)
and 9(Co), up to and including a temperature of 1100°C.

Austenitisation of Alloy 4(Si) at 1150°C only caused a
slight further reduction in the volume fraction of carbides,
this being less pronounced in this temperature range than for Alloys
3, 6(Mn), 7(Ni) and 9(Co).   However, on increasing the
temperature to 1200°C the converse was true, with a more

appreciable rate of carbide solution occurring in Alloy 4(Si).

The graphs of carbide content against austenitisation temperature for Alloys 5(Mo) and 10(W) had some similarities with those for Alloys 3, 4(Si), 6(Mn), 7(Ni) and 9(Co), but also some important disparities. An example of the latter category occurred as a result of austenitisation at $850^{\circ}C$. Carbide solubilities were much lower for Alloys 5(Mo) and 10(W) after this austenitising treatment than for the other steels.

There were virtually no changes in the carbide contents of Alloys 5(Mo) and 10(W) after austenitisation between 850 and $950^{\circ}C$. Raising the temperature to $1050^{\circ}C$ caused very slight increases in the solubility of this phase, this becoming more appreciable between 1050 and $1100^{\circ}C$. In the cases of Alloys 3, 4(Si), 6(Mn), 7(Ni) and 9(Co) there were virtually no changes in carbide contents in the temperature range 850 to $1100^{\circ}C$.

The rates of carbide solution, however, were greater for Alloys 5(Mo) and 10(W) than for the other steels, between temperatures of 1100 and $1200^{\circ}C$. In the case of Alloy 4(Si), though, the rate of solution of this phase was only slightly less than in these two steels in the range 1150 to $1200^{\circ}C$.

Finally, the fourth classification consisted of Alloy 8(Cr), the relationship for which in the temperature range 850 to $1100^{\circ}C$ was quite different to those for the other steels. Austenitisation of this steel at $850^{\circ}C$ caused only a slight decrease in the volume fraction of carbides, compared with the level present in the annealed condition. The reduction in carbide content of this steel, as a result of low temperature

austenitisation, was of a similar degree to that which occurred in Alloys 5(Mo) and 10(W) at this temperature, but considerably less than in the other steels.

Raising the austenitising temperature to 950, 1050 and 1100°C resulted in progressive increases in the solution rate of carbides in Alloy 8(Cr), whilst there was very little carbide solution over this temperature range for the other alloys. There was a slight reduction in the solution rate of carbides at temperatures between 1100 and 1150°C for Alloy 8(Cr), the gradient of the graph in this range being less than for Alloys 5(Mo) and 10(W).

Austenitisation of Alloy 8(Cr) at 1200°C caused a marked increase in the solution rate of carbides. The magnitude of this was similar to the other steels, with the exceptions of Alloys 4(Si), 5(Mo) and 10(W), which had greater solution rates of this phase over the corresponding temperature region.

4.4 Hardness Values

4.4.1 In the as-Cast Condition

The high purity steels, in the as-cast condition, had hardness values over quite a narrow range of 424 to 489 HV/30, with two exceptions. These were Alloys 1 and 2, which had hardnesses of 373 and 407 HV/30 respectively. All the hardness values for these steels are shown in TABLE 14.

However, the commercial purity steels had lower hardnesses, in the as-cast condition, than those of high purity. These former steels had values ranging from 213 HV/30 in the case of Alloy 11 to 259 HV/30 for Alloy 14. The hardness figures for the commercial purity steels are also shown in TABLE 14.

4.4.2 In the as-Cast and Annealed Condition

Annealing the ingots of all these steels at 800°C for a period of 6 hours resulted in marked softening taking place. This was particularly so for the high purity steels, which had hardness values between 201 and 234 HV/30 for Alloys 1 and 4(Si) respectively.

In the case of the commercial purity steels, the figures ranged from 104 HV/30 for Alloys 11 and 15 to 160 HV/30 for Alloy 14. The hardnesses of both the high, and commercial purity alloys are given in TABLE 15.

4.4.3 In the Forged Condition

The hardness value of each of the high and commercial purity steels after forging, showed a considerable increase over the corresponding figure in the as-cast and annealed

condition, as shown in TABLE 16. This increase was most marked in the case of the high purity alloys.

However, the hardness values of the high purity steels showed a wide variation, and could be divided into three classes. In one category were Alloys 5(Mo), 8(Cr) and 10(W), all of which had hardness values in excess of 380 HV/30. Alloys 3, 4(Si) and 6(Mn) had figures in the range 325 to 335 HV/30, but Alloys 1, 2, 7(Ni) and 9(Co) had lower values of 282 to 304 HV/30.

A similar trend was obtained in the hardness figures of the commercial purity steels in the forged condition, as occurred in both the as-cast and as-cast and annealed states. This was with Alloys 11 and 15 being somewhat softer than the other six commercial purity steels. These two alloys had hardness values of 162 and 159 HV/30 respectively, whilst the other steels had hardnesses ranging from 211 to 237 HV/30.

4.4.4   In the Annealed Condition

Annealing all the high and commercial purity steels after forging caused appreciable softening to occur, as shown in TABLE 17. This softening was most marked in the high purity steels, in which the reduction in hardness as a result of annealing was in the order of 100 HV/30. There was quite a wide range in the hardness values of these steels in the annealed condition, from a minimum of 206 HV/30 for Alloy 1 to a maximum of 266 HV/30 in the case of Alloy 4(Si).

The reduction in hardness after annealing the commercial

purity alloys was approximately 40 HV/30. Once again the hardnesses of Alloys 11 and 15 were below those of the other commercial purity steels, being 109 and 112 HV/30 respectively, compared with a range from 170 to 198 HV/30.

4.4.5   In the Carburised Condition

4.4.5.1 The Analysis for Carbon throughout the Carburised Cases of Alloys 11 and 14

Two alloys were selected for carbon analysis at varying positions throughout the carburised cases. These steels were Alloys 11 and 14, thereby representing the maximum and minimum limits of the vanadium contents of the alloys of commercial purity.

The forms of the graphs of carbon content against the distance from the outer edge of the specimen were the same for both steels, as shown in FIG. 93. At each corresponding distance from the outer surface of the sample, the carbon level of Alloy 14 was fractionally higher than that of Alloy 11.

These graphs could be divided into four different sections. The first of these was up to a distance of 1.25 mm. from the outer surfaces of the specimens, in which region the carbon contents varied very little. However, between 1.25 and 2.75 mm from the edge there was a considerable decrease in the carbon level in each case.

In the region 2.75 to 4.23 mm. from the outer surfaces of the specimens, the gradients of both graphs were slightly less than in the immediately preceding zone. The limits of the cases were 4.23 mm., beyond this distance the carbon contents of the cores were the same as those of these alloys in the

annealed

condition.

4.4.5.2 <u>Hardness Values in the Carburised Condition</u>

The graphs of hardness against the distance from the outer edge of the sample for the carburised steels were of similar forms, all consisting of four differing regions, as shown in FIGS. 94 and 95. These zones corresponded very closely with the different regions of the graphs of carbon content against the distance from the outer surface of the specimen for these steels.

The first region was of the form of a plateau, there being virtually no hardness change up to a distance of 1.25 mm. from the sample surface for each alloy. Hardness tests at positions further from the surfaces of the steels, up to a point 3.0 mm. away, revealed appreciable decreases in this property, this being particularly the case for Alloys 11 and 15.

Increasing the distances from the edge of these steels up to, and including a value of 4.23 mm., caused decreases in gradients of the graphs, compared to those between 1.25 and 3.0 mm. The most marked decreases in gradients within this region were for Alloys 11 and 15.

The final region was again of a plateau form and occurred at distances in excess of 4.23 mm. from the surfaces of all the steels. This was the core hardness, and in each case was virtually identical with the corresponding hardness in the annealed condition.

These graphs could be classed together in pairs according to the vanadium contents of the steels. For corresponding distances from the surfaces of the samples, the hardness

diminished in the order Alloys 14 and 18, 13 and 17, 12 and 16 and finally 11 and 15.

However, the hardness differences between the first six alloys, at corresponding positions, were not very marked. This was not so for the latter two steels at distances in excess of 2 mm. from their surfaces. Alloys 11 and 15 were appreciably softer at these positions in the carburised cases than were the other steels.

4.4.6   In the As-Hardened Condition

4.4.6.1 The High Purity Steels Containing Only Vanadium as an Alloying Addition

The hardness values of these steels, after varying austenitisation treatments and water quenching, are presented in TABLE 18.   Most of the hardness figures are for austenitisation times of 20 minutes, but in some instances values are quoted for longer periods of 30 and 45 minutes.

In the case of each alloy, the maximum hardness was attained by austenitisation at the optimum conditions to give an ideal as-hardened microstructure.   These were 920, 1000 and 1120°C for Alloys 1, 2 and 3 respectively, with the soaking time in each instance being 20 minutes.   The maximum hardness values achieved for Alloys 1, 2 and 3 were 841, 858 and 862 HV/30 respectively.

Differences in hardness values between these three steels were most marked after austenitisation at either very low or high temperatures.   The lowest temperature employed was 850°C, but even after austenitisation at this temperature for 20 minutes, Alloy 1 had quite a high hardness of 829 HV/30.

However, Alloy 2 had a lower hardness of 812 HV/30 and Alloy 3 a very low value of 772 HV/30 as a result of austenitisation under these conditions. The hardness of the latter steel was increased to 803 HV/30 after austenitising at 900°C for 20 minutes.

Austenitisation of Alloy 1 at temperatures in excess of 1050°C caused a considerable decrease in hardness. This was particularly so after austenitising at 1150 and 1200°C for 20 minutes, as a result of which the hardness figures were 762 and 702 HV/30 respectively.

This effect was not nearly so marked in the cases of Alloys 2 and 3. The former steel did show a slight decrease in hardness after austenitisation at temperatures above 1100°C, but still had a value of 786 HV/30 after austenitising at 1200°C for 20 minutes. However, in the case of Alloy 3 there was only a fractional fall in hardness after austenitisation at temperatures in excess of 1120°C. This steel in fact had a hardness of 836 HV/30 after austenitisation at 1200°C for 20 minutes and subsequent water quenching.

Increasing the austenitisation time to 30 and 45 minutes at certain temperatures had very little effect on the hardness values obtained for these steels after 20 minutes soak at the corresponding temperature, followed by water quenching. There was, however, one exception, this being Alloy 1 after austenitisation at 1150°C. The hardness of this steel after austenitising at this temperature and subsequent quenching was 762 HV/30, whilst this was reduced to 744 and 721 HV/30 as a result of increasing the soaking period to 30 and 45

minutes respectively, at this same temperature.

4.4.6.2 The High Purity Steels Containing Vanadium and a Second Alloying Addition

Peak hardnesses for these steels were attained by austenitisation in the temperature range 1100 to 1150°C, for a time of 20 minutes, followed by water quenching. The hardness values of all these alloys, after austenitisation treatments at varying temperatures, are presented in TABLE 19.

Austenitisation at 850°C resulted in all the steels having low hardness values, most of which were below 810 HV/30. However, raising the austenitising temperature to 900°C caused increases in the hardness figures of most of the alloys. The exception to this was Alloy 5 (Mo), which had a value of 796 HV/30.

Generally, austenitisation at temperatures between 950 and 1050°C resulted in increases in hardness readings of the alloys. All the steels had hardnesses in excess of 800 HV/30 after austenitising at 950°C for 20 minutes and subsequent water quenching, and in some cases these were of the order 850 to 860 HV/30 after treatment at 1050°C.

Peak hardness values were obtained by austenitising either under, or very close to, the conditions required to give the ideal microstructure of each particular alloy, as was the case for Alloys 1, 2 and 3. Maximum hardnesses for Alloys 6(Mn), 7(Ni) and 9(Co) were attained by austenitisation in the range 1100 to 1120°C, whilst this was the case for Alloys 4(Si), 5(Mo), 8(Cr) and 10(W) between 1120 and 1150°C. Austenitisation of these steels at 1200°C resulted in decreases in hardness of approximately 30 HV/30, compared with the corresponding value obtained after treatment at 1150°C, with the exception

of Alloy 7(Ni) which softened more appreciably.

In every case, with the exception of austenitisation at $950^{\circ}C$, Alloy 9(Co) had the lowest hardness of these steels after corresponding treatments. The maximum hardness of this steel was attained after austenitising at $1120^{\circ}C$, the value only being 830 HV/30.

The peak hardness values of the other steels were in a range 856 to 888 HV/30. In the lower part of this range were Alloys 4(Si), 6(Mn) and 7(Ni) whilst Alloys 5(Mo), 8(Cr) and 10(W) had maximum hardness readings of 877, 879 and 888 HV/30 respectively.

4.4.6.3   The Commercial Purity Steels

The carburised steels had all been given optimum austenitisation treatments. These conditions were austenitising at $860^{\circ}C$ in the cases of Alloys 11 and 15, $900^{\circ}C$ for Alloys 12 and 16, $940^{\circ}C$ for Alloys 13 and 17, and $1040^{\circ}C$ in the cases of Alloys 14 and 18. In each instance the soaking period was 20 minutes, and the quenchant employed was water.

The form of the graph of hardness against the distance from the surface of the specimen was the same for each of the carburised steels, as shown in FIGS. 96 and 97. From the sample surface to a distance 2.5 mm. within, there was only a relatively slight decrease in hardness. This is illustrated in the instance of Alloy 11, where the hardness reduction was 45 HV/5.

Between 2.5 and 2.75 mm. from the surface of each specimen, there was an increase in the gradient of the graph compared

with that up to a distance of 2.5 mm. This was taken a stage further at distances between 2.5 and 4.0 mm. from the sample edge, the gradient in this region being considerably greater than that in the immediately preceding part of the graph.

However, the gradient of each graph decreased in the region between 4.0 and 4.25 mm. from the specimen surface. The hardness at this latter distance was the first value which was obtained of the core, the extent of the carburised case being 4.23 mm. Increasing the distance more than 4.25 mm. resulted in the graph having a plateau form.

Differences in hardness values at corresponding distances from the specimen surfaces were only slight. However, these were consistent in that they could be divided into pairs according to vanadium content. At corresponding distances from the specimen surfaces the hardness figures decreased in the following order:- Alloys 14 and 18, 13 and 17, 12 and 16, and finally 11 and 15.

The most pronounced differences in the hardness values were at distances in excess of 3.25 mm. from the specimen surface. This effect was particularly marked in the hardnesses of the cores, with Alloys 14 and 18 having values of between 44 and 103 HV/5 greater than the other steels.

4.4.7   In the Hardened and Tempered Condition

4.4.7.1 The High Purity Steels containing only Vanadium as an Alloying Addition

4.4.7.1.1 After Austenitisation under Ideal Conditions

The graphs of hardness against tempering temperature for

these steels are presented in FIG. 98. In the cases of
Alloys 1 and 2, the forms of the graphs bore a close relation-
ship with each other, over the whole range of tempering
temperatures employed. However, the graph for Alloy 3 was
somewhat different to those of the other two steels at
temperatures between 300 and 500°C.

Increasing the tempering temperature from 300 to 550°C
resulted in a decrease in the rate of softening for Alloys 1
and 2, compared with in the region 200 to 300°C. Alloy 3
had a lower rate of softening than the other two steels between
300 and 500°C, but the gradients of the graphs were similar
for all these alloys in the range 500 to 550°C.

The graph for each of the steels was either of, or very
close to, a plateau form on tempering at temperatures in the
range 550 to 600°C. Tempering each steel at 700°C resulted
in considerable softening taking place, this being particularly
marked in the case of Alloy 3.

4.4.7.1.2 <u>After Austenitisation at 850°C for 20 Minutes</u>

The graphs of hardness against tempering temperature for
alloys which had been austenitised at this low temperature,
had some similarities with the tempering curves for these
steels, which had previously received an ideal austenitisation.
Those graphs of steels subjected to the former austenitisation
treatment are shown in FIG. 99.

The first similarity between the two sets of graphs was
that for each steel, there was no hardness reduction on
tempering at 100°C. In addition, samples which had been
subjected to a low temperature austenitisation treatment

softened appreciably on tempering at 200°C, but this was
less pronounced in the range 200 to 400°C.   This again was
in quite close agreement with steels which had received an
ideal austenitisation treatment.

Finally, in the temperature region 550 to 600°C, each
graph in the two series had only a very slight gradient.   The
hardness decreases within this range were in fact very slightly
more pronounced for the steels which had been subjected to the
low temperature austenitisation treatment.

There were, however, several important differences between
the two sets of graphs.   The most marked was that at all
tempering temperatures up to, and including 400°C, Alloy 1
had the highest hardness whilst that of Alloy 3 was the lowest.
This was a complete reversal of the values obtained on tempe-
ring steels which had been austenitised under ideal conditions.

Tempering at temperatures in excess of 400°C resulted
in Alloy 3 having the highest hardness.   A temperature,
however, of 700°C was required before the hardness of Alloy
2 exceeded that of Alloy 1.

A second major anomaly was that at every tempering
temperature the hardness of each alloy was higher after
previously receiving an optimum austenitisation treatment.
This effect was most marked in the case of Alloy 3 and least
for Alloy 1.

Another difference was that the gradient of each of the
graphs for steels, which had been subjected to low temperature
austenitisation, was greater in the temperature region of
100 to 150°C.   The converse, however, held in the range 600

to 700°C, in that the gradients for steels which had been ideally austenitised, were greater.

4.4.7.1.3 After Austenitisation at 1200°C for 20 Minutes

The graphs of hardness against tempering temperature, for steels which had been overheated during austenitisation, are presented in FIG. 100. These graphs bore a much closer resemblance to the tempering curves for alloys which had been ideally austenitised, than was the case for those which were underhardened.

Tempering curves for the overheated steels could be divided into the same sections as for those which had been subjected to ideal austenitisation treatments. There were, however, some variances between the two series of graphs within corresponding sections.

One of the differences was in the temperature range 550 to 600°C. Steels which had been austenitised at 1200°C gave a slight amount of secondary hardening on tempering within this temperature region, reaching a peak in every case at 600°C. However, each of the graphs for steels ideally aus-tenitised, were of a plateau form in this temperature range.

The hardness values of Alloys 1 and 2 were higher at all tempering temperatures up to, and including 500°C, as a result of ideal austenitisation. In the case of Alloy 3 this was only true up to a temperature of 200°C. Tempering this steel at 300 to 500°C inclusive, resulted in the overheated samples having slightly higher hardness values.

Even though secondary hardening occurred during tempering the overheated steels between 550 and 600°C, the hardness of

each of these alloys in this range was only slightly in excess of the corresponding hardness of the steel after previously receiving an ideal austenitisation treatment. The maximum variation was 16 HV/30, which was for Alloy 1 after tempering at 600°C.

4.4.7.2 The High Purity Steels Containing Vanadium and a Second Alloying Addition

4.4.7.2.1 After Austenitisation Under Ideal Conditions

The relationships between hardness and tempering temperature for these steels are presented in FIGS. 101, 102, 103 and 104. Many similarities existed between the various graphs, but once again, these were several important differences.

Within the temperature range 150 to 200°C the hardness values of all the steels decreased very markedly. The gradients of the graphs were similar in this region, with the exception of those for Alloys 4(Si) and 9(Co), which were lower than for the other steels.

The softening rate of the steels decreased in the temperature range 200 to 500°C. Alloy 4(Si) was quite resistant to softening between 200 and 400°C, but softened more appreciably than the other steels in the temperature region 400 to 500°C.

Every graph had a secondary hardening peak between 500 and 600°C. The hardness peak occurred at 600°C, with the exception of Alloy 9(Co), in which case this phenomenon was at the slightly lower temperature of 580°C. In decreasing order of magnitude, the most pronounced peaks were for Alloys 5(Mo), 10(W), 6(Mn) and 8(Cr). Tempering all the steels at

700°C resulted in appreciable softening.

4.4.7.2.2 <u>After Austenitisation at 1200°C for 20 Minutes</u>

The relationships between hardness and tempering tempera-
ture, for steels which had previously been austenitised at
1200°C, are shown in FIGS. 105, 106, 107 and 108.   Yet again
there were many similarities between these graphs and the
tempering curves for steels which had received an ideal auste-
nitisation treatment prior to tempering, but there were some
important differences.

Tempering at temperatures up to, and including 400°C,
resulted in Alloy 4(Si) being the most resistant to softening.
This steel once again softened more appreciably than the other
alloys in the range 400 to 500°C.

An important factor was that tempering the steels between
500 and 600°C resulted in considerable secondary hardening
occurring, which in all the cases reached a peak at 600°C.
These secondary hardening peaks were more marked for each steel
as a consequence of previous austenitisation at 1200°C, than
for those which had been ideally austenitised.

The most appreciable secondary hardening peak was for
Alloy 5(Mo), and was 100 HV/30.   This corresponding value
was only 56 HV/30 when the steel had previously been subjected
to an ideal austenitisation treatment.   Comparison of the
hardness peaks for other steels, which had been austenitised
at 1200°C before tempering, gave values of 80, 59, 57, 50
49 and 37 HV/30 for Alloys 10(W), 8(Cr), 6(Mn), 4(Si), 9(Co)
and 7(Ni) respectively.

4.4.7.3   The Commercial Purity Steels

The relationships between hardness and tempering tempe-
rature are given for the commercial purity steels in TABLES
20 to 25.   Graphs are presented for Alloys 11 and 14 in FIGS.
109 to 112, illustrating this relationship at carbon levels
within the carburised cases of 1.29, 0.80, 0.40 and 0.20 wt.
% respectively.

Tempering at 200°C resulted in the steels softening quite
appreciably, this effect being most marked in each alloy at
positions in the case where the carbon content was in the
high range of 0.80 to 1.29 wt. %.   The rate of softening of
the steels was less pronounced between 200 and 400°C, this
being particularly so for Alloys 14 and 18, at all carbon
levels within the cases.   These two steels did soften more
appreciably in the temperature range 400 to 500°C, particularly
at positions in the cases with a high carbon level (1.29 wt. %).

Tempering some of the steels between 500 and 600°C
resulted in the occurence of secondary hardening.   In
generally assessing the secondary hardening responses, these
alloys are best divided into pairs, according to vanadium
content.

The most marked secondary hardening was obtained in
Alloys 14 and 18, whilst quite considerable hardening peaks
were also achieved in Alloys 13 and 17.   Alloys 12 and 16,
however, only gave a small degree of secondary hardening,
and in fact Alloys 11 and 15 softened slightly within the
temperature range 500 to 600°C.

An important criteria was the carbon level at the position in the case where each hardness reading was taken. The most appreciable secondary hardening was obtained with a combination of low carbon (0.2 wt. %) and high vanadium contents. An extension of this fact was that secondary hardening was most pronounced in Alloys 12 and 16 in the cores, rather than the carburised cases. The carbon content of the former was only 0.08 wt. %.

In fact, presented in FIG. 113 are graphs showing the change in hardness after tempering at 600°C for 1 hour as opposed to treatment at 500°C for the same time, as a function of the carbon content in the carburised layers. Even though optimum secondary hardening for Alloys 14 and 18 was achieved at positions in the cases with low carbon contents, quite considerable secondary hardening was obtained over the whole range of carbon levels. A similar effect, although of less magnitude, was obtained for Alloys 13 and 17.

However, for Alloys 12 and 16 the degree of secondary hardening was consistent throughout the carburised layer. The most appreciable secondary hardening for these steels was in the cores, this being further illustrated in Table 26, which gives the hardness values of all the steels after tempering over the full range of temperatures. Secondary hardening at low carbon contents in the cores of Alloys 12 and 16 was as appreciable as in the cores of the steels with higher vanadium levels (i.e. Alloys 13, 14, 17 and 18). These latter steels had a much lower degree of secondary hardening in the cores than in the carburised cases.

Tempering Alloys 11 and 15 at 600°C as opposed to 500°C, revealed the softening which resulted was insensitive to carbon content. These steels softened by between 18 and 24 HV/5 over the range of carbon levels within the cases. The extent of softening in the cores for the two steels was very similar to that of the case, within this temperature range.

The relationships between variation in hardness after tempering at 600°C and 500°C as a function of vanadium content are presented in FIG. 114, for Alloys 11 to 14. These graphs are plotted for four carbon levels, namely 0.2, 0.4, 0.8 and 1.29 wt. %. Clearly in evidence is the fact that raising the vanadium concentration from 0.06 to 0.22 wt. % has the most pronounced effect on increasing secondary hardening response. Further increase in the vanadium content to 0.55 and 1.11 wt. % improved the degree of hardening, but this was only really appreciable at a carbon level of 0.2 wt. %, and to a lesser extent 0.4 wt. %.

The result of tempering all the steels at 700°C was that softening took place. This effect was quite appreciable for alloys with high vanadium contents, but tended to decrease with a reduction in the concentration of this element in the steels.

4.4.8   After Long Term Tempering at 560°C

4.4.8.1 The High Purity Steels Containing Only Vanadium as an Alloying Addition

There were some important variations in the relationships between hardness and tempering time at 560°C for these steels, as illustrated in FIG. 115. This was particularly the case

for tempering times in the range 16 and 120 hours.

Alloy 1 softened appreciably at times between 8 and 40 hours, but tempering beyond this latter period only caused a slight further reduction in hardness.   Softening was not as pronounced for Alloy 2 for times between 8 and 40 hours, but this steel did show a greater reduction in hardness than Alloy 1 for periods in the range 40 to 100 hours, with very little further softening in excess of this time.

There was only a slight reduction in hardness as a result of tempering Alloy 3 at times of up to, and inclusive of 40 hours.   The softening rate became progressively more pronounced at 70 and 120 hours, but decreased for times above this latter period.

4.4.8.2   The High Purity Steels Containing Vanadium and a Second Alloying Addition

Basically the relationships between hardness and tempering time at 560°C for these steels could be divided into three types.   All these graphs are presented in FIGS. 116 and 117.

The first classification consisted of Alloys 4(Si), 7(Ni) and 9(Co).   These steels were quite resistant to softening at short tempering times.   However, the hardness of the alloys appreciably decreased on tempering for longer periods up to 160 hours, but further increases in time only resulted in slight degrees of further softening.

Within the time range 40 to 100 hours, the relationship for Alloy 9(Co) was somewhat different from these other two

steels.   The former steel was more resistant to softening
at times between 40 and 70 hours, but the converse was the
case for periods in the range 70 to 100 hours.

The second category contained Alloys 6(Mn) and 8(Cr).
These steels were resistant to softening at times up to, and
including 16 hours, this being particularly the case for
Alloy 8(Cr). Tempering for periods between 16 and 160 hours
resulted in quite appreciable softening taking place, although
this was less pronounced than for steels in the first classi-
fication.   Very little further reduction in hardness occurred
at times in excess of 160 hours.

Alloys 5(Mo) and 10(W) formed the final classification.
These two steels exhibited 'secondary hardening' as a function
of tempering time at 560°C.   The hardness peak in both cases
occurred at a time of 16 hours, being slightly more pronounced
for Alloy 10(W).

Increasing the tempering time from 16 to 160 hours resulted
in only a slight degree of softening for Alloy 10(W), but this
effect was more appreciable for Alloy 5(Mo) in the corres-
ponding range.   Tempering both these steels between 160 and
220 hours resulted in no further decreases in hardness.

4.4.8.3   The Commercial Purity Steels

The relationships between hardness and tempering time
at 560°C are presented for Alloys 11 to 14 in FIGS. 118 to
121, and for all the commercial purity steels in TABLES 27
to 32.   These are shown for a wide range of carbon contents
in the carburised cases of the steels.   Alloys with very
similar vanadium levels (e.g. Alloys 11 and 15) had virtually

identical relationships between hardness and tempering time,
as was also the case for the relationships when tempered
for 1 hour at different temperatures. The steels can, there-
fore, be divided into pairs for the presentation of the results.

These steels varied most in tempering behaviour for times
between 1 and 16 hours. 'Secondary hardening' occurred for
some of these steels in this period, reaching a maximum in
every instance at a time of 16 hours.

The most pronounced 'secondary hardening' took place in
Alloys 14 and 18 and, in diminishing order of magnitude, this
phenomenon also occurred in Alloys 13 and 17, and also Alloys
12 and 16. However, Alloys 11 and 15 did not show a 'secondary
hardening' peak, and in fact softened slightly on tempering
for times in this range.

Once again the carbon level played a vital role in
governing the degree of 'secondary hardening', as is shown
in FIG. 122 for all the commercial purity steels. Changes
in hardness after tempering for 16 hours as against 1 hour
at $560^{\circ}C$, are presented for carbon contents ranging from 0.08
to 1.29 wt. %. Clearly, these graphs confirmed that the most
appreciable 'secondary hardening' for steels with the highest
vanadium levels (i.e. Alloys 13, 14, 17 and 18) was at the
low carbon concentration of 0.2 wt. %, whilst for Alloys 12
and 16 maximum hardening took place at the lower carbon content
of the core.

Graphs are presented in FIG. 123, showing the variation
in hardness after tempering for 16 hours at $560^{\circ}C$ as opposed
to 1 hour at this temperature, as a function of vanadium
content. These relationships are presented for Alloys 11

to 14, at carbon levels in the cases of 0.2, 0.4, 0.8 and
1.29 wt. %.

A pronounced improvement in 'secondary hardening' response
occurred on increasing the vanadium concentration from 0.06
to 0.22 wt. %.   This was further improved upon by progressively
raising the level of this element to 0.55 and 1.11 wt. %, but
this effect was less pronounced at the high carbon contents
of 0.8 and 1.29 wt. %.

Tempering all the commercial purity steels for times
between 16 and 160 hours caused softening to occur, this being
most marked for alloys with the highest vanadium contents.
Further increase in time to 220 hours resulted in virtually
no further reduction in hardness values.

4.5   Transmission Electron Microscopy

4.5.1 In the Forged Condition

The only significant difference within the high purity steels in the forged condition was in the inter-lamellar spacing of pearlite.   This spacing was greatest in Alloys 1, 2 and 3 (which only contained vanadium as an alloying addition) and in Alloys 4(Si), 6(Mn), 7(Ni) and 9(Co). These latter steels contained vanadium and a second alloying element, which was not a carbide former.

A transmission electron micrograph taken from a thin foil of Alloy 9(Co), in the forged condition, is shown in FIG. 124. The structure consisted of pearlite, which had quite a large inter-lamellar spacing, and a few relatively small primary carbides.   The width of the ferrite lamellae were considerably greater than those of cementite.

The structure did not have a high dislocation density, this being indicative that recovery had taken place during hot working.   Recrystallisation had also occurred to a considerable degree in this alloy, and the large grain shown in FIG. 124 had grown and enveloped small subgrains.

The inter-lamellar spacing of the pearlite that was present in Alloys 5(Mo), 8(Cr) and 10(W) was quite small. This is shown in FIG. 125, which is a transmission electron micrograph taken from a thin foil of Alloy 8(Cr), in the forged condition.   Both the ferrite and cementite lamellae were finer in Alloy 8(Cr) than those present in Alloy 9(Co), this being particularly the case for the former phase.

Fine primary carbides were also present in the structure of Alloy 8(Cr). This steel had a higher dislocation density in the forged condition than was the case for Alloy 9(Co), and recrystallisation in Alloy 8(Cr) had not occurred to such a high degree as in the steel which contained vanadium and cobalt.

4.5.2   In the as-Hardened Condition

The high purity steels, in the as-hardened condition, which were examined by means of transmission electron microscopy, had all been austenitised under optimum conditions. All these steels had structures of twinned martensite and contained very high dislocation densities.

Transmission electron micrographs taken from thin foils of Alloys 3, 4(Si), 8(Cr) and 10(W), in the as-hardened condition, are presented in FIGS. 126, 127, 128 and 129 respectively. The individual martensite plates can be seen in these micrographs, and marked changes in the orientations of these plates indicated regions where excessive shear had taken place.

4.5.3   In the Hardened and Tempered Condition
4.5.3.1 Carbon Extraction Replicas

A transmission electron micrograph, taken from a carbon replica, which had been extracted from Alloy 1 in the hardened and tempered condition, is presented in FIG. 130. The tempering treatment which this steel had been given was 23 hours at 560°C.

The matrix of this alloy had retained a slightly acicular nature, indicating that martensite was still present, and the grain boundaries could be clearly observed. Primary vanadium carbides, which had not been taken into solution during austenitisation, were present in the structure. A few of these carbides were positioned at grain boundaries, thereby causing pinning and restriction of grain growth.

Electron micrographs of carbon replicas, which had been extracted from Alloys 2 and 3 are shown in FIGS. 131 and 132. These steels had both been given long term tempering treatments at 560°C, for times of 70 and 190 hours respectively.

In the case of the micrograph of Alloy 2 (FIG. 131), grain boundaries could be observed along with primary vanadium carbides. Some of the vanadium carbides were once again present at grain boundaries. The matrix of this steel still had a very slightly acicular nature, and was not completely ferritic.

The matrix of Alloy 3 was not acicular after treatment at 560°C for 190 hours, as shown in FIG. 132. This long term tempering treatment had caused the martensite, which was present in this steel in the as-hardened condition, to transform to ferrite. Primary vanadium carbides were also present in the structure, the volume fraction of these being greater than those present in FIGS. 130 and 131, for Alloys 1 and 2 respectively.

4.5.3.2   Thin Foils

4.5.3.2.1 The High Purity Steels Containing Only Vanadium as an Alloying Addition

Tempering these steels at 600°C resulted in marked changes in the structures, compared with those obtained in the as-hardened condition.   This is illustrated in the case of Alloy 1 in FIGS. 133, 134 and 135.   These are transmission electron micrographs taken from thin foils of this steel after tempering at 600°C for varying times.

A relatively low magnification electron micrograph is shown in FIG. 133.   This was taken from a thin foil of Alloy 1, which had been tempered at 600°C for 16 hours.   The structure contained a high dislocation density, with several areas of dislocation tangles being present.   The matrix had a lath form and primary carbides were present.

The micrograph presented in FIG. 134 was also taken from a thin foil of Alloy 1, after tempering at 600°C for 16 hours. This micrograph was taken at a higher magnification than was the case for FIG. 133, and this allowed some very fine, precipitated vanadium carbide particles to be resolved. These precipitated carbides had either nucleated on or adjacent to regions of high dislocation density.

Precipitated vanadium carbide particles could also be observed in FIG. 135.   This was a micrograph of Alloy 1, taken from a thin foil after tempering at 600°C for 23 hours. Laths were not present in the matrix structure and dislocation lines were forming as well as tangled networks.   These factors indicated that a recrystallised type of structure was commencing to form.

Vanadium carbide particles had also precipitated in Alloys 2 and 3 after tempering at 600°C. Electron micrographs, taken from thin foils of Alloy 2 after tempering at 600°C for 16 and 23 hours, are presented in FIGS. 136 and 137 respectively. Once again the precipitates had nucleated either on or adjacent to regions of high dislocation density.

The matrix of this steel had a lath form after tempering at 600°C for 16 hours, but this was not so on increasing the time to 23 hours. This longer time had resulted in a lower dislocation density and a recrystallised type of structure was starting to form.

Grain growth had commenced to occur and in this micrograph, two primary carbides, which were present at a grain boundary, were having the effect of pinning the grain against further growth. There was, therefore, a marked bulge in the part of the grain boundary which was present between the two carbides.

Diffraction patterns, which were taken from a precipitated and two primary vanadium carbide particles, present in Alloy 2 after tempering at 600°C for 23 hours, are shown in FIGS. 138 and 139 respectively (there is a double diffraction pattern for the two primary carbides in the latter figure). In the case of the precipitated carbide, the zone axis of the diffraction pattern was $[211]$, whilst that of the matrix was $[011]$. However, for the primary carbides these directions were $[111]$ and $[120]$ respectively, with the patterns for both primary carbides having $[111]$ zone axes.

Vanadium carbides, which had precipitated in Alloy 3 as a result of tempering at 600°C are shown in FIGS. 140, 141 and 142. The volume fractions of vanadium carbide, which had precipitated on tempering at this temperature for times of 16, 23 and 40 hours were still quite low.

Tempering this steel at 600°C for periods of 16 and 23 hours, did not cause the lath form of the matrix to break down, as shown in FIGS. 140 and 141 respectively. The dislocation densities which were present in the steel after these two tempering treatments were still high and the precipitated vanadium carbide particles had nucleated on dislocations.

Increasing the tempering time of this steel to 40 hours at 600°C did cause the lath nature of the matrix to commence to transform into a ferritic structure. The electron micrograph, taken from a thin foil of Alloy 3 after this treatment is shown in FIG. 142. Some of the precipitated carbides had formed at lath boundaries.

The effect of increasing the tempering temperature to 700°C had the effect of producing a virtually fully recrystallis ed matrix for each of these steels. This is illustrated for Alloy 2 in FIGS. 143 and 144, which are electron micrographs taken from thin foils, after tempering for 7 and 24 hours respectively.

Tempering Alloy 2 for 7 hours at 700°C had resulted in the growth of dislocation-free grains to envelope subgrains, which had a recovered structure. The grain boundaries could be readily observed in FIG. 143 as also could the vanadium carbide particles.

A very similar structure was also observed after tempering this steel at 700°C for 24 hours, as shown in FIG. 144. Dislocation lines were still present as were some precipitated vanadium carbide particles. These precipitated particles tended to have a spherical shape after tempering at this temperature for 7 and 24 hours, rather than the rod-like form which was present after tempering at 600°C.

4.5.3.2.2 The High Purity Steels Containing Vanadium and a Second Alloying Addition

Transmission electron micrographs, taken from thin foils of all these steels, after tempering at 600 and 700°C, revealed that a greater volume fraction of vanadium carbide had precipitated than in Alloys 1, 2 and 3 after corresponding heat treatments. The electron microscopy results for these steels are most suitably divided into two sections, depending on whether the second alloying addition was a carbide-forming element.

In the case of Alloys 4(Si), 6(Mn), 7(Ni) and 9(Co), the second alloying addition was not a carbide former. Nevertheless, each of these alloying additions increased the volume fraction of vanadium carbide, which had precipitated on tempering at 600 and 700°C.

This effect was most pronounced in Alloys 4(Si) and 6(Mn). An electron micrograph, taken from a thin foil of the latter steel, after tempering at 600°C for 40 hours, is presented in FIG. 145. The micrograph illustrated that the matrix of this steel had retained a lath form after this tempering treatment, and also that many dislocations were present in the structure.

Most important, however, was the fact that a considerable number of vanadium carbide particles had precipitated on tempering, and these were present both within the laths and at lath boundaries.

Furthermore, appreciable volume fractions of precipitated V_4C_3 particles were present in Alloys 7(Ni) and 9(Co) after tempering at either 600 or 700°C, as shown for Alloy 9(Co) in FIG. 146. These particles had, in many cases, nucleated on dislocations. This steel still retained a high dislocation density, after tempering at 600°C for 40 hours, but the matrix did not have a pronounced lath structure.

Tempering Alloy 7(Ni) for 40 hours at 600°C also resulted in quite a considerable degree of precipitation of vanadium carbide, as shown in FIG. 147. The matrix of this steel was still of a lath form, with inter-lath widths, greater than those present in Alloys 3 and 6(Mn) after corresponding heat treatments.

An electron diffraction pattern, taken from a precipitated vanadium carbide particle, which was present in Alloy 7(Ni) after tempering at 600°C for 40 hours, is shown in FIG. 148. The zone axis of the diffraction pattern for the carbide was $\left[211\right]$, whilst that of the matrix was $\left[331\right]$.

Considerable volume fractions of precipitated carbides were present in Alloys 5(Mo) and 10(W), after tempering at 600°C. An electron micrograph, taken from a thin foil of Alloy 5(Mo), which had been tempered at 600°C for 40 hours, is presented in FIG. 149. The precipitated vanadium carbides and molybdenum carbides (Mo_2C) were aligned in the direction of the

laths.   These particles were of the form of rodlets or plates.

The structure of Alloy 10(W), after this corresponding heat treatment was very similar to that of Alloy 5(Mo).   An electron micrograph, taken from a thin foil of Alloy 10(W), after tempering at 600°C for 40 hours, is shown in FIG. 150. Once again the precipitates (V_4C_3 and W_2C) were aligned in the direction of the laths, and had a rodlet shape.   The dislocation densities present in both Alloys 5(Mo) and 10(W) after tempering under these conditions were high, with recrystallisation not having commenced.

Results of transmission electron microscopy, carried out on Alloy 8(Cr) after tempering at 600°C, revealed one very important difference compared with the structures obtained in the other steels, after corresponding tempering treatments. Cementite was still present in Alloy 8(Cr) after tempering at 600°C, whereas in the other steels this phase had redissolved at this temperature.

Electron micrographs, taken from thin foils of Alloy 8(Cr) after tempering for 8 hours at 600°C, are presented in FIGS. 151, 152 and 153.   The cementite particles were very coarse and were in the form of large thick rodlets.   These particles had the same orientation within an individual lath in these micrographs.   A high dislocation density was still present in this steel, after tempering under these conditions, but only a low volume fraction of precipitated vanadium and chromium carbides could be observed.

Increasing the tempering period at 600°C to 16 hours had the effect of causing some solution of cementite and more

pronounced precipitation of vanadium carbide and chromium carbide (Cr_7C_3). Electron micrographs, taken from a thin foil of this steel, after treatment under these conditions, are shown in FIGS. 154 and 155.

The precipitated vanadium carbides and chromium carbides were very fine in size and were in the form of rodlets. These particles had the same orientation within an individual lath.

A double electron diffraction pattern, taken from two primary vanadium carbide particles, which were present in Alloy 8(Cr) after tempering at $600^{\circ}C$ for 16 hours, is presented in FIG. 156. The zone axis for each carbide diffraction pattern was $\left[111\right]$, whilst this was $\left[120\right]$ in the case of the matrix.

A dark field electron micrograph, taken using a $(2\overline{2}0)$ V_4C_3 zone reflection, is shown in FIG. 157. This is the corresponding dark field for the bright field electron micrograph which is presented in FIG. 155, and shows the vanadium carbide particles with the same zone reflections.

Cementite was not present in Alloy 8(Cr) after tempering at $600^{\circ}C$ for 40 hours, as shown in FIG. 158. This phase had redissolved after this treatment, and the only precipitated carbides present were Cr_7C_3 and V_4C_3, the size of these particles being larger than those present after tempering at this temperature for 16 hours. These precipitated particles were of a spherical form, rather than the rodlets, which formed after tempering for the shorter time.

Furthermore, tempering this steel at $600^{\circ}C$ for 40 hours caused a marked reduction in dislocation density, compared with

that present after 16 hours at this temperature. The matrix had not retained a lath form and recrystallisation had taken place.

All the electron microscopy results, so far described for steels in the hardened and tempered condition, have concerned alloys which had received ideal austenitising treatments. The volume fractions, however, of vanadium carbide particles which had precipitated in these steels, on tempering at 600 and 700°C, were greatest when the prior austenitisation temperature was increased to 1200°C.

This is illustrated for Alloy 4(Si) in FIG. 159, which is an electron micrograph taken from a thin foil of this steel, after tempering at 600°C for 16 hours. Increasing the austenitisation temperature to 1200°C, rather than employing the optimum temperature, had more effect in improving the secondary hardening response of this steel on tempering, than was the case for any of the other alloys.

The matrix had a coarse lath form and a large volume fraction of precipitated V_4C_3 particles were aligned in the directions of the laths. These precipitated carbides had a rodlet shape. Furthermore, this sample had a high dislocation density.

4.6   The Determination of Retained Austenite

Retained austenite was not present in any of the high purity steels as a result of austenitisation under ideal conditions and subsequent water quenching.   This is illustrated for Alloy 8(Cr) in FIG. 160, the X-ray scan revealing only martensite peaks.

Austenitisation at $1200^{\circ}C$ for 20 minutes followed by water quenching still resulted in the absence of retained austenite in these alloys, with two exceptions.   These were Alloys 7(Ni) and 9(Co), which contained 12.8 and 9.5% by volume of austenite respectively after this heat treatment.

The X-ray scans for Alloys 7(Ni) and 9(Co), after austenitisation at $1200^{\circ}C$ and quenching, are presented in FIGS. 161 and 162 respectively.   These scans show the $(110)\alpha'$, $(200)_{\alpha'}$ $(211)\alpha'$, $(220)\alpha'$, $(200)_{\gamma}$, $(220)_{\gamma}$ and $(311)_{\gamma}$ peaks and were obtained using a low sensitivity, the full chart scale being 400 impulses/second.

In addition, high sensitivity scans using a full chart scale of 100 impulses/second, through the austenite peaks given by Alloys 7(Ni) and 9(Co) are shown in FIGS. 163 and 164 respectively.   The technique of step scanning allows considerably greater resolution of the peaks.

4.7   Electron Microprobe Analysis

4.7.1 Analysis of the Primary Carbides Present in the High Purity Steels in the as-Hardened Condition

The primary carbides present in these steels in the as-hardened condition, along with the analyses, are listed in TABLE 33.   Each given carbide analysis is the average of the analyses of five carbides of the same type as the particular carbide quoted.   It must be pointed out, however, that each carbon level was calculated by subtracting the total weight percentage of the elements present in a particular carbide from 100 wt. %.

Generally, the five analyses carried out on carbides of the same type in a particular steel yielded very consistent results, with the elements present not varying by more than 3 wt. %.   The one exception to this was Cr_7C_3, which was present in Alloy 8(Cr).   Electron microprobe analysis revealed that the iron and chromium contents of five carbides of this type in Alloy 8(Cr), varied by 10 wt. %.

Only one carbide was present in Alloys 1, 2, 3, 4(Si), 6(Mn), 7(Ni) and 9(Co) and this was the vanadium carbide, V_4C_3.   The vanadium carbides had very similar analyses in all these steels, with vanadium contents ranging from 78.6 to 80.1, iron between 3.8 and 4.6 and carbon from 15.7 to 17.0 wt. %.   Small amounts of the second alloying additions were present in the carbides in Alloys 4(Si), 6(Mn), 7(Ni) and 9(Co).

Two carbides were detected in each of the other three high purity steels in the as-hardened condition.   Vanadium

carbide was present in all these steels but the second carbide was Mo_2C in the case of Alloy 5(Mo), Cr_7C_3 in Alloy 8(Cr) and W_2C in Alloy 10(W).

The vanadium carbides present in Alloys 5(Mo), 8(Cr) and 10(W) contained less vanadium and iron than those present in the other high purity steels. Molybdenum, chromium and tungsten replaced these two elements in the vanadium carbide in Alloys 5(Mo), 8(Cr) and 10(W) respectively.

The average molybdenum content of the vanadium carbide which was present in Alloy 5(Mo) was 6.5 wt. %. Similarly the average chromium level of the vanadium carbide which had formed in Alloy 8(Cr) was 6.1 wt. % and the tungsten level of that in Alloy 10(W) was 7.4 wt. %. These values were very similar, but on an atomic scale both chromium and molybdenum replaced the vanadium and iron atoms present in vanadium carbide to a greater extent than did tungsten.

Molybdenum carbide (Mo_2C) was present in Alloy 5(Mo) in the as-hardened condition, this carbide containing an average of 79.3 molybdenum and 7.1 wt. % carbon. This carbon level was considerably lower than that of vanadium carbide. Vanadium was present in Mo_2C at 4.7 wt. % and iron replaced some of the molybdenum atoms.

Analysis of tungsten carbide (W_2C) in Alloy 10(W) revealed an average tungsten content of 86.4 wt. %. This carbide had lower carbon, vanadium and iron contents than the molybdenum carbide present in Alloy 5(Mo).

Finally, the chromium carbide, Cr_7C_3, in Alloy 8(Cr) contained an average of 50.6 chromium, 35.2 iron, 5.5 vanadium and 8.7 wt. % carbon. Iron, and to a lesser extent vanadium had replaced a considerable number of the chromium atoms in this carbide.

Vanadium carbide was present in each of these steels in the as-hardened condition, irrespective of the austenitisation temperature which had been employed. This was also the case for molybdenum carbide in Alloy 5(Mo) and tungsten carbide in Alloy 10(W). The exception, however, was chromium carbide which was only present in Alloy 8(Cr) after austenitising at temperatures up to, and including $1100^{\circ}C$, prior to quenching.

4.7.2 <u>The Partitioning of Elements Between the Martensitic Matrix and Carbide Phases in the High Purity Steels in the as-Hardened Condition</u>

An electron image, showing some of the vanadium carbides in Alloy 3 in the as-hardened condition, is presented in FIG. 165. This steel had been austenitised at $1200^{\circ}C$ for 20 minutes with subsequent water quenching. The carbides were in the form of stringers, with the directionality of these being due to hot working.

The X-ray image, showing the vanadium distribution over the same field shown in FIG. 165, is presented in FIG. 166. This photograph was taken, as were all the X-ray image photographs, using an exposure time equivalent to ten scans of the particular field.

Very high concentrations of vanadium, in the carbides shown in FIG. 166, could be observed on this X-ray image.

This clearly confirmed that these were in fact vanadium carbides. The partitioning of vanadium between both the martensitic matrix and vanadium carbides could be readily seen from this X-ray image.

Further X-ray images, illustrating the vanadium partitioning between the matrix and vanadium carbides are shown in FIGS. 167 and 168. The former of these is the vanadium distribution in Alloy 7(Ni), after austenitisation at 1200°C for 20 minutes followed by water quenching, whilst the latter X-ray image is for this same element in Alloy 8(Cr) after a corresponding heat treatment.

The chromium distribution between the matrix, chromium carbides and vanadium carbides in Alloy 8(Cr), is shown in FIG. 169. Austenitisation of this steel had been carried out at 1050°C for 20 minutes with subsequent water quenching.

This X-ray image clearly identifies three chromium carbide stringers. The intensity of chromium radiation obtained from the chromium carbides, however, illustrated that the chromium content of these was less than the vanadium levels of the vanadium carbides shown in FIGS. 166, 167 and 168. In addition, a band of vanadium carbide particles can be observed in FIG. 169, as the chromium contents of these are higher than the level of this element in the matrix.

Finally, the X-ray image, showing the partitioning of molybdenum between the matrix and molybdenum carbides in Alloy 5(Mo), is presented in FIG. 170. This steel had been austenitised at 1150°C for 20 minutes followed by water

quenching.

A stringer of molybdenum carbides is shown in this
X-ray image.   One of these carbides was of a large size,
whilst the remainder were very fine.   An accurate analysis
could be obtained from this large carbide but the other
carbides present were too small in size for this to be the
case.   Any attempts to analyse the small carbides would have
resulted in inaccuracies being incurred, as analysis would
also be obtained from the immediate areas surrounding the
particles.

4.7.3   <u>Matrix Analyses of the High Purity Steels in the
        Annealed and as-Hardened Conditions</u>

4.7.3.1 <u>The Matrix Vanadium Contents of the High Purity Steels
        Containing Only Vanadium as an Alloying Addition</u>

Graphs of the vanadium content of the matrix against
austenitisation temperature for Alloys 1, 2 and 3 are presented
in FIGS. 171, 172 and 173 respectively.   A point is plotted
on every graph showing the vanadium level of the ferritic
matrix of the steel in the annealed condition.   In each case
the austenitisation time was 20 minutes, and the quenchant
employed was water.   This was so for all the steels used in
this research, on which microprobe analysis was carried out.

The graphs were of similar forms, and consisted of three
regions.   In the first place, austenitisation of these steels
at 850°C resulted in slight increases in the vanadium contents
of the matrices, compared with the concentrations of this
element present in the annealed state.   The second region
occurred over an austenitisation temperature range of 850 to

1100°C inclusive, in which each graph was virtually of a plateau form.

Finally, the third region occurred at austenitisation temperatures in excess of 1100°C. Quite marked increases in the vanadium levels of the matrices of these three steels took place on austenitisation at a temperature of 1150°C, compared with corresponding contents obtained at temperatures below this value. This effect was more pronounced for each steel on austenitisation at 1200°C, with the gradient of the graph in the range 1150 to 1200°C being much greater than in any other region of the graph.

The vanadium contents of the matrices of these steels in the annealed state, was greatest for Alloy 3 and least for Alloy 1. Austenitisation at 850°C, however, resulted in the greatest increase in the matrix vanadium level for Alloy 1 and least for Alloy 3, compared with corresponding values obtained for these steels in the annealed condition.

An important fact was that the most critical austenitisation temperature range in these graphs was 1100 to 1200°C. Within the range 1100 to 1150°C, the gradient of the graph for Alloy 3 was the greatest whilst that of Alloy 1 was the lowest. This was also the case on austenitising at between 1150 and 1200°C, although the differences in the gradients between the three graphs were much more pronounced in this range, than in the immediately preceding temperature region.

4.7.3.2   <u>The Matrix Vanadium Contents of the High Purity</u>
          <u>Steels Containing Vanadium and a Second Alloying</u>
          <u>Addition</u>

Relationships between the vanadium contents of the
matrices of these steels and austenitisation temperature are
shown in FIGS. 174 to 177.   These graphs could be divided
into three regions, over the same temperature ranges as were
the corresponding graphs for Alloys 1, 2 and 3.

In the first instance, austenitisation of these steels
at 850°C caused marginal increases in the vanadium levels of
the matrices, compared with corresponding contents of this
element obtained on analysing these steels in the annealed
condition.   The second region extended over an austenitisation
temperature range of 850 to 1100°C inclusive.   Each of the
graphs was virtually of a plateau form over this temperature
range.

The final region was between austenitisation temperatures
of 1100 to 1200°C, with once again these being inclusive.
In the lower part of this temperature range, the matrix
vanadium contents of these steels increased, compared with
concentrations obtained in the immediately preceding temperature
region.   This effect was much more marked between 1150 and
1200°C, with the gradients of all these graphs being greatest
in this region.

In the annealed condition, the ferrite matrices of the
steels had very low vanadium contents, with the lowest level
being in Alloys 5(Mo) and 10(W) at 0.02 wt. % and the highest
in Alloys 7(Ni) and 9(Co) at 0.06 wt. %.   Despite, however,
these close similarities in the matrix vanadium contents of

the steels in the annealed state and the fact that the graphs had three corresponding sections, there were some important differences within corresponding austenitisation temperature ranges.

The first such case was only marginal and was in the austenitisation temperature range of 1050 to 1100°C. Austenitisation of Alloys 4(Si), 5(Mo), 6(Mn), 7(Ni), 9(Co) and 10(W) at 1100°C resulted in no increases in the matrix vanadium contents compared with corresponding values obtained after treatment at 1050°C. In the case of Alloy 8(Cr), however, this higher temperature treatment resulted in an increase in the vanadium level of the matrix of 0.02 wt. %.

Undoubtedly, the most critical region of each of the graphs was in the austenitisation temperature range of 1100 to 1200°C. Examination of the graphs at the lower part of this temperature range (i.e. 1100 to 1150°C) revealed that the gradients of the graphs for Alloys 5(Mo), 6(Mn) and 10(W) were very similar. The gradients of the graphs for Alloys 7(Ni), 8(Cr) and 9(Co) were greater than those for the previously mentioned steels, whilst that for Alloy 4(Si) was lower.

The gradients of the graphs for Alloys 6(Mn), 7(Ni) 8(Cr) and 9(Co) were very similar in the austenitisation temperature range of 1150 to 1200°C. This is illustrated by the fact the matrix vanadium contents of these steels increased by between 1.02 and 1.06 wt. % on austenitising at 1200°C, compared with the levels obtained after treatment at 1150°C.

In the cases of Alloys 4(Si), 5(Mo) and 10(W), however, the gradients were lower in this temperature range than for

the other four steels.   The vanadium contents of the
matrices of these steels increased by between 0.87 and 0.93
wt. % on austenitising at 1200°C, as opposed to 1150°C.
Austenitisation at 1200°C resulted in Alloy 7(Ni) having the
highest matrix vanadium content of 1.43 wt. % and Alloy 4(Si)
the lowest, at 1.06 wt. %.

4.7.3.3   The Matrix Molybdenum, Chromium and Tungsten
           Contents of Alloys 5(Mo), 8(Cr) and 10(W) Respectively

Graphs illustrating the relationships between the matrix
molybdenum, chromium and tungsten contents and austenitisation
temperature for Alloys 5(Mo), 8(Cr) and 10(W) are presented
in FIGS. 178, 179 and 180 respectively.   The relationships
between the matrix molybdenum and tungsten concentrations and
austenitisation temperature were quite similar to those for
the vanadium contents of the matrices against the same variable
for Alloys 5(Mo) and 10(W), as shown in FIGS. 174 and 176.

The graphs showing the variations in matrix molybdenum
and tungsten levels with austenitisation temperature were of
a plateau form up to, and including, an austenitisation
temperature of 1050°C.   Austenitisation at 1100°C resulted
in a slight increase in solution of these elements and this
effect became progressively more pronounced on austenitisation
at 1150 and 1200°C.   In fact austenitisation at 1200°C
resulted in a very marked increase in matrix molybdenum and
tungsten contents, compared with the corresponding levels
obtained after treatment at 1150°C.

Comparison of the matrix molybdenum and tungsten contents
with corresponding vanadium levels in Alloys 5(Mo) and 10(W)

respectively, revealed several interesting features. The first of these was that the molybdenum and tungsten concentrations of the ferrite, in the annealed condition, were higher than the vanadium contents of this phase.

Secondly, austenitisation of Alloys 5(Mo) and 10(W) at 850°C caused a very slight increase in matrix vanadium content, compared with the corresponding levels obtained in the annealed state. In the cases of the molybdenum and tungsten levels of the matrices of these steels, however, there were no increases as a result of this austenitisation treatment.

Austenitisation of these two steels at 1100°C caused slight increases in the matrix molybdenum and tungsten concentrations (0.02 and 0.06 wt. % respectively) compared with the levels obtained after treatment at 1050°C. This higher temperature treatment, however, did not result in any increases in the matrix vanadium contents of these steels.

The critical regions of these graphs were in the austenitising temperature range of 1150 to 1200°C. In this region, the gradient of the graph of matrix tungsten content against austenitisation temperature was in excess of the corresponding graph of vanadium level. The converse, however, held for molybdenum, with the gradient of the graph showing the level of this element as a function of austenitising temperature being less than the corresponding graph for vanadium.

Finally, the relationship between the chromium content of the matrix of Alloy 8(Cr) and austenitisation temperature

is shown in FIG. 179. This graph was of a totally different form to all the other graphs of matrix vanadium, molybdenum and tungsten levels as functions of austenitising temperature, in these high purity steels.

In the case of FIG. 179, there was a slight increase in the chromium content of the matrix as a result of austenitisation at 850°C, compared with the level obtained for Alloy 8(Cr) in the annealed state. The ferritic matrix of this steel, in the annealed condition, contained 0.16 wt. % of chromium.

Further raising of the austenitisation temperature to 950, 1050 and 1100°C caused progressive increases in the gradient of the graph shown in FIG. 179. The result of this was that the matrix of Alloy 8(Cr) contained 0.90 wt. % of chromium after austenitising at 1100°C.

Austenitisation of Alloy 8(Cr) at 1150°C caused only a slight further increase in the matrix chromium level. A slightly more pronounced rise in the content of this element in the martensitic matrix did result, however, after austenitising at 1200°C. The matrix chromium content, after this high temperature treatment, was 0.96 wt. %.

4.8   Scanning Electron Microscopy

4.8.1 The Distribution of Vanadium and Iron In Alloy 1 After Long Term Tempering

A scanning electron micrograph is presented in FIG. 181, and this shows a large particle in the ferrite matrix of Alloy 1, after tempering for 220 hours at 560°C. The ferrite grain boundaries can be clearly seen in this micrograph.

The distribution of iron over the field illustrated in FIG. 181, is given by the X-ray image shown in FIG. 182. A uniform distribution of iron occurred throughout the ferrite matrix, but none of this element was present in the large particle in the centre of the micrograph. The exposure time employed for this X-ray image was 15 seconds.

Similarly, the X-ray image showing the distribution of vanadium over this same field, is presented in FIG. 183. The exposure time used for this X-ray image was 20 minutes. Vanadium was uniformly distributed in the ferrite matrix, but this element was not present at all in the large particle. This, coupled with the fact that the particle had the definite feature of a phase (unlike for example a surface pore or hole), confirmed that the particle was graphite.

5. Discussion

5.1 Comparisons of the Secondary Hardening Responses of the Steels

This section covers both high and commercial purity steels, which had received an ideal austenitisation treatment prior to tempering. The effects of the prior austenitisation temperature on the secondary hardening responses of these alloys are discussed later.

A very significant result from this research was that high purity steels, which contained only vanadium as an alloying addition, did not show a secondary hardening peak on tempering in the temperature range of 550 to 600°C. The hardness value of each of these alloys remained virtually constant as a result of tempering at varying temperatures within the secondary hardening range for vanadium steels.

These alloys, therefore, did resist softening in this temperature region. Very appreciable softening of these steels occurred on tempering between 150 to 550°C. The fact, however, that this did not continue in the higher temperature range of 550 to 600°C was due to one factor. This was the hardening caused by the precipitation of particles of V_4C_3.

This hardening counterbalanced the softening of each steel, which took place as a result of both carbon depletion and reduction in tetragonality of the crystal structure of the matrix. The volume fraction, however, of precipitated V_4C_3 particles was insufficient to result in a true secondary hardening peak occurring in the critical tempering temperature range.

A simple graphical construction can be employed in order to assess the secondary hardening response of a steel, which resists softening but does not give a hardness peak, over the temperature range at which secondary hardening should take place. This consists of extending the graph of hardness against tempering temperature from 550 to 600°C, employing the same gradient as in the range 500 to 550°C.

The graphical extension, therefore, allowed the hardness value to be determined for the steel at a tempering temperature of 600°C, which would have been attained if the steel had continued softening at the same rate in the range 550 to 600°C as in the preceding region of 500 to 550°C. Subtraction of this hardness value from the maximum hardness actually achieved by the steel in the range 550 to 600°C gave a hardness figure (ΔH) which was equivalent to the secondary hardening response of the steel. A hypothetical case, showing how this was carried out, is presented in FIG. 184.

On this basis the high purity steels, which contained only vanadium as an alloying addition, 'secondary hardened' to very similar degrees. The exact values of ΔH were 32, 30 and 37 HV/30 for Alloys 1, 2 and 3 respectively. This clearly confirms that increasing the vanadium content of high purity vanadium steels does not improve the secondary hardening response

Effectively the carbon levels of these three steels could be considered as constant, ranging from 0.78 to 0.81 wt. %. A carbon content of 0.80 wt. % had been selected as this level is usually employed in high speed steels. The vanadium contents of the alloys varied from 0.39 to 1.62 wt. %, as the level of

this element in most high speed steels is in the range 1 to 2 wt. %.

Calculation of the stoichiometric vanadium:carbon ratio to form vanadium carbide, using the carbide formula as $VC_{0.875}$ (i.e. intermediate between V_4C_3 and VC), revealed a ratio of 4.86 : 1. The vanadium : carbon ratios of the high purity vanadium steels which were employed in this research were less than this value, ranging from 0.50 : 1 to 2.00 : 1. Nevertheless, the steel with the lowest ratio gave a comparable secondary hardening response to that obtained from the alloy with the highest ratio.

The fact, however, that the vanadium : carbon ratios of these steels varied from that required for stoichiometry, does not explain why secondary hardening peaks were not obtained on tempering in the critical temperature range. In fact, Isizuka [130] determined that secondary hardening occurred in a whole range of commercial purity vanadium steels, with vanadium : carbon ratios varying from 0.41 : 1 to 9.87 : 1. Furthermore, Nishida and Tanino [129] found that vanadium contents in excess of 0.1 wt. % resulted in secondary hardening taking place in commercial purity vanadium steels.

The addition of individual alloying elements to a steel with the same base composition as Alloy 3 (i.e. 0.81 carbon and 1.62 wt. % vanadium) produced some interesting results. These additions were made at a level of 1 wt. %, with the exception of tungsten at 2 wt. %, and in each case a secondary

hardening peak occurred as a result of tempering in the range 500 to 600°C.

A further point from these results was that for each of these steels, a slight amount of hardening took place on tempering between 500 and 550°C, thereby extending the secondary hardening peak over a temperature region of 100°C. In the case of the high purity steels which contained only vanadium as an alloying addition, quite considerable softening occurred on tempering between 500 and 550°C, and for each steel the plateau region only extended over the range 550 to 600°C. This clearly confirmed that nucleation of V_4C_3 was taking place appreciably more readily in steels containing vanadium plus a second alloying addition.

Molybdenum had the most pronounced effect in improving the secondary hardening response which had been obtained from the alloy with base composition, and resulted in a secondary hardening peak of 56 HV/30. The following other elements had decreasing effects on the degree of secondary hardening obtained in steels containing vanadium:- tungsten, manganese, chromium, with silicon and nickel being equal, and cobalt.

Electron microscopy results revealed that molybdenum, tungsten and chromium carbides had precipitated along with vanadium carbide in the corresponding steels, on tempering in the critical temperature range. These carbides contributed to the secondary hardening of these steels along with vanadium carbide, although in the case of chromium carbide this effect was not very pronounced.

A very important revelation, from the examination by means of transmission electron microscopy, was that the volume fraction of precipitated vanadium carbide particles was greater in each of the steels which contained vanadium and a second alloying addition, than in the alloys where only vanadium had been added. This was surprising for the steels, in which the second alloying addition was a carbide former. Confirmation of this was achieved by means of dark field electron microscopy.

Calculation, however, of the values of ΔH for these steels revealed some changes in the previously mentioned secondary hardening order. A point which must be made is that in the calculation of the values of ΔH for these steels, the extension from the graph was made at a temperature of 500°C and not 550°C. This was because these steels secondary hardened over the temperature range 500 to 600°C, and not just between 550 and 600°C.

In terms of decreasing ΔH values obtained, the order of elements was silicon, manganese, with molybdenum and tungsten equal, nickel, cobalt and chromium. The extent of the range was between a maximum ΔH value of 132 HV/30 and a minimum figure of 69 HV/30. In fact, the steel which contained silicon had a ΔH value of 38 HV/30 in excess of that of the next steel, in which manganese was present, in the previous list.

The steel which contained silicon softened very appreciably in the tempering range 400 to 500°C. This explains, therefore, how this steel, which only showed a small secondary hardening peak, could have such a high value of ΔH. Conversely, in cases where the second alloying element was a carbide former (particularly molybdenum and tungsten), the degree of softening between temperatures of 400 and 500°C was less pronounced than

for the other steels.   The outcome of this was, that although these three steels gave pronounced secondary hardening peaks, the ΔH values were lower than that for the alloy in which silicon was present.

Some of the commercial purity steels showed secondary hardening peaks as a result of tempering in the critical temperature range.   The commercial purity steels had been carburised, thereby allowing comparisons to be made between the hardening responses of these alloys at varying positions within the carburised cases.

The commercial purity steels with the lowest vanadium contents (i.e. 0.05 and 0.06 wt. %) did not give secondary hardening peaks at any of the carbon levels in the carburised cases.   These steels however, did resist softening somewhat in the temperature range 500 to 600°C.

An increase in the vanadium level of the commercial purity steels to 0.22 and 0.24 wt. % did cause secondary hardening to occur on tempering.   The degree of secondary hardening shown by each of these steels throughout the carburised case was very consistent.   Undoubtedly, the reason for this consistency was that, even at positions in the cases with low carbon contents, the vanadium:carbon ratios were still well below that required by stoichiometry for $VC_{0.875}$ formation.

This theory also held to a lesser extent for carburised steels with vanadium levels of 0.53 and 0.55 wt. %, as the vanadium : carbon ratios for these alloys was lower, at all points in the cases, than the stoichiometric value.   These

steels gave quite considerable secondary hardening peaks on tempering, with these being most pronounced at positions in the carburised cases with low carbon contents.

Further confirmation of the importance of the vanadium : carbon ratio in determining the secondary hardening response was given by the two commercial purity steels with highest vanadium levels (1.11 and 1.13 wt. %). These steels had secondary hardening peaks of 40 and 34 HV/5 respectively at a position in the cases with a carbon content of 1.29 wt. %.

The amount of secondary hardening, shown by these steels increased with decreasing carbon levels in the cases, so much so that the hardness peaks were 75 HV/5 for both steels at a point where the content of this element was 0.20 wt. %. In fact the vanadium : carbon ratios at this position were slightly in excess of that required for stoichiometry. Nevertheless, these ratios were closer to stiochiometry than those given by carbon levels at other positions in the cases where hardness readings were taken.

The fact, therefore, that maximum secondary hardening response was obtained at a point in each carburised case where the vanadium : carbon ratio was near to the requirement of stoichiometry, reveals how important this criterion is in controlling the degree of secondary hardening in vanadium steels. This factor could also be utilised to achieve optimum secondary hardening in high speed tool steels.

An interesting point was that the steels with vanadium levels of 0.22 and 0.24 wt. % showed the most appreciable secondary hardening peaks at the low carbon concentrations of

the cores.   The vanadium : carbon ratios for the cores of these steels were closer to the requirement of stoichiometry than at positions in the carburised cases, so much so that the secondary hardening peaks of the former were as pronounced, in this corresponding region, as for steels with higher vanadium contents.

A presentation is made in FIG. 185 which shows vanadium and carbon levels which give corresponding hardness variations for steels tempered at $600^{\circ}C$, as opposed to $500^{\circ}C$, with in each case the time being 1 hour.   This diagram clearly illustrates the beneficial effect of relatively high vanadium and low carbon concentrations in giving optimum degrees of secondary hardening.

High vanadium and carbon contents gave similar secondary hardening responses to steels with medium carbon and vanadium levels (0.4 - 0.6 wt. %).   An increase in carbon concentration for steels with low vanadium contents had very little effect on secondary hardening.

Instances where the vanadium : carbon ratios were very high (i.e. the cores of the high vanadium steels), the secondary hardening response was limited due to low volume fractions of V_4C_3 which precipitated on tempering.   This was as a direct result of the low matrix carbon content, with very little of this element available to react with vanadium to form V_4C_3.

Steels with vanadium : carbon ratios less than the need for stoichiometry would contain higher proportions of vanadium in the form of carbides prior to hardening, than alloys with the ideal ratio.   The greater availability of carbon in the

former steels caused more vanadium atoms to react with this element to form V_4C_3, and therefore, more vanadium present in the form of carbide. This reduced the matrix vanadium level, thereby lessening the secondary hardening response on tempering.

Vanadium carbide particles would certainly precipitate in the commercial purity steels during slow cooling from the carburising temperature. These carbides would be fine and more readily dissolved during austenitisation than the larger carbides which formed during the freezing of the molten high purity alloys. This factor contributed to both, the excellent secondary hardening peaks of steels with compositions in the cases close to the stoichiometric vanadium : carbon ratio, and also quite good responses from alloys with ratios varying from the ideal.

A final point in connection with the commercial purity steels, was that these secondary hardened in the temperature range 500 to 550°C, as well as between 550 and 600°C. Sufficient vanadium carbide precipitation must have occurred in the lower temperature region to both counteract the softening of the steel and produce a hardening peak. This, therefore, was similar to the effect obtained from the high purity steels which contained vanadium and a second alloying addition.

5.2   The Significance of Tempering Time on Secondary Hardening

Tempering time was shown to be of less importance than tempering temperature, as far as secondary hardening was concerned.   Hardening peaks occurred during tempering the high purity steels containing molybdenum and tungsten, and in all the commercial purity alloys except the two with lowest vanadium levels, on tempering for periods up to 16 hours at 560°C.

The peaks were less pronounced than those obtained in tempering curves relating hardness changes with variation in temperature, particularly for the commercial purity steels. Nevertheless, quite considerable hardness peaks were achieved for the high purity steels containing molybdenum and tungsten, and for commercial purity alloys with high vanadium contents, at positions in the carburised cases with low carbon levels.

A diagram is presented in FIG. 186 which relates vanadium and carbon concentrations that gave corresponding hardness variations for steels tempered for 16 hours, as opposed to 1 hour, at 560°C.   The beneficial effect of low carbon and high vanadium levels on 'secondary hardening' with variation in time is clearly illustrated.   Once again, therefore, the importance of stoichiometric ratio was confirmed.

Hardness variations were insensitive to carbon content at low vanadium concentrations (0.06 - 0.15 wt. %).   Further increase, however, in the vanadium level showed that steels with quite low carbon and vanadium contents of 0.08 and 0.22 wt. % respectively gave similar peaks to alloys with medium carbon and vanadium concentrations.   The form of this diagram

was very similar to FIG. 185, for steels tempered at 600 and 500°C, except that in this instance the hardness variations were of a lower magnitude.

5.3 The Effects of Nitrogen and Aluminium on Secondary Hardening

The carburised steels could be divided into two groups, depending on the nitrogen contents. In the first series the alloys had levels of this element between 0.007 and 0.008, whilst in the second, the nitrogen concentrations were considerably higher, ranging from 0.015 to 0.018 wt. %. An important factor was, therefore, to compare the secondary hardening responses of alloys from these two groups. Most significance was placed on steels in each group which had similar vanadium contents, and hardness readings had been taken at positions with corresponding carbon levels in the cases.

Very little difference was obtained between the secondary hardening peaks of corresponding alloys in these two groups. This confirmed, therefore, that nitrogen was not assisting in the secondary hardening mechanism to any appreciable extent.

The reason for this was that, even at positions in the carburised cases where the carbon contents were low or in the cores, the carbon levels were considerably in excess of those of nitrogen. This was so even in the steels with high nitrogen contents. The net result was that vanadium carbide was the predominant precipitating phase in the secondary hardening temperature range, with nitrogen being present in precipitated vanadium carbonitride.

Nitrogen, however, does play a significant role in the precipitation mechanism of vanadium steels with very low carbon and high nitrogen levels. This is because vanadium carbide or even vanadium carbonitride precipitation in these steels is very limited and the precipitation of vanadium nitride(s) takes

place.

Hrivnak [167] in fact, carried out a detailed study of compositions of vanadium steels which were required to cause vanadium nitride to precipitate. His results revealed that, in steels with low nitrogen contents, vanadium carbide or vanadium carbonitride precipitated on tempering at $600^{\circ}C$. In alloys, however, which contained more nitrogen than carbon (the levels used were 0.060 and 0.02 wt. % respectively), the face centred cubic vanadium nitride (VN) precipitated at between 600 and $700^{\circ}C$. Furthermore, tempering at temperatures in excess of this range caused the hexagonal vanadium nitride (V_2N) to precipitate.

A further factor of importance was to assess the effect of aluminium on the secondary hardening responses of the commercial purity steels. Seven of these steels had aluminium contents ranging from 0.025 to 0.040 wt. %, whilst the other alloy contained 0.079 wt. % of this element. This latter steel was in the group of alloys with low nitrogen levels, but with a high vanadium content of 1.11 wt. %.

The outcome of tempering these steels in the secondary hardening temperature range was that the degrees of secondary hardening obtained were insensitive to the aluminium contents. This fact was confirmed by the steel with a high aluminium level not giving a more pronounced secondary hardening peak than the alloy with a corresponding vanadium content, but con- taining less aluminium. In addition, comparison of the secondary hardening peaks of steels containing 0.55 and 0.53 wt. % vanadium, but with aluminium levels of 0.040 and 0.025

wt. % respectively, yielded this same conclusion.

Viswanathan and Beck, [158] whilst working on the stress rupture properties of chromium-molybdenum-vanadium steels, did find that increased aluminium contents resulted in a rise in the volume fraction of precipitated V_4C_3 particles, after carrying out stress rupture tests for varying times at $593^{\circ}C$. The two steels on which the research was undertaken had carbon contents of 0.3 wt. %, with chromium and molybdenum being present at a level of 1.2 wt. %, and manganese at 0.9 wt. %. Vanadium was a secondary element in these steels at 0.25 wt. %.

The silicon contents of the alloys were 0.25 and 0.14 wt. %, and nickel was also present at 0.15 and 0.40 wt. % respectively. Furthermore, analysis for the minor elements in these steels revealed that the aluminium levels were 25 and 237 parts per million respectively. Several other elements were also present at impurity levels.

Vanadium carbide precipitated in preference to $M_{23}C_6$ in the steel with higher aluminium content. The resultant was that this alloy had excellent rupture strength at $593^{\circ}C$, but poor ductility. In the other steel, however, $M_{23}C_6$ and V_4C_3 precipitated particles were present in approximately equal volume fractions after stress rupture tests, for varying times, at this temperature.

No explanation, however, is given by these authors, as to why the increased aluminium content of the steel matrix (virtually all the aluminium was present in the matrix phase) resulted in increased precipitation of vanadium carbide. In fact, there was very little difference between the hardness

values of the two steels, after undergoing stress rupture tests at $593^{\circ}C$ for corresponding times.

The fact, however, that aluminium additions did not improve the secondary hardening responses of commercial purity steels used in this research is a very interesting point. This factor will be discussed in the following section.

5.4 Consideration of the Factors Governing the Secondary Hardening of Steels Containing Vanadium

There is no doubt that the secondary hardening of vanadium steels is caused by the precipitation of V_4C_3. Strain fields around the precipitated particles result in hardening, as does the resistance of the particles to dislocation movement.

Vanadium carbide particles nucleate on dislocations, and on lattice defects in general. The high purity steels, which contained only vanadium as an alloying addition, had quite high dislocation densities after hardening and then tempering in the critical temperature region of 550 to 600°C.

Only a small volume fraction of V_4C_3 particles were precipitated, however, as a result of tempering in this range, despite the relatively high dislocation densities of the alloys. The resultant was that true secondary hardening did not occur in these steels, thereby indicating that a high dislocation density is not the crucial factor in controlling the precipitation of V_4C_3.

Retained austenite was not playing a significant role in the tempering responses of the steels used in this research. When present, this phase either transforms to bainite on holding at the tempering temperature, or to martensite on cooling, whilst precipitates can nucleate in austenite. However, austenite was not present in any of the high purity steels after optimum austenitisation, and was only present in the alloys containing nickel and cobalt after high temperature treatment at 1200°C.

Austenitisation at $1200^{\circ}C$ had caused appreciable solution of V_4C_3, with resultant excessive grain growth of austenite. Such austenite is more stable than that formed at lower temperatures, and this phase is likely to be present in steels containing strong austenite stabilising elements, after high temperature austenitisation and quenching. Nickel and cobalt are both strong austenite stabilisers, but were not present at high enough levels to cause appreciable volume fractions of retained austenite in vanadium steels, in the as-hardened state.

A further important factor to consider when investigating secondary hardening response, is the analysis of the matrix of the particular steel in question. Only atoms which are present in the martensitic matrix of an alloy in the as-hardened condition, can react with other atoms on tempering at certain critical temperatures to result in the precipitation of carbides or intermetallic compounds.

The high purity steels, which only contained vanadium as an alloying addition, had matrices with low vanadium contents after receiving optimum austenitisation treatments. In each of these steels, a much higher proportion of the vanadium present was in the form of carbide, rather than dissolved in the matrix after this austenitisation treatment. Furthermore, because vanadium has combined with carbon to form V_4C_3, a presumption can be made to the effect that a low matrix vanadium content similarly means a low carbon level in this phase.

A vastly different situation however, occurred in samples of these steels which had been austenitised at $1200^{\circ}C$ for 20

minutes and water quenched. This high temperature treatment
resulted in considerable increases in the matrix vanadium
contents of these steels.

Comparison of the secondary hardening responses of these
two series of samples revealed very little difference. The
specimens which had been previously austenitised at $1200^{\circ}C$
gave very slight secondary hardening peaks on tempering between
550 and $600^{\circ}C$, whereas the hardness was constant in this
temperature range for samples which had received an ideal prior
austenitisation treatment. Furthermore, the magnitude of the
secondary hardening peaks for alloys which had been austen-
itised at the high temperature, prior to tempering, were
virtually the same for all three steels.

The inference to be drawn from these results is that in
very high purity steels, containing only vanadium as an alloying
addition, a high matrix vanadium content in the as-hardened
condition, is not sufficient alone to give a good secondary
hardening response on tempering. This is an unusual finding,
because the general theory has been that a high matrix level
of any strong carbide-forming element, would give conditions
for optimum secondary hardening on tempering, as a result of
a very high volume fraction of precipitated particles of the
particular carbide in question.

Vanadium carbide is a very stable carbide and difficult
to take into solution during austenitisation. In fact, one
of the objectives of this research project was to attempt to
alloy high speed steels in such a manner that a higher degree
of solubility of V_4C_3 could be achieved during austenitisation,

and hence give improved secondary hardening response due to V_4C_3 precipitation on tempering.

Tungsten carbide and molybdenum carbide are also both very stable carbides, and appreciable solution of these only occurs in high speed steels at temperatures in excess of 1200°C. These carbides are, therefore, competing to be taken into solution with V_4C_3 during the austenitisation of high speed steels, and so limited solubility of each is only to be expected. This is particularly the case for V_4C_3, which is the most stable of these three carbides and hence has the lowest solubility during austenitisation.

The fact, however, that a large number of nucleation sites (dislocations) for V_4C_3 together with a high matrix vanadium content, did not cause marked secondary hardening to occur in vanadium steels, suggests that another factor is crucial in controlling the precipitation of this carbide. Relationships between hardness and tempering temperature for both, the commercial purity steels which had been carburised, and the high purity alloys which contained vanadium and a second alloying addition, revealed some important factors.

In the first place, the vital significance of purity in controlling the secondary hardening response was revealed, this being particularly illustrated by the hardness results for the commercial purity steels. These alloys, with the exception of the two steels with very low vanadium contents (0.05 and 0.06 wt. %), gave secondary hardening peaks on tempering in the critical temperature range at all carbon compositions within the carburised cases.

The highest vanadium content of these alloys was only 1.13 wt. %, and this was considerably below the level of this element (1.62 wt. %) in one of the high purity steels which contained only vanadium as an alloying addition. This commercial purity steel, however, gave far superior secondary hardening response, at all carbon levels in the carburised case, to the high purity alloy with a vanadium content of 1.62 wt. %.

Comparison of the remainder of the analyses of these two steels revealed that the commercial purity alloy contained several elements which were not present in the high purity steel. The most important of these elements were, as expected, silicon and manganese, which were present at levels of 0.30 and 0.76 wt.%. respectively.

Other elements were present at very low levels in the commercial purity steel, these being aluminium, nitrogen, sulphur, phosphorus, copper, tin, chromium and nickel. Aluminium and nitrogen had very little effect on secondary hardening response, and the other elements were present at such low levels as to be considered likewise ineffective.

Silicon or manganese, therefore, appear to be having the effect of improving the degree of secondary hardening of vanadium steels. A further possibility is that this improvement is an accumulation of the influence of both these elements. In order to assess the effects that individual elements are having on secondary hardening, however, the necessity is to study the tempering curves for high purity steels containing vanadium and a second alloying element in conjunction with

the findings obtained from electron metallographic examination.

A point which must be made here is that the effect of the prior austenitisation treatment on secondary hardening response will be discussed in a later section. In this comparison, however, the maximum secondary hardening for each steel is mentioned, and this always resulted after previous austenitisation at the high temperature of $1200^{\circ}C$.

All the alloying additions to vanadium steels resulted in great improvements in the secondary hardening responses of these steels. Very marked secondary hardening peaks were obtained, as a result of tempering at temperatures between 500 and $600^{\circ}C$.

The magnitudes of these secondary hardening peaks were, in diminishing order of the second alloying addition:- molybdenum, tungsten, chromium, manganese, silicon, cobalt and nickel respectively. Comparison, however, of the ΔH values for these steels, revealed some changes in this order. The steel containing silicon had the highest ΔH value, whilst the remainder of the order was unchanged, apart from cobalt preceding chromium and nickel doing likewise with manganese.

Additions of each of the three carbide-forming elements, used as secondary alloying additions, to vanadium steels had, in general, the greatest effect in the improvement of the degree of secondary hardening. This was particularly the case as far as molybdenum and tungsten were concerned, with this being only to be expected, as these are secondary hardening elements in their own right.

Examination by means of a transmission electron microscope revealed that molybdenum carbide (Mo_2C) and tungsten carbide (W_2C) were precipitated in the respective steels, after tempering at $600^{\circ}C$. Undoubtedly, some hardening resulted from the precipitation of these carbides in the particular alloys in question.

Similarly, the chromium carbide Cr_7C_3, precipitated at this temperature in the steel which contained chromium as the additional alloying element. Chromium is not a true secondary hardening element, but the precipitation of either Cr_7C_3 or $Cr_{23}C_6$ on tempering results in chromium steels resisting softening at temperatures between 500 and $550^{\circ}C$. The type of chromium carbide which is precipitated is dependent on the chromium : carbon ratio of the particular steel.

The important factor, however, was that the addition of molybdenum, chromium or tungsten to vanadium steels, increased the volume fraction of V_4C_3 particles which precipitated on tempering at $600^{\circ}C$. This was confirmed for these alloys by employing dark field transmission electron microscopy using V_4C_3 zone reflections.

A possible explanation for the increased nucleation rate of V_4C_3 caused by the addition of molybdenum, chromium or tungsten to a steel containing vanadium is that V_4C_3 is nucleating on the precipitated carbides of these elements, on tempering in the critical temperature range. This particularly appeared to be likely when chromium was present. The chromium carbide, Cr_7C_3, precipitates on tempering at between 500 and $600^{\circ}C$, i.e. fractionally below the temperature

range required for the precipitation of V_4C_3.

The precipitation of Mo_2C and W_2C takes place over virtually the same temperature range as for V_4C_3. This, however, does not rule out the possibility of these carbides acting as nuclei for V_4C_3 embryo. Precipitation temperatures for Mo_2C, W_2C and V_4C_3 are always expressed as a range, and the possibility must exist that the first two carbides mentioned nucleate at a fractionally lower temperature than V_4C_3.

The nucleation of one phase on another is not uncommon. A precipitated particle represents a discontinuity in the matrix lattice crystal structure, although is not intrinsic with this crystal structure, and in this respect is different from a vacancy or dislocation. The fact that the discontinuities exist means that these must be potential nucleation sites for the embryos of other phases.

Examination by means of an electron microscope of the structures of the three steels in question, revealed that V_4C_3 nucleated on dislocations. This, however, does not completely eliminate the possibility of V_4C_3 nucleating on another precipitated carbide.

Even in cases where one phase has nucleated on another, the likelihood exists that these will appear as only one phase on a bright field electron micrograph. An element of good fortune is required to age a sample at the ideal temperature and for the correct time to enable the observation to be made, by means of transmission electron microscopy, that one phase had nucleated on a particle which had precipitated at a lower temperature.

Nucleation of a phase, either on a particle or a
dislocation are cases of heterogeneous nucleation. The
alternative nucleation technique of homogeneous nucleation
very rarely, if ever, takes place in practice.

The energy of a cluster of atoms in a crystal lattice
depends upon location, and is greater for groups of atoms at
structural imperfections than for atoms in perfect regions.
This clustering process must take place before nucleation
can occur. The energy, therefore, needed to form a nucleus
is nearly always less if the nucleus forms at one of these
high energy locations. A dislocation is such a location,
and so is a particle, although in the latter instance much
depends on whether the particle is coherent or incoherent
with the matrix phase.

In cases where the interface between the particle which
is acting as the nucleation site and the matrix is incoherent,
the interfacial energy value is large, and this governs the
formation energy of the new precipitate. The interfacial
energy of coherent interfaces is appreciably less than that
of the incoherent type, thus the latter have much more driving
force in their action as nucleation sites for further embryo
of a different phase, as this will result in a greater redu-
ction in interfacial energy.

Nucleation of some V_4C_3 embryo did undoubtedly occur on
dislocations, in steels used in this research. An important
factor is, therefore, to consider the free energy required
for such nucleation to take place.

Research was carried out on this subject by Cahn. [168]
He presented a simple model of nucleation on dislocations, and made the assumptions of an elastic model of a dislocation and an incoherent interphase interface.

Cahn [168] deduced that the free energy of formation of a nucleus consisted of three terms, namely the volume free energy, the surface energy and a strain energy term, which is negative on account of the release of the strain energy of the dislocation.   The value of ΔG for a cylindrical nucleus of unit length and radius r is given by:-

$$\Delta G = - A \log r + 2\pi \gamma r + \pi r^2 . \Delta G_v \qquad \dots\dots\text{EQUATION 12.}$$

Where A is given by dislocation theory in terms of the elastic constants.

γ = Interfacial energy per unit area of the interface between the matrix and the precipitating phase.

ΔG_v = Difference between the free energy of the matrix and precipitating phase per unit volume of the precipitating phase measured on bulk samples.

On occasions when $\left| 2A . \Delta G_v \right| < \pi \gamma^2$, the term ΔG passes through a minimum at a nucleus radius r_0, and a maximum at a value of r_c.   The value of r_0 is approximately equal to the size of a Cottrell atmosphere, and is given by the following equation:-

$$r_0 = - \frac{\gamma}{2 \Delta G_v} \left[1 - \left(1 + \frac{2A \Delta G_v}{\pi \gamma^2} \right)^{\frac{1}{2}} \right] \qquad \dots\dots\text{EQUATION 13}$$

The barrier against nucleation is the difference between the values of ΔG at embryo radii of r_c and r_0.   When

$\left| 2A \cdot \Delta G_V \right| > \pi \gamma^2$ there is neither a minimum nor maximum in the graph showing the relationship between the free energy of formation of a nucleus on a dislocation and the radius of the nucleus. This means that there is no barrier to nucleation taking place.

Substituting reasonable values for the parameters, the nucleus radii r_o and r_c have values at approximately 2 and $10\overset{o}{A}$ respectively. On this basis, nucleation on a dislocation is 10^{78} more rapid than homogeneous treatment.

This generalised treatment by Cahn, is not strictly applicable to the precipitation of V_4C_3 in a martensitic matrix, as in this case the original precipitate is coherent with the matrix. Nevertheless, this treatment shows that dislocations are very much preferred nucleation sites, as a considerably lower free energy is required for a nucleus to form on such a site than if this same nucleus was forming homogeneously in the matrix lattice.

There are two final points, however, to consider on the precipitation of V_4C_3 in steels containing vanadium and a second alloying addition which is a carbide-forming element. The first of these is that the precipitation of the carbide of the second alloying element (molybdenum, chromium or tungsten) could lower the free energy required for V_4C_3 precipitation.

Precipitation of a carbide at a very slightly lower temperature than that required for V_4C_3 precipitation, would effectively increase the vanadium content of the matrix, due to depletion in this phase of the second carbide-forming

element.   This higher effective vanadium concentration would enable vanadium and carbon atoms to combine more readily in the matrix, thereby reducing the free energy required for V_4C_3 precipitation.   Overall this would lead to a synergistic effect, whereby the combined secondary hardening response of two elements would be greater than the corresponding sum of their individual effects.

The second factor is that molybdenum, chromium and tungsten dissolve to appreciably greater extents in V_4C_3 than do non carbide-forming elements.   Analysis revealed that primary vanadium carbides contained 6.5, 6.1 and 7.4 wt. % of molybdenum, chromium and tungsten respectively in the three separate alloys.

However, on an atomic basis, molybdenum and chromium replace vanadium atoms in V_4C_3 to a greater extent than does tungsten, this fact having also been established in research carried out on high speed tool steels.   In addition, the steel in which molybdenum was present showed a slightly more pronounced secondary hardening peak than the alloy which contained tungsten.

The fact that molybdenum can enter into solid solution in precipitated V_4C_3 to a greater degree than tungsten and that the former alloying addition results in slightly more secondary hardening in vanadium steels, suggests that the two factors are related.   The inference must be that both molybdenum and tungsten, but particularly the former, in solid solution in V_4C_3, increase the coherency stresses slightly

between this precipitate and the martensitic matrix, thereby resulting in improved secondary hardening response.

Chromium is not a secondary hardening element alone, and there was no surprise in the fact that the steel containing this element gave an inferior secondary hardening peak to those in which molybdenum and tungsten were present. A further factor could, however, be based on the atomic radius of chromium in relation to those of molybdenum and tungsten. Chromium atoms have a smaller radius than those of both molybdenum and tungsten, and also slightly less than that of vanadium. This could lead to chromium atoms, present in solid solution in precipitated V_4C_3, creating smaller coherency stresses between this precipitate and the matrix, than would the larger molybdenum and tungsten atoms, when dissolved in this precipitate.

5.4.1 Steels Containing a Second Alloying Addition which is not a Carbide-Forming Element

These four steels, which contained individually silicon, manganese, nickel and cobalt in addition to vanadium, really hold the key as to the factor which is governing the precipitation of V_4C_3, and hence controlling the secondary hardening response. These alloys all showed considerably superior degrees of secondary hardening than steels which only contained vanadium as an alloying addition.

Silicon and manganese had the greatest effects of the non carbide-forming elements, in improving the secondary hardening response of vanadium steels. These two alloying

additions resulted in secondary hardening peaks in vanadium steels, particularly when previously austenitised at $1200^{\circ}C$, only slightly below those obtained in alloys in which either molybdenum or tungsten was present along with vanadium. In fact the steel in which silicon was present as the second alloying addition, had a higher ΔH value than any of the other alloys, when austenitisation prior to tempering had been carried out at $1200^{\circ}C$.

Furthermore, the fact that these non carbide-forming elements did give such marked improvements in the secondary hardening of vanadium steels, suggests that molybdenum, chromium and tungsten were not contributing to any appreciable extent to the hardening due to V_4C_3 precipitation. This means that carbides of these elements are unlikely to act as nucleation sites for V_4C_3 embryo. In addition, these elements do not appear to have a very marked effect on the coherency stresses between precipitated V_4C_3 particles and the martensitic matrix, by dissolving in this precipitate.

The inference to be made, therefore, is that molybdenum, chromium and tungsten are basically improving the secondary hardening responses of steels containing vanadium by precipitation of their own carbides. Precipitation of either molybdenum carbide or tungsten carbide result in secondary hardening in their own right, and chromium carbide precipitation also causes steels to resist softening between 500 and $600^{\circ}C$. The precipitated carbides Mo_2C, Cr_7C_3 and W_2C were identified by means of electron diffraction patterns, in the respective steels, during carrying out transmission electron microscopy.

Consideration of the reason why silicon, manganese, nickel and cobalt improve the secondary hardening of vanadium steels leads to several possible explanations. The first of these is that a transition carbide is formed, prior to V_4C_3 precipitation. Formation of such a transition carbide could lower the activation energy for V_4C_3 formation. This means that the precipitation of V_4C_3 would take place in two stages, with the intermediate phase being very important in assisting the formation of the final precipitate.

However, no such intermediate phase was identified by means of transmission electron microscopy. Furthermore, these four elements only dissolved in primary vanadium carbide to very small degrees, thereby meaning that an intermediate carbide based on Fe V X C (X = silicon, manganese, nickel or cobalt) was highly unlikely to form prior to V_4C_3 precipitation.

A second possibility is that each of these four alloying elements is retarding the diffusion of vanadium atoms in the martensite lattice, to sites where reaction occurs with carbon to form V_4C_3. The diffusion of vanadium in the matrix lattice is the rate controlling step in the formation of V_4C_3, as the atomic radius of this element is greater than that of carbon. In addition, vanadium dissolves in iron to form a substitutional solid solution, whilst carbon is present at interstitial positions in the lattice.

Comparison of the atomic radii of silicon, manganese, nickel and cobalt with that of α-iron, reveals that silicon has the biggest discrepancy. The atomic radius of silicon

is considerably less than that of α-iron, and so the presence of this element causes marked contraction in localised regions of the iron lattice. Silicon, therefore, would be expected to retard the diffusion of vanadium atoms (which have a very similar atomic radius to α-iron atoms) to reaction sites with carbon atoms, within the iron matrix, for the formation of V_4C_3.

However, if silicon and the other non carbide-forming elements were having a marked effect on the diffusion of vanadium atoms in the iron matrix, the secondary hardening peaks of these steels would be moved to higher temperatures. Samples of these four alloys were in fact austenitised at $1200^{\circ}C$ for 20 minutes, water quenched followed by tempering at either 610 or $620^{\circ}C$ for 1 hour.

In fact, increasing the tempering temperature from 600 to $620^{\circ}C$ for these steels resulted in slight softening taking place. This showed that silicon, manganese, nickel and cobalt were not appreciably retarding the diffusion of vanadium atoms to reaction sites with carbon atoms in the matrices, at temperatures within the secondary hardening range.

Tempering for times in excess of 1 hour at a temperature of $560^{\circ}C$, confirmed that these elements were not retarding the precipitation of V_4C_3. Steels containing vanadium and any one of these elements did not show hardening peaks, on tempering for times ranging from 1 to 220 hours. These alloys resisted softening up to, and including a time of 23 hours, but softened on tempering in excess of this time.

The series of samples which had been subjected to long term tempering at 560°C had been ideally austenitised. The matrix vanadium contents of these alloys were quite low, and so appreciable 'secondary hardening' response could not be expected.

This was particularly the case with respect to silicon, thereby, causing difficulty in the assessment of the degree of 'secondary hardening' of this steel during long term tempering. The matrix vanadium level of this alloy was very low after optimum austenitisation, the result of which was that the vast proportion of vanadium present in the matrix had precipitated in the form of V_4C_3 as a result of tempering for 1 hour at 560°C. Therefore, only a small concentration of vanadium was available for further precipitation on tempering at this temperature for longer times.

Silicon retarded the precipitation of Fe_3C in the temperature range 200 to 400°C. In fact, the steel containing vanadium and silicon did not soften as appreciably as the other alloys in this temperature range. The effect of silicon was to retard the diffusion of *carbon* atoms in the matrix to reaction sites with *iron* atoms, to form cementite. This was as a result of the atomic diameter of silicon being considerably less than that of α-iron.

Chromium had the effect of retarding the growth rate of Fe_3C and hence reducing the rate of softening. This element dissolves to quite a large extent in Fe_3C, with resultant decrease in the rate of growth of this phase. Illustration of this fact is given by results of electron microscopy, which

showed that cementite was only present in one alloy after tempering at $560^{\circ}C$, and this contained vanadium and chromium.

Cementite in fact, precipitated readily in all the other steels at temperatures between 200 and $400^{\circ}C$. Carbon atoms can easily diffuse through the tempered martensite lattice to reaction sites with iron atoms to form Fe_3C, and nucleation of this phase occurs very readily in the tempering of the vast majority of steels in this temperature range.

The steels which contained molybdenum and tungsten did give hardening peaks on tempering between 1 and 16 hours at $560^{\circ}C$, with the actual peak occurring at the latter time. These peaks were due to the precipitation of two secondary hardening carbides in each alloy, namely V_4C_3 and Mo_2C in the first case and V_4C_3 and W_2C in the second steel. In addition, these two alloys had received an ideal prior austenitisation treatment, which had been at a slightly higher temperature than employed for the other high purity steels. This meant that the matrix levels of secondary hardening elements were greater in the alloys containing molybdenum and tungsten than was the case for the other steels, thereby allowing greater volume fractions of secondary hardening carbides to precipitate in the former alloys.

Tempering these two steels for times in excess of 16 hours resulted in softening taking place. This was due to the growth of precipitated particles, thereby causing a reduction in coherency stresses between these and the matrix. The process, therefore, leads to overageing or Ostwald ripening as this is sometimes termed.

A very important factor now is to consider the sizes
of the atoms of the various elements investigated, and the
effects of these on the solid solution hardening of α-iron.
The term atomic diameter must be qualified here, and this is
in accordance with the classical definition by Hume-Rothery.[169]
He defined the atomic diameter of an element as the closest
distance of approach of the atoms in the crystal structure.

On this basis, Hume-Rothery developed the term of size
factor. This governs the formation of substitutional solid
solutions, with complete solid solubility only occurring in
alloy systems where the atomic diameters do not vary by more
than 15%. Valency, crystal structure and position in the
electro-chemical series also influence the formation of solid
solutions, but these factors are less crucial than the size
effect. Solid solutions can be formed in alloy systems
involving elements with differences in these requirements,
providing that the atomic diameters are favourable.

The atomic diameter of α-iron is 2.48 Å, and comparison
of the atomic diameters of the alloying elements which were
present in the high purity alloys, revealed that these were
all within 15% of this value, as shown in FIG. 187. These
elements, therefore, had favourable size factors to form solid
solutions in α-iron.

These elements, with the exception of silicon, are tran-
sition elements, as also is iron. Vanadium, manganese,
chromium, nickel, cobalt and iron are all in the first
transition period. Chromium, nickel and cobalt have atomic
diameters only very slightly in excess of that of α-iron.

Vanadium and manganese have also atomic diameters greater than α-iron, but these differences are more pronounced than is the case for chromium, nickel and cobalt.

Molybdenum is present in the second transition period, whilst tungsten is in the third series. Both these elements have atomic diameters greater than α-iron, and in fact are very similar to that of manganese. Silicon was the only alloying element used in these steels with an atomic diameter less than α-iron.

Each of these alloying elements forms a substitutional solid solution in ferrite. Carbon, however, has only a very small atomic diameter and is present at the intersticies in this phase. The fact that this element was present at very similar levels in all of these high purity steels, meant that the solid solution hardening effects due to this element being dissolved in the martensitic matrices of these alloys, in the as-hardened condition, only varied very slightly.

A surprising fact is that only a limited amount of information is available concerning the hardening effects of elements present in substitutional solid solution in pure ferrite. The data are complicated by variations in grain size and the presence of small amounts of impurities in the different alloys. Significant data is difficult to attain because of the presence of trace amounts of elements which dissolve interstitially in ferrite. The two most important elements in this respect are carbon and nitrogen, with as little as 0.0005 wt. % of the former element resulting in quite a marked increase in the stress necessary to cause a

specified very small level of plastic strain.

The classical research on the solid solution hardening effects of different elements, forming substitutional solid solutions in ferrite, was carried out by Lacy and Gensamer.[170] These co-workers produced a list, showing the effectiveness of various elements on the solid solution hardening of pure ferrite. The order, based on additions of equal weight, in terms of increasing solid solution hardening effect in α-iron was chromium, nickel, molybdenum, manganese and silicon. Furthermore, this order was unchanged for equal atomic percentages of these elements.

Bain [171] and Rees, Hopkins and Tipler [172] also undertook research on the effectiveness of these same elements on the solid solution hardening of α-iron. They both obtained the same order, in terms of increased solid solution strengthening of α-iron, which was as follows:- chromium, molybdenum, nickel, manganese and silicon. This list was for additions of equal weight percentages of these elements.

The order is identical to that determined by Lacy and Gensamer, [170] with one exception, this being that the positions of nickel and molybdenum were interchanged. This interchange of positions was only very slight, as nickel and molybdenum were adjacent to each other in the order found by Lacy and Gensamer. [170]

In addition, Rees, Hopkins and Tipler [172] determined the solid solution hardening effects in terms of equal atomic percentages of these elements. On this basis the order became chromium, nickel, silicon, manganese and molybdenum

for increased magnitude of hardening.   The positions of
the elements in this list are slightly different to the
corresponding order obtained by Lacy and Gensamer, [170] with
silicon and molybdenum being interchanged.   Silicon has the
lowest atomic weight of these alloying elements, and molybdenum
the highest, so a reversion of positions in the list was
plausible.

However, Rees, Hopkins and Tipler [172] are prepared to
accept the orders, in terms of both atomic and weight perce-
ntage additions given by Lacy and Gensamer, [170] for the
solid solution hardening effects of these elements in pure
ferrite.   The former co-workers admit to variations in the
grain sizes of their steels, which would be expected to cause
inaccuracies in the results.   This was particularly the case
for the iron-silicon alloy, which had a very coarse grain
size, and thereby tending to reduce the hardening response.

The other elements, not mentioned in these lists but
which were used as alloying additions in the high purity
steels employed in this research, are vanadium, cobalt and
tungsten.   Each of these elements forms a substitutional
solid solution when dissolved in ferrite, but with quite
differing hardening responses.

Vanadium has a position between those of nickel and
molybdenum in the order of effectiveness of elements in the
strengthening of α-iron.   This was so in terms of additions
of either equal atomic or weight percentage.

Cobalt gives a very similar degree of solid solution
hardening as nickel, when dissolved in α-iron.   The presence

of tungsten in this phase, however, resulted in more pronounced strengthening, with the amount of hardening, in terms of additions of equal atomic percentages, being slightly superior to that resulting from the addition of molybdenum.

The degree of hardening which resulted from the presence of tungsten, however, in terms of equal weight percentages is very limited. This is due to the very high atomic weight of tungsten. On this basis, the effectiveness of this element, in the strengthening of α-iron is very low, being only just superior to that of chromium.

An important factor now is to consider the influence of carbon on the substitutional solid solution hardening responses of elements dissolved in α-iron. Only very small carbon contents are required for the hardening effect, due to the presence of this element, to become more pronounced than that resulting from the solid solution hardening of an element dissolved substitutionally in ferrite. Carbon is present at interstitial sites in the ferrite lattice and exerts a very pronounced hardening effect. Furthermore, the carbides formed result in appreciable strengthening.

The strengthening effect due to the presence of carbides can be reduced if these are of a large spheroidised form. In such a case, steels can have carbon contents as high as 0.1 wt. %, where a more pronounced substitutional solid solution hardening effect is being exerted than that due to the presence of carbon.

A vital point in connection with the presence of carbon is whether the alloying elements in a particular steel are

carbide formers. This depends on the relative affinities that individual elements have for iron and carbon. Consideration must now be made of these factors, along with the degrees of solid solution hardening, for the alloys employed in this research.

Vanadium was present in all the steels used in this research. The high purity alloys, with only two exceptions, had virtually the same vanadium levels. These exceptions were steels in which this element was the only alloying addition.

The solid solution hardening effects, due to vanadium being dissolved in martensite, for these alloys in the as-hardened condition, were reasonably constant. Vanadium has a considerably greater affinity for carbon than for iron, thereby meaning that V_4C_3 is very stable. Vanadium carbide is, therefore, very difficult to take into solution during austenitisation, and for this reason, the vanadium matrix contents of these steels, in the as-hardened state, did not generally vary very appreciably. This resulted in the solid solution hardening effects, due to the presence of vanadium in the martensitic matrices of these alloys, being quite consistent.

Undoubtedly, the most important series of alloys employed in this research were those of high purity, which contained vanadium and a second alloying element. An important point was now to consider the solid solution hardening effect of each of the second alloying additions.

Actually the matrix phase after tempering these alloys
for 1 hour at temperatures within the secondary hardening
range was tempered martensite, but virtually identical solid
solution hardening effects exist between elements dissolved
in this phase and in ferrite.   Furthermore, the martensitic
matrix, after tempering at temperatures between 500 and $600^{\circ}C$,
has lost a considerable degree of the tetragonality that this
phase had in the as-hardened condition, and the crystal
structure approached very closely to the body centred cubic
structure of ferrite.

A very close relationship exists between the degree of
solid solution hardening and the atomic diameters of the
elements involved, with more pronounced hardening occurring
with a larger difference in diameter between the solvent and
solute atoms.   Lattice distortion occurs due to the presence
of solute atoms and the resultant localised lattice strains
cause the solid solution hardening.

In the case where the atomic diameters of solvent and
solute atoms vary by more than 15%, only very limited solid
solubility will take place.   Appreciable hardening will,
therefore, occur but this may be more than counterbalanced
by the limitation in solubility.

Consideration can now be made of the atomic diameters
of the second alloying elements used in the high purity steels,
along with the resultant solid solution hardening effects
in ferrite.   The atomic diameters of these elements, along
with that of ferritic iron, are as follows:- α-iron 2.48,
silicon 2.35, molybdenum 2.72, manganese 2.73, nickel 2.49,

chromium 2.49, cobalt 2.49 and tungsten 2.74 $\overset{o}{A}$.

The order of effectiveness of these elements, in terms of additions of equal atomic percentages, on the solid solution hardening of ferrite is directly related to the differences in sizes of atoms of these elements with the atomic diameter of ferrite. This is in close agreement to the orders given by Lacy and Gensamer [170] and Rees, Hopkins and Tipler [172] for equivalent atomic percentage additions, for although their results differed slightly, the overall patterns were very similar. Furthermore, phosphorus gives the highest degree of solid solution hardening in ferrite of any element present in commercial purity steels, and the atomic diameter of this element is only 2.18 $\overset{o}{A}$, being considerably smaller than that of ferritic iron.

There is very little doubt over the order of effect, of the elements used as second alloying additions in the high purity steels on the solid solution hardening of ferrite in terms of additions of equal weight percentages. The full list, in order of increased hardening effect is chromium, tungsten, nickel, cobalt, molybdenum, manganese and silicon.

The relationship between the secondary hardening responses of these high purity steels and the solid solution hardening effect in ferrite of the second alloying addition, provides some very important information, as the former was seen to be very dependant on the latter. A fact which should be mentioned here is that all the additions were in terms of equal weight percentages (1 wt. %), with the exception of tungsten, which was present at 2 wt. %.

Comparisons of the magnitudes of the secondary hardening peaks of these alloys, after optimum prior austenitisation, revealed the following order, in terms of increasing secondary hardening response as a function of the second alloying addition:- nickel, silicon, cobalt, chromium, manganese, tungsten and molybdenum. Even more revealing is to consider the ΔH values, which take into account the softening of the steels at tempering temperatures just below the secondary hardening range. The corresponding order in this case is chromium, cobalt, nickel, tungsten, molybdenum, manganese and silicon.

Some slight similarity exists between the order in terms of the magnitudes of the secondary hardening peaks and the solid solution hardening effects in ferrite of the second alloying elements. However, there is a very close relationship between this latter phenomenon and the ΔH values for these steels. The orders of effectiveness of the second alloying additions on these factors are virtually identical, with only the position of tungsten being misplaced. Furthermore, these orders are identical when comparisons are made between these elements for additions of equal weight percentages.

A further fact is that the ΔH values for these steels, after prior austenitisation at 1200°C, are very similar to those already mentioned. The only exceptions are that chromium gives a fractionally superior secondary hardening response to nickel and cobalt, and molybdenum is slightly better in this respect than manganese, in vanadium steels.

Direct comparisons between the effects that the second alloying additons, which were non-carbide forming elements, had on the secondary hardening of vanadium steels is fully justified. Only fractional amounts of these elements were present in V_4C_3, and the partitioning of each of these elements was very strongly in favour of the matrix phase in these alloys. The order, therefore, in terms of increased secondary hardening response, can be given conclusively as follows:- nickel, cobalt, manganese and silicon.

However, in the cases where the second alloying element is a carbide former, the situation is more complex. This is due to two factors, the first of these being the secondary hardening effect due to the precipitation of the carbide of the second alloying addition (i.e. Mo_2C, Cr_7C_3 and W_2C). In the second place is the consideration of the levels of these elements which are dissolved in the matrices of the steels.

The hardening effects due to the precipitation of these three carbides have already been discussed. Results showing the partitioning of molybdenum, chromium and tungsten between the carbide and matrix phases of these steels are very relevant to this consideration. The vast proportion of chromium was present in the matrix phase after optimum austenitisation. Partitioning of molybdenum and tungsten, however, were more in favour of the carbide phases, for all austenitising temperatures with the exception of $1200^\circ C$.

A consideration should now be made of each of these elements in turn. Chromium dissolves quite readily in ferrite but the resultant amount of solid solution hardening

is low. This element gives a very limited degree of precipitation hardening on its own account, and the important point now is to consider these factors in terms of the effect of this element on the secondary hardening response of a vanadium steel.

A combination of these phenomena, due to the presence of chromium, only leads to very limited secondary hardening of a vanadium steel. The fact that chromium appeared higher than some of the other elements, in the order of increasing effectiveness on the secondary hardening responses of these steels, was entirely attributable to the hardening caused by the precipitation of Cr_7C_3. Chromium had the least pronounced effect of the elements investigated, in improving the secondary hardening of vanadium steels, as confirmed by the ΔH values.

The situation was even more complex with respect to molybdenum and tungsten. Consideration of the degrees of secondary hardening due to the precipitation of Mo_2C and W_2C and the solid solution hardening of the matrices due to the presence of these elements was difficult to accurately assess.

Even the low molybdenum and tungsten matrix contents of these steels, after optimum austenitisation, resulted in appreciable solid solution hardening taking place. Nevertheless, this effect did not have quite the same significance on the degree of secondary hardening of these alloys as the hardening caused by the precipitation of Mo_2C and W_2C, which

was appreciable.

Prior austenitisation at $1200^{\circ}C$ caused appreciable solubility of Mo_2C and W_2C, with resultant high levels of solid solution hardening of the martensite matrices. Tempering these steels after this treatment resulted in the occurrence of very appreciable secondary hardening peaks. This high degree of secondary hardening was very much an indirect function of the solid solution hardening effect in martensite of molybdenum and tungsten.

Elimination of the secondary hardening effect due to the precipitation of Mo_2C and W_2C in these alloys, provided a very interesting conclusion to be drawn. This was that the contributions of these elements, in terms of equal weight percentages, on the secondary hardening responses of vanadium steels, were exactly as given by the order of effectiveness of these on the solid solution hardening of ferrite.

Tungsten, therefore, was only slightly more effective than chromium in improving the secondary hardening, resulting from the precipitation of V_4C_3 in vanadium steels. The effect of molybdenum in this respect was intermediate between those of cobalt and manganese.

The final consideration to be made in this section is why an element which gives pronounced solid solution hardening in ferrite should greatly increase the nucleation rate of V_4C_3. This is in fact very much a function of the inter- actions between solute atoms and dislocations.

There is an interaction between subsitutional solute atoms and dislocations of the edge orientation. A solute

atom, of different atomic diameter to the solvent atoms, causes distortion of the lattice of the latter with resultant strain. These distortions may be partially removed if the solute atom is positioned close to the centre of a dislocation.

The overall outcome is that the free energy of the crystal will be lowered when a small solute atom takes the place of a larger solvent atom in the compressed region of a dislocation in, or even close to, the extra plane of a dislocation. In a similar manner, large solvent atoms are attracted to lattice positions below the edge, the expanded area of the dislocation.

There is little reaction between substitutional solute atoms and screw dislocations. The presence of substitutional atoms causes a lattice distortion which is spherical in shape, whilst the strain field due to a screw dislocation is nearly pure shear. A condition of pure shear is equivalent to two equal principal strains, one of these being tensile and the other compressive. Lattice strains of this nature will not react appreciably with the spherical strain produced as a result of the presence of substitutional solute atoms.

Solute atoms, however, are attracted towards edge dislocations due to the interactions of the respective strain fields. The rate of movement of the solute atoms under these attractive forces is governed by the rate at which they can diffuse through the lattice. This means at high temperatures, where diffusion rates are rapid, the solute atoms concentrate quickly round dislocations.

These regions of solute atoms segregated round dislocations can act as nucleation sites for another phase. This is particularly the case when solute atoms have a mutual attraction. The dislocations, therefore, act as sinks for solute atoms, and unidirectional flow occurs towards the dislocations. Diffusion continues until the solute concentration in the crystal is reduced to the point where this is in equilibrium with the newly formed phase.

The fact that greater volume fractions of V_4C_3 were precipitated in steels containing vanadium and a second alloying addition than in steels containing only vanadium supports this theory. Clearly the greater the solid solution hardening effect of the second alloying addition, the higher the nucleation rate of V_4C_3. This means that raising the free energy of the matrix lattice by the presence of solute atoms, results in an increase in the nucleation rate of V_4C_3.

Vanadium carbide nucleates originally to reduce the free energy in the regions where solute atoms are present along with dislocations. The V_4C_3 particles are of very small size ($\approx 20 \overset{o}{A}$) and are coherent with the matrix. However, the particles grow with further tempering with the result that marked precipitation hardening takes place. Maximum hardening occurs when the particles are at the largest size at which coherency can be maintained with the matrix.

Electron microscopy results confirmed that V_4C_3 particles nucleated on dislocations. The fact that only a small volume fraction of these particles precipitated in steels containing only vanadium suggested that a high dislocation density alone

was insufficient to create a high nucleation rate of V_4C_3.
The presence of solute atoms in the regions of dislocations
was essential to produce this high nucleation rate with
resultant precipitation hardening.

A mention should be made here of aluminium, the atomic
diameter of which is only just within the favourable size
zone to form a complete substitutional solid solution in
ferritic iron. This element, therefore, results in very
marked solid solution hardening of ferrite, and on this basis
could have been expected to improve the secondary hardening
responses of the commercial purity steels employed in this
research, as a result of increasing the nucleation rate of
V_4C_3.

The fact that this did not occur was due to the solid
solution hardening effect of aluminium in the matrices of
these steels being considerably less than those of silicon
and manganese. Both these elements were present at much
greater concentrations in these steels than was aluminium.
Silicon and manganese have been found to have the greatest
effect on the nucleation rate of V_4C_3, of the elements
investigated in this research, and both were responsible for
the very appreciable degrees of secondary hardening which
occurred in the commercial purity steels with vanadium contents
between 0.53 and 1.13 wt. %.

5.5 Factors Influencing the Solubility of Vanadium Carbide in Austenite

Several processes occur during the dissolution of carbides. Firstly the bonds in the carbide lattice, between metal atoms and carbon are broken, and these elements go into solid solution. Carbon and the corresponding alloying element diffuse from the carbide/austenite interface into the austenite, and iron diffuses towards the boundary.

The bonds between metal and carbon atoms in the carbide lattice must, therefore, be broken before the diffusion processes come into operation in the dissolution of carbides in austenite. Carbon has a small atomic diameter and the diffusion rate of this element from carbide to austenite is high, with diffusion taking place via interstices in the austenite. However, the kinetics of the diffusion of metal atoms in this direction from the carbide/austenite interface are much lower, owing to the greater diameter of these atoms. This means that, of the diffusion processes occurring in carbide dissolution in austenite, the diffusion of metal atoms is the rate controlling process.

An important factor was to ascertain whether the elements employed in the steels in this research had an effect on the strength of the bonds between vanadium and carbon atoms in the V_4C_3 lattice. In addition, determination of whether the composition of the austenite affected the transfer and diffusion of vanadium and carbon atoms during the dissolution of V_4C_3 was crucial. The significance of more pronounced solubility of V_4C_3 during austenitisation was that this would

lead to a higher vanadium content in the martensitic matrix of the steel in the as-hardened condition. More vanadium, therefore, would be available to react with carbon in the formation of V_4C_3 during tempering, with resultant improved precipitation hardening response.

Only a very small amount of vanadium was present in the ferritic matrices of all the high purity steels, in the annealed state, with the vast proportion of vanadium being in the form of V_4C_3. Very little dissolution of V_4C_3 occurred at austenitising temperatures below $1150^{\circ}C$, and appreciable solubility did not take place until the employment of an austenitisation temperature of $1200^{\circ}C$.

Soaking time was considerably less important than austenitisation temperature in governing the dissolution of V_4C_3 in austenite. Employment of soaking times of 30 and 45 minutes, at varying temperatures, for steels in which vanadium was the only alloying addition, only slightly increased the dissolution rate of V_4C_3 in austenite, compared with that obtained after a soak for 20 minutes.

An increase in the vanadium content of steels which contained only vanadium as an alloying addition, resulted in higher levels of this element in the martensitic matrices, when austenitisation was carried out at temperatures of $1150^{\circ}C$ and above. Proportionally, however, these increases were less pronounced than the ratios of the vanadium contents of these alloys.

The individual additions of manganese, nickel, chromium and cobalt to steels containing vanadium, increased the

dissolution rate of V_4C_3 in austenite at temperatures in
excess of $1100^{\circ}C$. Particularly effective in this respect
~~dissolution rate of V_4C_3 in austenite at temperatures in~~
were nickel and cobalt.

Molybdenum, tungsten and silicon decreased the dissolution rate of V_4C_3 in austenite to similar degrees, with one exception. This was in the steel which contained both vanadium and silicon after austenitisation at $1150^{\circ}C$, for only very slight dissolution of V_4C_3 took place after this treatment. Appreciable dissolution of this carbide occurred after austenitisation at $1200^{\circ}C$, but nevertheless the matrix vanadium content of this steel was lower than those of all the other alloys after corresponding high temperature treatments.

The non-carbide forming elements had the effect of weakening the interatomic bonds between vanadium and carbon atoms in the V_4C_3 lattice, with resultant increase in the kinetics of dissolution of this carbide in austenite. On this basis, manganese would be expected to have the least effect of these elements, with the exception of silicon. In fact, silicon is a stronger carbide former than manganese but this former element has a greater affinity to stabilise ferrite than to react with carbon.

Chromium is a carbide forming element and is quite soluble in V_4C_3. The fact that this element is not a very strong carbide former coupled with the moderately high solubility of chromium in V_4C_3, is sufficient to weaken the interatomic bonds in this carbide lattice, with resultant improvement in the kinetics of the dissolution of V_4C_3 in austenite. Solution of Cr_7C_3 commenced at $900^{\circ}C$ and was complete at $1100^{\circ}C$, which is a very similar temperature range

to that required for the dissolution of chromium carbides in high speed steels.

Molybdenum and tungsten, however, are such strong carbide formers that even the quite high solubilities of these elements in V_4C_3 are not sufficient to reduce the interatomic bond strengths between atoms in the V_4C_3 lattice. Furthermore, the dissolution rates of Mo_2C and W_2C were only slightly in excess of that of V_4C_3 during austenitisation, with intense solution of the former two carbides only occuring at $1200^{\circ}C$.

5.5.1   The Effect of Austenite Composition

Consideration must also be made of the effect of the composition of the austenite on the diffusion of vanadium atoms from V_4C_3 into austenite. In the first place, if the diffusion coefficient of vanadium in austenite is independent of concentration, then the concentration distribution for semi-infinite solids is given by Equation 14:-

$$C = C_b \left[1 - \text{erf.} \ (Z) \right] \qquad \ldots\ldots\text{Equation 14.}$$

Where C_b = The boundary concentration of the diffusing element.

erf. (Z) = The function of error.

The relationship between Z, the diffusion coefficient and time is as follows:-

$$Z = \frac{x}{2 \ (Dt)^{\frac{1}{2}}} \qquad \ldots\ldots\text{Equation 15.}$$

Where x = Diffusional distance of the particular element.
  D = Diffusion coefficient.

  t = Time.

Graphs are presented in FIGS. 18c to 191, showing the relationships between $\log_{10}$ [matrix vanadium content] and the reciprocal of the austenitisation temperature in $^{\circ}A$, for Alloys 1, 3, 4(Si), 6(Mn), 7(Ni) and 9(Co). These graphs allow several important observations to be made on the solution of V_4C_3 during austenitisation.

There was an increase in the matrix vanadium content of Alloy 1 after austenitisation in the temperature range 850 to 950°C. The reason was that this steel contained quite a high volume fraction of cementite in the annealed condition, and this carbide dissolved at these low temperatures Vanadium atoms can replace some of the iron atoms in the cementite lattice, thereby causing an increase in the matrix vanadium content when this carbide dissolves.

The graphs for the other alloys, however, were virtually of a plateau form after austenitising in this corresponding temperature range. This was because these steels had higher vanadium levels than Alloy 1, resulting in less free carbon being available to react with iron to form Fe_3C.

All the graphs were of a plateau form for austenitisation temperatures between 950 and 1100°C. Vanadium carbide was very stable in this temperature range, with the rate controlling step for dissolution being the bond strength between metal and carbon atoms in the carbide lattice.

However, austenitising at temperatures slightly in excess of 1100°C caused a reduction in bond strength between atoms in the V_4C_3 lattice in all the steels, with commencement of solution of V_4C_3 . Most effective in this respect were the

steels containing non-carbide forming elements, and in particular nickel and cobalt, as these had the least affinity for carbon of the alloying elements employed in the high purity steels.

There was a change, therefore, in the rate controlling step for the dissolution of V_4C_3 at temperatures slightly in excess of $1100^{\circ}C$, with the crucial stage becoming the diffusion rate of vanadium atoms from the carbide to austenite. The graphs for all the steels, with the exception of that containing silicon, were close to linearality at increased temperatures up to and including $1200^{\circ}C$, indicating no further change in the rate controlling step.

In the case of the alloy in which silicon was present, there was an appreciable increase in the solubility of V_4C_3 on austenitising between 1150 and $1200^{\circ}C$, compared with in the immediately preceding temperature region. The limited solubility of V_4C_3 in the range 1100 to $1150^{\circ}C$ was due to the retardation effect of silicon on the diffusion rate of vanadium atoms away from the carbide lattice and into austenite. This was nullified at temperatures in excess of $1150^{\circ}C$, as the diffusion rate of vanadium atoms was greatly increased, so much so that the effect of silicon in causing localised contraction of the austenite lattice became insignificant.

Graphs of $\log_{10}\left[\text{matrix vanadium content}\right]$ allow very approximate comparisons to be made for the changes in activation energy for the solution of V_4C_3 at varying austenitisation temperatures. The time for a pre-determined percentage

solution of V_4C_3 during austenitising was not determined for steels in this research, so activation energies could not be calculated with any degree of accuracy.

A factor, however, of more significance in this research, was the determination of the equilibrium temperature for the solution of V_4C_3 in the alloys. The equilibrium temperature was obtained by extending the graph in the austenitisation temperature range 1150 to 1200°C to meet the line (or extension of the line) for temperatures between 950 and 1100°C. Therefore, the equilibrium temperature gives a guide as to the temperature for the onset of solution of V_4C_3 during austenitisation.

The calculated equilibrium temperatures were 1124, 1115, 1135 and 1112 for Alloys 1, 3, 4(Si) and 6(Mn) respectively, and 1100°C for both Alloys 7(Ni) and 9(Co). These temperatures clearly confirm the beneficial effect of nickel and cobalt additions in increasing the solution rate of V_4C_3, and also the deleterious effect of the presence of silicon in this respect.

The solubility of V_4C_3 during austenitisation of the steels employed in this research was in excess of that achieved in high speed steels. This is because of the presence of large volume fractions of carbides in the latter steels, and the comparative solution rates of these during austenitisation. Vanadium carbide is the most stable of these carbides, and only limited solubility of V_4C_3 can be expected in an austenite lattice partially saturated by the dissolution of less stable carbides.

5.6 The Significance of the Matrix Vanadium Content of the Steels on the Resultant Secondary Hardening Responses

The importance of the matrix vanadium content on secondary hardening response was clearly illustrated in results obtained from the high purity steels which contained vanadium and a second alloying element. Prior austenitising these steels at $1200^{\circ}C$ resulted in markedly superior secondary hardening responses on tempering than those obtained after optimum prior austenitisation.

This was most clearly shown by the alloy which contained silicon, as only limited secondary hardening occurred on tempering this steel after previously employing an optimum austenitisation treatment. Only very limited dissolution of V_4C_3 resulted from this austenitising treatment but much more appreciable solubility of this carbide took place after austenitisation at $1200^{\circ}C$. This resulted in a considerably higher vanadium content in the martensitic matrix of the steel in the as-hardened condition, with a very appreciable secondary hardening response being achieved after tempering in the range 500 to $600^{\circ}C$.

However, a high matrix vanadium level for a steel, in the as-hardened state, is only significant if a considerable number of nucleation sites are available for V_4C_3 embryo, during tempering. This was the case for the steels which contained another alloying element apart from vanadium. The presence of each of the secondary alloying additions resulted in solid solution hardening of the matrix, and the regions of lattice distortion were nucleation sites for V_4C_3 embryo.

The steels which only contained vanadium as an alloying addition did not give true secondary hardening on tempering in the critical temperature range, after ideal prior austenitisation. An increase in the austenitising temperature to 1200°C only resulted in very slight hardening peaks occurring on tempering. These steels contained quite high matrix vanadium contents after this austenitisation treatment, with in each case a higher proportion of vanadium dissolved in the matrix than in the form of carbide. This was insufficient, however, to give a good secondary hardening response due to the shortage of sites for the nucleation of V_4C_3.

Further vindication of the significance of the effect of matrix analysis on secondary hardening response was given by the tempering hardness results for the commercial purity steels. These alloys (with the exception of those containing only 0.05 and 0.06 wt. % vanadium) secondary hardened to marked degrees on tempering between 500 and 600°C, and also showed hardening peaks during long term tempering. These results were partially due to the high matrix vanadium levels of these steels, but the major factor was the quite high silicon and manganese contents of the matrices, which allowed the vanadium dissolved in the matrices to be fully utilised by the provision of sufficient nucleation sites.

Vanadium was present at high levels in the matrices of these steels as a direct result of the low carbon contents in the as-cast condition. This meant that very little carbon was available to react with vanadium to form V_4C_3, thereby resulting in the vast proportion of vanadium being dissolved

in the ferritic matrix. Carburising these steels at 920$^{\mathrm{o}}$C
for 24 hours did not appreciably alter this situation, although
some fine V_4C_3 particles did precipitate during cooling from
this temperature.

5.7 The Graphitisation of Steels Containing Vanadium

A very surprising aspect of this research was that some of the high purity vanadium steels graphitised during long term tempering at $560^{O}C$. Vanadium is a very strong carbide-forming element and the graphitisation of these steels, therefore, is very unusual.

Each of the high purity steels which contained only vanadium as an alloying addition, graphitised during long term tempering at $560^{O}C$. These steels had effectively the same carbon contents but varying vanadium levels. The tempering time required for the commencement of graphitisation decreased with a reduction in the vanadium level of the alloy. Furthermore, tempering these steels for corresponding periods of time revealed that both the volume fraction and size of the graphite rosettes were greater with a decrease in the vanadium content of the alloy.

The addition of molybdenum, manganese, chromium or tungsten to a high purity vanadium steel prevented graphite formation during long term tempering, even after a period of 220 hours. In addition, none of the commercial purity alloys graphitised as a result of this tempering process.

However, the presence of silicon, nickel or cobalt in vanadium steels still caused graphitisation to occur during long term tempering. The addition of cobalt resulted in graphite formation after tempering for a period of 100 hours, which was the same time required for the steel which only contained vanadium as an alloying addition. A slightly longer time of 120 hours was necessary for this phenomenon

Graphite forms in these steels due to the high carbon and silicon contents, and in one case the high nickel level. Even the presence of the carbide-forming elements molybdenum, chromium and tungsten is not sufficient to totally counteract the graphitisation effects of carbon, silicon and nickel, with the result that a relatively high proportion of the carbon present in the alloys is in the form of free graphite rather than carbide.

However, the high purity steels employed in this research, with only one exception, contained considerably greater atomic percentages of carbide-forming element(s) than was the case for the graphitic tool steels. The carbide-forming element in the high purity steels was vanadium, which has a greater affinity for reaction with carbon than molybdenum, chromium and tungsten, which are present in the graphitic tool steels.

Furthermore, the high purity alloys only had carbon contents of approximately one half of those of the graphitic tool steels, yet graphite formed in these former steels after treatment at a temperature of only $560^{\circ}C$. In the case of the graphitic tool steels, annealing or normalising in a temperature range of 800 to $950^{\circ}C$ only resulted in partial transformation of carbide to graphite. All these factors, therefore, made the formation, and the ease with which this occurred, of graphite in steels containing vanadium very unusual.

The vanadium : carbon ratio was not a controlling factor on whether the steels graphitised. Certainly graphitisation was most appreciable in the high purity steels which contained only vanadium as an alloying addition, at low vanadium : carbon

ratios.   However, none of the commercial purity alloys
graphitised during long term tempering at 560°C, and some of
these contained only small amounts of vanadium.   Graphite
was not present in these steels even at positions in the
carburised cases with high carbon contents (1.5 wt. %).

The original theory as an explanation for the graphiti-
sation of these steels, was that cementite had been the source
of graphite formation.   Cementite is not a true equilibrium
phase and is not as stable as graphite, and employment of the
correct conditions causes the former phase to decompose into
graphite.

This transformation never takes place in the vast majority
of steels.   The reason is that the nucleation of cementite in
iron, supersaturated with carbon, occurs much more readily than
the nucleation of graphite.   When carbon is precipitated from
solid solutions of ferrite or austenite, the resultant phase
is nearly always cementite, or alloy carbides but not graphite.
Once cementite has formed this phase is stable, and may be
considered for practical purposes as an equilibrium phase.

However, cementite is considerably less stable than
vanadium carbide and this latter carbide certainly would not
be expected to decompose into graphite.   In these steels,
therefore, the most likely occurrence was that cementite had
decomposed into graphite, with iron diffusing into the matrix
during long term tempering at 560°C.

The fact that cementite was found to be present, by means
of electron microscopy, in only one of the high purity alloys
after tempering at 560°C, disproved this theory.   This was

the steel which contained chromium and in fact this did not graphitise. The phase which had decomposed into graphite was undoubtedly primary vanadium carbide, for the graphite particles were present in many cases in the form of stringers, with the same directionality as that induced on the carbides by hot working.

There were also two other important aspects to the long term tempering results, apart from the fact that graphite formed in some of vanadium steels. The alloys which contained silicon, nickel or cobalt did not graphitise to such an extent as those where vanadium was the only alloying addition. These three elements are all strong graphitisers and were expected to cause more pronounced graphitisation of high purity vanadium steels.

The second factor concerns manganese, the addition of which to a high purity vanadium steel prevented graphitisation. This was a slight surprise as manganese aided the dissolution of V_4C_3 during austenitisation. Manganese, nickel and cobalt in fact all increased the dissolution of V_4C_3 during austenitisation and this fact must be used in the consideration of the effect of these elements on graphitisation.

Similar mechanisms are involved in a carbide going into solution during austenitisation and a carbide decomposing into graphite. The only difference is that in graphite formation the carbon atoms do not diffuse away, along with the metal atoms, from the carbide lattice and into the matrix.

There are three vital factors, therefore, in controlling graphite formation. These are the bond strength between

metal and carbon atoms in the carbide lattice, the degree
of saturation of the matrix, and the graphite stabilising
effects of the other elements present in the steel.

Silicon, nickel and cobalt are all strong graphitising
elements and also reduce the bond strength between vanadium
and carbon atoms in the V_4C_3 lattice. However, the vast
proportions of these elements, present in the high purity
alloys in the as-hardened condition, were dissolved in the
martensitic matrices. This meant that partial saturation
of this phase occurred, causing a restriction on the amount
of vanadium which could dissolve in the matrices during
tempering.

Vanadium atoms, therefore, diffused from V_4C_3 in to the
matrix of each of these steels, until partial saturation of the
martensite took place. When this occurred vanadium atoms
could no longer readily diffuse from the carbide, and so the
graphitisation was restricted. This factor more than counter-
acted the other two effects of these elements on graphitisation
and was responsible for the fact that the addition of silicon,
nickel or cobalt did not cause more pronounced graphitisation
of vanadium steels.

A greater amount of vanadium could diffuse from the
vanadium carbides to allow graphite to form in the high purity
steels which only contained vanadium as an alloying addition,
as the martensitic matrices were not partially saturated by
the presence of a non-carbide forming alloying addition.
The fact that graphitisation was more pronounced in these
steels with a reduction in the vanadium content, was due to
the matrix being less saturated with the lower the level of this

element in the alloy, therefore, enabling this phase to accept more vanadium atoms from the carbides.

Very little manganese dissolved in V_4C_3, with the vast proportion of this element present in the steel, being dissolved in the matrix. Manganese did have an effect in increasing the dissolution of V_4C_3 during austenitisation, as a result of decreasing the bond strength between vanadium and carbon atoms in the carbide lattice. This effect was quite pronounced as more manganese was dissolved in this carbide than was the case of silicon, nickel or cobalt.

The stability of carbides during austenitisation can only partially be compared with stability and resistance to graphitisation on tempering. This is because the solubility of elements in austenite is greater than in ferrite or martensite, and a considerable number of vanadium atoms can diffuse from primary vanadium carbides before saturation of the matrix lattice occurs during austenitisation. Saturation of the ferrite matrix occurs at much lower concentrations of vanadium, particularly if a non-carbide forming element is present in the steel.

Manganese is a stronger carbide-forming element in steel than silicon, nickel or cobalt. Of even more importance is the fact that the solubility of manganese in ferrite is less pronounced than that of nickel or cobalt in this phase. This is because the atomic diameter of manganese varies more with that of ferritic iron than do those of nickel and cobalt. Binary equilibrium diagrams are shown for iron-manganese and iron-nickel in FIGS. 192 and 193.

The presence, therefore, of over 1 wt. % of manganese in the martensitic matrix was a crucial factor in preventing graphitisation taking place. This element also caused the most appreciable dissolution of V_4C_3 during austenitisation, thereby meaning that the matrix vanadium content of this steel was higher than those of the other alloys. The martensitic matrix saturation due to the presence of manganese and vanadium was sufficient to prevent any further solubility of vanadium atoms, preventing diffusion of these atoms from the V_4C_3 lattice and also preventing graphitisation.

Graphitisation did not occur during long term tempering of the commercial purity steels and this was undoubtedly due to the presence of manganese in these alloys. The manganese was sufficient to prevent graphitisation at positions within the carburised cases where the carbon contents were high.

Silicon has, like manganese, limited solubility in ferrite, owing to the quite large difference in atomic radius of this element compared to that of ferritic iron. The graphite stabilising effect of silicon, however, was still sufficient to cause graphitisation in a vanadium steel containing this element. However, the limited solubility of manganese in ferrite coupled with the fact that this element does not stabilise graphite, resulted in manganese preventing graphitisation of a vanadium steel.

Hypothetical free energy curves are shown in FIG. 194 for a tempering treatment where graphite formation is about to commence. The free energy of graphite is lower than that of V_4C_3 for this tempering temperature and time, but the highest

free energy curve is for the dissolution of vanadium in the martensitic or ferritic matrix. Only if this free energy can be surpassed will graphitisation occur, and this free energy will be very high if the matrix is already saturated with a non-carbide forming element. In such cases graphitisation will be restricted or not take place at all.

The addition of molybdenum, chromium or tungsten to a vanadium steel prevented graphitisation occurring on long term tempering. These elements are strong carbide-formers, and do not weaken the bonds between metal and carbon atoms in the V_4C_3 lattice. These elements, therefore, do not stabilise graphite, and also restrict the dissolution of V_4C_3 in austenite. This latter fact means that the matrices of these alloys have lower vanadium contents in the as-hardened condition, than was the case for the other steels. All these factors contribute to molybdenum, chromium and tungsten preventing graphitisation of vanadium steels.

5.8 Application of the Results from this Research to High Speed Tool Steels

5.8.1 Secondary Hardening Response

The major contribution to the secondary hardening of high speed steels is the hardening caused by the precipitation of V_4C_3. Precipitation of this carbide is vitally dependant on the availability of nucleation sites within the martensitic matrix. This research has shown that these sites are dislocations surrounding solute atoms, and that the nucleation rate of V_4C_3 increases with the presence in the steel of elements which have atomic diameters varying considerably with that of ferritic iron. Non-carbide forming elements are particularly significant in this respect, as these are virtually completely dissolved in the matrix, whilst elements which are carbide-formers are not present in the matrix to such high degrees.

Cobalt is an element which has been known for some time to improve the secondary hardening response of high speed steels. This element is present in many of these alloys at concentrations between 5 and 12 wt. %. Some examples of steels which contain cobalt are T4, T5, T6, T15, M30 and M33.

No conclusive explanation has been presented as to why cobalt has a beneficial effect on the degree of secondary hardening of these steels, although there are two postulations. The first of these is that this element retards the growth of the secondary hardening precipitates W_2C, Mo_2C and V_4C_3. This was thought to improve both the secondary and hot hardnesses of high speed steels.

Cobalt is also known to increase the melting point of high speed steels, thereby allowing the employment of higher austenitisation temperatures. The resultant of this is increased solution of primary M_6C and V_4C_3 during austenitisation, with higher martensitic matrices contents of molybdenum, tungsten and vanadium for these steels in the as-hardened condition. Then higher matrices contents of these elements leads to a greater volume fraction of secondary hardening carbides precipitating on tempering between 550 and $600^{\circ}C$.

However, the results obtained from this research suggest that neither of these effects of cobalt is vitally important in explaining the effect of this element on secondary hardening. Even though no high speed steels were employed in this research, an explanation can be given as to why cobalt improves the secondary hardening response of high speed steels.

Cobalt does not cause very pronounced lattice distortion and solid solution hardening when dissolved in ferrite. However, when present in high speed steels at the appreciable concentrations of between 5 and 12 wt. %, the solid solution hardening effect of this element in the martensitic matrix will be quite considerable. The regions of lattice distortion due to the presence of cobalt atoms, have high energies and act as nucleation sites for the secondary hardening carbides. This increased nucleation rate for Mo_2C, W_2C and V_4C_3 improves the secondary hardening response of the steel.

On this basis, therefore, exists the possibility of improving the degree of secondary hardening of high speed

steels. Silicon and manganese additions improve the secondary hardening responses of vanadium steels to a greater extent than does cobalt. These two elements are present at relatively small levels (0.3 wt. %) in high speed steels, and increasing these additions would lead to even more pronounced secondary hardening. Cobalt could still be employed as an alloying addition, but at lower levels than 5 wt. %, thereby still allowing some beneficial effect in the employment of higher austenitising temperatures.

Excessively high austenitisation temperatures are to be avoided because of the increase in retained austenite. This means that very high cobalt contents are not necessary, and in any case, in terms of increasing the nucleation rate of V_4C_3, silicon and manganese are more effective than cobalt. The manganese content, however, should be restricted to 2 wt.% to avoid an increase in retained austenite, which even in normal high speed steels is excessively high at a volume fraction of 15 to 25%.

5.8.2 The Dissolution of Primary Carbides During Austenitisation

The primary carbides M_6C and V_4C_3 are difficult to take into solution during the austenitisation of high speed steels, this particularly being the case for the latter of these carbides. Great importance surrounds the dissolution of these carbides, as optimum secondary hardening cannot be achieved unless the matrix is sufficiently enriched with metal and carbon atoms, which have diffused from primary carbides during

austenitisation.

High speed steels contain large concentrations of carbide-forming elements. Results from this research have shown that adding a second strong carbide-forming element (tungsten or molybdenum) to a vanadium steel, reduces the dissolution rate of V_4C_3. Application of this to high speed steels shows the great problem in alloying high speed steels in a manner to increase the dissolution rate of the stable primary carbides present.

Fortunately the elements which increased the nucleation rate of V_4C_3 on tempering, also increased the dissolution rate of V_4C_3 during austenitisation, with one exception. This was silicon, which had the most pronounced effect in increasing the nucleation rate of V_4C_3 during tempering.

High speed steels are austenitised in the temperature range 1220 to $1300^{\circ}C$, and at such elevated temperatures silicon willnot have such a pronounced retardation effect on the dissolution rate of V_4C_3. These steels, therefore, could contain quite appreciable silicon contents, providing correct alloying is achieved with manganese, cobalt or even nickel, and still have improved dissolution rates for primary carbides than occur in current high speed steels.

The maximum silicon content to be employed is 2 wt. %, and a manganese level of 1 to 2 wt. %, whilst small additions of cobalt or nickel could also be made to prevent silicon having a retardation effect on the dissolution of primary carbides. There is a small group of silicon tool steels,

but these alloys only have very small concentrations of carbide-forming elements present. Little research has been undertaken on these steels and the effect of silicon on carbide precipitation during tempering has not been appreciated.

5.8.3   The Economics of High Speed Steels

High speed steels are very costly materials. These steels contain appreciable concentrations of alloying additions and these are very expensive. The current prices of the alloying additions employed in high speed steels, for a weight of 1 kilogram of metal in each case, are as follows:- ferro-molybdenum £7.00, ferro-vanadium £6.50, ferro-tungsten £11.80, ferro-chrome £0.865 and cobalt £7.51.

The high prices of ferro-molybdenum, ferro-vanadium, ferro-tungsten and cobalt have given great importance to research to try and reduce the cost of these steels, without impairing the metal cutting properties. These attempts have been to reduce the concentration of the alloying additions made to these steels, in the development of the so-termed semi-high speed steels.

This research has illustrated the importance of alloying a steel to the requirements of the stoichiometric ratio of the carbide concerned, in order to obtain optimum secondary hardening response. High speed steels generally have metal : carbon ratios in excess of the stoichiometric requirement for the carbides concerned. This results in excess primary carbide in the steels, which is helpful in giving good wear resistance. However, this is not as important in this respect

as the matrix composition, which also governs secondary hardening response and hot hardness.

Stoichiometric alloying would, therefore, give a slight reduction in the cost of high speed steels. This, however, would be less pronounced than the cost reduction by raising the silicon and manganese contents and reducing the molybdenum and tungsten levels. Ferro-silicon and ferro-manganese are both cheap alloying additions, the prices being £0.31 and £0.26 per kilogram of silicon and manganese respectively.

Stoichiometric alloying of a steel containing 0.85 carbon, 1/2 silicon and 1/2 wt. % manganese could be achieved by making carbide-forming additions to levels of 3.0 vanadium, 2.0 chromium, 2.0 tungsten and 1.0 molybdenum. This would allow the beneficial effect of silicon and manganese on secondary hardening response to be achieved. Furthermore, vanadium would be present at a concentration greater than those of the other carbide-forming elements, and this would be significant as this element contributes the most to the secondary hardening of high speed steels.

Tungsten and molybdenum are present in this steel to allow two more secondary hardening carbides to precipitate on tempering. This effect tends to give improved secondary hardening than that due to the precipitation of just one carbide. Chromium is present to increase the dissolution rate of the primary carbides during austenitisation, increase hardenability, cause resistance to tempering by precipitation of $M_{23}C_6$ and reduction in the amount of scaling during annealing

and hardening.   This element is always present in high
speed steels at 4 to 4.5 wt. %, but reduction in this concentration would be more than compensated by the higher
vanadium, silicon and manganese levels.

Such a steel would be considerably cheaper than high
speed steel, costing only £531 for alloying additions per
tonne of steel, compared with £1223 for M2 high speed steel.
In fact M2 is one of the cheaper high speed steels, as this
is not one of the super grades and does not contain cobalt.
This low alloy tool steel should be capable of meeting most
tooling applications such as drills, reamers, hacksaw blades,
slitting cutters etc. and may even be able to cope with the
demands of tool bits, for which hot hardness and wear resistanc
are at a premium.

6. Conclusions

The main inference to be drawn from this research is that high purity vanadium steels do not show true secondary hardening peaks on tempering in the temperature range 500 to 600°C. These steels had vanadium : carbon ratios below the stoichiometric ratio for V_4C_3, but nevertheless the fact that these alloys did not secondary harden was very surprising.

Commercial purity steels did show secondary hardening peaks, with just two exceptions, over a wide range of vanadium and carbon contents. The exceptions were alloys which had the very low vanadium levels of 0.05 and 0.06 wt. %. In some instances the secondary hardening peaks were appreciable, with these being optimum at positions in the carburised cases where the vanadium : carbon ratio was either at, or very close to, the stoichiometric ratio for V_4C_3. This clearly illustrates the importance of alloying a steel in such a manner as to attain the stoichiometric ratio for the carbide(s) concerned, if optimum secondary hardening is to be achieved.

Each of the high purity steels which contained vanadium plus a second alloying addition, showed a true secondary hardening peak on tempering. Some of these peaks were considerable, particularly in the steels in which silicon, molybdenum, manganese or tungsten were present. All the alloying additions employed increased the nucleation rate of V_4C_3 on tempering in the critical secondary hardening range.

Previous research has shown that V_4C_3 nucleates on dislocations during tempering. This research in fact

confirmed the nucleation mechanism of V_4C_3 on dislocations. However, the high purity steels which only contained vanadium as an alloying addition, had very high dislocation densities in the as-hardened condition, but this was not sufficient to give an appreciable nucleation rate of V_4C_3 on tempering.

The important factors were the distortion and free energy of the matrix lattice caused by the presence of solute atoms in localised regions, with high values of these two terms leading to a considerable degree of solid solution hardening. Distortion of the matrix lattice and resultant free energy are directly related to the difference in atomic diameters between the solute element and ferritic iron, being greater for a more pronounced size anomaly.

These solute atoms are attracted towards edge dislocations, as a result of the interactions of the respective strain fields. Tempering at relatively high temperatures causes the solute atoms to diffuse rapidly to positions around edge dislocations. The distorted matrix lattice regions around solute atoms, which contain high dislocation densities, have high free energies and are, therefore, potential nucleation sites for another phase. This is in a similar manner to grain bounda-ries, sub-grain boundaries and vacancies being potential nucleation sites, as these are all regions of high free energy.

The fact that V_4C_3 was confirmed to nucleate on dis-locations, in conjunction with the very poor secondary hardening responses of the high purity steels which only contained vanadium as an alloying addition, very much supported the theory that the dislocations which acted as nucleation

sites were those surrounded by solute atoms.   In fact, V_4C_3
did precipitate in these high purity steels on tempering,
but the nucleation rate of this phase was low.   Vanadium
was the only other element present in the martensitic matrices
of these steels apart from iron and carbon, and the lattice
distortion and resultant solid solution hardening due to the
presence of vanadium was relatively small.

However, the addition of a second alloying element
resulted in further lattice distortion and solid solution
hardening of the matrix, and in some cases this was quite
pronounced.   Comparison firstly of the secondary alloying
additions which were non-carbide forming elements showed that,
in terms of increased secondary hardening response due to
V_4C_3 precipitation, the order was nickel, cobalt, manganese
and silicon.   This is the same order as the effectiveness
of these elements, in terms of equal weight percentages, on
the solid solution hardening of ferrite.   These elements,
therefore, all increase the nucleation rate of V_4C_3 on
tempering, and in this same order.

Consideration of the effects of secondary alloying
additions, which were carbide-forming elements, on the second-
ary hardening of vanadium steels was more difficult.   These
were secondary hardening elements in their own right, with
the exception of chromium, which retards softening at tempering
temperatures up to $550^{\circ}C$, but does not give a true secondary
hardening peak.

Molybdenum and tungsten both retard the dissolution of
V_4C_3 on austenitisation.   This resulted in the matrices of

these alloys containing lower vanadium contents than in most of the other steels, after corresponding austenitisation and quenching treatments. These elements solid solution harden ferrite appreciably, but this effectiveness is somewhat reduced (particularly in the case of tungsten) when comparisons are made with other elements in terms of additions of equal weight percentages, owing to their high atomic weights.

Nevertheless, sufficient nucleation sites are present in the matrix for the appreciable nucleation of V_4C_3, and the other secondary hardening carbides Mo_2C and W_2C, during tempering. The nucleation of Mo_2C and W_2C, with the resultant precipitation hardening more than compensates for the reduction in alloy content of the matrix. Molybdenum was intermediate between cobalt and manganese in the effect on the secondary hardening of vanadium steels due to V_4C_3 precipitation, whilst tungsten was slightly less effective in this respect than nickel.

Chromium improved the dissolution of V_4C_3 on austenitisation to a small degree. This element, however, causes only very slight solid solution hardening of ferrite with very little lattice distortion. This led to a shortage of nucleation sites for V_4C_3 embryo, with the result that this element was the least effective of those investigated in improving the secondary hardening of vanadium steels due to V_4C_3 precipitation. The steel which contained chromium did show a secondary hardening peak, this being aided by the precipitation of Cr_7C_3.

The matrix vanadium content of each of the high purity steels which contained vanadium and a second alloying addition, in the as-hardened condition, was very important in governing the height of the secondary hardening peak obtained on tempering. More pronounced secondary hardening peaks were attained with higher matrix vanadium levels, as sufficient nucleation sites were present in these alloys to accommodate the increased number of V_4C_3 embryo. This was not the case, however, for the steels which only contained vanadium as an alloying addition, as sufficient nucleation sites were only available for a limited amount of V_4C_3 embryo, and so the high matrix vanadium contents were not fully utilised.

All the high purity steels had ferrite matrices which contained only very small levels of vanadium, in the annealed state. Vanadium is in fact a strong ferrite stabilising element, but has a greater affinity to react with carbon. This means that V_4C_3 is very stable and difficult to take into solution during austenitisation, but this must be achieved to a considerable degree if optimum secondary hardening response is to be attained on tempering.

The dissolution rate of a primary carbide during austenitisation is dependent on two factors. These are the bond strength between metal and carbon atoms in the carbide lattice and the diffusion rate of metal atoms from the carbide, via the interface and into the austenite lattice. Diffusion of carbon atoms from the carbide and into the austenite lattice is not the rate controlling process, as carbon has a small atomic diameter and is able to readily diffuse into the

austenite lattice via interstitial sites.

Dissolution of V_4C_3 in austenite commenced in a tempe-
rature range of 1100 to 1150°C for the steels, and became
appreciable at 1200°C.   The non-carbide forming elements only
dissolved to small extents in V_4C_3, but nevertheless these
elements all decreased the bond strength between vanadium and
carbon atoms in this carbide lattice.   Manganese was particularl
effective in this respect, as this element dissolved more
appreciably in V_4C_3 than the other non-carbide forming elements.

Manganese, nickel and cobalt had no appreciable effect
on the diffusion rate of vanadium atoms from V_4C_3 to austenite.
The resultant, therefore, in adding these elements to a
vanadium steel was to increase the dissolution rate of V_4C_3
during austenitisation, this being entirely due to the
weakening of the bond strength between vanadium and carbon
atoms in the carbide lattice.

Silicon, however, was the only element employed in the
steels which had an atomic diameter less than that of ferrite.
This element had a contracting effect on the ferrite lattice,
thereby retarding the diffusion of vanadium atoms from V_4C_3
to the austenite lattice, with this more than outweighing the
beneficial contribution of silicon in decreasing the bond
strength between vanadium and carbon atoms in the carbide
lattice.   The outcome was that silicon retarded the dissolu-
tion of V_4C_3 during austenitisation, with very little solution
of this carbide occurring after treatment at 1150°C.

Additions of the strong carbide- forming elements,
molybdenum and tungsten, to a vanadium steel decreased the

dissolution rate of V_4C_3 during austenitisation. These
strong carbide forming elements dissolved quite markedly
in V_4C_3, but did not weaken the bonds between vanadium and
carbon atoms in the carbide lattice. In addition, Mo_2C
and W_2C are very stable carbides and difficult to dissolve
during austenitisation. However, these two carbides are
slightly less stable and dissolved more appreciably than
V_4C_3 on austenitisation, with the resultant that the disso-
lution rate of V_4C_3 was reduced.

Chromium is not such a strong carbide-forming element
as molybdenum and tungsten, and the addition of chromium to
vanadium steels slightly reduced the bond strength between
vanadium and carbon atoms in the V_4C_3 lattice. This, coupled
with the fact that chromium dissolved quite considerably in
V_4C_3, led to this element increasing the dissolution rate of
V_4C_3 on austenitisation.

A very surprising feature of this research was that some
of the high purity vanadium steels graphitised during long
term tempering at $560^{\circ}C$. In the early stages of the work,
the theory was that cementite had decomposed into graphite,
but results obtained from transmission electron microscopy
revealed that cementite was present in only one of the steels
after tempering at $560^{\circ}C$. This steel contained chromium and
vanadium as alloying additions and in fact did not graphitise
on tempering. Primary vanadium carbides had undoubtedly
decomposed into graphite on tempering, with the graphite
particles having the same directionality as the primary carbides
had as a result of hot working.

Another surprising result was that graphitisation was most appreciable in the steels which only contained vanadium as an alloying addition. More expected was the finding that graphitisation occurred more readily the lower the vanadium : carbon ratio of the alloy.

The addition of silicon, nickel or cobalt to high purity vanadium steels resulted in graphitisation taking place on long term tempering at 560°C, but not as readily as in steels which contained only vanadium as an alloying addition. These are all strong graphitising elements and the reduced degree of graphitisation as a result of their addition was due to partial saturation of the tempered martensite matrix.

Vanadium atoms must diffuse from V_4C_3 to the matrix for graphitisation to occur and this is dependent on the matrix being able to accept these atoms. Additions of 1 wt. % of silicon, nickel or cobalt, in conjunction with 1.6 wt. % vanadium, caused partial saturation of the tempered martensite matrix, with the result that only a limited number of vanadium atoms, diffusing from the primary carbides, could dissolve in the matrix, thus restricting graphitisation.

Additions of molybdenum, chromium, tungsten or manganese to high purity vanadium steels prevented graphitisation occurring, even after tempering for 220 hours at 560°C. This was not in the least surprising as far as the first three elements were concerned, as these are all strong carbide-formers.

Manganese, however, is not a strong carbide-forming element but has a greater affinity for carbon than nickel or cobalt. Furthermore, manganese is not a graphitising element. A factor of even more importance in this case is that the atomic diameter of manganese differs quite appreciably with that of iron. This alloy also had a high matrix vanadium content in the as-hardened condition, and so this phase was partially saturated with vanadium and manganese. The resultant of this was that no further vanadium could readily dissolve in the matrix by diffusing from primary carbides during tempering, thereby preventing graphitisation.

None of the commercial steels, even those with low vanadium contents and at positions in the carburised cases with high carbon levels, graphitised during long term tempering. This was entirely due to the quite high manganese contents (0.72 to 0.78 wt. %) of these steels.

The results of this research allowed a low alloy tool steel to be developed, which could be expected to have a wide range of tooling uses. This was achieved by a compromise between optimum secondary hardening response and appreciable dissolution of primary carbides on austenitisation.

Vanadium was the main carbide-forming element present in this steel, although molybdenum, chromium and tungsten were also present. Silicon and manganese were also present as both these elements considerably increase the nucleation rate of V_4C_3, and probably also Mo_2C, Cr_7C_3 and W_2C, on tempering. In addition, manganese increases the dissolution rate of V_4C_3 on austenitising, this counteracting the reduction

in this phenomenon caused by the addition of silicon.

Such a steel would cost less than half the price of high speed steels, price being a major consideration for tool steels today.   Nevertheless, this steel would be expected to have both good wear resistance and hot hardness, both these factors being very important for tool steels. This steel could be employed for a wide range of tooling applications, necessitating either one or both of these requirements.

7. Recommendations for Further Work

An important propagation of this research would be to determine whether other high purity steels, which in each case contain only one alloying element which is a strong carbide-former and causes secondary hardening in commercial purity steels, show true secondary hardening peaks on tempering. Evidence from this research suggests that the high purity steels containing these elements would not, like vanadium steels of similar purity, show a true secondary hardening peak. The elements which this would apply to are molybdenum, tungsten, titanium, tantalum, niobium and zirconium.

Further research would be beneficial on the effects of silicon, manganese and possibly other elements on the secondary hardening of these steels. This would enable further evidence to be gleaned on the theory that the nucleation sites for carbide embryo are dislocations surrounding solute atoms, and that the greater the mismatch between these atoms and those of the ferritic parent matrix, the higher the nucleation rate of the carbides.

Low alloy steels cover a very wide range of applications, and many of these steels contain elements which cause secondary hardening on tempering in the critical temperature range. Alloy design could be employed for these steels to obtain optimum secondary hardening response in cases where this is an important criteria.

However, the major outlet for this work is in the field of tool steels. This covers the range high speed steels, hot and cold work tool steels and shock resisting tool steels. The greatest application is to high speed steels, as these have the highest concentration of alloying elements, but there is some significance in these results, and suggestions for further research, for the other steels as well.

Additional research could be undertaken on stoichiometric alloying of these steels to determine whether this has as critical an effect on secondary hardening response as in vanadium steels. Alloy design should also be applied to the levels of non-carbide forming elements present, as these can greatly influence the secondary hardening response.

Cobalt additions of between 5 and 10 wt. % improve the degree of secondary hardening and hot hardness of high speed steels. This phenomenon appears to be due to the additional nucleation sites for carbides provided by dislocations surrounding cobalt atoms in the matrix. The atomic diameter of cobalt does not differ appreciably with that of α-iron, so other non-carbide forming elements could be employed at greater levels in these steels, which cause greater mismatch with the matrix, hence more nucleation sites and more pronounced precipitation hardening.

Silicon and manganese were the non-carbide forming elements which were found to give the most appreciable precipitation hardening in vanadium steels. Unfortunately, silicon retards the dissolution of V_4C_3 on austenitisation, and this is a very important criteria for high speed steels. Research must be

undertaken to achieve an optimum compromise between dissolution rate of the primary carbides on austenitising and maximum secondary hardening response on tempering, for only by achieving satisfactory results in the former can good response be obtained for the latter phenomenon.

The fact that high purity vanadium steels graphitised during long term tempering at 560°C was of more theoretical than practical significance, illustrating how unstable primary carbides can be in these alloys. Graphitic tool steels could be vacuum melted using high purity charges, but these would be costly, and this would more than outweigh the beneficial property of these alloys in graphitising at considerably lower temperatures than commercial purity graphitic tool steels. Similarly, in the field of cast irons, the cost of high purity alloy additions and vacuum melting would not render this an economical venture.

Nevertheless, further research could be carried out on high purity steels containing just one alloying addition, which is a strong carbide-forming element, other than vanadium. Great interest would surround whether such steels graphitised during long term tempering at 560°C, and if this was the case, the effect of other alloying elements on this phenomenon would add greatly to the theories postulated in this thesis.

8.   Appendix

8.1   Quantitative Metallography

8.1.1 Basic Relationship

Consider the volume fraction of a hypothetical phase, α.

$$P_f = \frac{P_\alpha}{P} \quad \ldots\ldots\ldots\ldots\text{EQUATION 16.}$$

Where P_f = Point fraction of α phase.

P_α = Number of points falling in α phase.

P = Total number of points stipulated on plane

of polish.

Point counts may be classed as either systematic or random.   There is some difficulty in achieving a random array of points, so often a systematic array is employed and an assumption is made that the distribution of the phase being measured is random.   Justification can be made if the point spacing is sufficiently large so as to be in excess of the maximum intercept length in the phase being measured.   This was so in the case of the quantitative metallography carried out in this research.

8.1.2   Experimental Errors

8.1.2.1   Sectioning Errors

Observed projected area fraction always greater than true area fraction.

$$V_f = A_f = A'_f - \frac{S_v}{4} t \quad \ldots\ldots\ldots\ldots\text{EQUATION 17.}$$

Where V_f = Volume fraction.

A_f = Areal fraction.

A_f' = Apparent areal fraction.

S_v = Surface area of second phase per unit volume of sample.

t = "Depth of etch".

Note:- $S_v = \dfrac{2N}{L} = 2N_L$ ....EQUATION 18.

Where N = Number of α-phase boundary intercepts in a line of length L.

N_L = Average number of α-phase boundary intercepts per unit length of line.

8.1.2.2 Errors due to lack of Resolution in Microscope

$$\frac{\delta V_f}{V_f} = \frac{\delta A_f}{A_f} = \frac{\lambda}{2NA} \cdot \frac{L_a^b}{A_f} = \text{Relative error} \dots\dots\text{EQUATION 1}$$

Where δA_f = Apparent areal fraction of phase boundary

$= \delta V_f$.

λ = Wavelength of light used.

L_a^b = α-phase boundary length per unit area of plane of polish.

NA = Numerical aperture of objective lens.

8.1.2.3 Statistical Errors

8.1.2.3.1 Statistical Parameters

Examine 'n' sub-areas which constitute the sample from the entire specimen. Let V_f on the sub-areas be x_1, x_2, x_3, ...x_n

Sample mean $= \bar{x} = \dfrac{\sum\limits_{i=1}^{i=n} x_i}{n}$ .... EQUATION 20.

As the number of sub-areas increases, so the frequency of the value of x recorded approaches a normal distribution. The distribution of values of x about the mean for the sample of 'n' sub-areas, $\bar{x}$, is given by the standard deviation of the values of x for the sample. This is measured in terms of the variance of the sample, V_x where:-

$$V_x = \frac{\sum\limits_1^n (x - \bar{x})^2}{n - 1} \quad \text{........ EQUATION 21}$$

The standard deviation of the mean for the sample, σ_x is:-

$$\sigma_x = V_x^{\frac{1}{2}} = \left(\frac{\sum\limits_1^n (x - \bar{x})^2}{n - 1} \right)^{\frac{1}{2}} \quad \text{......... EQUATION 22}$$

The requirement is now to know how good an estimation of the true mean for the entire specimen, μ_x, is the mean of the (n) sub-areas, $\bar{x}$. To determine this, an analysis is carried out several times on (n) sub-areas. Then the standard deviation of the true mean (standard error), $\sigma_{\bar{x}}$ is:-

$$\sigma_{\bar{x}} = \frac{\sigma_x}{n^{\frac{1}{2}}} \quad \text{......... EQUATION 23.}$$

$$\therefore \sigma_{\bar{x}} = \left(\frac{\sum\limits_1^n (x - \bar{x})^2}{n (n - 1)} \right)^{\frac{1}{2}}$$

For a normal distribution:-

67% of the values of $\bar{x}$ fall within $\mu_x \pm \sigma_{\bar{x}}$

95% " " " " " " " $\mu_x \pm 1.96\, \sigma_{\bar{x}}$

99% " " " " " " " $\mu_x \pm 2.58\, \sigma_{\bar{x}}$

The relative error of the mean $= \dfrac{\sigma_{\bar{x}}}{\bar{x}} =$ Coefficient of variation.

Also, proportional variance $=$ (relative error)$^2 = \dfrac{(\sigma_{\bar{x}})^2}{\bar{x}}$

8.1.2.3.2 Assessment of Statistical Errors

For systematic point counting the proportional variance

$= \dfrac{1}{P_\alpha} (1-P_f)$ ....EQUATION 24.

Where P_α = Number of points in α particles in total number of points P.

P_f = Point fraction of $\alpha = \dfrac{P_\alpha}{P}$

Assumptions:-

1. The α phase occurs as randomly distributed, discrete particles. This implies V_f is small.

2. P is very much greater than 1.

3. Point spacing is greater than maximum intercept length in α phase particles, i.e. $P_\alpha \simeq N_\alpha$.

From the previously mentioned relationships, the relative error $\left(\dfrac{\sigma_{V_f}}{V_f}\right)$ can be calculated for systematic point counting.

For 100 observations on a structure comprising a random dispersion of spherical particles of uniform size, the relative error is approximately of the order of 10.5%.

8.1.3 Number of Points counted to give Desired Accuracy and Confidence Limits

8.1.3.1 Volume Fraction of Graphite

An approximate volume fraction of 3% graphite was taken as an average value for the samples on which point counting was undertaken. The necessity was to determine the total

number of points to be counted to give an accuracy of graphite volume fraction of $\pm$ 1%, with a level of confidence of 95%.

$$2\sigma_{V_f} = 0.01$$

$$V_f = 0.03$$

$$\therefore \quad \frac{2\sigma_{V_f}}{V_f} = \frac{0.01}{0.03} = 0.3333$$

$$\therefore \quad \frac{\sigma_{V_f}}{V_f} = 0.1667$$

$$\left(\frac{\sigma_{V_f}}{V_f}\right)^2 = \frac{1}{P} = (0.1667)^2 = 0.0278$$

$$\therefore \quad P_{graphite} = \frac{1}{0.0278} = \underline{36 \text{ points in the graphite}}$$

Total number of points to be counted $= P = \dfrac{P_{graphite}}{V_f}$

$$= \frac{36}{0.03} = \underline{1200 \text{ points}}$$

8.1.3.2 Volume Fraction of Primary Carbides

These determinations were carried out by means of transmission electron microscopy. Nevertheless, the same analysis can be applied to determine the number of points to be counted for desired accuracy and confidence level, as was applied to results obtained by means of optical metallography.

An approximate volume fraction of 10% primary carbides was taken as an average value for specimens on which quantitative metallography was carried out. Once again an accuracy of $\pm$ 1% and a confidence level of 95% was required for the results.

$$2\sigma_{V_f} = 0.01$$

$$V_f = 0.1$$

$$\therefore \quad \frac{2\sigma_{V_f}}{V_f} = \frac{0.01}{0.1} = 0.1$$

$$\therefore \quad \frac{\sigma_{V_f}}{V_f} = 0.05$$

$$\left(\frac{\sigma_{V_f}}{V_f}\right)^2 = \frac{1}{P} = (0.05)^2 = 0.0025$$

$$\therefore \quad P_{carbides} = \frac{1}{0.0025} = \underline{400 \text{ points in the primary carbides}}$$

Total number of points to be counted $= P = \dfrac{P_{carbides}}{V_f}$

$$= \frac{400}{0.1} = \underline{4000 \text{ points}}$$

8.2 The Accuracy of the Matrix Analyses Carried out by Means of the Electron Microprobe

8.2.1 Confidence Limits of the Mean Count Rates

The examples taken are the matrix analyses carried out on Alloys 1 and 3 after austenitisation at $1200^{\circ}C$ for 20 minutes and subsequent water quenching.

Alloy 1

$$\text{Mean} = \bar{x} = \frac{\Sigma x}{n}$$

Where n = Number of matrix analyses undertaken = 20

$$\therefore \bar{x} = \frac{2986.0}{20} = 149.3 \text{ pulses/sec.}$$

$$\text{Variance} = \sigma^2 = \frac{\Sigma(x - \bar{x})^2}{n}$$

$$\therefore \sigma^2 = \frac{633.85}{20} = 31.69$$

Standard deviation = $\sigma = 5.629$

$$\text{Standard error} = s = \frac{\sigma}{(n-1)^{\frac{1}{2}}}$$

$$\therefore s = \frac{5.629}{(20-1)^{\frac{1}{2}}} = \frac{5.629}{4.359} = 1.291$$

The sample distribution was of the form of a normal distribution. Hence for the 95% confidence limit the mean of the population is $\bar{x} \pm 1.96s$ pulses/sec, and the 99% limit $\bar{x} \pm 2.58s$ pulses/sec.

The 95% confidence limit = $149.3 \pm 1.96 \times 1.291$

$$149.3 \pm 2.5$$

$$\underline{146.8 \text{ to } 151.8 \text{ pulses/sec.}}$$

The 99% confidence limit = $149.3 \pm 2.58 \times 1.291$

$$= 149.3 \pm 3.3$$

$$= \underline{146.0 \text{ to } 152.6 \text{ pulses/sec.}}$$

Alloy 3

$$\text{Mean} = \bar{x} = \frac{\Sigma x}{n}$$

$$\therefore \bar{x} = \frac{6356.2}{20} = 317.8 \text{ pulses/sec.}$$

$$\text{Variance} = \sigma^2 = \frac{\Sigma(x - \bar{x})^2}{n}$$

$$\therefore \sigma^2 = \frac{722.66}{20} = 36.13$$

$$\therefore \text{Standard deviation} = \sigma = 6.01$$

$$\text{Standard error} = s = \frac{\sigma}{(n-1)^{\frac{1}{2}}}$$

$$\therefore s = \frac{6.01}{(20-1)^{\frac{1}{2}}} = \frac{6.01}{4.359} = 1.379$$

Once again the sample distribution was of the form of a normal distribution. Therefore, the 95% confidence limit for the mean of the population is $\bar{x} \pm 1.96$ s pulses/sec., and the 99% limit $\bar{x} \pm 2.58$s pulses/sec.

$$\text{The 95\% confidence limit} = 317.8 \pm 1.96 \times 1.379$$
$$= 317.8 \pm 2.7$$
$$= \underline{315.1 \text{ to } 320.5 \text{ pulses/sec.}}$$

$$\text{The 99\% confidence limit} = 317.8 \pm 2.58 \times 1.379$$
$$= 317.8 \pm 3.6$$
$$= \underline{314.2 \text{ to } 321.4 \text{ pulses/sec.}}$$

8.2.2 Accuracy of the Scaler

The scaler is a digital device, thereby meaning that the accuracy is limited only by statistics. The relative standard deviation (σ) in the measurement of a mean counting rate of n/sec. is given by:-

$$\sigma = \frac{1}{(nt)^{\frac{1}{2}}} \qquad \dots\dots\dots\text{EQUATION 25}$$

Where t is the counting time.

Taking a low mean counting rate (e.g. the counts for vanadium present in the matrix of Alloy 1 after austenitisation at 1200°C and subsequent water quenching), with a value of n = 149.3 pulses/sec.

$$\therefore \sigma = \frac{1}{(149.3 \times 10)^{\frac{1}{2}}} = 0.026 = \underline{2.6\%}$$

An example of a high count rate obtained in this research was the counts obtained for vanadium from the pure vanadium standard. When analysis was carried out on the above mentioned sample, the count rate for vanadium from the standard was 17666.2 pulses/sec.

$$\therefore \sigma = \frac{1}{(17666.2 \times 10)^{\frac{1}{2}}} = 0.0024 = \underline{0.24\%}$$

8.2.3 Accuracy of the Ratemeter

The ratemeter is basically an analogue device, and some error is certain to arise in the electronics, quite apart from statistical factors. This error is less than 1% on a full scale counting rate, but can be as high as 3% if only a low scale deflection is employed.

8.2.4 Dead Time Correction

After subtracting the mean background count rate (obtained from positions on either side of the peak) from the peak count rate, the number of counts (n'), due to the emission at the characteristic wavelength, can be determined. The value of n' so obtained must, in every instance, be corrected to compensate for the loss of counts as a result of coincidences in the arrival of X-ray quanta in the proportional counter. The statistical probability of such coincidences occurring increases

with the counting rate, and n' is related to n, which is the true counting rate, by the following expression:-

$$n = \frac{n'}{1 - n'p} \qquad \ldots\ldots\ldots\text{EQUATION 26}$$

Where p = Paralysis time of the counting channel, and was set at 5 microseconds.

8.3 Retained Austenite Present in Alloy 7(Ni) and Alloy 9(Co) After Austenitisation at 1200°C and Subsequent Water Quenching

The integrated intensity of a diffraction line is given by the following equation:-

$$I_{(hkl)} = n^2 \, Vm \, (LP) \, e^{-2m} \, (Ff)^2 \quad \ldots\ldots\ldots \text{EQUATION 27}$$

Where $I_{(hkl)}$ = Integrated intensity for a special (hkl) reflection.

n = Number of cells in 1 cm^3

V = Volume exposed to the X-ray beam.

(LP) = Lorentz - Polarization factor

m = Multiplicity of (hkl)

e^{-2m} = Debye-Waller temperature factor

F = Structure factor

f = Atomic factor

The term V/v^2 can be substituted for n^2V, where v is the volume of the unit cell.

Denoting the ratio between the integrated intensities of martensite and austenite as P, then

$$P = \frac{I \text{ martensite } (\alpha)}{I \text{ austenite } (\gamma)} = \frac{V_\alpha v_\gamma^2 \, m_\alpha (LP)_\alpha \, e_\alpha^{-2m} (F_\alpha f_\alpha)^2}{V_\gamma v_\alpha^2 \, m_\gamma (LP)_\gamma \, e_\gamma^{-2m} (F_\gamma f_\gamma)^2}$$

$$\ldots\ldots\ldots \text{EQUATION 28}$$

A factor G was then defined, and can be determined for any combination of martensite and austenite peaks. In this case the peaks employed were $(200)_\alpha$ and $(200)_\gamma$.

$$G = \frac{V_\alpha v_\gamma^2 \, m_\alpha (LP)_\alpha \, e_\alpha^{-2m} (F_\alpha f_\alpha)^2}{V_\gamma v_\alpha^2 \, m_\gamma (LP)_\gamma \, e_\gamma^{-2m} (F_\gamma f_\gamma)^2} \quad \ldots\ldots\ldots \text{EQUATION 29}$$

Each factor was determined from International Tables,[173] although in some cases further expansion is necessary.

8.3.1 Lorentz Polarisation Factor

The Lorentz factor is as follows:-

$$\left(\frac{1}{\sin 2\theta}\right)(\cos\theta)\left(\frac{1}{\sin 2\theta}\right) = \frac{\cos\theta}{\sin^2 2\theta} = \frac{1}{4\sin^2\theta\cos\theta}$$

.........EQUATION 30

This term is combined with the polarization factor, $\frac{1}{2}(1 + \cos^2 2\theta)$ to give the combined Lorentz-Polarisation factor. Omission of a constant factor of $\frac{1}{8}$ gives an equation as follows:-

$$\text{Lorentz Polarisation factor} = \frac{1 + \cos^2 2\theta}{\sin^2\theta\cos\theta}$$

.......EQUATION 31

8.3.2 Debye-Waller Temperature Factor

The Debye temperature has only been determined for ferrite, and an assumption has been made that this value is applicable to both martensite and austenite. The mid-range value of 420°K has been used, from the range of values, given in the International Tables. Slight variations in the Debye temperature have a negligible effect on the temperature factor.

8.3.3 Atomic Scattering Factor

If the wavelength of the radiation employed is very near to the absorption edge of iron, then corrections must be made to the atomic scattering factor to allow for dispersion. In this case, however, the irradiating (molybdenum $K\alpha$) wavelength was not close to the absorption edge of the sample, so no corrections had to be made to the atomic scattering factor.

The intensity factors for the α_{200} and γ_{200} peaks, for Alloys 7(Ni) and 9(Co) are presented in Table 35. Very slight corrections were made to allow for the alloy content

of both steels.   Calculation of the G factors, for the peak

combination $\gamma_{200} - \alpha_{200}$, revealed values of 2.17 and 2.22

for Alloys 7(Ni) and 9(Co) respectively.

Alloy 7(Ni)

The ratio between the integrated intensities of martensite

and austenite, $P = \dfrac{63.45}{20.15} = 3.149$.

(The intensities were determined by means of the equation

area $= \dfrac{\text{base x perpendicular height}}{2}$, the accurate traces of

the peaks being made by means of a planimeter).

Carbides were present in this sample:-

$$\alpha + \gamma + \text{carbide} = 1 \quad \ldots\ldots\ldots\text{EQUATION 32}$$

$$\therefore \% \gamma = \dfrac{1 - \text{carbide}}{1 + GP} \times 100 \quad \ldots\ldots\ldots\text{EQUATION 33}$$

The volume fraction of primary carbide = 0.2%

$$\therefore \% \gamma = \dfrac{1 - 0.002}{1 + 2.17 \times 3.149} \times 100 = \underline{12.8\%}$$

Alloy 9(Co)

$$P = \dfrac{56.40}{13.17} = 4.283$$

The volume fraction of primary carbide = 0.3%

$$\therefore \% \gamma = \dfrac{1 - 0.003}{1 + 2.22 \times 4.283} \times 100 = \underline{9.5\%}$$

8.4 Electron Diffraction

All measurements from the electron diffraction patterns were taken from negatives, by means of a travelling microscope. This was to avoid inaccuracies caused by the distortion of photographic prints during preparation.

The ratio method was employed to index the diffraction patterns. This method allows the indices of diffraction spots from cubic crystals to be determined, without the necessity for determining the camera constant, λL. The constant, however, was used in the calculations of the spacings.

Derivation of the zone axis $[u, v, w]$ for each diffraction pattern, was made by using the following expressions:-

$$u = k_1 l_2 - k_2 l_1 \quad \ldots\ldots\text{EQUATION 34}$$

$$v = l_1 h_2 - l_2 h_1 \quad \ldots\ldots\text{EQUATION 35}$$

$$w = h_1 k_2 - h_2 k_1 \quad \ldots\ldots\text{EQUATION 36}$$

Where $h_1 k_1 l_1$ and $h_2 k_2 l_2$ are the indices of any two spots in the diffraction pattern, other than the central spot or two spots on either side of the central spot. The following equation must hold for any spot on the diffraction pattern:-

$$hu + kv + lw = 0 \quad \ldots\ldots\ldots\text{EQUATION 37.}$$

8.5   X-ray Map for Carbon

An X-ray map was obtained for carbon on a field containing graphite, this being present in Alloy 1 after tempering for 220 hours at $560^{\circ}C$.   This was achieved by means of an EDAX ECON Energy Dispersive Detector on a PSEM 500 electron microscope.   The several regions of high carbon concentration clearly confirm the presence of graphite rosettes.

CHAPTER 9

9.   References

1.   H.J. Goldschmidt, J. Iron Steel Inst., Dec. 1948, 160, 345

2.   H.J. Goldschmidt, J. Iron Steel Inst., Mar. 1952, 170, 189

3.   K. Becker, Physikalische Zeitschrift, 1933, 34, 185.

4.   E. Maurer, H. Döring and R. Pulewka, Archiv für das
        Eisenhüttenwesen, 1940, 13, 337.

5.   A. Osawa and M. Oya, Science Reports of the Tôhoku
        Imperial University, 1930, 19, (1), 95.

6.   F. Wever, A. Rose and H. Eggers, Mitt. Kaiser-Wilhelm
        Inst. Elsenforsch, 1936, 18, 239.

7.   G. Steven, A.E. Nehrenberg and T.V. Philip, Trans. A.S.M.,
        1964, 57, 925.

8.   T. Mukherjee, in 'Materials for Metal Cutting', I.S.I.
        Spec. Rep. 126, 1970, 61.

9.   W. Crafts and J.L. Lamont, Trans. A.I.M.E., 1949, 180,
                                                            471.

10.   M.G. Gedberg, M.F. Sidelkovsky, M.F. Melnikov, N.N. Kazek
        and V.A. Lektyushin, Zavod. Lab., 1968, 34, (4), 454.

11.   G. Steven, A. Hauser, W. Neumeyer and J. Capenos, Trans.
        A.S.M., 1969, 62, 180.

12.   K. Bungardt, E. Haberling, A. Rose and H.H. Weigand,
        D.E.W. Tech. Ber., July 1972, 12, (2), 111.

13.   G. Preis and G. Lennartz, Arch. Eisenhüttenwes., Aug. 1975
        46, (8), 509.

14.   E. Horn, D.E.W. Tech. Ber., Oct. 1972, 12, (3), 217.

15.   E. Haberling and H. Kiesheyer, D.E.W. Tech. Ber., Oct.
        1972, 12, (3), 213.

16.   R. Schlatter and J. Stepanic, Metal Prog., June 1976, 56.

17.   A. Fischer and E. Kohlhaas, Prakt. Metallogr., Aug. 1975,
        12, (8), 393.

18.   E. Haberling, A. Rose and H.H. Weigand, Stahl u. Eisen,
        July 1973, 93, (14), 645.

19.   T.K. Jones and T. Mukherjee, J. Iron Steel Inst., Jan.
        1970, 208, (1), 90.

20.   H.J. Goldschmidt, 'Interstitial Alloys', Butterworths,
        1967, 105.

21.	R. Gullberg, J. Iron Steel Inst., Jan. 1971, 209, (1), 71.

22.	A.M. Baikov, L.I. Baranova, I.K. Kupalova and V.M. Aleksandrova. Sbornik Trudov Vses. Nauchno-Issled. Instrum. Inst., 1972, 1, 43.

23.	A.M. Baikov, L.I. Baranova and I.K. Kupalova, Met. Sci. Heat Treat., May-June 1974, 16, (5-6), 533.

24.	G. Lennartz and G. Preis, D.E.W. Tech. Ber., 13, 55.

25.	G. Hoyle, Alloy Metals Rev., Mar. 1965, 12, (115), 3.

26.	F.D. Richardson, J. Iron Steel Inst., Sept. 1953, 175, 33.

27.	J.P. Gill, Trans. A.S.M. 1936, 24, 735.

28.	F. Kayser and M. Cohen, Metal Progress, 1952, 61, (6), 79.

29.	J. Chodorowski, K. Jurczak and J. Lampe, J. Iron Steel Inst., Nov. 1968, 206, (11), 1131.

30.	S. Koshiba, S. Kimura and H. Horado, J. Iron Steel Inst. Japan, Nov. 1960, 46, 1554.

31.	T. Sato, T. Nishizawa and K. Murai, J. Iron Steel Inst. Japan, May 1959, 45, 511.

32.	V.I. Arkharov, I.S. Kvater and S.T. Kiselev, Bulletin of Academy of Sciences of U.S.S.R., June 1947, 749.

33.	A. Ivanov, Stal, 1950, 8, 317.

34.	M. Nikanorov, Dissert. Leningr. Politekhn. Inst., 1952, 76.

35.	T. Malkiewicz, Z. Bojarski and J. Foryst, Prace Inst. Hutniczych, 1959, 11, 267.

36.	A.P. Gulyaev, I.K. Kupalova and V.A. Landa, Ind. Lab., Mar. 1965, 31, (3), 362.

37.	A.N. Popandopulo, Metal Sci. Heat Treat., Nov. - Dec. 1970, 12, (11-12), 1030.

38.	H. Arnfelt, Iron and Steel Institute, Carnegie Scholarship Memoirs, 1928, 17, 1.

39.	W.P. Sykes and K.R. Van Horn, Trans. A.I.M.E., 1933, 105, 198.

40.	H. Arnfelt and A. Westgren, Jernkontorets Ann., 1935, 119, 185.

41.	A. Westgren, Sci. Rep. Tôhoku Imp. Univ., Honda Aniv., 1936, 852.

42. H.J. Goldschmidt, J. Iron Steel Inst., May 1957, 186, 68.

43. I.K. Kupalova, V.A. Landa, A.I. Malinkina and M.N. Fadyushina, Met. Sci. Heat Treat., Jan-Feb. 1969, 11, (1-2), 45.

44. V.A. Brostrem and Yu. A. Geller, Metal Sci. Heat Treat., Jan-Feb. 1970, 12, (1-2), 32.

45. I.K. Kupalova and Ye. M. Stepnov, Phys. Met. Metallogr., 1970, 30, (5), 240.

46. T. Murakami and A. Hatta, Sci. Rep. Tôhoku Univ., Honda Anniversary Vol., 1936, 882.

47. K. Kuo, J. Iron Steel Inst., 1955, 181, 128.

48. M. Massin, Mém. Sci. Rev. Mét., Dec. 1971, 68, (12), 845.

49. T. Malkiewicz, Z. Bojarski and J. Foryst, J. Iron Steel Inst., Sept. 1959, 193, 25.

50. G. Hoyle, J. Iron Steel Inst., Aug. 1960, 195, 454.

51. F.B. Pickering, J. Iron Steel Inst., Aug. 1960, 195, 450.

52. T. Malkiewicz, J. Iron Steel Inst., Aug. 1960, 195, 456.

53. Z. Bojarski, J. Iron Steel Inst., Nov. 1961, 199, 267.

54. B.L. Averbach, 'Tool Steels', Climax Molybdenum Company, 1960.

55. P.K. Koh, in 'The Electron Microprobe', 1966, 604.

56. H.B. Sansa, J.M. Arcas, F.E. Masoliver and A.T. Espallargas, Tech. Met., Sept. - Oct. 1973, 28, (198), 29.

57. A.P. Gulyaev, Stal, 1946, 3, 188.

58. J. Chodorowski, K. Jurczak and J. Lampe, J. Iron Steel Inst., Sept. 1971, 209, (9), 750.

59. L. Colombier, Traitement Thermique, May 1970, (50), 39.

60. J.E. Bridge, Jr., G.N. Maniar and T.V. Philip, Met. Trans., Aug. 1971, 2, (8), 2209.

61. G. Hoyle, Met. Reviews, 1964, 9, (33), 49.

62. Z. Hegedus and L. Acs, Gep, 1967, (3), 101.

63. A.N. Popandopulo, Met. Sci. Heat Treat., Sept. - Oct. 1974, 16, (9-10), 799.

64. A.P. Gulyaev, I.K. Kupalova and A.M. Baikov, Met. Sci. Heat Treat., July - Aug. 1972, 14, (7-8), 680.

65. M. Cohen and P. Koh, Trans. A.S.M., 1939, 27, 1015.

66. C.H. White and R.W.K. Honeycombe, J. Iron Steel Inst., Jan. 1961, 197, 21.

67. P. Payson, Trans. A.S.M., 1959, 51, 60.

68. J.H. Holloman and L.D. Jaffe, Trans. A.I.M.E., 1945, 162, 223.

69. K. Kuo, J. Iron Steel Inst., July 1953, 174, 223.

70. G. Hobson and D.S. Tyas, Metals and Materials, May 1968, 2, (5), 144.

71. E. Tekin and M.H. Richman, Metallography, Sept. 1970, 3, (3), 327.

72. S.G. Cope, J. Iron Steel Inst., Aug. 1960, 195, 452.

73. T. Mukherjee, Metals and Materials, July 1968, 2, (7), 224.

74. T. Mukherjee, R. Stumpf, J. Sellars and S. McGtegart, J. Iron Steel Inst., 1969, 207, 621.

75. A.H. Michel and J. Papier, Rev. Mét., 1954, 51, (6), 425.

76. A.R. Johnson, S.M. Thesis, Massachusetts Institute of Technology, 1956.

77. R. Lévêque and A. Condylis, Mém. Sci. Rev. Mét., Feb. 1971, 68, (2), 87.

78. E. Horn, D.E.W. Techn. Ber., Dec. 1974, 13, (3), 171.

79. L. Colombier and R. Lévêque, Mém. Sci. Rev. Mét., 1968, 65, 229.

80. E. Kunze, D.E.W. Techn. Ber., Sept. 1971, 11, (3), 184.

81. I.K. Kupalova, A.M. Baykov and M.M. Kubayev, Phys. Met. Metallogr., 1972, 33, (1), 175.

82. I. Sato, T. Nishizava and K. Murai, J. Iron Steel Inst. Japan, 1958, 44, 4.

83. N. Shönberg, Acta Chem. Scand., 1954, 8, 624.

84. H.J. French and T.G. Digges, Trans. Amer. Soc. Steel Treat., 1925, 8, 681.

85. N.T. Gudtsov and K.M. Gelfand, Izv. Akad. Nauk S.S.S.R., O.T.N. No. 1, 1947.

86. E. Zmihorski, J. Iron Steel Inst., March 1969, 207, (3), 319.

87. A.P. Gulyaev and I.K. Kupalova, Met. Sci. Heat Treat., July-Aug. 1970, 12, (7-8), 666.

88. A. Mazur, J. Krawiarz and E. Kaliszewski, Hutnik (Katowice), Feb. 1971, 38, (2), 103.

89. A.N. Popandopulo, Met. Sci. Heat Treat., July-Aug. 1971, 13, (7-8), 672.

90. V.K. Chandhok, J.P. Hirth and E.J. Dulis, Trans. A.S.M., 1963, 56, 677.

91. E. Williams, Metals and Materials, 1967, 1, (2), 50.

92. D. Rousseau, Aciers Spéciaux, 1973, 24, 18.

93. D.J. Blickwede, M. Cohen and G.A. Roberts, Trans. A.S.M., 1950, 42, 1161.

94. M. Mortier, Mét. Const. Mécan, Mar. 1964, 96, (3), 239.

95. E. Elsen, G. Elsen and M. Markworth, Metall, Apr. 1965, 19, (4), 334.

96. I.F. Zaitsev, V.P. Rogovtsev and V.M. Doronin, Met. Sci. Heat Treat., Jan-Feb. 1973, 15, (1-2), 95.

97. J. Mortier, Mét. Constr. Mécan, Oct. 1971, 103, (10), 431.

98. A.B. Kinzel and C.O. Burgess, Trans. A.I.M.E., 1932, 100, 257.

99. G.A. Roberts, 1966 Howe Memorial Lecture - Iron and Steel Division, Trans. A.I.M.E., July 1966, 236, 950.

100. R. Harder and J. Grove, Trans. A.I.M.E. 1933, 105, 88.

101. H.H. Weigand and E. Haberling, D.E.W. Techn. Ber., Sept. 1971, 11, (3), 134.

102. Yu. A. Geller, Yu. G. Ivanov and L.S. Kremnev, Stal, Apr. 1972, 4, 355.

103. W. Oertel and A. Grutzner, 'Die Schnelldrehstable', Dusseldorf, Verlag Stahleisen, 1931.

104. B. Wadell, Metals and Materials, Jan. 1973, 7, (1), 38.

105. J.T. Berry, 'High Performance, High Hardness High Speed Steels', Climax Molybdenum Company, 1970.

106. E. Houdremont, H. Bennek and H. Schrader, Trans. A.I.M.E 1935, 116, 260.

107. E. Houdremont, F.K. Neumann and H. Schrader, Arch. Eisenhuttenwesen, 1942, 16, 57.

108. W. Koch and H.J. Wiester, Stahl u. Eisen, 1949, 69, 80.

109. K. Kuo, J. Iron Steel Inst., Nov. 1956, 184, 258.

110.   A.K. Seal and R.W.K. Honeycombe, J. Iron Steel Inst.,
       Jan. 1958, 188, 9.

111.   A.K. Seal and R.W.K. Honeycombe, J. Iron Steel Inst.,
       Apr. 1958, 188, 343.

112.   R.G. Baker and J. Nutting, in 'Precipitation Processes
       in Steels', I.S.I. Spec. Rep. 64, 1959, 1.

113.   E. Smith, Fifth Int. Conf. on Elect. Mic., Vol. 1,
       Academic Press, 1962, CC-10.

114.   R.B. Nicholson and J. Nutting, Phil. Mag., 1958, 3, 531.

115.   E. Hornbogen, J. Appl. Phys., Feb. 1961, 32, (2), 135.

116.   E. Hornbogen, Acta Met., May 1962, 10, 525.

117.   E. Hornbogen, Acta Met., Dec. 1962, 10, 1187.

118.   W. Sorbo, H.N. Treaftis and D. Turnbull, Acta Met.,
       1958, 6, 401.

119.   J.M. Silcock, Phil. Mag., 1959, 4, 1187.

120.   C. Chiou, H. Herman and M.E. Fine, Trans. A.I.M.E.,
       1960, 218, 299.

121.   E. Smith and J. Nutting, J. Iron Steel Inst., Dec. 1957,
       187, 314.

122.   J.J. Irani and R.W.K. Honeycombe, Fifth Int. Conf. on
       Elect. Mic., Vol. 1, Academic Press, 1962, HH-9.

123.   J.J. Irani and R.W.K. Honeycombe, Third Europ. Reg.
       Conf. on Elect. Mic., Vol. A, Prague 1964, 207.

124.   R.W.K. Honeycombe, in 'High-Alloy Steels', I.S.I. Spec.
       Rep. 86, 1964, 1.

125.   D.L. Speirs, W. Roberts, P. Grieveson and K.H. Jack,
       Second Intern. Conf. on Strength of Metals and Alloys,
       Vol. 2, 1970, 601.

126.   Yu. I. Ustinovshchikov, I.M. Kovenskiy and V.A. Vlasov,
       Phys. Met. Metallogr., 1976, 41, (1), 82.

127.   E. Tekin and P.M. Kelly, J. Iron Steel Inst., July
       1965, 203, (7), 715.

128.   L.S. Livshits and V.S. Shcherbakova, Russ. Met., 1969,
       (5), 93.

129.   T. Nishida and M. Tanino, Nippon Kinzoku Gakkai-Si,
       1965, 29, (7), 728.

130.   H. Isizuka, Japan Steel Works Techn. Rev., 1963, no.
       15, 1610.

131.   K. Aoki and M. Tanino, Yawata Techn. Rep., June 1966,
       no. 255, 159.

132. M.I. Goldshteyn, Trudy Ural Nauchno. - Issled. Inst. Chern. Met., 1966, (5), 170.

133. M.I. Goldshteyn and V.M. Farber, Phys. Metals Metallogr., 1968, 26, (6), 68.

134. J. Friedel, 'Les Dislocations', Gauthier Villars, Paris, 1956.

135. A. Kelly and R.B. Nicholson, 'Precipitation Hardening', Progress in Materials Science, Vol. 10, Pergamon Press, 1963.

136. T. Frnka, Second Intern. Conf. on Strength of Metals and Alloys, Vol. 2, 1970, 590.

137. D. Raynor, J.A. Whiteman and R.W.K. Honeycombe, J. Iron Steel Inst., 1966, 204, 349.

138. E. Smith, Acta Met., 1966, 14, (5), 583.

139. M. Tanino and T. Nishida, Trans. Japan Inst. Metals, Apr. 1968, 9, (2), 103.

140. M.I. Goldshteyn, Povysh. Konstruktivin Prochnosti Stalei i Splavov, Russian Collect., Moscow, 1970, (1), 51.

141. R.W.K. Honeycombe, Foundation of National Research Inst. for Metals, Proceedings, Tokyo, Japan 1966, 44.

142. J.M. Darbyshire and J. Barford, Acta Met., Apr. 1967, 15, (4), 671.

143. J.A. Whiteman and S.R. Keown, J. Sheffield Univ. Met. Soc., 1971, 10, 30.

144. V.M. Farber and B.Z. Belenky, Trudy Ural. Nauchno. - Issled. Inst. Chern. Met., 1971, (11), 227.

145. M.I. Goldshteyn, Trudy Ural. Nauchno. - Issled. Inst. Chern. Met., 1971, (11), 200.

146. A.T. Davenport, J. Iron Steel Inst., May 1968, 206, (5), 499.

147. M. Tanino and T. Sato, J. Iron Steel Inst. Japan, Dec. 1973, 59, (14), 1971.

148. S.W.K. Shaw and A.G. Quarrell, J. Iron Steel Inst., Jan. 1957, 185, 10.

149. W. Crafts and J.L. Lamont, Trans. A.I.M.E., 1950, 188, 561.

150. K.J. Irvine and F.B. Pickering, J. Iron Steel Inst., Feb. 1960, 194, 137.

151. W. Crafts and J.L. Lamont, Metals Tech., Sept. 1948, 2439.

152. F.B. Pickering, in 'Precipitation Processes in Steels', I.S.I. Spec. Rep. 64, 1959, 23.

153. Yu. A. Geller, V.F. Moiseev and A.O. Aranovich, Met. Sci. Heat Treat., Mar-Apr. 1971, $\underline{13}$, (3-4), 193.

154. L. Colombier and R. Lévêque, Mém.Sci. Rev. Mét., Jan. 1969, $\underline{66}$, (1), 1.

155. H.G. Suzuki, T. Sato and M. Tanino, Proc. Internat. Conf. Sci. Technol. Iron Steel, Tokyo, Sept. 1970, (2), 1082.

156. S.K. Biswas and A.K. Seal, Trans. Indian Inst. Metals, Dec. 1968, $\underline{21}$, (4), 21.

157. R.W.K. Honeycombe and A.K. Seal, in 'Precipitation Processes in Steels', I.S.I. Spec. Rep. 64, 1959, 44.

158. R. Viswanathan and C.G. Beck, Metall. Trans. A., Nov. 1975, $\underline{6A}$, (11), 1997.

159. Z. Cochnar and J. Cadek, Sb. Vedec Praci Vysoka Skoly Banske Ostravo, 1965, $\underline{11}$, (5), 795.

160. E. Staska, R. Blöch and A. Kulmburg, Mikrochim. Acta. 1970, Suppl. 4, 62.

161. Z. Cochnar, M. Zemcikova, R. Freiwillig and J. Cadek, Kovove Mat., 1973, $\underline{11}$, (2), 98.

162. A.G. Rakhshtadt, K.A. Lanskaya, N.M. Suleimanov and L.V. Katkova, Met. Sci.Heat Treat., May-June 1975, $\underline{17}$, (5-6), 477.

163. M.A. Gervasyev, A.L. Vinitskiy and M.I. Goldshteyn, Phys. Met. Metallogr., 1975, $\underline{40}$, (5), 143.

164. S.G. Guterman and M.I. Goldshteyn, Phys. Met. Metallogr., 1964, $\underline{17}$, (2), 145.

165. L.I. Kogan and R.I. Entin, Dokl. Akad. Nauk S.S.S.R., 1954, $\underline{94}$, 4.

166. M.A. Gervasyev, M.I. Goldshteyn, L.M. Panfilova and V.K. Rudenko, Phys. Met. Metallogr., 1974, $\underline{38}$, (5), 127.

167. I. Hrivnak, Czechoslov. J. Physics, 1969, $\underline{B19}$, (8), 987.

168. J.W. Cahn, Acta Met., 1957, $\underline{5}$, 169.

169. W. Hume-Rothery, 'Elements of Structural Metallurgy', Inst. of Metals Monog. and Report Series No. 26, 1966.

170. C.E. Lacy and M. Gensamer, Trans. A.S.M., 1944, $\underline{32}$, 88.

171. E.C. Bain, 'Function of Alloying Elements in Steel', Cleveland, A.S.M., 1939, 65.

172.   W.F. Rees, B.E. Hopkins and H.R. Tipler, J. Iron
        Steel Inst., May 1954, <u>177</u>, 93.

173.   International Tables for X-ray Crystallography, Kynock
        Press, 1962.

CHAPTER 10

10. Tables

Table 1

Composition of High Speed Steels

A.I.S.I. Designation	Designation quoted in text if either Designation in text different to or no A.I.S.I. Designation	Analysis (wt. %).									
		C	Mn	Si	S	P	Cr	V	W	Mo	Co
T1		0.75	0.30	0.30	0.03 max.	0.03 max.	4.00	1.00	18.00	–	–
T2		0.85	=	=	=	=	4.00	2.00	18.00	–	–
T3	R3	1.10	=	=	=	=	4.00	3.00	18.00	–	–
T4		0.75	=	=	=	=	4.25	1.00	18.50	–	5.00
T6	SK5	0.80	=	=	=	=	4.00	1.80	19.50	–	12.00
T9		1.25	=	=	=	=	4.00	4.00	18.00	–	–
T15		1.55	=	=	=	=	4.50	5.00	13.00	0.70	5.00
M1		0.80	=	=	=	=	4.00	1.00	1.50	8.50	–
M2	Mo30	0.85	=	=	=	=	4.00	2.00	6.00	5.00	–
M4		1.30	=	=	=	=	4.00	4.00	6.00	4.50	–
M7		1.00	=	=	=	=	4.00	2.00	1.50	8.50	–
M10		0.90	=	=	=	=	2.00	2.00	–	8.25	–

Specimen											
M15	—	1.55	"	"	"	"	4.50	5.00	6.50	4.00	5.00
M33	—	0.90	"	"	"	"	4.00	1.20	1.50	9.50	8.00
M34	—	0.90	"	"	"	"	4.00	2.00	1.50	3.00	3.00
M35	—	0.85	"	"	"	"	4.00	2.00	6.50	5.00	8.50
M36	—	0.85	"	"	"	"	4.00	2.00	6.00	5.00	8.50
M41	—	1.10	"	"	"	"	4.25	2.00	6.00	5.00	8.50
M42	—	1.10	"	"	"	"	4.00	6.75	3.75	3.75	5.00
M46	—	1.25	"	"	"	"	4.00	1.15	1.50	9.50	8.00
M50	—	0.85	"	"	"	"	4.00	3.20	2.00	8.00	8.25
D950		0.95	"	"	"	"	4.00	1.00	—	4.50	—
Mo325		1.00	"	"	"	"	4.00	1.10	1.70	5.00	—
Kono310		1.25	"	"	"	"	3.75	2.50	3.00	3.00	—
Sw9		0.90	"	"	"	"	4.25	3.25	10.50	4.00	10.00
SW9C		1.15	"	"	"	"	4.00	2.00	9.00	—	—
SW12		0.90	"	"	"	"	4.00	2.00	9.00	—	—
SW12C		1.15	"	"	"	"	4.00	2.00	12.00	—	—
SKC		1.05	"	"	"	"	4.25	2.00	12.00	—	5.00
SK5C		1.05	"	"	"	"	4.25	1.00	18.00	—	5.00

Table 2

Carbon Contents Necessary for Stoichiometric Balance with Carbide-Forming Elements (Hoyle[25])

Element	Carbide	Wt. % Carbon for 1 wt. % Element
Chromium	Cr_7C_3	0.099
Chromium	$Cr_{23}C_6$	0.060
Tungsten	W_2C	0.033
Molybdenum	Mo_2C	0.063
Vanadium	V_4C_3 (VC)	0.206

Table 3

Free Energies of Formation of Carbides at $298°K$ (Richardson[26])

Carbide	Free Energy of Formation (cal./mol. of Metal Atoms)
TaC	−64,000
TiC	−43,000
ZrC	−37,000
SiC	−12,300
VC	−12,000
WC	−8,400
$\frac{1}{7}Cr_7C_3$	−7,200
$\frac{1}{23}Cr_{23}C_6$	−4,400
$\frac{1}{3}Mn_3C$	−1,100
$\frac{1}{3}Fe_3C$	+1,500
$\frac{1}{2}Co_2C$	+1,700
$\frac{1}{3}Ni_3C$	+2,500

Table 4

Solubility during Austenitisation of the Primary Carbides present in High Speed Steels

Author(s)	Expt. Technique	Carbides (in some cases with volume fractions) present in steel in the annealed condition			Aust. Temp. (°C)	Carbides (in some cases with volume fractions) present in steel in the as-hardened condition			Comments on carbide solubility
eed on research aken									
Kayser and Cohen (28)	Preferential etching	M_6C	19.0		1280	M_6C	9.7		
		MC	0.9			MC	0.5		
		$M_{23}C_6$	9.0						
5		M_6C	11.5		1250	M_6C	4.5		
		MC	10.4			MC	8.5		
		$M_{23}C_6$	10.1						
Massin (48)	Electrolytic extraction & chemical analysis				1050 to 1250				M_6C slowly into solution at 1050°C, intensive solution 1200°C. Appreciable solution MC at 1250°C.

s for full range of steels on which research undertaken by these authors presented in FIG. 4. Results own in FIG. 5. for carbide contents of alloys as function of austenitisation temperature. Analyses of e steels given in Table 1.

Steel	Investigator	Technique	Carbides (temp. °C)	Comments
SW9	Malkiewicz, Bojarski and Foryst (49)	Electrolytic Extraction followed by chemical & X-ray diffraction analysis	M_6C, $M_{23}C_6$ — 900 to 1300; M_6C, MC, $M_{23}C_6$ — 900 to 1260. M_6C, $M_{23}C_6$ (after austenitisation at temperatures below 1100°C). M_6C, MC, $M_{23}C_6$ (after austenitisation at temperatures below 1100°C)	Solution of MC required slightly higher temperature than M_6C. $M_{23}C_6$ commenced dissolution at 900°C. Degree of carbide solution fairly insensitive to soaking time (providing not less than 1 minute).
M and SW9	Pickering (51)			Rate of solution of M_6C much greater in SW9 than T1.
M and SW9	Mackiewicz (52)			Solution rates of M_6C similar in both steels.

...s presented in Figs. 6 and 7, showing carbide contents of steels as function of soaking time at various ...itising temperatures.

	Author	Method	Phase		Temp. (°C)	Phase		Notes
T1 and SW9	Bojarski (53)	Electrolytic Extraction & X-ray diffraction analysis.			900 to 1300			
T1	Averbach (54)	Electrolytic Extraction & chemical analysis	M_6C MC $M_{23}C_6$	18.5 1.5 9.0	1290	M_6C MC	10.0 0.5	
M2			M_6C MC $M_{23}C_6$	16.0 3.0 9.0	1220	M_6C MC	7.5 1.5	
T1	Koh (55)	Electron microprobe analysis	M_6C	29.0	1290	M_6C	21.0	
M2			M_6C MC	15.0 2.2	1230	M_6C MC	15.0 1.3	No M_6C dissolved during austenitisation of M2.

268.

	Method	Total carbide volume fraction:-		Total carbide volume fraction:-	
Sansa, Mesoliver, Arcas and Espallarges (56)			1200 to 1260		Minimum soaking time of 2 minutes to approach maximum carbide solubility.
W9 W9C W12 W12C Chodorowski, Jurczak and Lampe (29)	Electrolytic extraction followed by chemical and x-ray diffraction analysis.	18.9 23.0 19.9 24.0	1230 1170 1250 1190	5.5 9.4 8.5 11.73	
W9 Gulyaev (57)	Electrolytic extraction and chemical analysis	16.4	1240	7.0	
Chodorowski, Jurczak and Lampe (58) K5 K5C KC	Electrolytic extraction followed by chemical & x-ray diffraction analysis	30.1 30.7 23.1	1270 1220 1190	15.7 18.3 11.6	Cobalt increased the solution rates of M_6C and MC.

Colombier (59)	Electrolytic extraction & X-ray diffraction analysis		1205 to 1280	Ratio M_6C:MC in as-hardened condition:- 97:3 T1, 92:8 T2, 87:13 M1, 61:39 M10, 44:56 M4
Bridge, Jr., Maniar and Philip (60)	Electrolytic extraction & X-ray diffraction analysis	M_6C MC $M_{23}C_6$ M_2C	740 to 1130	M_6C (after austenitisation at temperatures below 1110°C) MC $M_{23}C_6$ (after austenitisation at temperatures below 1010°C) M_2C.	Increasing temperature from 740 to 1130°C caused solution of 2.7 M_2C and 0.5wt.% MC.

No.	Reference	Method	Composition	Carbides	Temperature / treatment	Comments
3	Hegedus and Acs (62)	Transmission Electron microscopy	...with base composition 1, 4 chromium, ...dium and cobalt. ...en contents ...from 0.4 ...t.% and ...enum from ...wt.%.		1240 to 1300	Austenitisation at 1275°C resulted in solution of half the total carbide content.
	Popandopulo (63)	Electrolytic extraction and X-ray diffraction analysis		M_6C MC $M_7C_3(M_{23}C_6)$ Total carbide volume fraction:- 18% for high-molybdenum/low-tungsten steel, increasing with tungsten content to 2% for high-tungsten steel	1200 for high-molybdenum content of two low-tungsten /high-molybdenum steels to 1230 for low-molybdenum /high-tungsten steels	10wt.% of total carbide content of two low-tungsten /high-molybdenum steels. Two steels with high tungsten contents:- 45 and 60wt.%.
	Gulyaev, Kupalova and Baikov (64)	Electrolytic extraction and X-ray diffraction analysis	...with compo-...identical ...matrix solid ...ons or ...en-type, ...en/ ...en - ...and molybdenum- ...high speed steels -hardened ...ion, (carbon 0.34, ...en 0.22 to ...wt.%).		Samples annealed at 700°C for 10 hours	Opinion was that solubility of M_6C in austenite greatest when $K=0.7$

(28)   For given vanadium level, high-tungsten high speed steels favour formation of M_6C rather than MC, whilst converse true for high-molybdenum steels. This in agreement with (23) (37).

(48)   Results in good agreement with (28).

(49) M_6C most predominant carbide in both steels in annealed and as-hardened states, and tungsten favours formation of M_6C rather than MC. Both findings in good agreement with (28) (2)(50) These workers demonstrated inaccuracies in research by both of whom were of opinion that M_6C not dissolved at all during austenitisation of high speed steels. Both authors had employed soaking times of less than 1 minute, and had not approached equilibrium conditions for carbide solution.

(51)   In discussion of research by, (49) this author drew his conclusion on carbide solubility. Different positions which the two alloys occupy with respect to Fe-W-Cr-V-C equilibrium system could explain this phenomenon.

(52)   This author could not fully agree with opinion of (51) on solution rates of M_6C in SW9 and T1. He endorses his opinion by stating there were only slight differences in tungsten contents of matrices of the steels (Fig. 8) after corresponding austenitisation treatments. Volume fraction of M_6C, however, much greater for T1 in both annealed and as-hardened states.

(53)   Lattice parameter of M_6C constant at austenitisation temperatures less than $1250^\circ C$. Increase in lattice parameter at $1250^\circ C$ due to diffusion processes between matrix and carbide, with occurrence of coagulation. M_6C shown to have polygonal form owing to coagulation at temperatures at, or in excess of $1250^\circ C$.

(54)   Results for T1 in good agreement with (28). Austenitisation had not altered ratio of M_6C:MC, as present in steels in annealed condition. This also found to be case by (24) for high speed steels with relatively low vanadium contents.

(55)   Austenitisation and quenching had enriched matrix of T1 by 5.4 tungsten, 0.2 chromium, 0.1 vanadium and 0.2 wt. % carbon, with no change in manganese content. M2 had even less change in matrix analysis as result of hardening, with little carbide solution occurring. Results not in agreement with (28) (49) (54) (56). Surprisingly no mention made of $M_{23}C_6$ being present in steels in annealed state. High alloy content of matrices in annealed condition due to inaccuracies imparted in analysis as result of presence of high volume fraction of carbides. This had effect of giving low carbide solubilities in steels during austenitisation.

(56)   Minimum time for maximum carbide solubility in excess of corresponding time found by (49) for T1 and SW9 over much wider temperature range.

(29)   Increasing carbon content of SW9 and SW12 caused reduction in level of each of carbide forming elements in matrices in as-hardened condition.   This due to greater volume fractions of stable carbides, M_6C and MC.

(57)   These results in reasonable agreement with those of [29] for SW9.

(58)   To determine the effect of cobalt alone on carbide solubility, these authors had to compare results with those obtained for SW12C.[29]   Vast proportion of cobalt present in SK5, SK5C and SKC, in the annealed condition, dissolved in matrix.

(59)   Ratio M_6C:MC very high in tungsten-type high speed steels in as-hardened state, but much lower for molybdenum-type steels.   When vanadium present at 4wt.%, and above, in tungsten or molybdenum-type steels, MC predominant carbide after hardening.

(60)   Authors very surprised to find M_2C (Mo_2C) in this steel in both annealed and as-hardened states.   Very little phase analysis has been carried out on high speed steels containing molybdenum but with absence of tungsten. Presence of molybdenum favoured formation of M_2C, but only at high carbon levels.[14] M_2C shown to be metastable and easily dissolved during austenitisation.[14] [17]. However, [60] did determine some of M_2C present in M50 was metastable and had greater dissolution rate during austenitisation than $M_{23}C_6$ and M_6C.   Some of M_2C present was of stable form and difficult to dissolve.   Austenitising temperatures used were low, even for molybdenum-type high speed steels.   Hoyle[61] showed molybdenum caused reduction in eutectic temperature of these alloys to extent that usual austenitisation range 1180 to 1220°C .   These authors, however, demonstrated M_6C readily dissolved in M50, even at quite low temperatures. M_6C very stable and difficult to dissolve in tungsten-type high speed steels.[48][49] Conclusion drawn by [60] that tungsten critical element to stabilise M_6C.   Absence of tungsten in M50 decreased solvus of M_6C below normal austenitising temperature.

(62)   Polygonisation of carbides commenced at temperature of 1275°C.   This due to coalescence of individual carbides. Higher temperatures, caused carbides to increase in size, ultimately forming ledeburitic structure.

(63)   With decreasing amounts of tungsten in steels, the volume fraction of MC and M_7C_3 increases.   After austenitisation, martensitic matrix of alloy with highest tungsten level contained only 6.1 wt.% of this element. Analysis of this phase in two high-molybdenum/low-tungsten steels revealed that virtually all molybdenum present in alloys dissolved in matrices.   Vast proportion of cobalt present in alloys dissolved in matrix, in both annealed and as-hardened states, this in good agreement with (58).

(64)   Defined factor K, relating molybdenum content to total molybdenum and tungsten level, as follows:-

$$K = \frac{\text{Mo at \%}}{(W+Mo)\text{ at \%}} \quad \ldots\ldots\text{EQUATION } 38$$

Equiatomic replacement of tungsten with molybdenum up to value K = 0.7, led to equiatomic replacement in carbides. Combined matrix tungsten and molybdenum content greatest when K = 0.7.   Advised use of this value for optimum performance from high speed steels, concluding that replacement of high proportion of tungsten with molydbenum was desirable.

Table 5

Hardness of Primary Carbides (Fischer and Kohlhaas [17])

Carbide	Hardness ($HV_{0.025}$)
MC	2300-2500
M_2C	1700-1900
M_6C	1400-1600

Table 6

Composition of the High Purity Steels

Alloy Designation	Analysis (wt. %)								
	C	V	Si	Mo	Mn	Ni	Cr	Co	W
1	0.78	0.39	–	–	–	–	–	–	–
2	0.78	0.79	–	–	–	–	–	–	–
3	0.81	1.62	–	–	–	–	–	–	–
4(Si)	0.80	1.64	0.97	–	–	–	–	–	–
5(Mo)	0.79	1.64	–	1.02	–	–	–	–	–
6(Mn)	0.80	1.64	–	–	0.97	–	–	–	–
7(Ni)	0.82	1.63	–	–	–	1.03	–	–	–
8(Cr)	0.83	1.63	–	–	–	–	1.00	–	–
9(Co)	0.83	1.61	–	–	–	–	–	0.97	–
10(W)	0.83	1.59	–	–	–	–	–	–	1.99

Table 7

Composition of the Commercial Purity Steels

Alloy Designation	Analysis (wt. %)										
	C	V	Si	Mn	S	P	Cr	Mo	W	Al	N
11	0.086	0.06	0.27	0.74	0.015	0.009	0.05	0.01	–	0.027	0.007
12	0.083	0.22	0.29	0.76	0.017	0.009	0.04	0.01	–	0.030	0.008
13	0.086	0.55	0.29	0.75	0.012	0.007	0.06	0.02	–	0.040	0.007
14	0.086	1.11	0.30	0.75	0.019	0.007	0.08	0.01	–	0.079	0.007
15	0.080	0.05	0.30	0.78	0.020	0.009	0.04	0.02	–	0.032	0.016
16	0.079	0.24	0.27	0.78	0.015	0.010	0.06	0.01	–	0.030	0.015
17	0.080	0.53	0.26	0.72	0.013	0.007	0.05	0.02	–	0.025	0.018
18	0.082	1.13	0.30	0.76	0.015	0.007	0.04	0.01	–	0.031	0.018

Table 8

Carbon Contents at Varying Positions in the Carburised Case
of Alloy 12

Distance from Specimen Surface (mm.)	Carbon Content (wt. %)
0.25	1.29
0.50	1.29
0.75	1.27
1.00	1.25
1.25	1.22
1.50	1.15
1.75	1.06
2.00	0.96
2.25	0.86
2.50	0.75
2.75	0.64
3.00	0.52
3.25	0.42
3.50	0.32
3.75	0.22
4.00	0.14
4.25 (Core)	0.08

Table 9

Austenitisation Temperatures and Soaking Times Employed
During Hardening for the High Purity Steels Containing only
Vanadium as an Alloying Addition. The Optimum Austenitising
treatment has been underlined in each instance.

Austenitisation Temperature (°C)	Soaking Time (mins.)	Alloy Designation
850	20	1, 2 and 3
900	20	1, 2 and 3
920	20	1
920	30	1
920	45	1
950	20	1, 2 and 3
1000	20	1, 2 and 3
1000	30	2
1000	45	2
1050	20	1, 2 and 3
1100	20	1, 2 and 3
1120	20	3
1120	30	3
1120	45	3
1150	20	1, 2 and 3
1200	20	1, 2 and 3

Table 10

Austenitisation Temperatures and Soaking Times Employed During Hardening for the High Purity Steels containing Vanadium and a Second Alloying Addition.   The Optimum Austenitising Treatment is presented for each alloy.

Austenitisation Temperature (°C)	Soaking Time (mins.)	Alloy Designation	Optimum Austenitisation Treatment
850	20	All Alloys	–
900	"	" "	–
950	"	" "	–
1000	"	" "	–
1050	"	" "	–
1100	"	" "	–
1120	"	" "	Alloys 4(Si), 6(Mn), 7(Ni) and 9(Co).
1150	"	" "	Alloys 5(Mo), 8(Cr) and 10(W).
1200	"	" "	–

Table 11

Austenitisation Temperatures and Soaking Times employed during Hardening for the Commercial Purity Steels.   Only Optimum Austenitisation Treatments were used.

Austenitisation Temperature (°C)	Soaking Time (Mins.)	Alloy Designation
860	20	11 and 15
900	"	12 " 16
940	"	13 " 17
1040	"	14 " 18

Table 12

Grain Size of the High Purity Steels, Containing only Vanadium as an Alloying Addition, after varying Austenitisation Treatments During Hardening.

Austenitisation Temperature (°C)	Soaking Time (mins.)	A.S.T.M. Grain Size		
		Alloy 1	Alloy 2	Alloy 3
850	20	9	9	11
900	20	8	9	11
920	20	8	–	–
920	30	8	–	–
920	45	7	–	–
950	20	7	8	11
1000	20	7	8	11
1000	30	–	8	–
1000	45	–	8	–
1050	20	5	7	10
1100	20	3	4	8
1120	20	–	–	7
1120	30	–	–	7
1120	45	–	–	7
1150	20	1	2	6
1200	20	1	1	4

300.

Table 13

Grain Size of the High Purity Steels, containing Vanadium and a Second Alloying Addition, after Varying Austenitisation Treatments during Hardening

Austenitisation Temperature (°C)	Soaking Time (mins.)	A.S.T.M. Grain Size						
		Alloy 4(Si)	Alloy 5(Mo)	Alloy 6(Mn)	Alloy 7(Ni)	Alloy 8(Cr)	Alloy 9(Co)	Alloy 10(W)
850	20	11	11	11	11	11	11	11
900	20	11	11	11	11	11	11	11
950	20	11	11	11	11	11	11	11
1000	20	11	11	11	11	10	11	11
1050	20	10	10	10	10	9	10	10
1100	20	9	9	8	8	8	8	9
1120	20	9	9	8	8	8	8	9
1150	20	8	8	6	6	7	6	8
1200	20	4	4	4	4	4	4	4

Table 14

Hardness of the Steels in the As-Cast Condition

Alloy Designation	Hardness (HV/30)
1	373
2	407
3	431
4 (Si)	477
5 (Mo)	459
6 (Mn)	483
7 (Ni)	438
8 (Cr)	440
9 (Co)	424
10 (W)	489
11	213
12	243
13	249
14	259
15	215
16	239
17	246
18	254

Table 15

Hardness of the Steels in the As-Cast and Annealed Condition

Alloy Designation	Hardness (HV/30)
1	201
2	204
3	211
4 (Si)	234
5 (Mo)	229
6 (Mn)	229
7 (Ni)	205
8 (Cr)	207
9 (Co)	204
10 (W)	216
11	104
12	141
13	153
14	160
15	104
16	140
17	150
18	152

Table 16

Hardness of the Steels in the Forged Condition

Alloy Designation	Hardness (HV/30)
1	293
2	302
3	325
4 (Si)	332
5 (Mo)	395
6 (Mn)	335
7 (Ni)	304
8 (Cr)	385
9 (Co)	282
10 (W)	388
11	162
12	211
13	216
14	237
15	159
16	216
17	216
18	235

Table 17

Hardness of the Steels in the Annealed Condition

Alloy Designation	Hardness (HV/30)
1	206
2	223
3	240
4 (Si)	266
5 (Mo)	229
6 (Mn)	256
7 (Ni)	207
8 (Cr)	235
9 (Co)	207
10 (W)	221
11	109
12	170
13	183
14	198
15	112
16	172
17	180
18	190

Table 18

Hardness of the High Purity Steels, containing only Vanadium as an Alloying Addition, after varying Austenitisation Treatments During Hardening.

Austenitisation Temperature (°C)	Soaking Time (mins.)	Hardness (HV/30)		
		Alloy 1	Alloy 2	Alloy 3
850	20	829	812	772
900	20	829	823	803
900	30	832	823	806
900	45	830	821	808
920	20	841	-	-
920	30	836	-	-
920	45	834	-	-
950	20	840	842	822
1000	20	829	858	841
1000	30	-	852	-
1000	45	-	854	-
1050	20	820	837	845
1100	20	802	837	858
1120	20	-	-	862
1120	30	-	-	854
1120	45	-	-	855
1150	20	762	813	851
1150	30	744	813	844
1150	45	721	806	844
1200	20	702	786	836

Table 19

Hardness of the High Purity Steels, containing Vanadium and a Second Alloying Addition, after varying Austenitisation Treatments during Hardening.

Austenitisation Temperature (°C)	Soaking Time (mins.)	Hardness (HV/30)						
		Alloy 4(Si)	Alloy 5(Mo)	Alloy 6(Mn)	Alloy 7(Ni)	Alloy 8(Cr)	Alloy 9 (Co)	Alloy 10(W)
850	20	802	798	808	812	812	772	805
900	"	804	796	818	822	820	802	810
950	"	832	820	820	848	842	804	841
1000	"	843	829	839	855	870	806	841
1050	"	849	846	839	857	875	803	856
1100	"	849	856	854	864	870	819	856
1120	"	855	856	856	864	876	830	872
1150	"	865	877	851	842	879	817	888
1200	"	833	842	815	788	842	778	849

Hardness of the Carburised Steels in the As-Hardened Condition, and after Tempering at varying temperatures for 1 hour. Each hardness value is at a position in the Carburised case where the Carbon Content is 1.29 wt. %.

Table 20.

Alloy Designation	As.Hard.	Hardness (HV/5) Tempering Temperature (°C)										
		100	150	200	300	400	500	550	560	580	600	700
11	900	900	883	724	607	487	307	295	293	290	287	222
12	916	914	898	743	642	540	388	392	395	398	403	291
13	919	920	906	761	659	594	466	481	483	490	494	353
14	941	941	930	788	698	643	530	551	555	563	570	391
15	891	889	871	721	600	504	324	314	311	307	305	243
16	913	909	891	733	622	534	392	399	401	405	409	283
17	921	924	910	766	661	589	468	485	488	493	499	347
18	933	930	920	780	686	637	528	541	546	553	562	379

Hardness of the Carburised Steels in the As-Hardened Condition, and after Tempering at varying temperatures for 1 hour. Each hardness value is at a position in the Carburised case where the carbon content is 1.00 wt. %.

Table 21

Alloy Designation	As.Hard.	Hardness (HV/5) Tempering Temperature (°C)										
		100	150	200	300	400	500	550	560	580	600	700
11	880	876	857	707	580	473	310	299	293	287	285	225
12	891	894	877	728	613	526	385	391	393	398	401	281
13	899	895	880	736	637	564	459	475	478	486	491	340
14	914	914	901	761	670	615	527	546	550	558	564	384
15	884	885	865	716	593	492	321	313	308	303	300	227
16	894	894	874	728	610	522	383	393	394	397	400	279
17	899	890	877	735	629	569	466	484	486	492	499	343
18	916	918	906	764	662	612	520	538	541	550	558	377

Hardness of the Carburised Steels in the As-Hardened Condition, and after Tempering at varying temperatures for 1 hour. Each hardness value is at a position in the carburised case where the Carbon Content is 0.80 wt.%.

Table 22

Alloy Designation	As Hard	Hardness (HV/5) Tempering Temperature (°C)										
		100	150	200	300	400	500	550	560	580	600	700
11	858	858	838	699	562	464	300	290	288	284	282	229
12	871	868	850	708	585	499	370	377	378	380	383	260
13	881	879	863	725	617	554	447	463	466	461	478	318
14	891	891	877	739	647	592	520	543	547	557	565	376
15	854	854	832	695	551	450	296	287	282	278	275	227
16	871	873	854	709	596	506	362	374	375	374	377	262
17	888	887	871	728	614	542	453	474	468	480	486	326
18	892	892	876	735	651	581	512	534	539	547	553	364

Hardness of the Carburised Steels in the As-Hardened Condition, and after Tempering at varying temperatures for 1 hour. Each hardness value is at a position in the carburised case where the Carbon Content is 0.60 wt.%.

Table 23

Alloy Designation	As Hard	Hardness (HV/5) Tempering Temperature (°C)										
		100	150	200	300	400	500	550	560	580	600	700
11	805	800	779	665	548	453	292	280	276	272	268	226
12	816	816	799	685	575	493	360	367	371	373	378	256
13	832	824	809	691	620	541	440	456	461	468	475	287
14	848	842	827	709	631	574	494	516	523	531	541	338
15	798	797	775	657	545	459	295	282	278	275	270	229
16	804	804	783	668	566	477	361	372	373	373	377	250
17	837	832	814	700	609	539	437	452	455	465	473	299
18	844	844	827	707	619	559	477	499	504	512	522	329

Hardness of the Carburised Steels in the As-Hardened condition, and after Tempering at varying temperatures for 1 hour. Each hardness value is at a position in the carburised case where the Carbon Content is 0.40 wt. %.

Table 24

Alloy Designation	As Hard	Hardness (HV/5) — Tempering Temperature (°C)										
		100	150	200	300	400	500	550	560	580	600	700
11	679	679	656	571	474	390	285	278	271	267	261	202
12	700	702	682	598	494	429	320	328	351	333	336	231
13	715	710	693	602	546	488	396	416	420	427	433	248
14	743	743	728	631	568	510	422	446	451	461	472	270
15	681	686	662	577	483	401	283	273	271	266	257	205
16	707	705	684	596	503	401	334	346	348	353		235
17	709	709	692	602	539	432	391	407	412	421	429	249
18	752	745	731	646	572	523	427	449	453	463	473	264

Hardness of the Carburised Steels in the As-Hardened condition, and after Tempering at varying temperatures for 1 hour. Each hardness value is at a position in the carburised case where the Carbon Content is 0.20 wt. %.

Table 25

Alloy Designation	As Hard	Hardness (HV/5) — Tempering Temperature (°C)										
		100	150	200	300	400	500	550	560	580	600	700
11	421	421	400	355	307	271	236	224	220	217	214	181
12	456	454	435	393	306	278	284	238	292	295		204
13	492	492	474	427	363	319	335	340	346	362		219
14	535	535	522	472	436	401	364	402	412	425	439	264
15	429	425	404	353	312	280	237	228	224	219	213	180
16	447	444	427	391	349	310	270	277	281	284	288	201
17	482	482	467	427	387	352	326	343	349	355	371	222
18	532	529	513	469	425	394	362	396	406	421	437	267

Hardness of the cores of the Carburised Steels in the As-Hardened condition, and after tempering at varying temperatures for 1 hour.

Table 26

Alloy Designation	Carbon Content of Core (wt. %)	Hardness (HV/5) Tempering Temperature (°C)											
		As Hard	100	150	200	300	400	500	550	560	580	600	700
11	0.083	349	349	339	302	259	217	194	185	181	176	174	133
12	0.086	361	359	348	310	275	242	219	227	232	237	243	169
13	0.086	368	365	355	312	287	260	236	248	253	256	264	193
14	0.086	382	381	372	323	304	286	253	261	265	268	273	226
15	0.079	349	346	339	300	259	213	191	181	177	174	169	137
16	0.080	352	352	344	309	273	244	218	225	229	234	240	174
17	0.080	373	370	358	319	291	265	238	248	254	258	263	200
18	0.082	382	382	375	326	309	289	257	264	267	270	276	224

Table 27

Hardness of the Carburised Steels after Tempering for varying times at 560°C. Each hardness value is at a position in the carburised case where the Carbon Content is 1.29 wt.%

Alloy Designation	Tempering Time at 560°C (hrs.)												
	1	2	5	8	16	23	40	70	100	120	160	190	220
						Hardness (HV/5)							
11	293	292	291	291	289	288	282	262	260	256	254	254	253
12	395	395	397	398	401	397	390	379	370	366	360	359	357
13	483	484	487	490	498	494	483	468	448	435	405	404	402
14	555	557	562	570	582	582	577	561	538	518	492	492	492
15	311	309	309	308	305	303	298	287	273	268	264	261	261
16	401	400	403	403	406	401	396	384	373	367	366	364	362
17	488	488	490	494	503	498	490	473	452	442	411	411	409
18	546	547	553	558	571	571	563	548	527	508	483	482	482

Table 28

Hardness of the Carburised Steels after Tempering for varying times at 560°C. Each hardness value is at a position in the carburised case where the Carbon Content is 1.00 wt.%

Alloy Designation	Tempering Time at 560°C (hrs.)												
	1	2	5	8	16	23	40	70	100	120	160	190	220
						Hardness (HV/5)							
11	293	293	291	291	288	286	280	271	260	256	255	254	252
12	393	396	397	399	400	395	389	379	367	361	357	356	354
13	478	479	483	487	495	493	482	466	446	433	402	401	400
14	550	552	556	563	578	577	568	554	533	515	487	487	487
15	308	306	304	303	301	299	293	283	272	266	262	260	258
16	394	394	396	398	401	398	393	382	373	363	360	359	358
17	486	487	489	491	502	499	489	471	452	439	408	407	405
18	541	544	550	553	567	566	557	544	522	504	477	475	475

312.

Table 29

Hardness of the Carburised Steels after Tempering for varying times at 560°C. Each hardness value is at a position in the carburised case where the Carbon Content is 0.80 wt. %

Alloy Designation	Tempering Time at 560°C (hrs.) Hardness (HV/5)												
	1	2	5	8	16	23	40	70	100	120	160	190	220
11	288	287	287	286	282	280	273	263	254	247	247	247	247
12	378	380	382	383	389	387	385	376	362	354	353	352	352
13	466	467	471	474	483	481	472	456	439	427	400	398	398
14	547	548	555	560	576	574	563	548	529	515	485	485	485
15	282	280	279	279	276	274	268	257	249	243	242	242	242
16	375	376	378	380	385	382	381	371	359	351	349	349	348
17	474	476	479	481	491	490	480	462	445	430	404	404	403
18	539	541	547	551	567	563	553	536	519	503	477	477	476

Table 30

Hardness of the Carburised Steels after Tempering for varying times at 560°C. Each hardness value is at a position in the carburised case where the Carbon Content is 0.60 wt. %

Alloy Designation	Tempering Time at 560°C (hrs.) Hardness (HV/5)												
	1	2	5	8	16	23	40	70	100	120	160	190	220
11	276	275	275	273	272	271	265	256	248	241	240	240	240
12	371	373	374	376	382	380	378	371	360	353	349	348	348
13	461	463	466	469	482	480	474	452	436	424	398	397	397
14	523	525	528	535	557	554	545	533	517	505	477	477	477
15	278	277	275	274	272	270	264	255	248	242	242	242	242
16	373	373	375	377	385	380	378	369	357	351	347	346	346
17	455	456	459	463	478	476	468	454	440	428	404	402	402
18	504	505	509	515	537	532	523	508	496	482	455	455	454

Hardness of the Carburised Steels after Tempering for varying times at 560°C. Each hardness value is at a position in the carburised case where the Carbon Content is 0.40 wt. %.

Table 31.

Alloy Designation	Tempering Time at 560°C (hrs.) Hardness (HV/5)												
	1	2	5	8	16	23	40	70	100	120	160	190	220
11	271	271	270	270	267	266	262	254	246	240	239	238	238
12	331	331	334	337	344	343	341	336	330	326	322	318	318
13	420	422	427	433	447	445	445	426	412	400	379	378	378
14	451	453	461	469	492	491	486	475	463	454	434	430	430
15	271	270	269	267	265	263	258	250	243	236	234	233	233
16	346	348	350	351	357	354	351	344	339	336	329	329	329
17	412	415	420	427	440	438	432	422	411	402	383	383	382
18	453	454	463	469	490	487	481	469	457	447	423	421	420

Hardness of the Carburised Steels after Tempering for varying times at 560°C. Each hardness value is at a position in the carburised case where the Carbon Content is 0.20 wt. %.

Table 32

Alloy Designation	Tempering Time at 560°C (hrs.) Hardness (HV/5)												
	1	2	5	8	16	23	40	70	100	120	160	190	220
11	220	219	219	219	218	218	217	213	208	206	206	204	204
12	288	289	293	297	308	307	304	295	286	278	258	257	256
13	340	342	349	356	375	374	370	360	350	341	322	319	317
14	412	414	423	431	466	465	459	449	436	426	407	402	402
15	224	222	220	220	218	218	218	214	207	206	204	201	201
16	281	281	284	287	297	297	295	285	276	266	250	248	248
17	349	352	358	363	385	381	376	365	358	348	329	328	324
18	406	410	422	430	467	467	462	451	439	430	412	410	408

Per Cent.

Type M2.

Type M10.

Weight %
Atomic %

Type T1.

C W Mo Cr V Fe
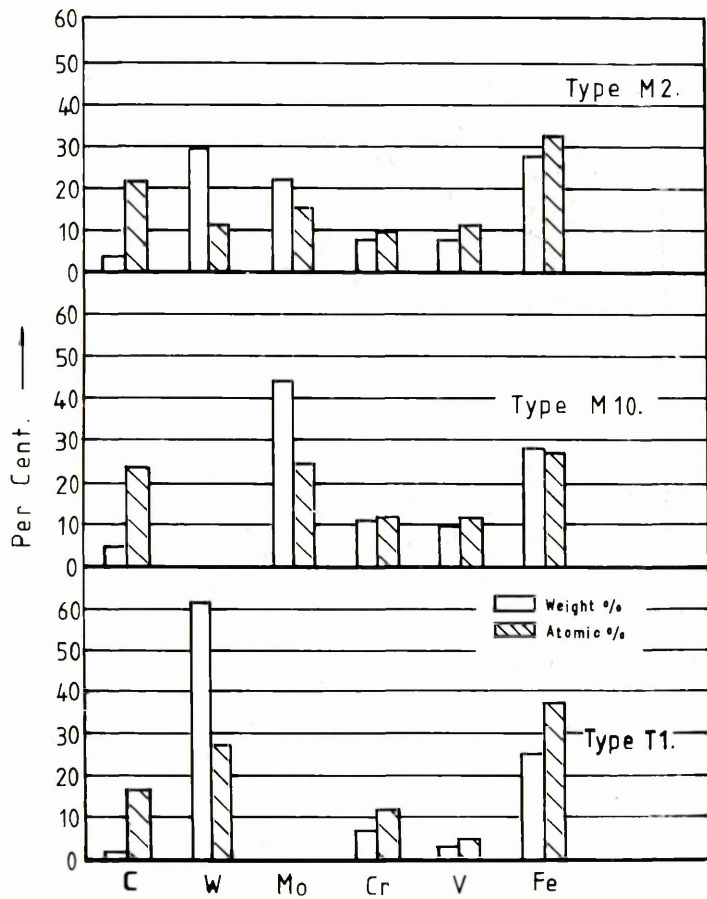
Composition of Carbides present in the High Purity Steels in the As-Hardened Condition

Table 32

Alloy Designation	Carbides Present	Analysis (wt. %)									
		Cr	Fe	Mo	W	V	C	Si	Mn	Ni	Co
1	V_4C_3	—	4.4	—	—	78.6	17.0	—	—	—	—
2	V_4C_3	—	4.44	—	—	78.9	16.7	—	—	—	—
3	V_4C_3	—	4.1	—	—	79.6	16.3	—	—	—	—
4(Si)	V_4C_3	—	4.5	—	—	78.9	16.4	0.1	—	—	—
5(Mo)	V_4C_3	—	2.6	6.5	—	75.0	15.9	—	—	—	—
"	Mo_2C	—	8.9	79.3	—	4.7	7.1	—	—	—	—
6(Mn)	V_4C_3	—	4.3	—	—	79.2	16.2	—	0.3	—	—
7(Ni)	V_4C_3	—	4.0	—	—	80.1	15.7	—	—	0.2	—
8(Cr)	V_4C_3	6.1	2.8	—	—	75.4	15.7	—	—	—	—
"	Cr_7C_3	50.6	35.2	—	—	5.5	8.7	—	—	—	—
9(Co)	V_4C_3	—	3.8	—	—	80.1	15.9	—	—	—	0.2
10(W)	V_4C_3	—	2.8	—	7.4	74.6	15.2	—	—	—	—
"	W_2C	—	6.3	—	86.4	2.9	4.4	—	—	—	—

Table 34

Composition of Graphitic Tool Steels

Grade of Graphitic Tool Steel	Analysis (wt.%)						
	C	Si	Mn	Cr	Mo	Ni	W
1	1.50	0.80	0.30	—	0.25	—	—
2	1.50	0.65	0.30	—	0.50	—	2.80
3	1.50	1.25	1.25	0.35	0.50	1.75	—

315.

Table 35

Intensity Factors for certain Martensite and Austenite Peaks

Intensity Factor	Alloy 7(Ni)		Alloy 9(Co)	
	α 200	γ 200	α 200	γ 200
Bragg Angle (Θ)	14.40°	11.50°	14.40°	11.45°
Multiplicity (M)	6	6	6	6
Lorentz Polarization (LP)	29.51	47.42	29.51	47.82
Debye-Waller (e^{-2m})	0.910	0.943	0.910	0.945
Atomic Scattering (f)	14.5	16.2	14.5	16.3
Structure Factor (F)	2	4	2	4
$1/v^2$ (v is volume of unit cell)	1.79x10^{-3}kx units	4.68x10^{-4}kx units	1.79x10^{-3}kx units	4.68x10^{-4}kx units
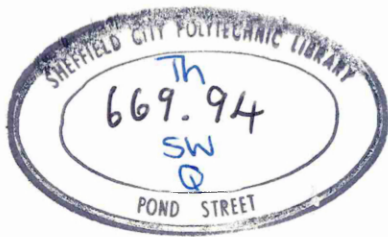
11.   Figures

FIG. 1.   Relationship between atomic and weight percentages of the elements present in T1 and M2 high speed steels (Gill [27]).

FIG. 2.   Chemical analysis of carbide extracted from M2, M10 and T1 high speed steels (Kayser and Cohen [28]).

Liq

Liq+δ+γ

Liq+δ+η Liq+δ

δ

Liq +γ

1345°

α(δ)+ξ

Liq+γ+η 1085°

γ+η

x

α(δ) α(δ)+γ+η

+η A

Y+θ+η

785°

α(δ)
+η+ξ

α+θ+η

1600

1400

1200

1000

800

600

Temperature (°C)

0   0,4   0,8   1,2   1,6   2,0

Carbon content (Wt %) ⟶

- - - - - Kuo's   modification

— · — Goldschmidt modification

Volume percentage of carbide ⟶

30

25

20

15

10

5

0

Total M₆C M₂₃C₆ MC (T1 1290°C)
Total M₆C M₂₃C₆ MC (T4 1290°C)
Total M₆C M₂₃C₆ MC (T2 1290°C)
Total M₆C M₂₃C₆ MC (M1 1205°C)
Total M₆C M₂₃C₆ MC (M2 1220°C)
Total M₆C M₃C₆ MC (M10 1205°C)
Total M₆C M₂₃C₆ (M4 1220°C)
Total M₆C M₂₃C₆ MC (T15 1250°C)

T 1   T 4   T 2   M 1   M 2   M10   M 4   T 15

1290°C 1290°C 1290°C 1205°C 1220°C 1205°C 1220°C 1250°C

FIG. 3.   Constitutional diagram for T1 high speed steel.
This is a binary section through the quaternary Fe-W-Cr-C system
at 18W and 4 wt. % Cr (Murakami and Hatta [46]).   Also shown are
the modifications at high (Kuo [47]) and low (Goldschmidt [42])
temperatures.

FIG. 4.   Volume fractions of carbides in high speed steels.
Open and cross-hatched bars indicate volume fractions in annealed
and as-hardened conditions.   Austenitisation was carried out at
commercial hardening temperatures.   (Kayser and Cohen [28]).

Weight Percentage Of Carbide.

18-4-2 (T2)
18-4-1-5 (T4)
18-4-1 (T1)
12-5-5-5 (T15)
6-5-4-2 (M2)
1½-9-4-1 (M1)
6-5-4-4 (M4)
0-9-4-2 (M10)

As Annealed.

Austenitising Temperature, °C.

Carbide content (Wt %)

900 °C
1000 °C
1100 °C
1200 °C
1230 °C

Austenitising time, min
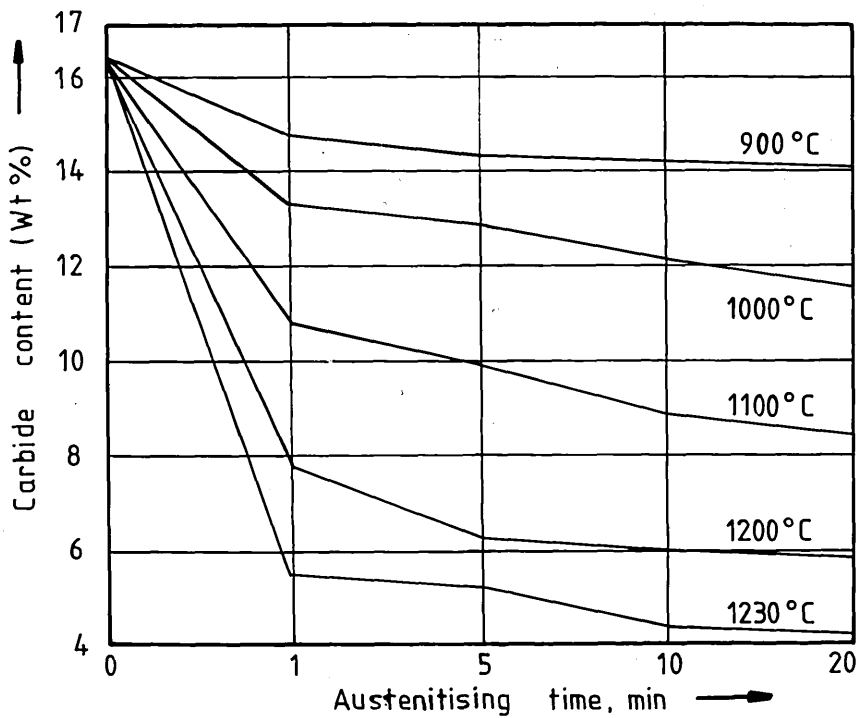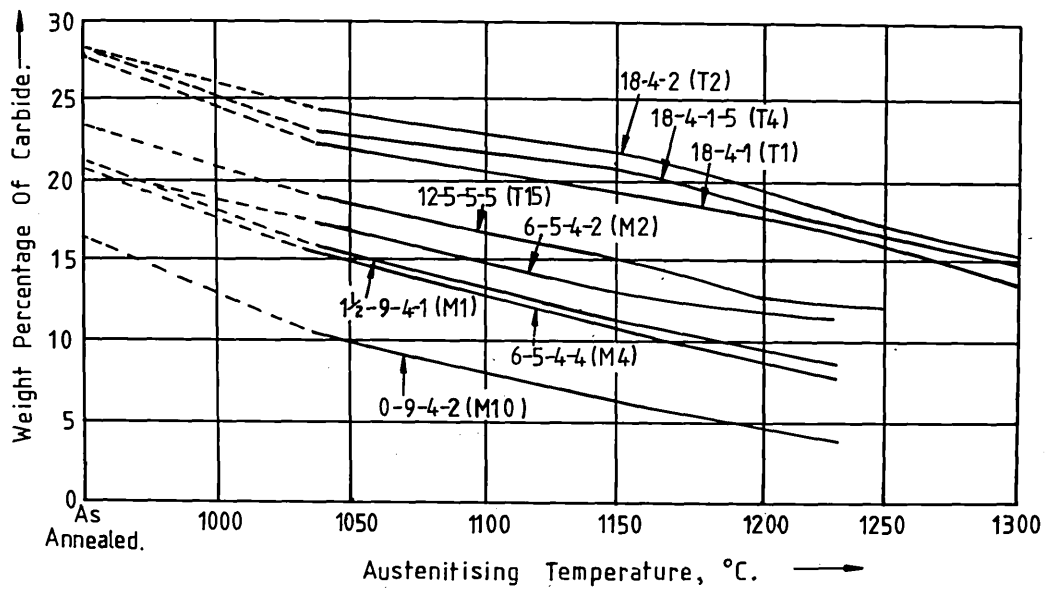
FIG. 5.   Relationship between total carbide content, in
terms of weight percentage, and austenitisation temperature for
several high speed steels (Kayser and Cohen [28]).

FIG. 6.   Relationship between total carbide content, in
terms of weight percentage, and soaking time at several
austenitisation temperatures, for T1 high speed steel (Malkiewicz,
Bojarski and Foryst [49]).
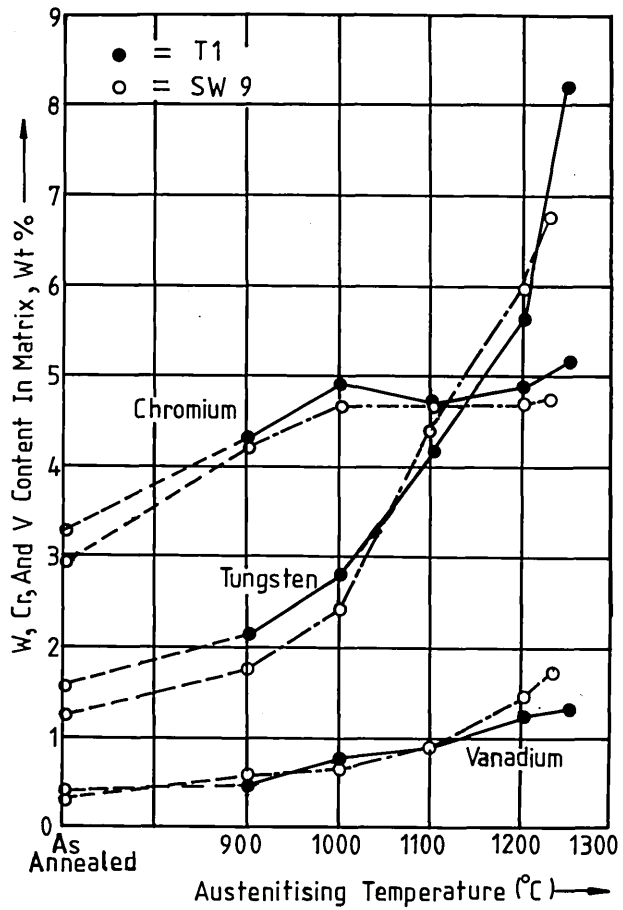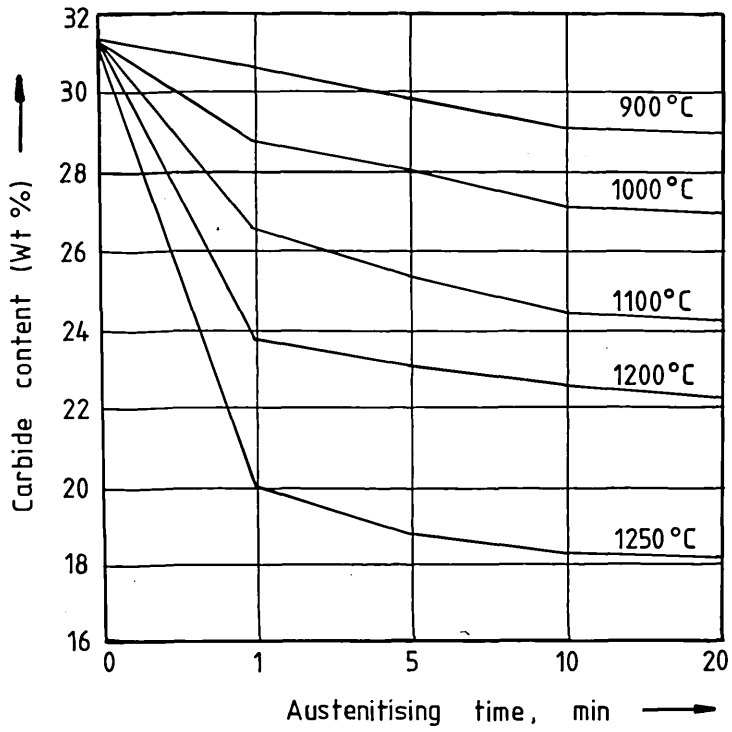
FIG. 7.   Relationship between total carbide content, in terms of weight percentage, and soaking time at several austenitisation temperatures, for SW9 high speed steel (Malkiewicz, Bojarski and Foryst [49]).

FIG. 8.   Relationship between matrix tungsten, chromium and vanadium levels and austenitisation temperature, for T1 and SW9 high speed steels in the as-hardened state (Malkiewicz, Bojarski and Foryst·[49]).

Top figure

Rockwell C hardness (y-axis): 70, 65, 60, 55, 50, 45, 40, 35, 30

1220°C

1190°C

Parameter = T (20 + logt)

x-axis: 10,000 18,000 26,000 34,000 42,000

Bottom figure

Weight Percentage Carbon In Steel (y-axis): 2·50, 2·25, 2·00, 1·75, 1·50, 1·25, 1·00, 0·75, 0·50, 0·25, 0

Numbers refer to casts used

(6) Not Forgeable
(12) Not Forgeable
(18) Not Forgeable
(24) Not Forgeable
(30) Not Forgeable

(5) Not Forgeable

(11) MC (2·4) M₆C (9·5) M₂₃C₆(15·6)

(17) MC (8·4) M₆C(9·5) M₂₃C₆(14·2)

(26) MC (14·1) M₆C (10·7) M₂₃C₆(6·8)

(29) MC (12·6) M₆C (18·6) M₂₃C₆ (Tr)

M₆C + MC + M₂₃C₆

(4) M₆C (9·3) M₂₃C₆(22·2)

(10) MC (2·8) M₆C (10·0) M₂₃C₆(12·0)

(16) MC (5·6) M₆C (15·9) M₂₃C₆(4·8)

(22) MC(9·5) M₆C(12·0) M₂₃C₆(Tr.)

(28) MC (8·8) M₆C (19·0) M₃R₂(Tr)

M₆C + M₂₃C₆

6-5-4-2 High Speed Steels
5-5-4-2

M₆C + MC + M₃ R₂

(3) M₆C (12·6) M₂₃C₆(15·6)

(9) MC(1·7) M₆C(13·0) M₂₃C₆(8·5)

(15) MC (5·0) M₆C (13·6) M₂₃C₆(Tr)

(21) MC (6·2) M₆C (16·9) M₃R₂(Tr)

(27) MC(8·5) M₆C (2·9) M₃R₂(13·2)

(2) M₆C (13·4) M₂₃C₆ (7·2)

(8) MC (0·8) M₆C(11·1) M₂₃C₆(5·5)

(14) MC (1·9) M₆C (14·7) M₃R₂(Tr)

M₆C + MC + M₃ R₂

(20) MC (3·0) M₆C (0·5) M₃R₂(18·9)

(23) MC (3·4) M₃R₂(26·8)

(1) M₆C + M₃R₂ M₆C (2·3) M₃R₂(15·3)

(7) M₆C (2·9) M₃R₂ (16·2)

(13) MC (Tr) M₆C (2·4) M₃R₂(16·0)

(19) MC (1·2) M₃R₂(19·0)

MC + M₃ R₂

(25) MC (3·8) M₃R₂(26·4)

x-axis: 0 1 2 3 4 5 6 7 8 9 10 11

Weight Percentage Vanadium In Steel

FIG. 9.   Master tempering curve for high speed steel, presenting the relationship between hardness and the parameter M = T (20 + log t), where t = Time (Hours) and T = absolute temperature on Fahrenheit scale (^{O}F + 460) ^{O}A (Holloman and Jaffe [68]).

FIG. 10.   Identification and volume fractions of excess phases present in annealed high speed steel of base composition M2, as a function of the vanadium and carbon contents (Blickwede, Cohen and Roberts [93]).

Austenite + M₆C + MC (+M₂₃C₆ below 1149°C) (+δ above 1038°C)

Austenite +
M₆C + MC
(+M₂₃C₆
below
1093°C)

Ferrite + M₆C
+MC (+Austenite
above 1149°C)

Potentially useful highspeed steels

Austenite +
M₆C(+M₂₃C₆
below 1149°C)
(+δ above
1093°C)

Ferrite +
M₆C+MC

Ferrite +M₆C+
MC (+M₃R₂ below
1093°C)

2.00
1.75
1.50
1.25
1.00
0.75
0.50
0.25
0

Carbon content (Wt %)

⑪ ⑰ ㉖ ㉙
④ ⑩ ⑯ ㉒ ㉘
③ ⑨ ⑮ ㉑ ㉗
② ⑧ ⑭ ⑳ ㉓
① ⑦ ⑬ ⑲ ㉕

0 1 2 3 4 5 6 7 8 9 10 11

Vanadium (Wt %)

Ferrite + M₆C
(+M₃R₂ below 1093°C)

Ferrite + MC
(+M₃R₂ below 1093°C)

2.0
1.8
1.6
1.4
1.2
1.0
0.8
0.6
0.4
0.2
0

Carbon (Wt %)

Not Forgeable

Increasing Ret Aust.

Ferrite At Grain Boundary

Increasing Ret. Aust.

Constant Retained Aust.

Optimum Combination Of V & C.

Potentially
Useful High
Speed
Steels.

Increasing Vanadium Carbide

Ferritic
(Not Quench Hardenable)

0 1 2 3 4 5 6 7 8 9 10

Vanadium (Wt.%)

FIG. 11. Phase relationships in high speed steel of base composition M2, containing varying vanadium and carbon contents, after austenitisation at temperatures between 925 and 1260°C and subsequent quenching (Blickwede, Cohen and Roberts [93]).

FIG. 12. General correlation of the effects of vanadium and carbon in high speed steels of base composition M2 (Blickwede, Cohen and Roberts [93]).
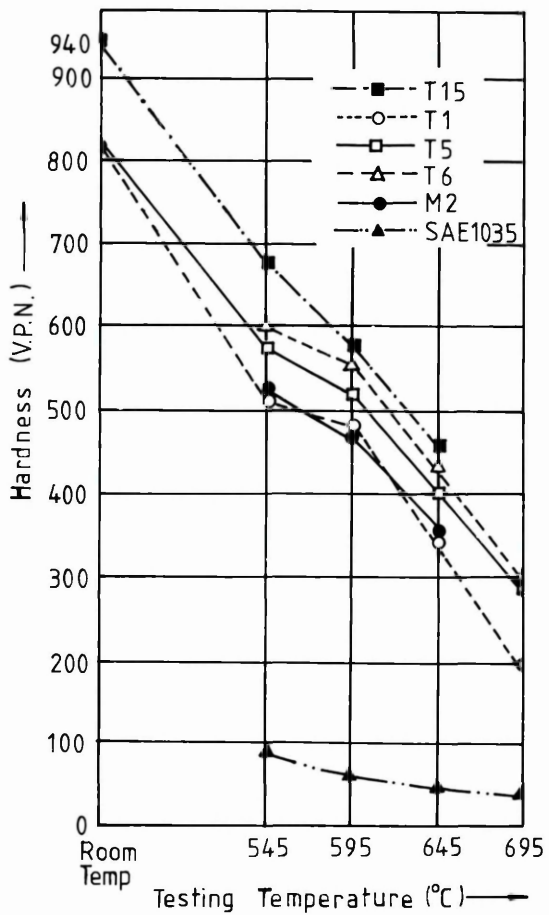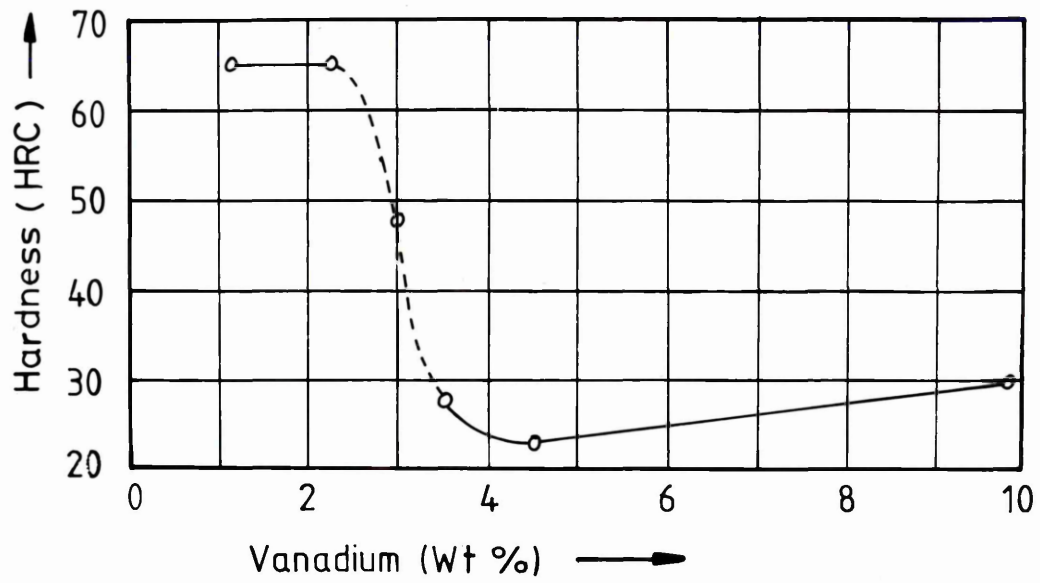
FIG. 13. Effect of vanadium in high speed steel with base composition T1, on the hardness after austenitising at 1285°C with subsequent oil quenching (Kinzel and Burgess [98]).

FIG. 14. Effect of temperature on the hardness of several high speed steels. These steels had previously been fully hardened (Harder and Grove [100]).
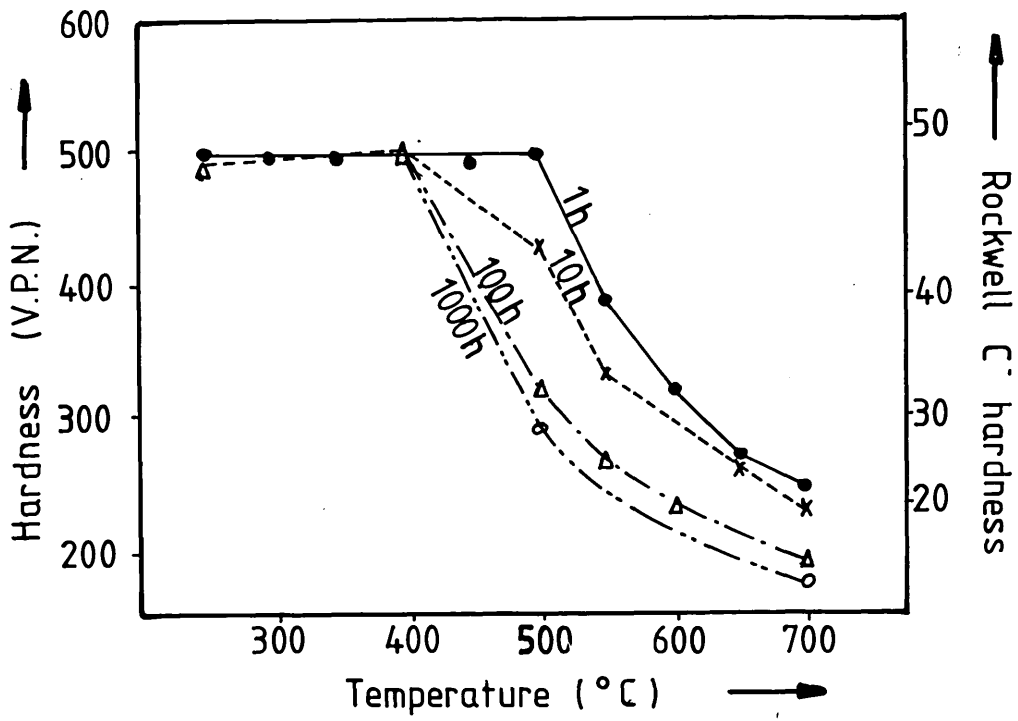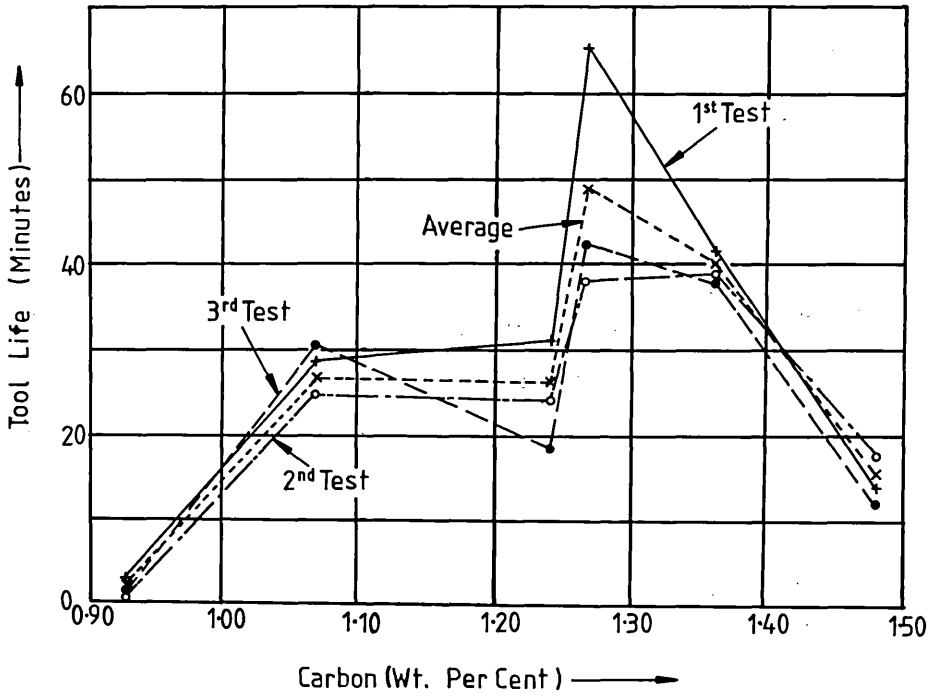
FIG. 15.   Lathe tool cutting tests on high speed steels with base composition 19 W, 4 Cr and 4 wt. % V, but with varying carbon contents (Oertel and Grutzer [103]).

FIG. 16.   Relationship between hardness and temperature for varying tempering times, for a steel containing 0.21 C and 9.09 wt. % Cr (Seal and Honeycombe [110]).

Hardness (V.P.N.) →

600

500

400

300

200

Rockwell (°C)

50

40

30

20

300   400   500   600   700

Temperature (°C) →

1000 h

100 h

10 h

1 h

d(110) VC = 2.95 Å   d(010)∝-Fe = 2.86 Å

d(001) VC = 4.17 Å

d(001)∝-Fe = 2.86 Å

[001] VC
[001]∝-Fe

(001) VC
(001)∝-Fe

(110) VC   (100)∝-Fe

(010)∝-Fe
(1̄10) VC

[110] VC
[100]∝-Fe

[1̄10] VC
[010]∝-Fe

— o — VC
— ● — ∝-Fe
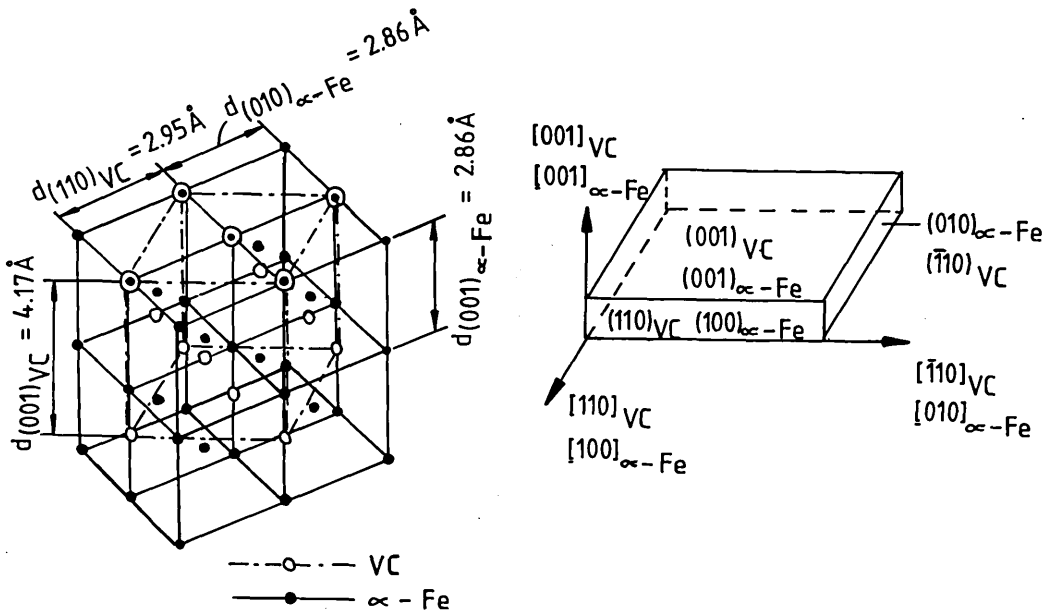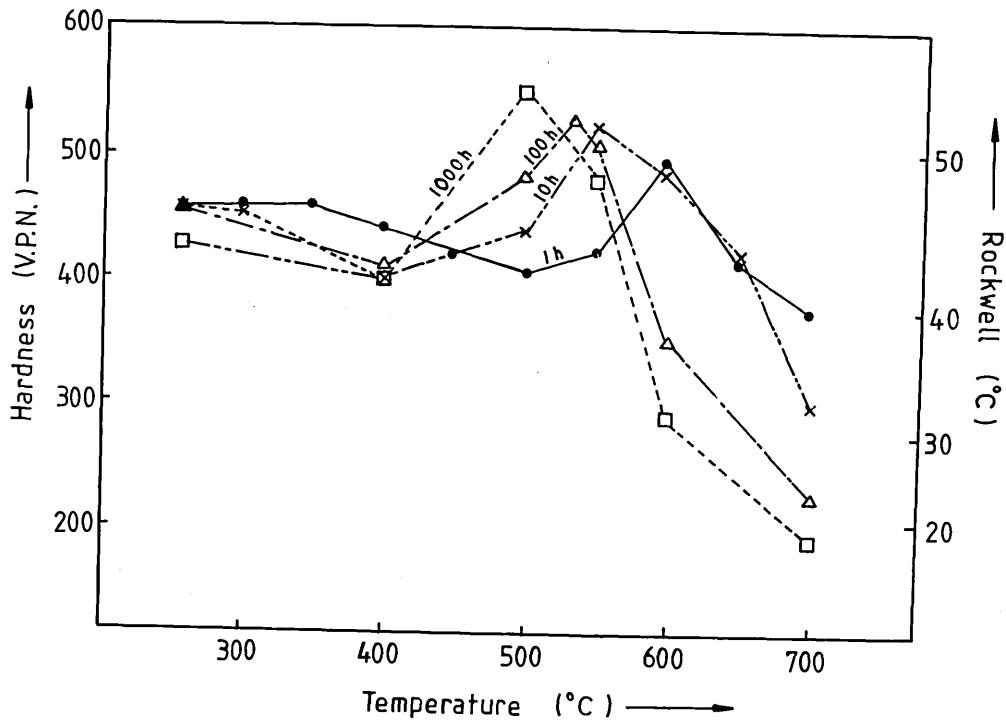
FIG. 17. Relationship between hardness and temperature for varying tempering times, for a steel containing 0.23 C and 0.97 wt. % V (Seal and Honeycombe [110]).

FIG. 18. Crystallographic relationship between vanadium carbide and α - iron (Goldshteyn and Farber [133]).
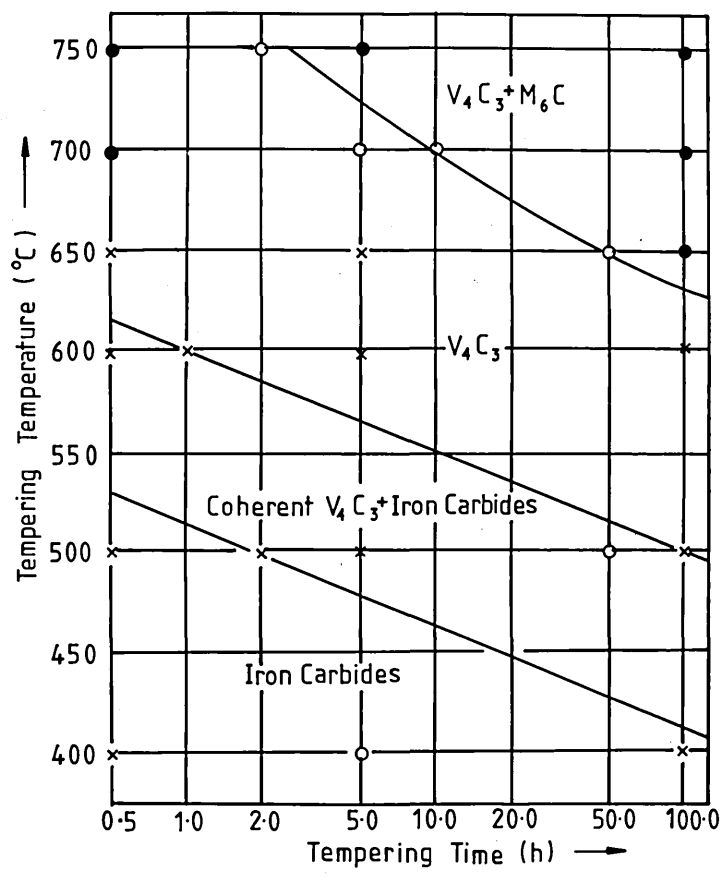
FIG. 19. Effect of temperature and time on the nature of carbides formed in a Mo-V steel after isothermal tempering, with time plotted on log scale (Baker and Nutting [112]).
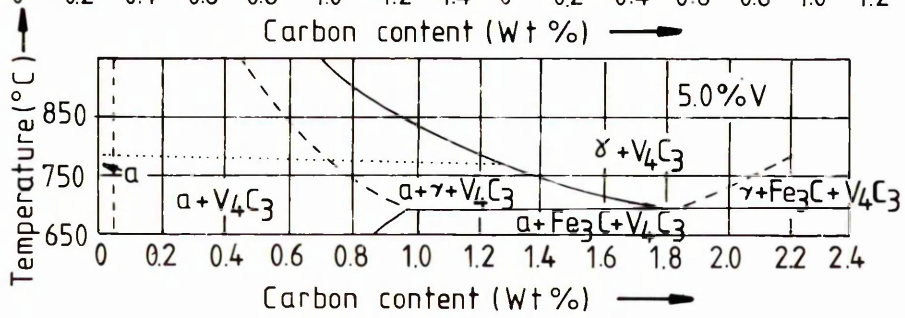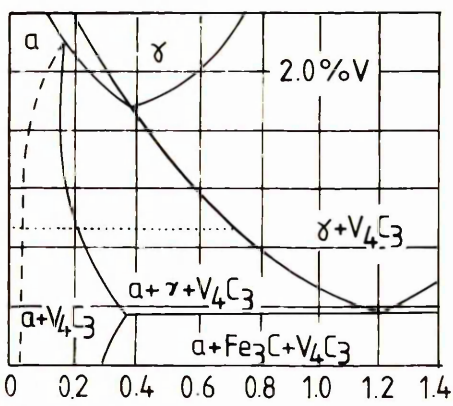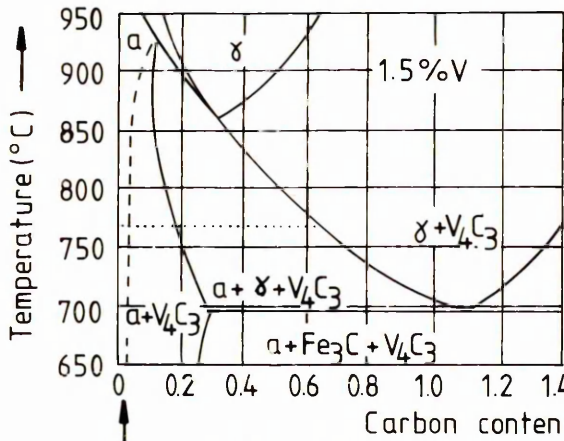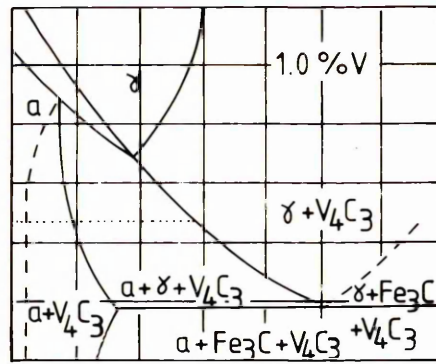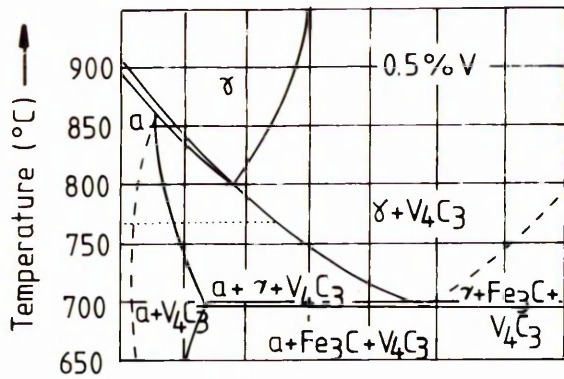
FIG. 20.   Vertical sections through the C-Fe-V ternary system at varying vanadium concentrations (Wever, Rose and Eggers [6]).
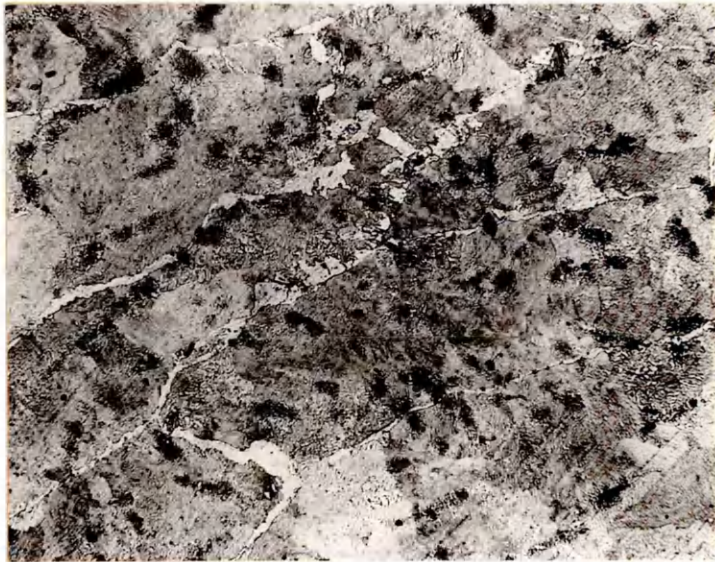
In cases where no details are presented of austenitisation and quenching conditions during hardening, for samples in the hardened and tempered state, the hardening treatment had been ideal.

FIG. 21. Optical micrograph of Alloy 1 (0.78C and 0.39 wt. % V) in the as-cast condition. Transverse section, magnification:- x150.

FIG. 22. Optical micrograph of Alloy 3 (0.81C and 1.62 wt. % V) in the as-cast condition. Transverse section, magnification:- x150.

FIG. 23. Optical micrograph of Alloy 10 (W), (0.83 C, 1.59 V and 1.99 wt. % W) in the as-cast condition. Transverse section, magnification:- x240.

FIG. 24. Optical micrograph of Alloy 9(Co), (0.83 C, 1.61 V and 0.97 wt. % Co) in the as-cast condition. Transverse section, magnification:- x240.
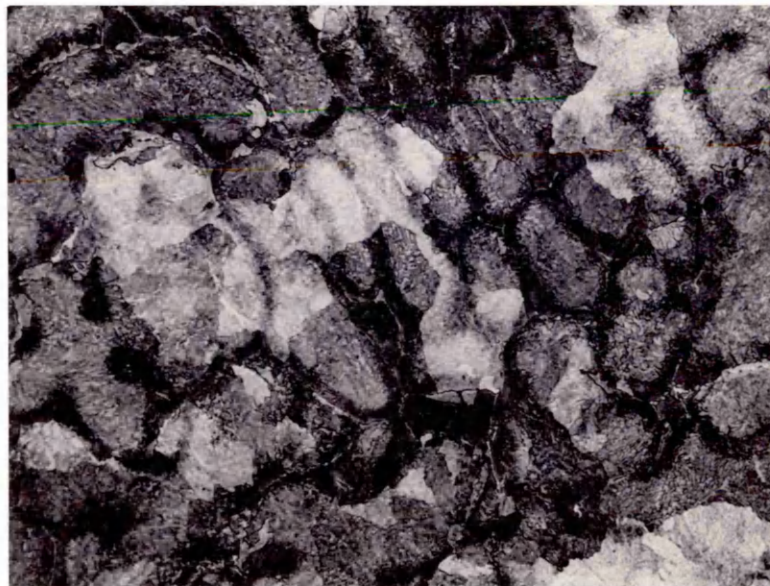
FIG. 25.   Optical micrograph of Alloy 5 (Mo),(0.79 C,
1.64 V and 1.02 wt. % Mo) in the as-cast condition.   Transverse
section, magnification:- x240.

FIG. 26.   Optical micrograph of Alloy 6 (Mn),(0.80 C,
1.64 V and 0.97 wt. % Mn) in the as-cast condition.   Transverse
section, magnification:- x240.
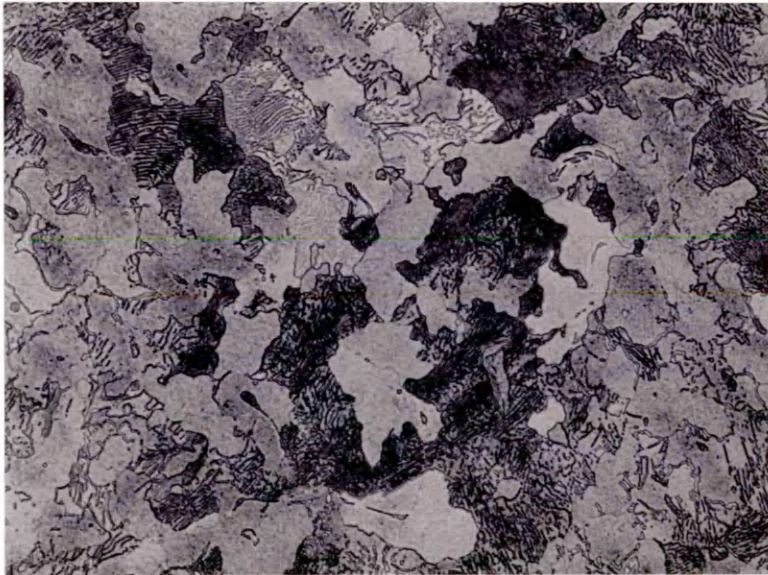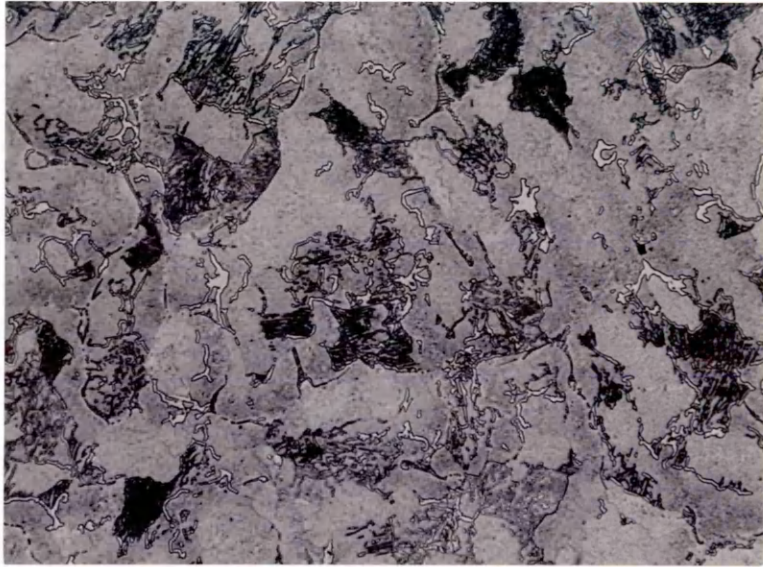
FIG. 27.   Optical micrograph of Alloy 10 (W) in the
as-cast and annealed condition.   Transverse section,
magnification:- x240.

FIG. 28.   Optical micrograph of Alloy 9 (Co) in the
as-cast and annealed condition.   Transverse section,
magnification:- x240.

FIG. 29.　Optical micrograph of Alloy 9 (Co) in the forged condition.　Longitudinal section, magnification:- x240.

FIG. 30.　Optical micrograph of Alloy 10 (W) in the forged condition.　Longitudinal section, magnification:- x240.
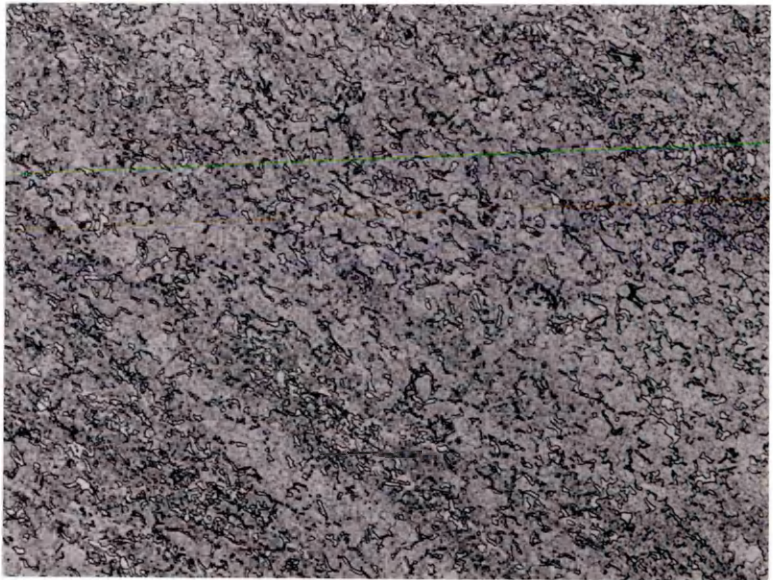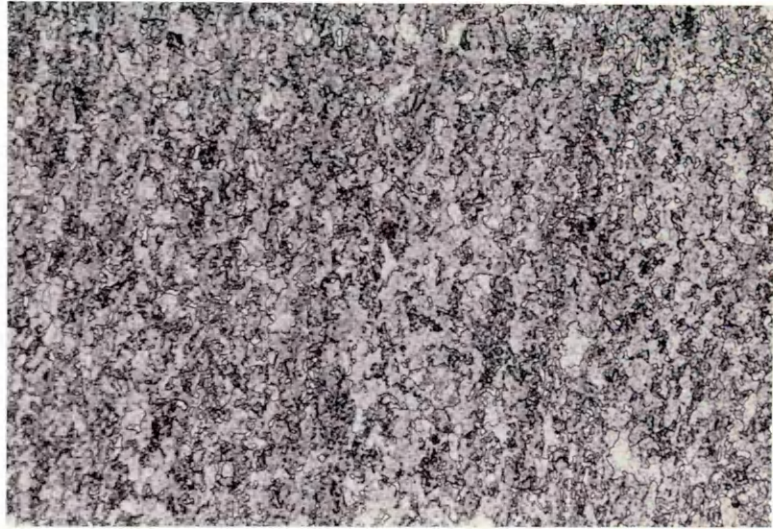
FIG. 31.   Optical micrograph of Alloy 9 (Co) in the
annealed condition.   Longitudinal section, magnification:- x240.

FIG. 32.   Optical micrograph of Alloy 10 (W) in the
annealed condition.   Longitudinal section, magnification:-
x240.
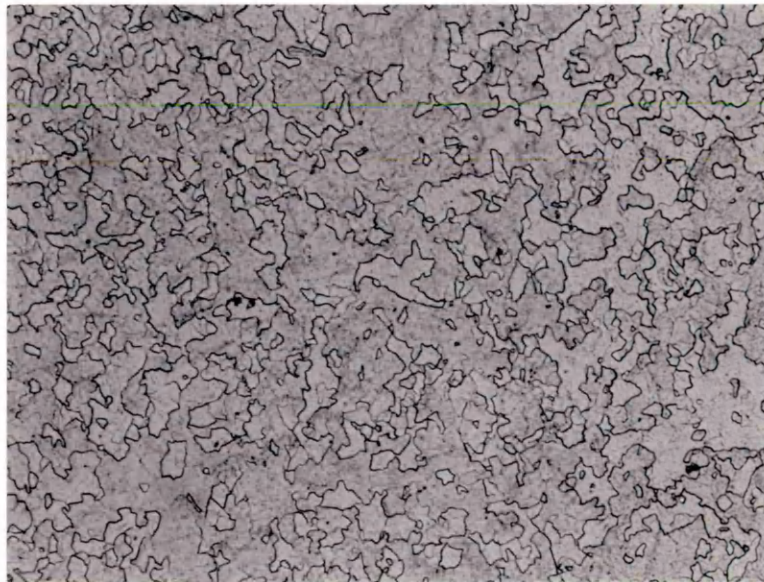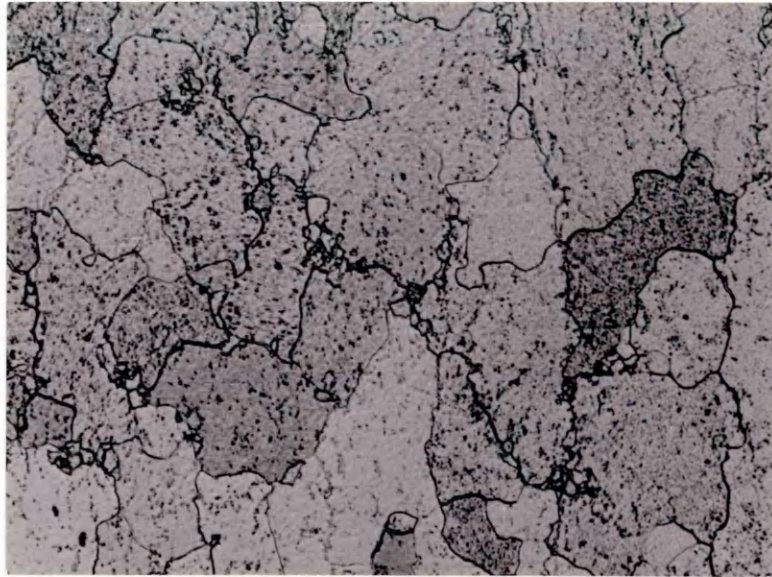
FIG. 33. Optical micrograph of Alloy 11 (0.086C, 0.27 Si, 0.74 Mn and 0.06 wt. % V) in the annealed condition. Transverse section, magnification:- x240.

FIG. 34. Optical micrograph of Alloy 14 (0.086 C, 0.30 Si, 0.75 Mn and 1.11 wt. % V) in the annealed condition. Transverse section, magnification:- x240.
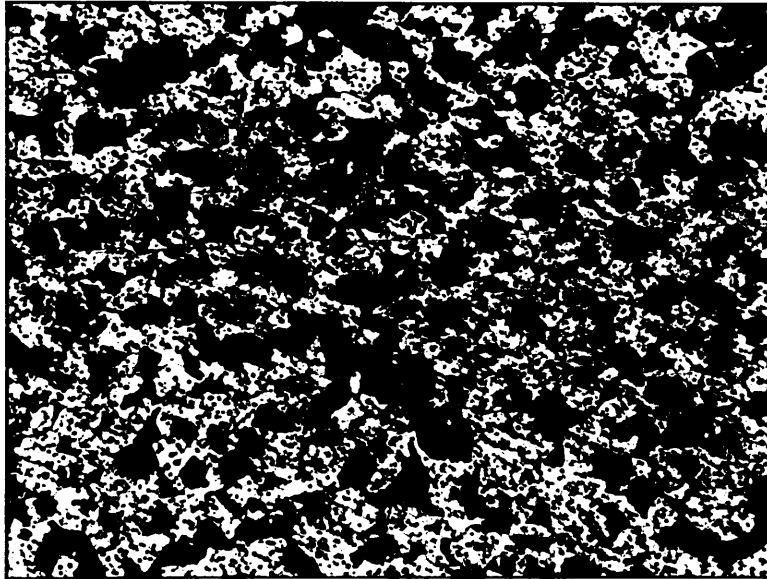
FIG. 35.   Optical micrograph of Alloy 14 in the carburised condition.   The microstructure shown is at a depth of 2mm. (1.03 wt. % C) from the specimen surface.   Transverse section, magnification:- x320.

FIG. 36.   Optical micrograph of Alloy 14 in the carburised condition.   The microstructure shown is at a depth of 3mm. (0.55 wt. % C) from the specimen surface.   Transverse section, magnification:- x320.
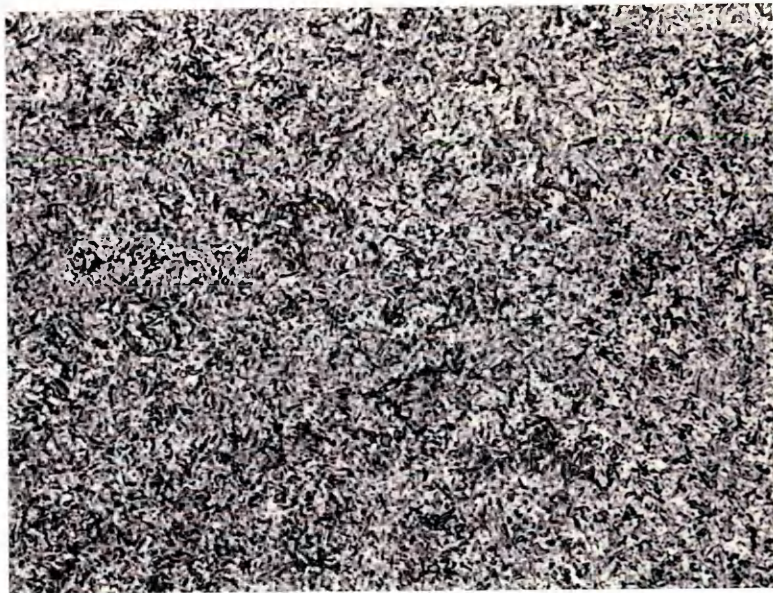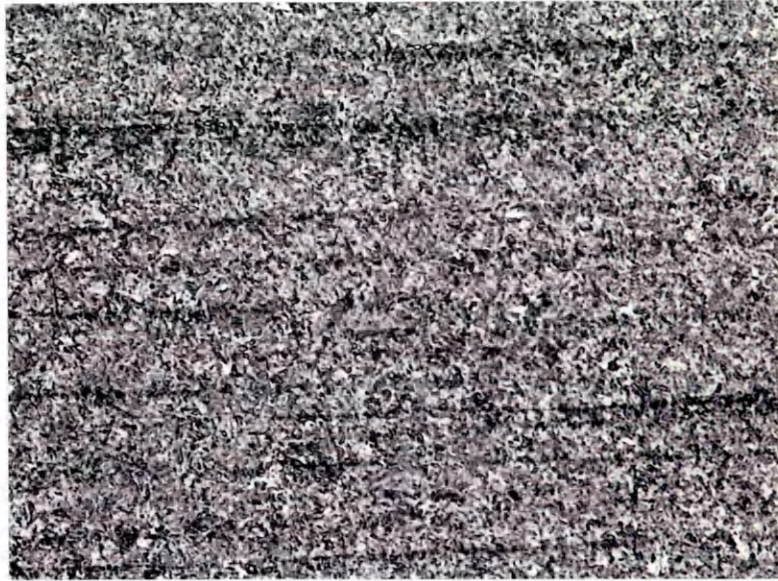
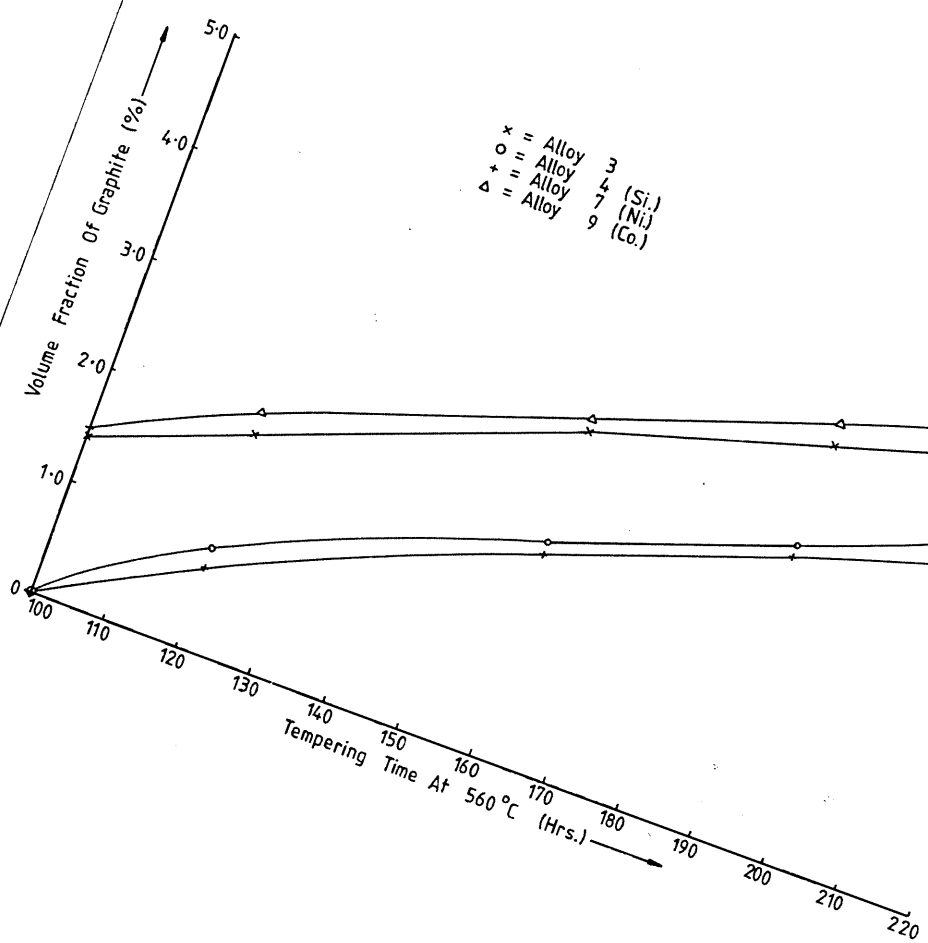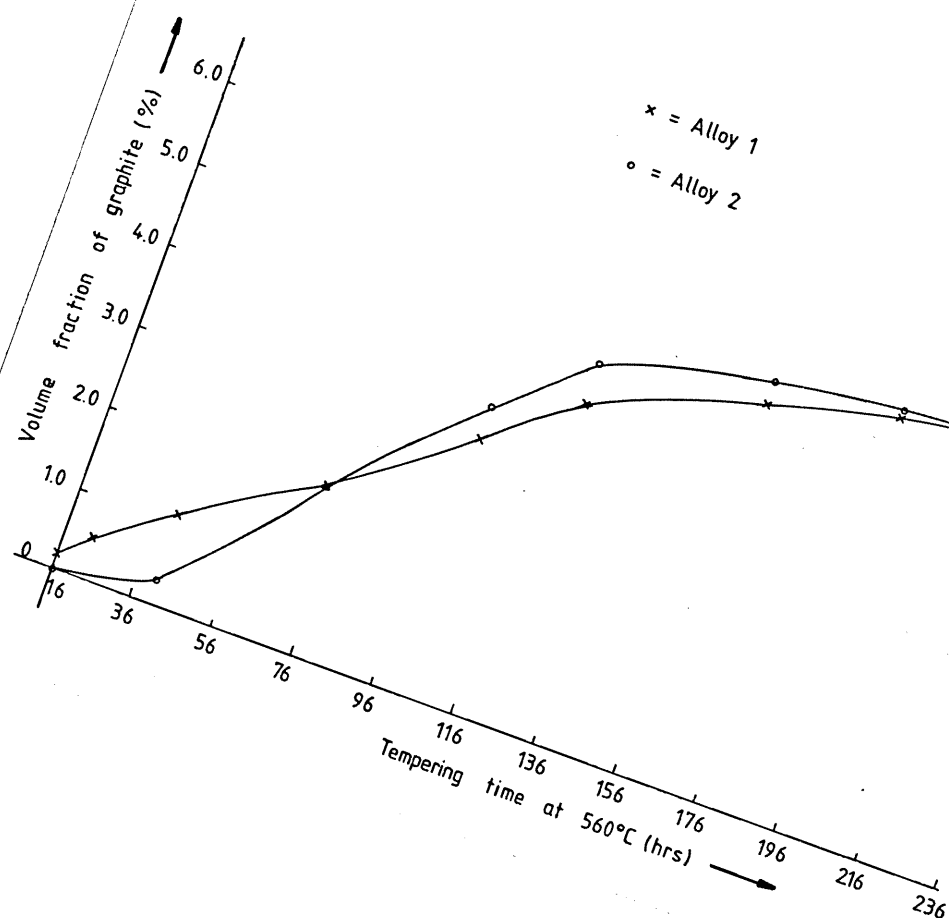FIG. 37. Optical micrograph of Alloy 2 (0.78 C and 0.79 wt. % V) in the as-hardened condition. Austenitisation was carried out at 860°C for 20 minutes, with subsequent water quenching. Longitudinal section, magnification:- x240.

FIG. 38. Optical micrograph of Alloy 1 in the as-hardened condition. Austenitisation was carried out at 920°C for 20 minutes, with subsequent water quenching. Longitudinal section, magnification:- x240.
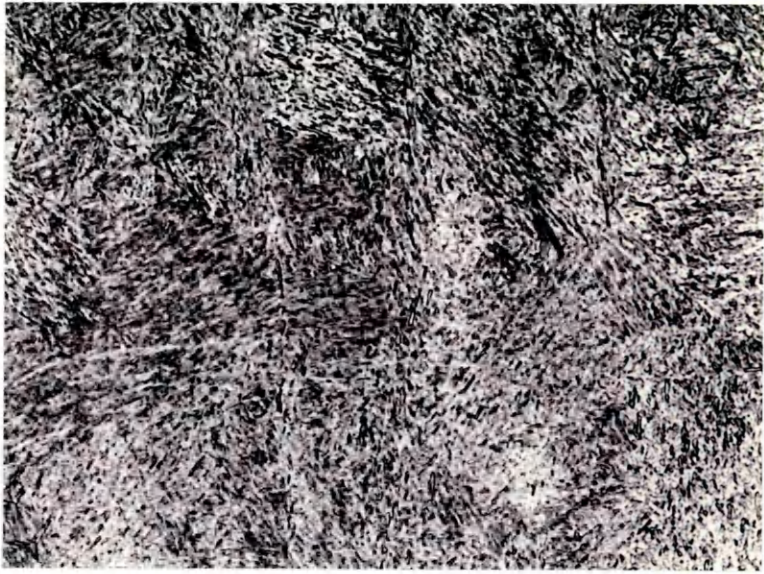
FIG. 39.   Optical micrograph of Alloy 1 in the as-hardened
condition.   Austenitisation was carried out at 1150°C for 20
minutes, with subsequent water quenching.   Transverse section,
magnification:- x240.

FIG. 40.   Optical micrograph of Alloy 2 in the as-hardened
condition.   Austenitisation was carried out at 1000°C for 20
minutes, with subsequent water quenching.   Longitudinal section,
magnification:- x240.

FIG. 41.   Optical micrograph of Alloy 3 in the as-hardened condition.   Austenitisation was carried out at 1120°C for 20 minutes, with subsequent water quenching. Longitudinal section, magnification:- x240.

FIG. 42.   Optical micrograph of Alloy 2 in the as-hardened condition.   Austenitisation was carried out at 1150°C for 20 minutes, with subsequent water quenching.   Transverse section, magnification:- x240.
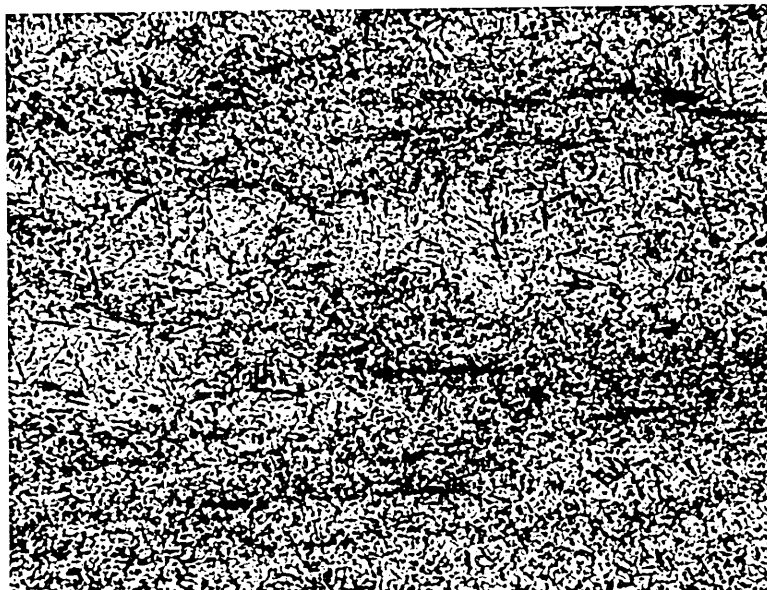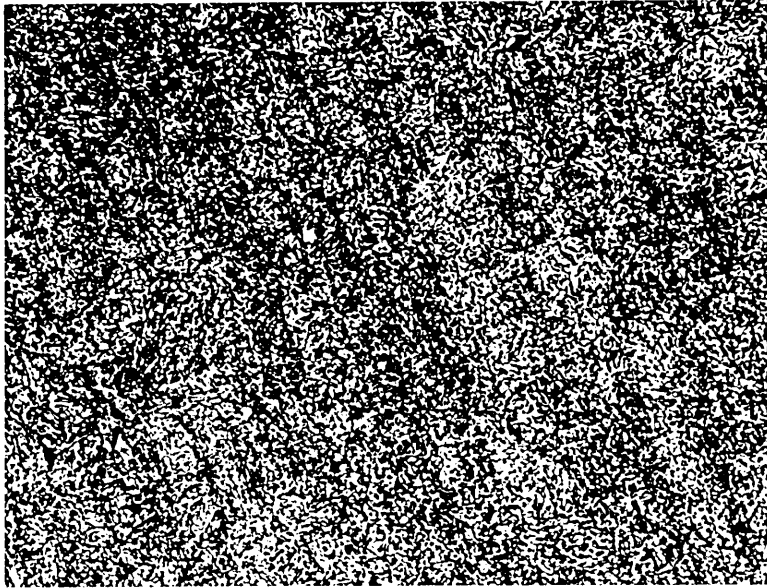
FIG. 43.   Optical micrograph of Alloy 3 in the as-hardened condition.   Austenitisation was carried out at 1150°C for 20 minutes, with subsequent water quenching.   Longitudinal section, magnification:- x240.

FIG. 44.   Optical micrograph of Alloy 3 in the as-hardened condition.   Austenitisation was carried out at 1150°C for 45 minutes, with subsequent water quenching.   Longitudinal section, magnification:- x240.

FIG. 45. Optical micrograph of Alloy 4 (Si), (0.80 C,
1.64 V and 0.97 wt. % Si) in the as-hardened condition.
Austenitisation was carried out at 1120°C for 20 minutes, with
subsequent water quenching. Longitudinal section, magnification:
x300.

FIG. 46. Optical micrograph of Alloy 8 (Cr), (0.83 C,
1.63 V and 1.00 wt. % Cr) in the as-hardened condition.
Austenitisation was carried out at 1150°C for 20 minutes, with
subsequent water quenching. Longitudinal section, magnifica-
tion:- x300.
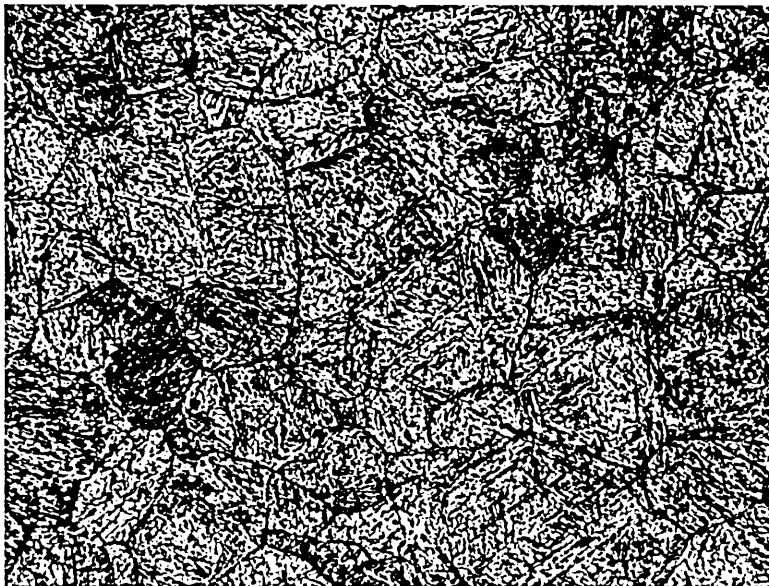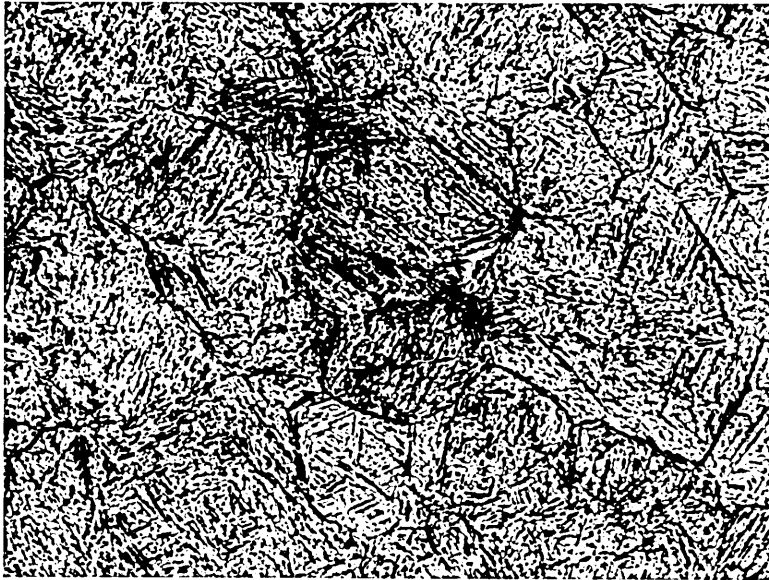
FIG. 47. Optical micrograph of Alloy 6 (Mn) in the
as-hardened condition. Austenitisation was carried out at
1200°C for 20 minutes, with subsequent water quenching.
Transverse section, magnification:- x300.

FIG. 48. Optical micrograph of Alloy 10 (W) in the
as-hardened condition. Austenitisation was carried out at
1200°C for 20 minutes, with subsequent water quenching.
Transverse section, magnification:- x300.
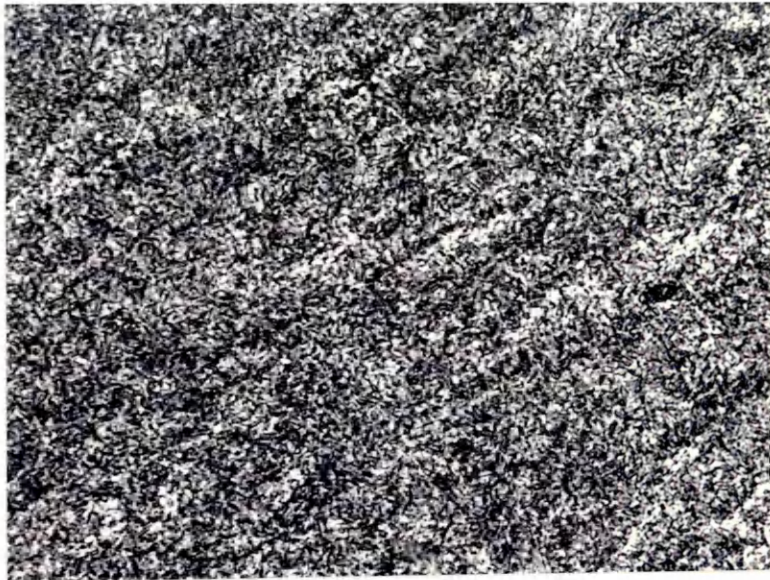
FIG. 49. Optical micrograph of Alloy 5 (Mo) in the as-hardened condition. Austenitisation was carried out at $1100^{\circ}C$ for 20 minutes, with subsequent water quenching. Longitudinal section, magnification:- x300.

FIG. 50. Optical micrograph of Alloy 7 (Ni),(0.82 C, 1.63 V and 1.03 wt. % Ni) in the as-hardened condition. Austenitisation was carried out at $1100^{\circ}C$ for 20 minutes, with subsequent water quenching. Longitudinal section, mangification:- x300.
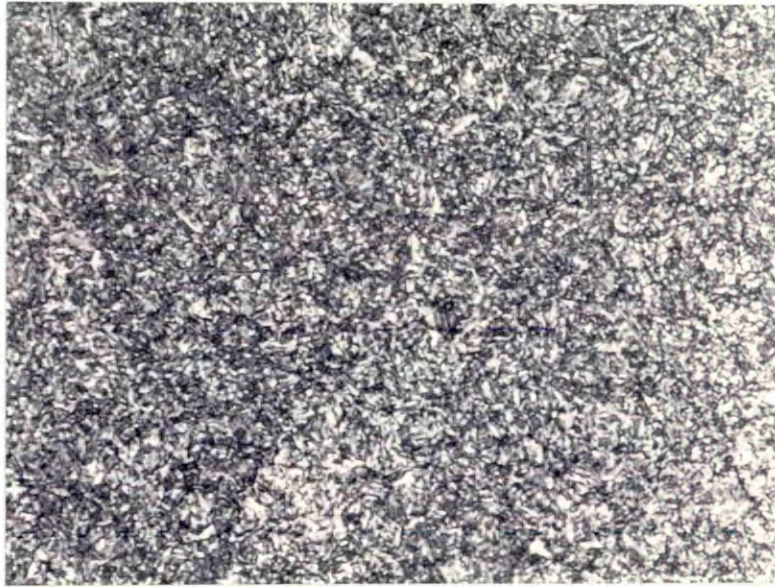
FIG. 51. Optical micrograph of Alloy 17 (0.080 C, 0.26 Si, 0.72 Mn and 0.53 wt. % V) after carburisation and hardening. Austenitisation was carried out at 940°C for 20 minutes, with subsequent water quenching. The microstructure shown is at a depth of 2mm. (1.01 wt. % C) from the specimen surface. Transverse section, magnification:- x320.

FIG. 52. Optical micrograph of Alloy 3 in the hardened and tempered condition. Tempering was carried out at 300°C for 1 hour. Longitudinal section, magnification:- x240.
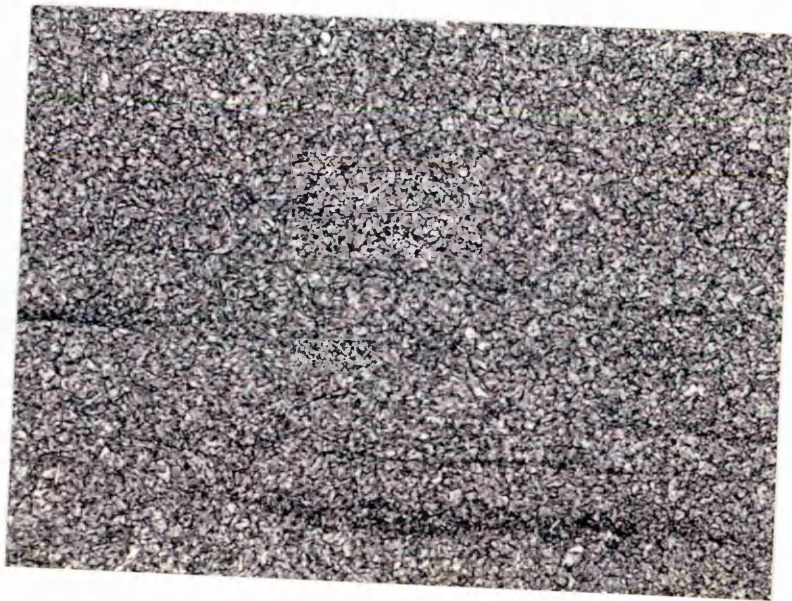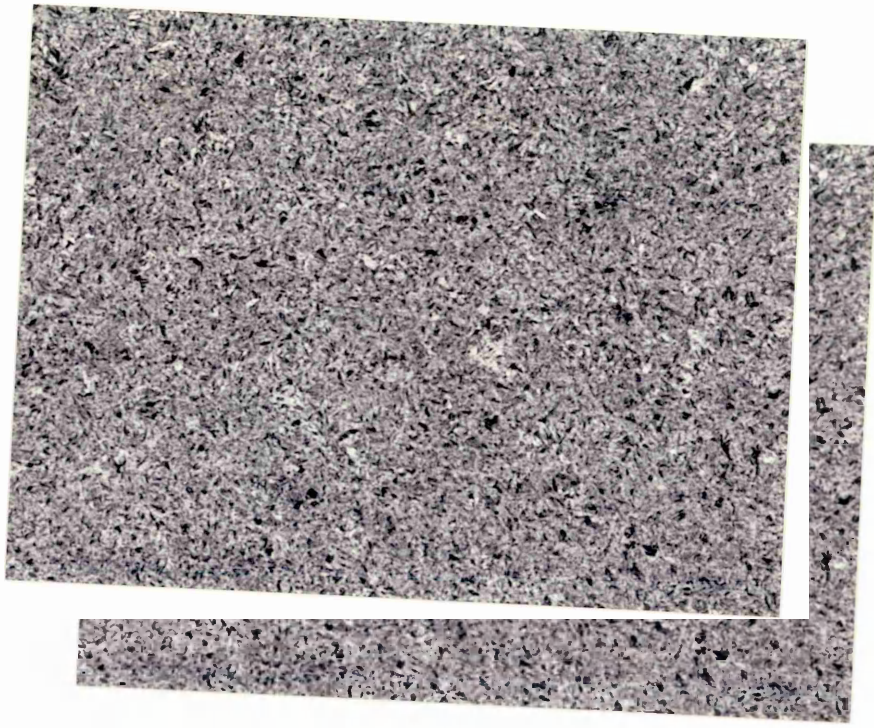
FIG. 53. Optical micrograph of Alloy 1 in the hardened and tempered condition. Tempering was carried out at 400°C for 1 hour. Longitudinal section, magnification:- x240.

FIG. 54. Optical micrograph of Alloy 1 in the hardened and tempered condition. Tempering was carried out at 500°C for 1 hour. Longitudinal section, magnification:- x240.

FIG. 55.   Optical micrograph of Alloy 3 in the hardened and tempered condition.   Tempering was carried out at 500°C for 1 hour.   Longitudinal section, magnification:- x240.

FIG. 56.   Optical micrograph of Alloy 2 in the hardened and tempered condition.   Tempering was carried out at 700°C for 1 hour.   Longitudinal section, magnification:- x240.
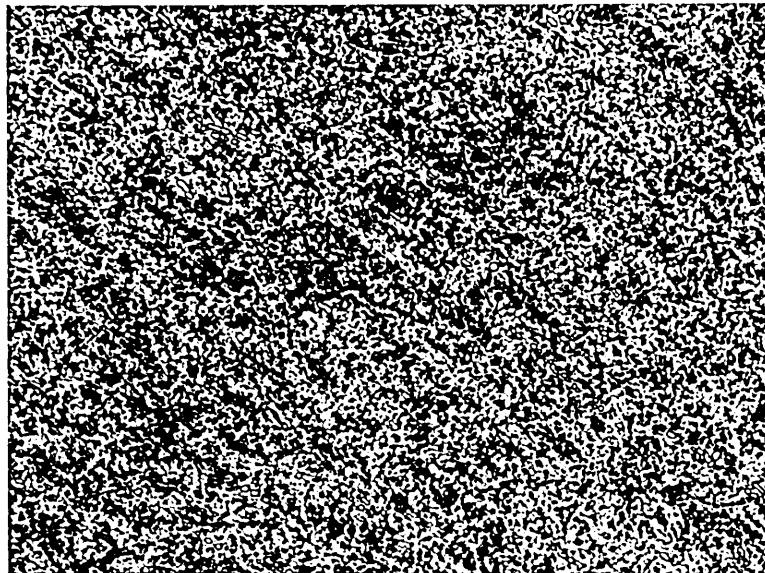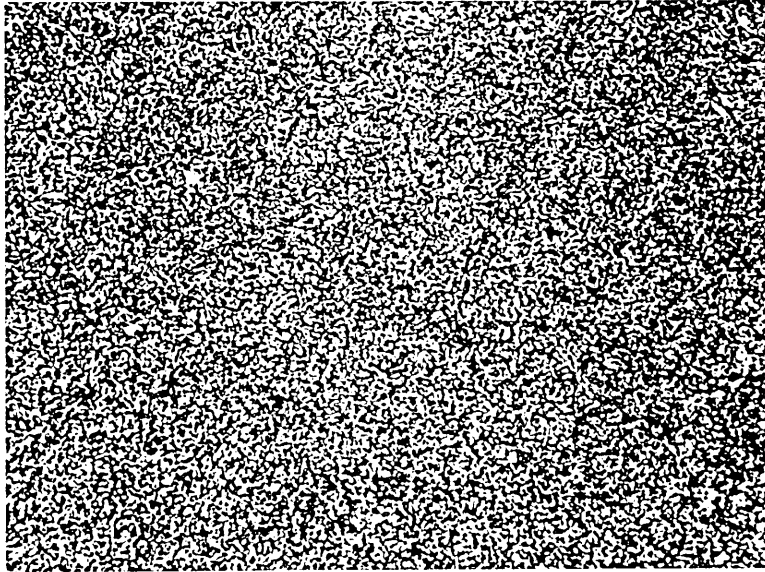
FIG. 57. Optical micrograph of Alloy 3 in the hardened and tempered condition. Tempering was carried out at 700°C for 1 hour. Longitudinal section, magnification:- x240.

FIG. 58. Optical micrograph of Alloy 6 (Mn) in the hardened and tempered condition. Tempering was carried out at 300°C for 1 hour. Longitudinal section, magnification:- x310.
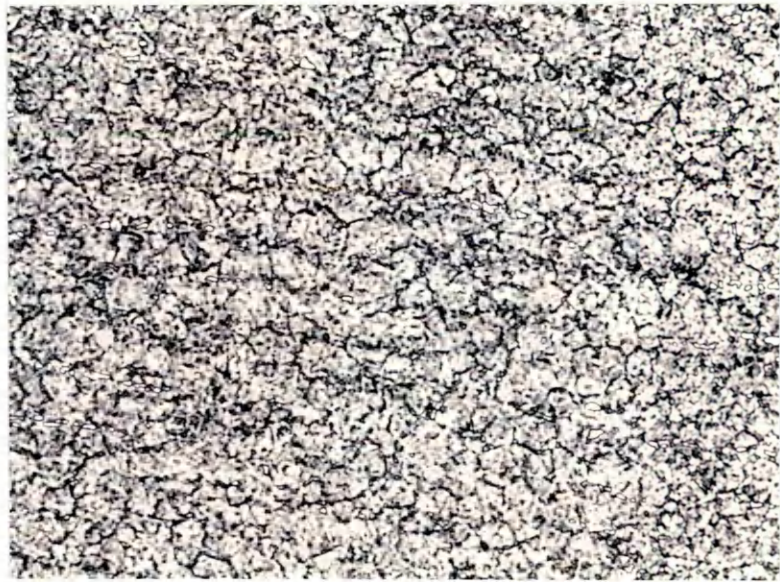
FIG. 59.   Optical micrograph of Alloy 7 (Ni) in the hardened and tempered condition.   Tempering was carried out at 500°C for 1 hour.   Longitudinal section, magnification:- x310.

FIG. 60.   Optical micrograph of Alloy 5 (Mo) in the hardened and tempered condition.   Tempering was carried out at 600°C for 1 hour.   Longitudinal section, magnification:- x310.
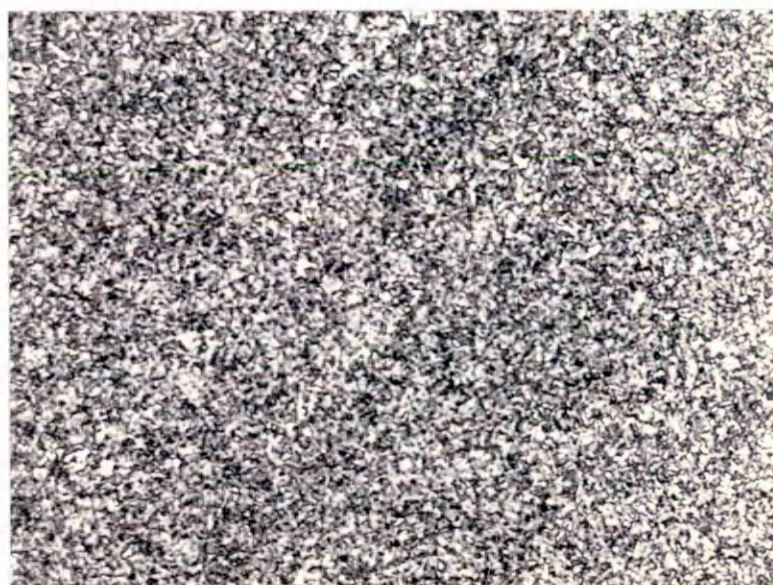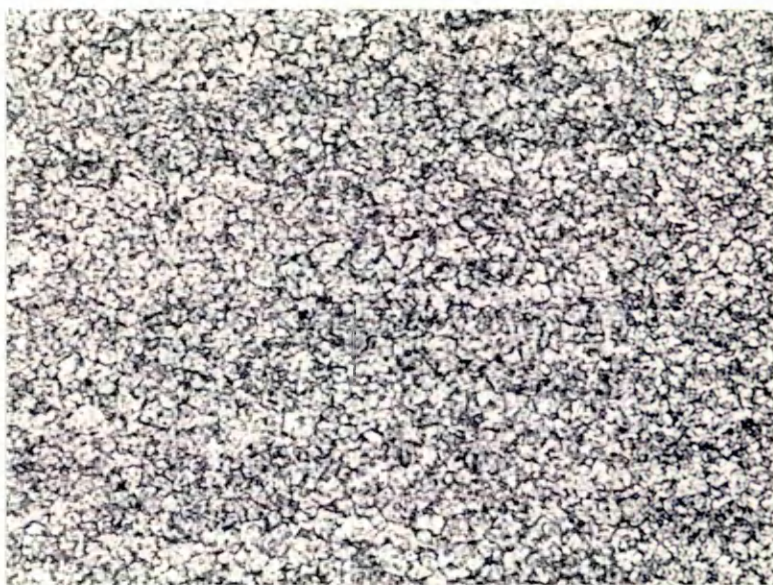
FIG. 61. Optical micrograph of Alloy 7 (Ni) in the hardened and tempered condition. Tempering was carried out at 600°C for 1 hour. Longitudinal section, magnification:- x310.

FIG. 62. Optical micrograph of Alloy 9 (Co) in the hardened and tempered condition. Tempering was carried out at 700°C for 1 hour. Longitudinal section, magnification:- x310.

FIG. 63. Optical micrograph of Alloy 18 (0.082 C, 0.30 Si, 0.76 Mn and 1.13 wt. % V) in the carburised, hardened and tempered condition. Tempering was carried out at 700°C for 1 hour. The microstructure shown is at a depth of 2mm. (1.00 wt. % C) from the specimen surface. Transverse section, magnification:- x310.

FIG. 64. Optical micrograph of Alloy 15 (0.080 C, 0.30 Si, 0.78 Mn and 0.05 wt. % V) in the carburised, hardened and tempered condition. Tempering was carried out at 550°C for 1 hour. The microstructure shown is at a depth of 1mm. (1.25 wt. % C) from the specimen surface. Transverse section, magnification:- x310.

FIG. 65.   Optical micrograph of Alloy 13 (0.086 C,
0.29 Si, 0.75 Mn and 0.55 wt. % V) in the carburised, hardened
and tempered condition.   Tempering was carried out at 600°C
for 1 hour.   The microstructure shown is at a depth of 1mm.
(1.28 wt. % C) from the specimen surface.   Transverse section,
magnification:- x310.

FIG. 66.   Optical micrograph of Alloy 1 in the hardened
and tempered condition.   Tempering was carried out at 560°C
for 16 hours.   Longitudinal section, magnification:- x240.
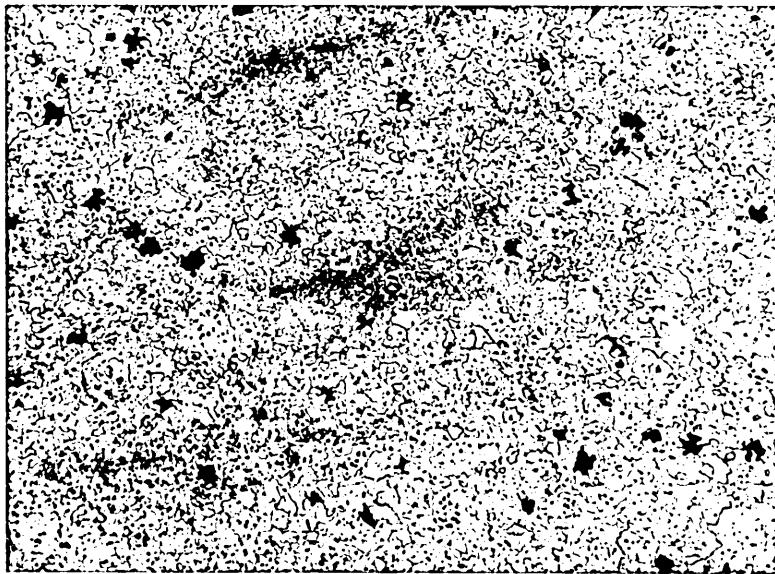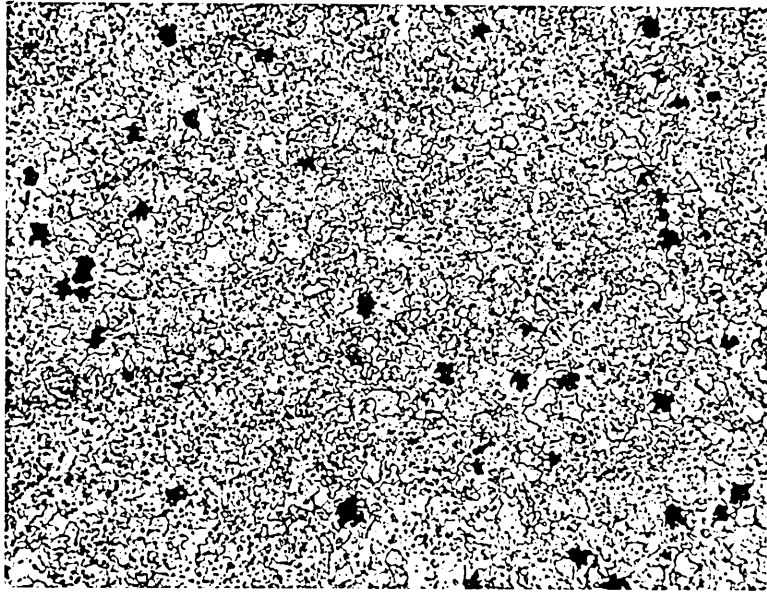
FIG. 67.   Optical micrograph of Alloy 1 in the hardened
and tempered condition.   Tempering was carried out at 560°C
for 120 hours.   Longitudinal section, magnification:- x240.

FIG. 68.   Optical micrograph of Alloy 1 in the hardened
and tempered condition.   Tempering was carried out at 560°C
for 160 hours.   Longitudinal section, magnification:- x240.
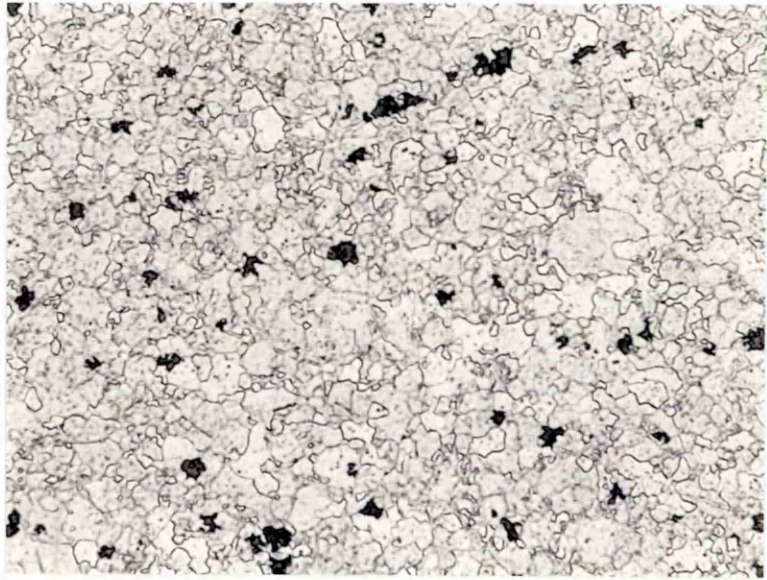
FIG. 69.   Optical micrograph of Alloy 1 in the hardened
and tempered condition.   Tempering was carried out at 560°C
for 190 hours.   Longitudinal section, magnification:- x240.

FIG. 70.   Optical micrograph of Alloy 1 in the hardened
and tempered condition.   Tempering was carried out at 560°C
for 190 hours.   Longitudinal section, unetched condition,
magnification:- x240.
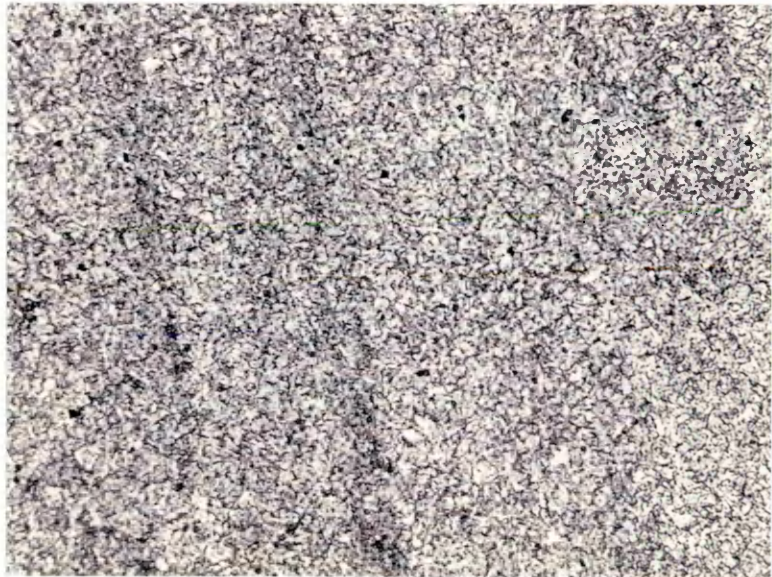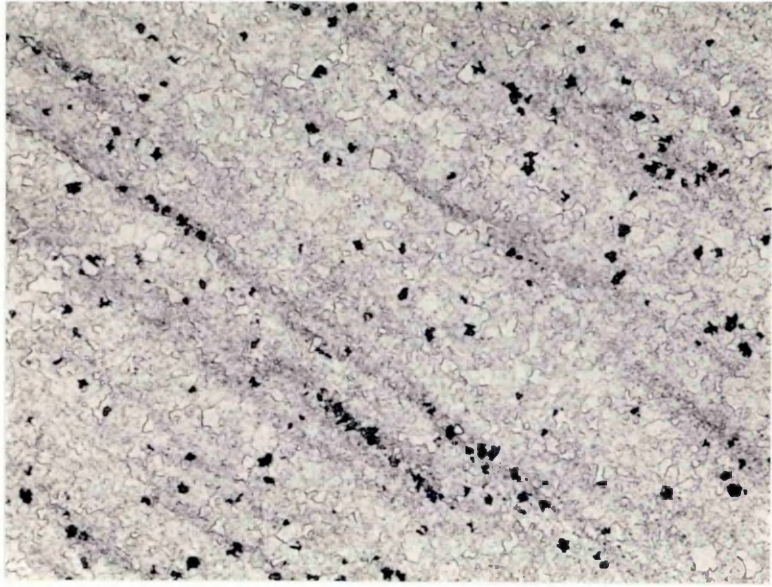
FIG. 71.   Optical micrograph of Alloy 1 in the hardened
and tempered condition.   Tempering was carried out at 560°C
for 100 hours.   Longitudinal section, magnification:- x240.

FIG. 72.   Optical micrograph of Alloy 2 in the hardened
and tempered condition.   Tempering was carried out at 560°C
for 40 hours.   Longitudinal section, magnification:- x240.
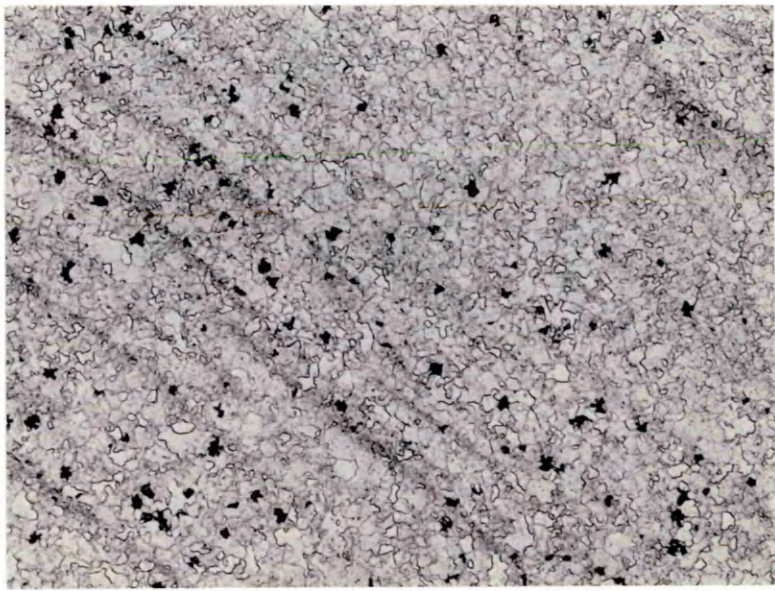
FIG. 73. Cptical micrograph of Alloy 2 in the hardened and tempered condition. Tempering was carried out at $560^{\circ}C$ for 70 hours. Longitudinal section, magnification:- x240.

FIG. 74. Optical micrograph of Alloy 2 in the hardened and tempered condition. Tempering was carried out at $560^{\circ}C$ for 160 hours. Longitudinal section, magnification:- x240.
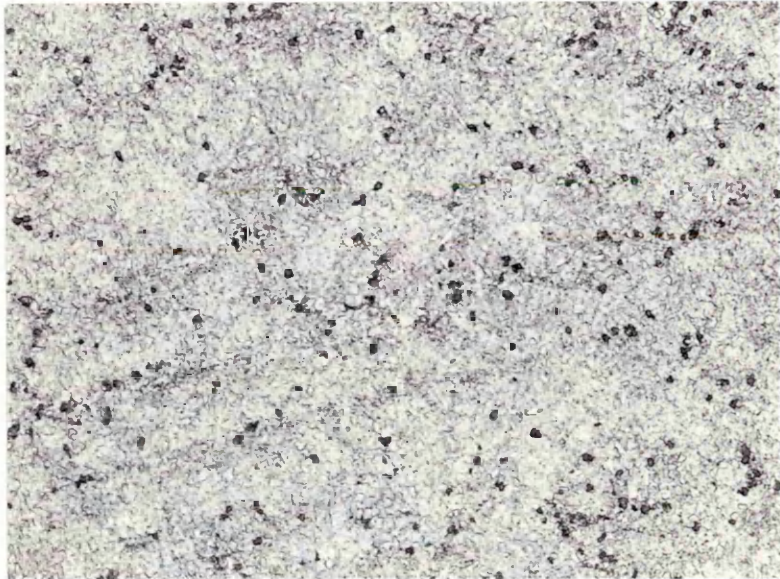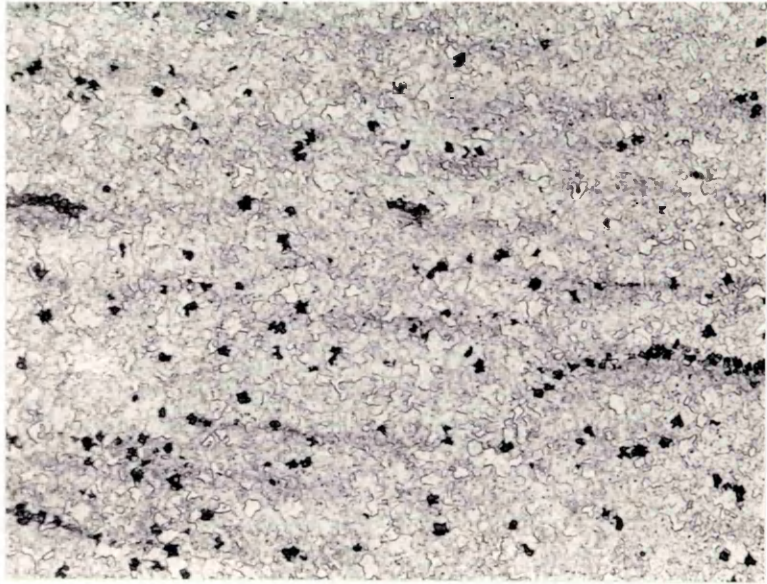
FIG. 75. Optical micrograph of Alloy 2 in the hardened and tempered condition. Tempering was carried out at 560°C for 220 hours. Longitudinal section, magnification:- x240.

FIG. 76. Optical micrograph of Alloy 3 in the hardened and tempered condition. Tempering was carried out at 560°C for 190 hours. Longitudinal section, magnification:- x240.
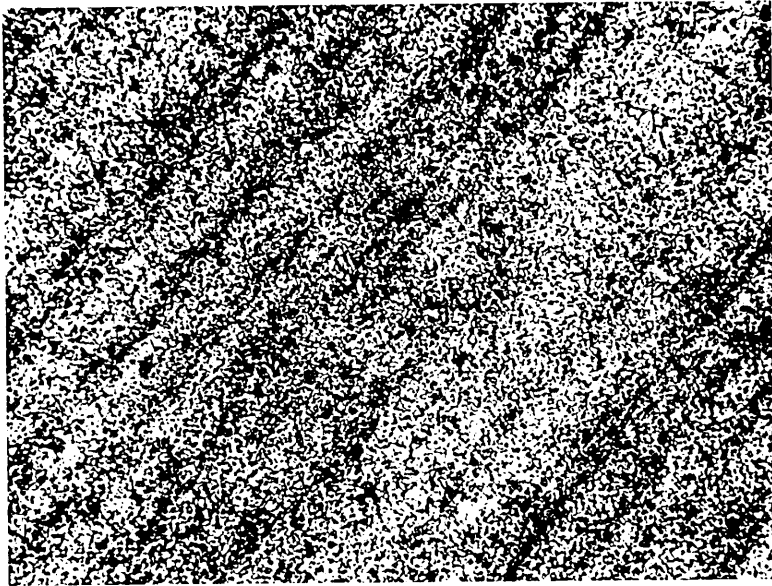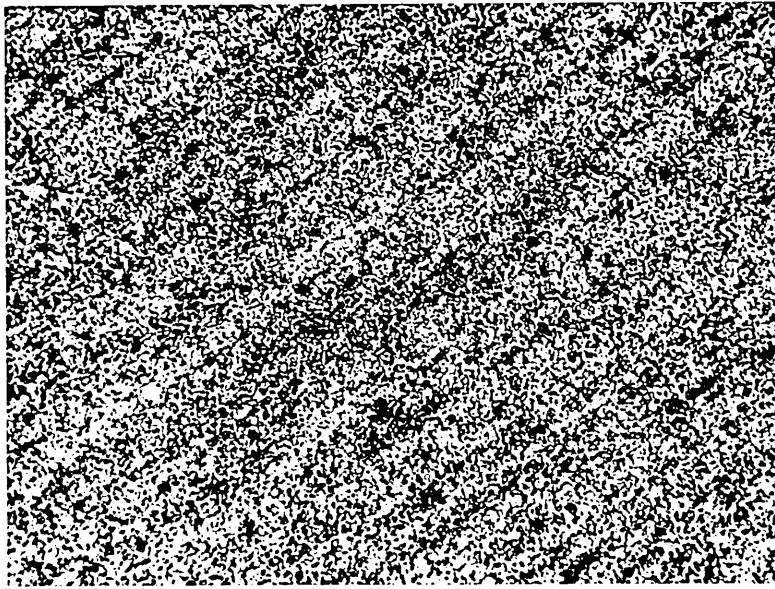
FIG. 77.   Optical micrograph of Alloy 3 in the hardened and tempered condition.   Tempering was carried out at $560^{\circ}C$ for 100 hours.   Longitudinal section, magnification:- x240.

FIG. 78.   Optical micrograph of Alloy 3 in the hardened and tempered condition.   Tempering was carried out at $560^{\circ}C$ for 160 hours.   Longitudinal section, magnification:- x240.
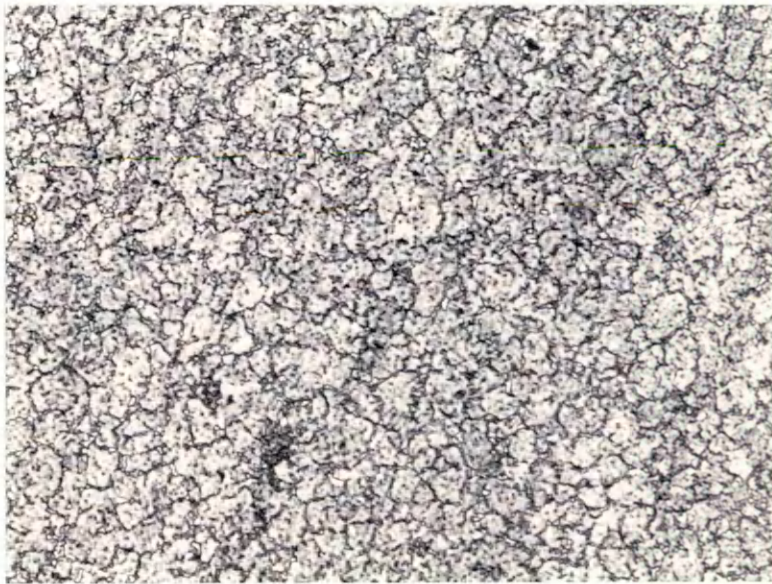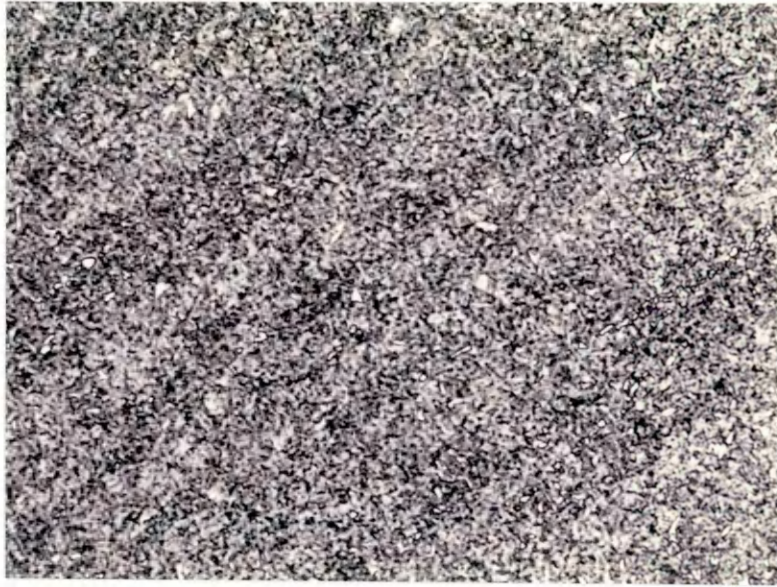
FIG. 79. Optical micrograph of Alloy 8 (Cr) in the hardened and tempered condition. Tempering was carried out at 560°C for 220 hours. Longitudinal section, magnification:- x310.

FIG. 80. Optical micrograph of Alloy 10 (W) in the hardened and tempered condition. Tempering was carried out at 560°C for 220 hours. Transverse section, magnification:- x310.
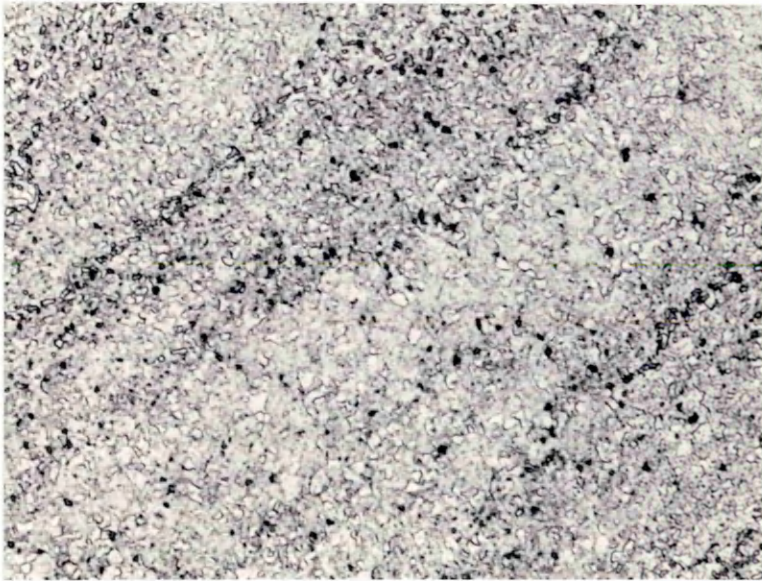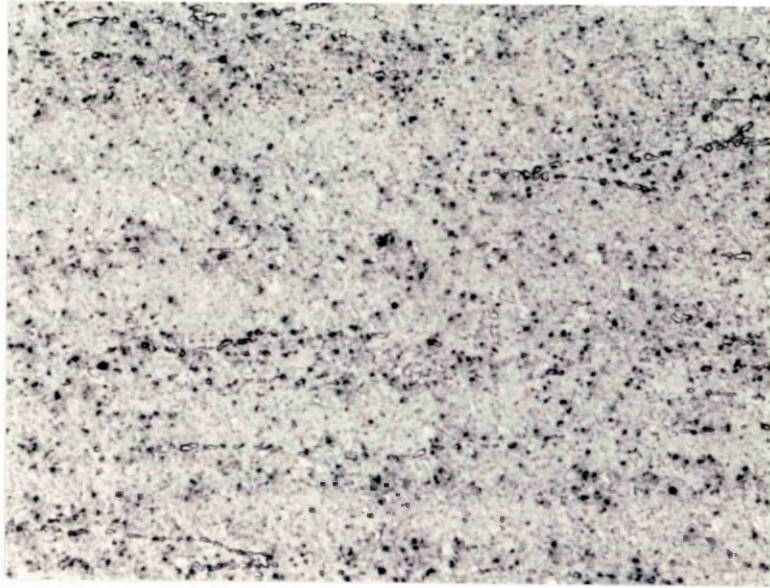
FIG. 81.   Optical micrograph of Alloy 4 (Si) in the
hardened and tempered condition.   Tempering was carried out
at 560°C for 220 hours.   Longitudinal section, magnification:-
x310.

FIG. 82.   Optical micrograph of Alloy 7 (Ni) in the
hardened and tempered condition.   Tempering was carried out
at 560°C for 220 hours.   Longitudinal section, magnification:-
x310.
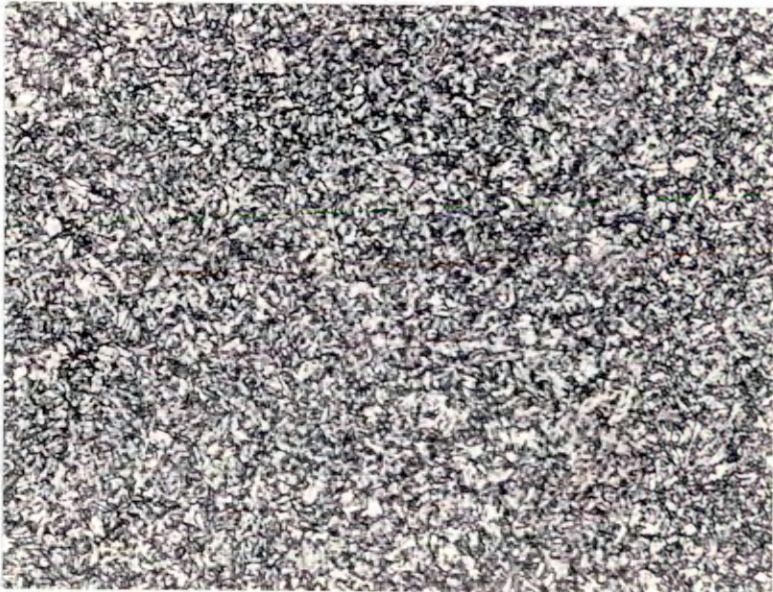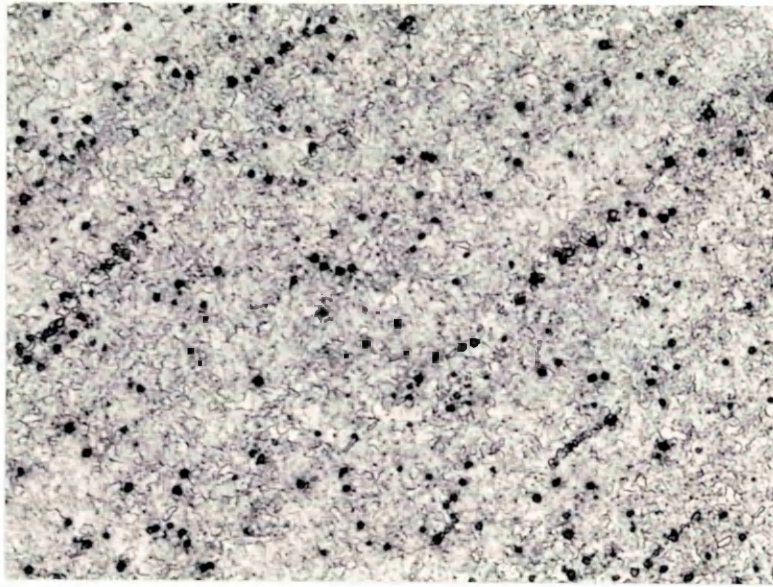
FIG. 83.   Optical micrograph of Alloy 9 (Co) in the
hardened and tempered condition.   Tempering was carried out
at 560°C for 220 hours.   Longitudinal section, magnification:-
x310.

FIG. 84.   Optical micrograph of Alloy 18 in the carburised,
hardened and tempered condition.   Tempering was carried out at
560°C for 220 hours.   The microstructure shown is at a depth
of 1mm. (1.28 wt. % C) from the specimen surface.   Transverse
section, magnification:- x310.
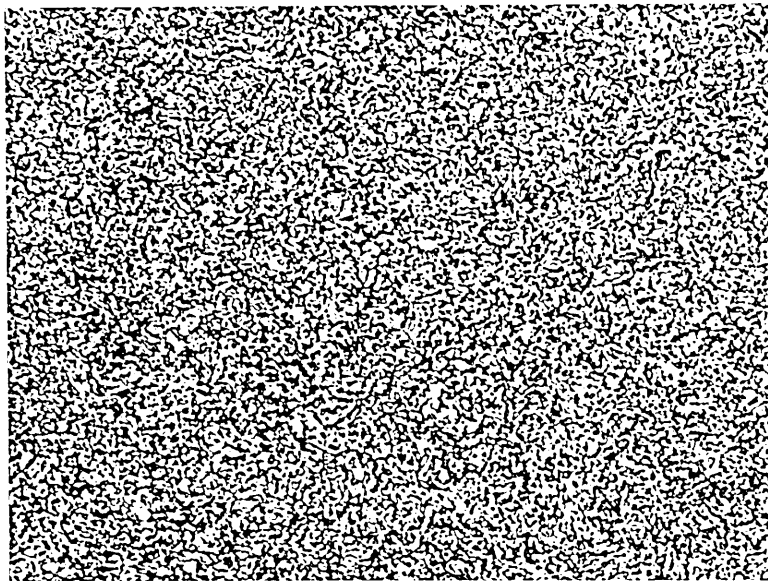
FIG. 85.   Optical micrograph of Alloy 14 in the carburised,
hardened and tempered condition.   Tempering was carried out at
560°C for 220 hours.   The microstructure shown is at a depth
of 1mm. (1.30 wt. % C) from the specimen surface.   Transverse
section, magnification:- x310.

Volume fraction of graphite (%)

× = Alloy 1

○ = Alloy 2

Tempering time at 560°C (hrs)

16 36 56 76 96 116 136 156 176 196 216 236

6.0 5.0 4.0 3.0 2.0 1.0 0

Volume Fraction Of Graphite (%)

× = Alloy   3
○ = Alloy   4
+ = Alloy   7 (Si.)
△ = Alloy   9 (Ni.)
        9 (Co.)

Tempering Time At 560°C (Hrs.)

100 110 120 130 140 150 160 170 180 190 200 210 220

5.0 4.0 3.0 2.0 1.0 0

FIG. 86.   Volume fraction of graphite present in Alloys
1 and 2, as a function of the tempering time at 560°C.

FIG. 87.   Volume fraction of graphite present in Alloys
3, 4(Si), 7(Ni) and 9(Co), as a function of the tempering time
at 560°C.
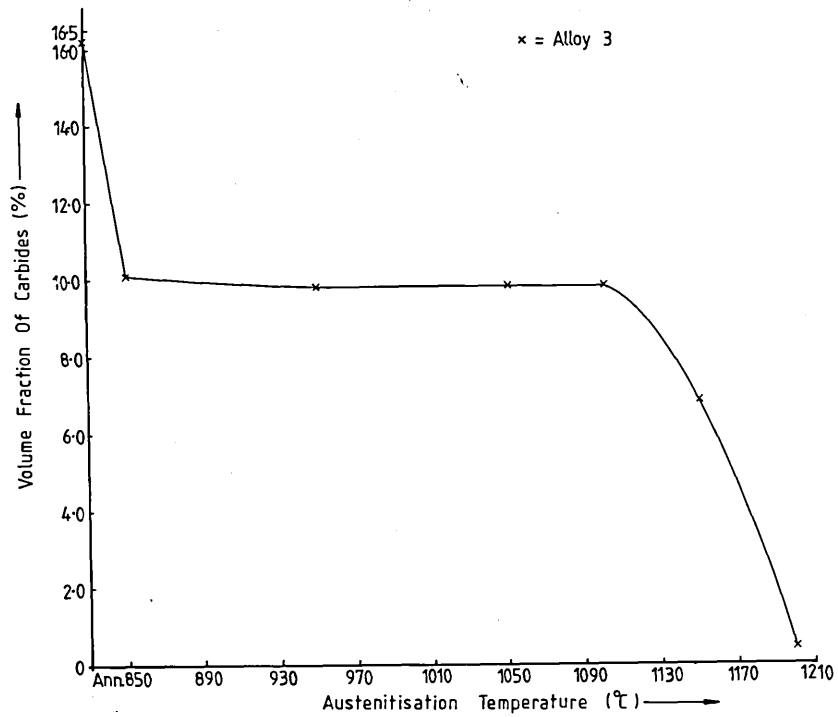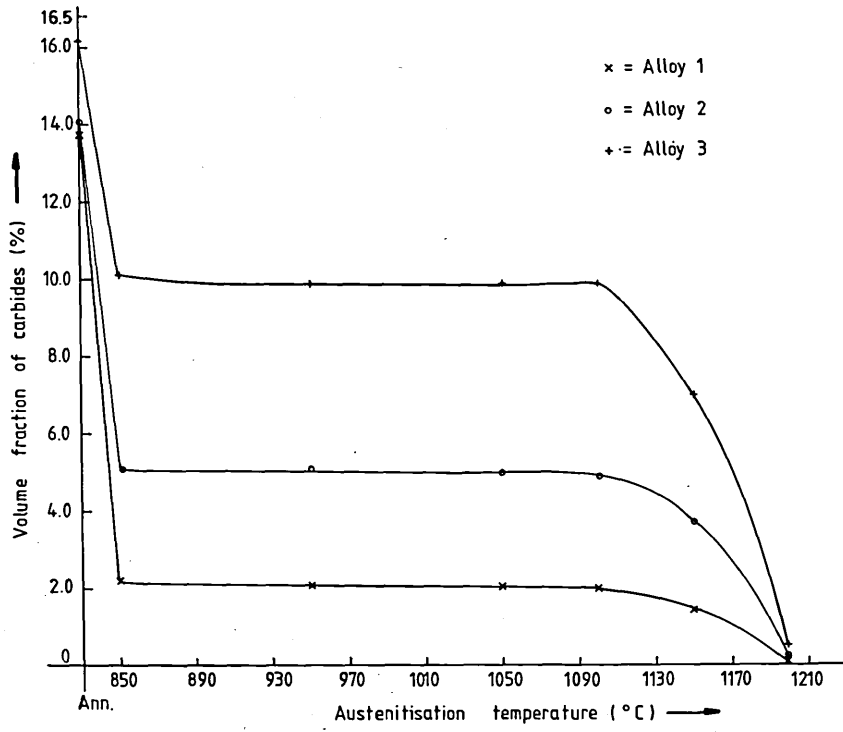
FIG. 88.   Effect of austenitisation temperature during
hardening on the volume fraction of primary carbide present
in Alloys 1, 2 and 3.   The soaking time employed was 20 minutes
in each instance.

FIG. 89.   Relationship between volume fraction of primary
carbide and austenitisation temperature during hardening for
Alloy 3.   The soaking time employed was 45 minutes in each
instance.

Distance From Specimen Surface (mm.)

0.25 0.5 1.0 1.5 2.0 2.5 3.0 3.5 4.0 4.5 5.0

Carbon Content (wt%)

0.08 0.28 0.48 0.68 0.88 1.08 1.28 1.48

× = Alloy 11
○ = Alloy 14

Austenitisation temperature (°C)

Ann. 850 890 930 970 1010 1050 1090 1130 1170 1210

Volume fraction of carbides (%)

0 4.0 8.0 12.0 16.0 20.0

x = Alloy 9 (Co)
o = Alloy 10 (W)
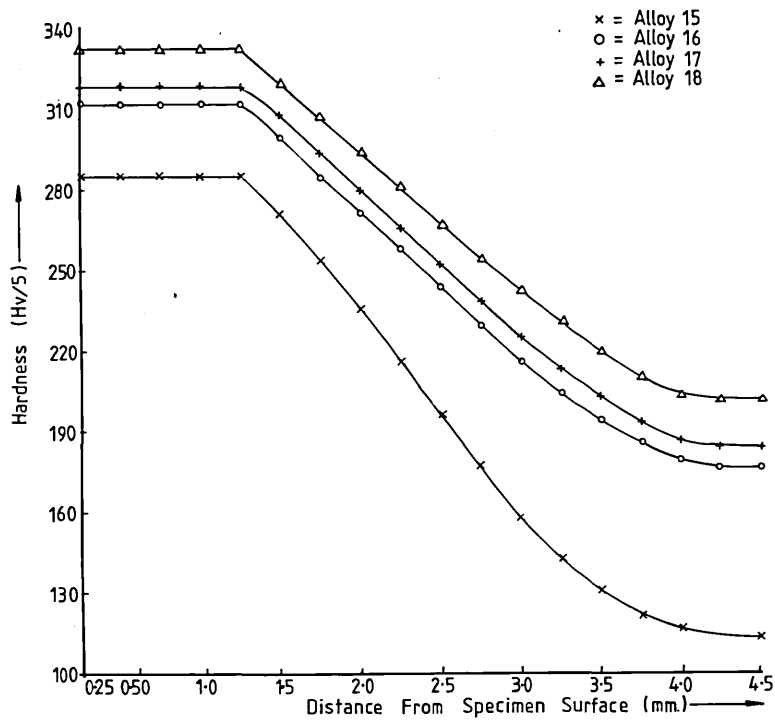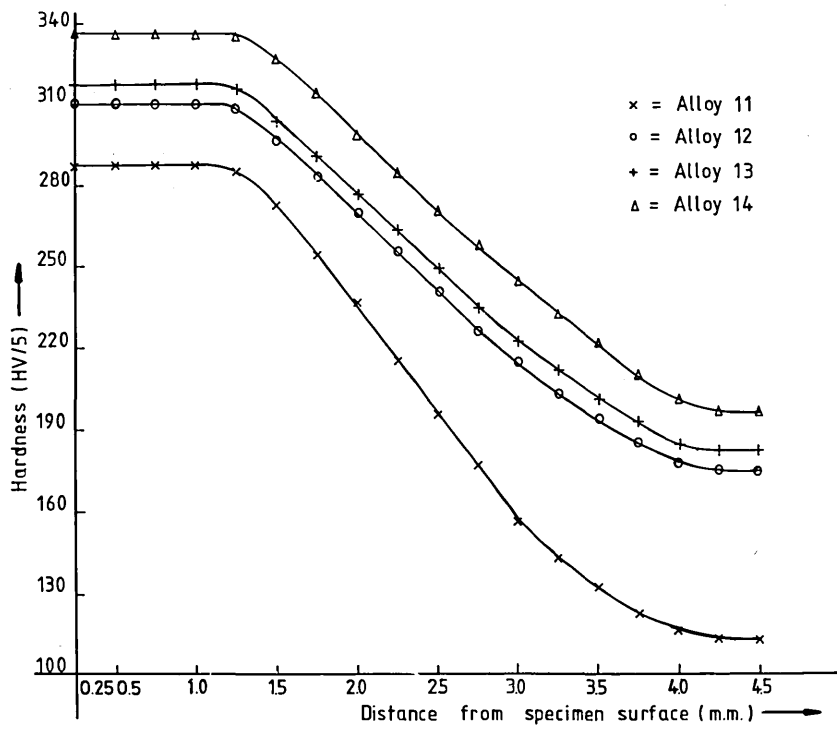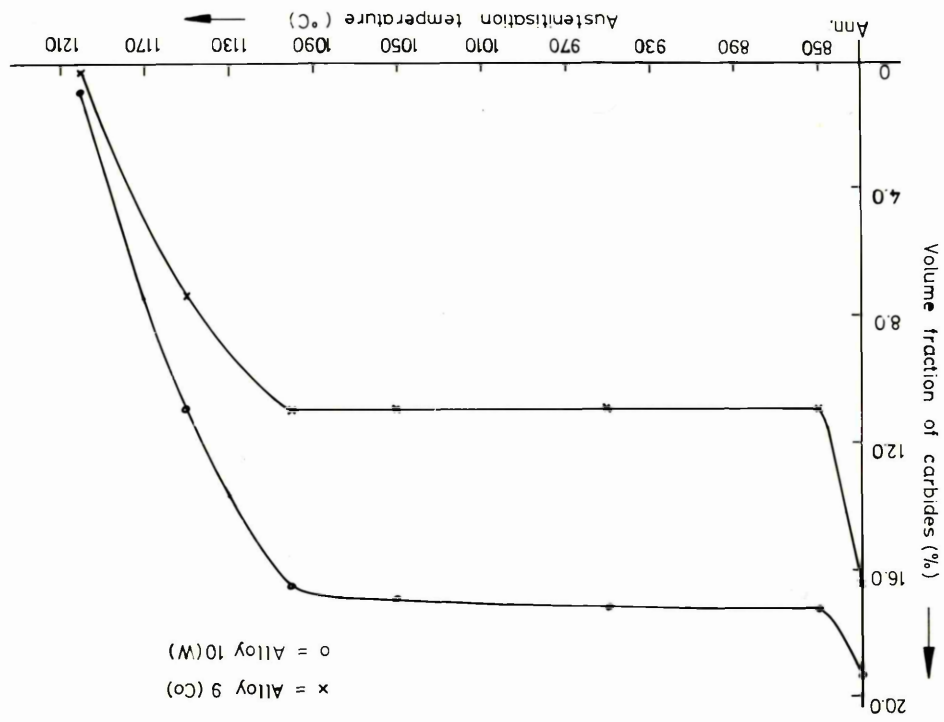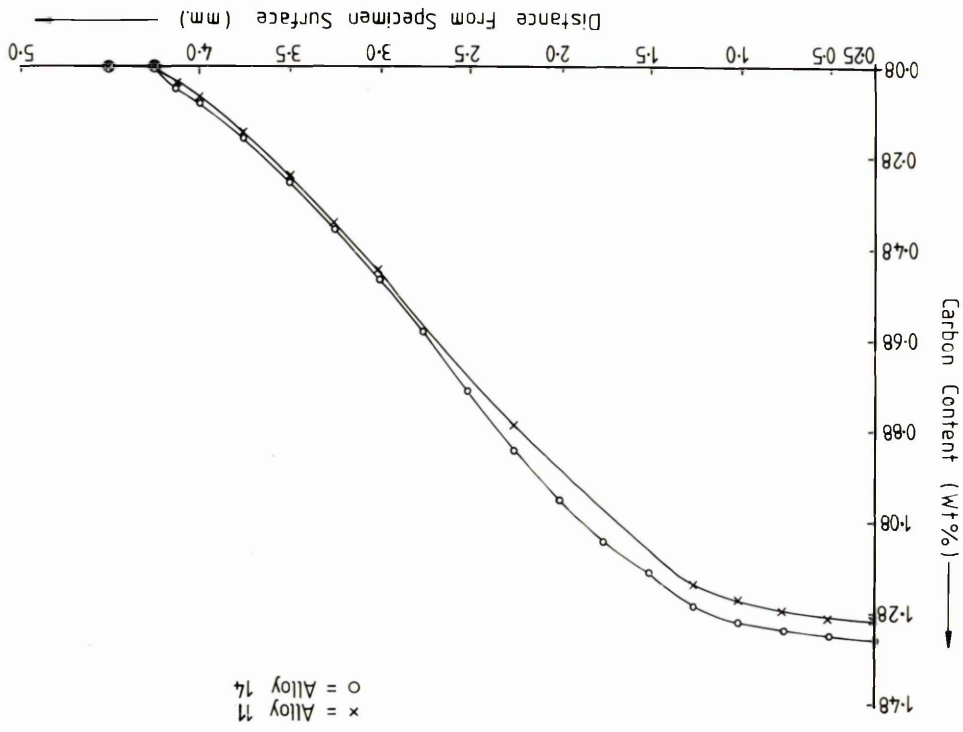
FIG. 90.   Effect of austenitisation temperature during
hardening cn the volume fraction of primary carbide present
in Alloys 4(Si), 5(Mo) and 7(Ni).   The soaking time employed
was 20 minutes in each instance.

FIG. 91.   Relationship between volume fraction of primary
carbide and austenitisation temperature during hardening for
Alloys 6(Mn) and 8(Cr).   The soaking time employed was 20
minutes in each instance.

FIG. 92.   Effect of austenitisation temperature during hardening on the volume fraction of primary carbide present in Alloys 9(Co) and 10(W).   The soaking time employed was 20 minutes in each instance.

FIG. 93.   Relationship between carbon concentration and depth beneath specimen surface for Alloys 11 and 14.   This was as a result of pack carburisation at $920^{o}C$ for 24 hours.

FIG. 94.   Effect of carbon content on hardness for
Alloys 11, 12 (0.083 C, 0.29 Si, 0.76 Mn and 0.22 wt. % V),
13 and 14 in the carburised condition.

FIG. 95.   Relationship between hardness and carbon
content for Alloys 15, 16 (0.079 C, 0.27 Si, 0.78 Mn and
0.24 wt. % V), 17 and 18 in the carburised condition.
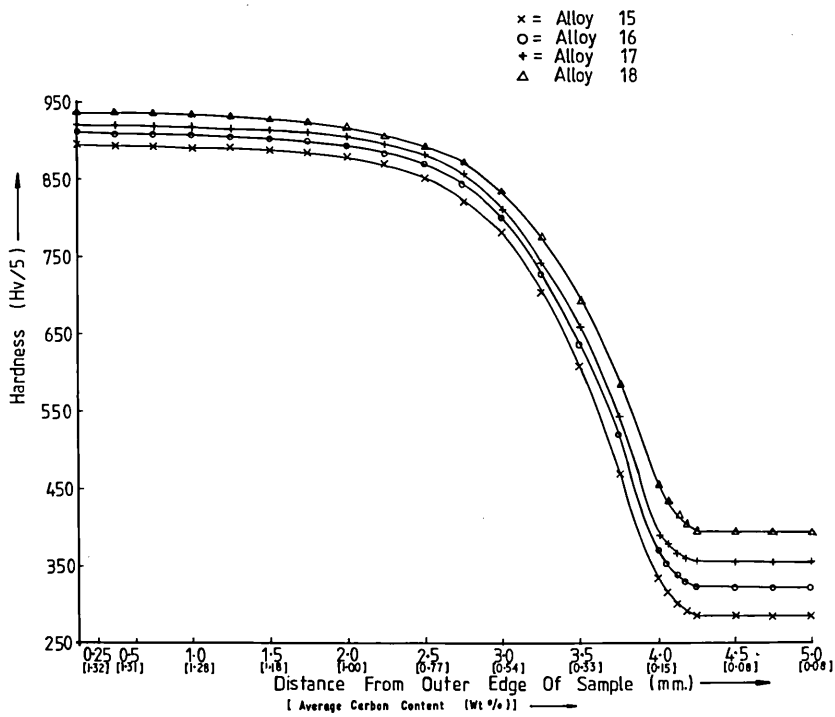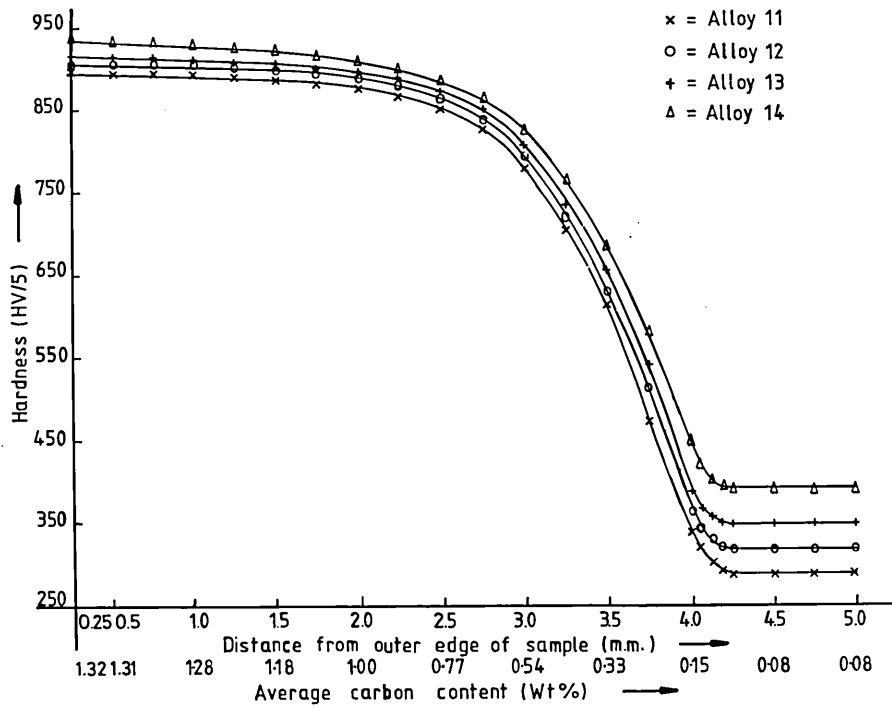
FIG. 96. Effect of carbon content on hardness for Alloys 11, 12, 13 and 14 in the carburised and hardened condition.

FIG. 97. Relationship between hardness and carbon content for Alloys 15, 16, 17 and 18 in the carburised and hardened condition.
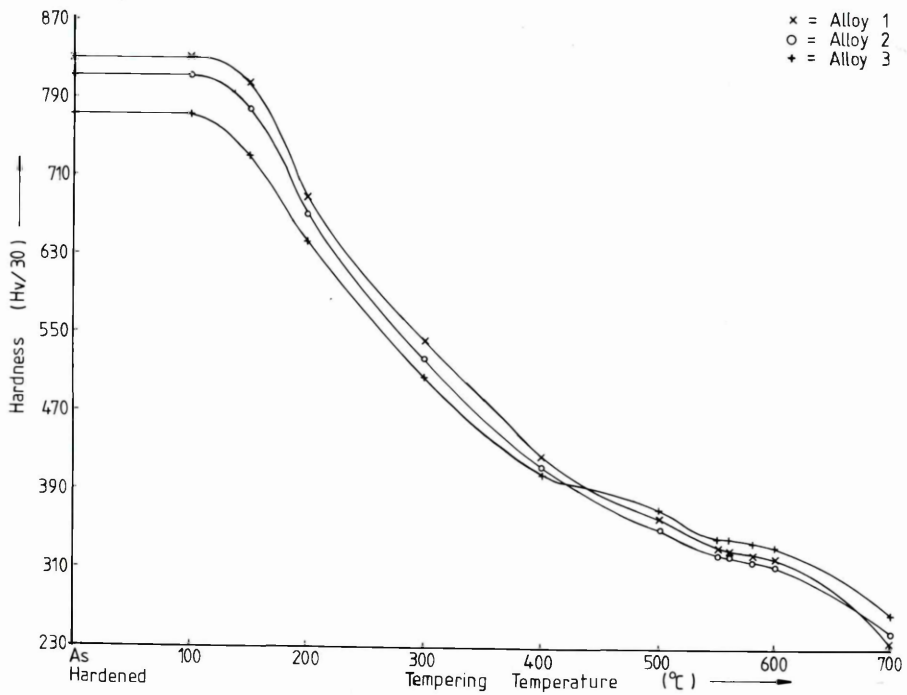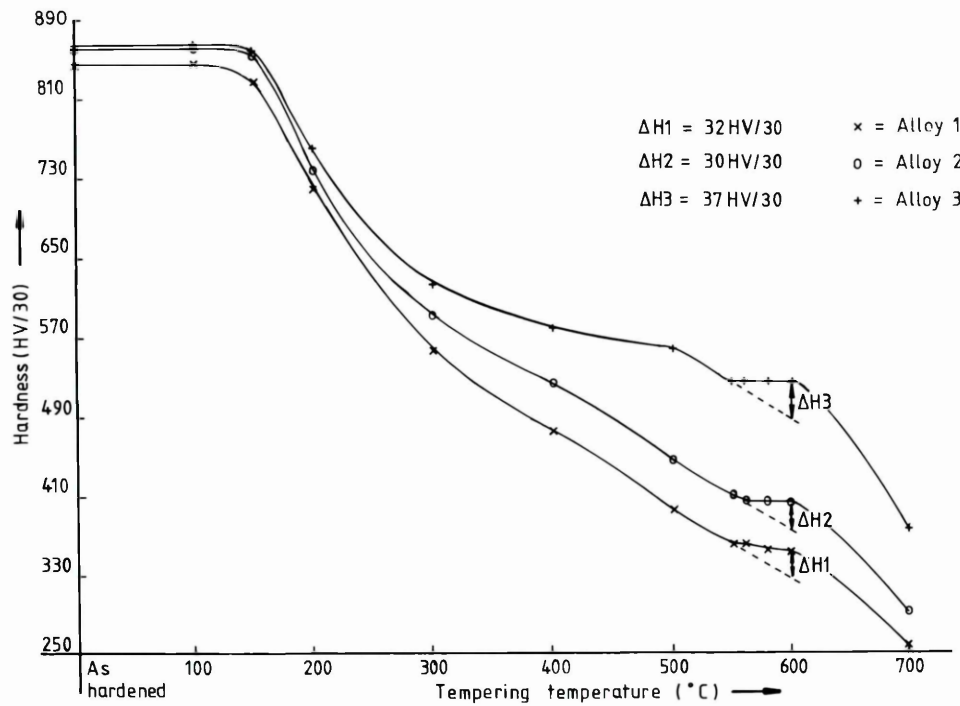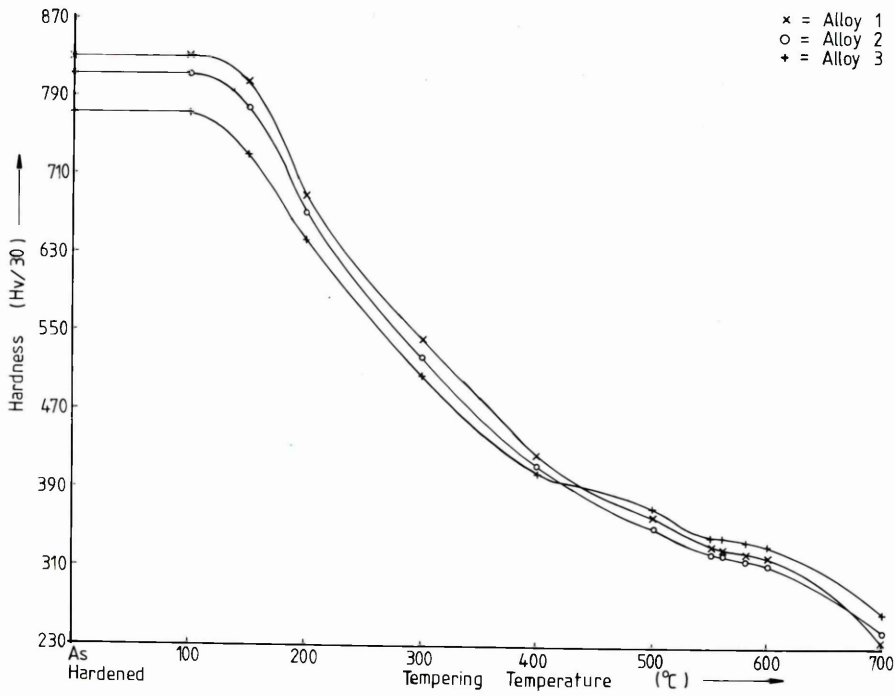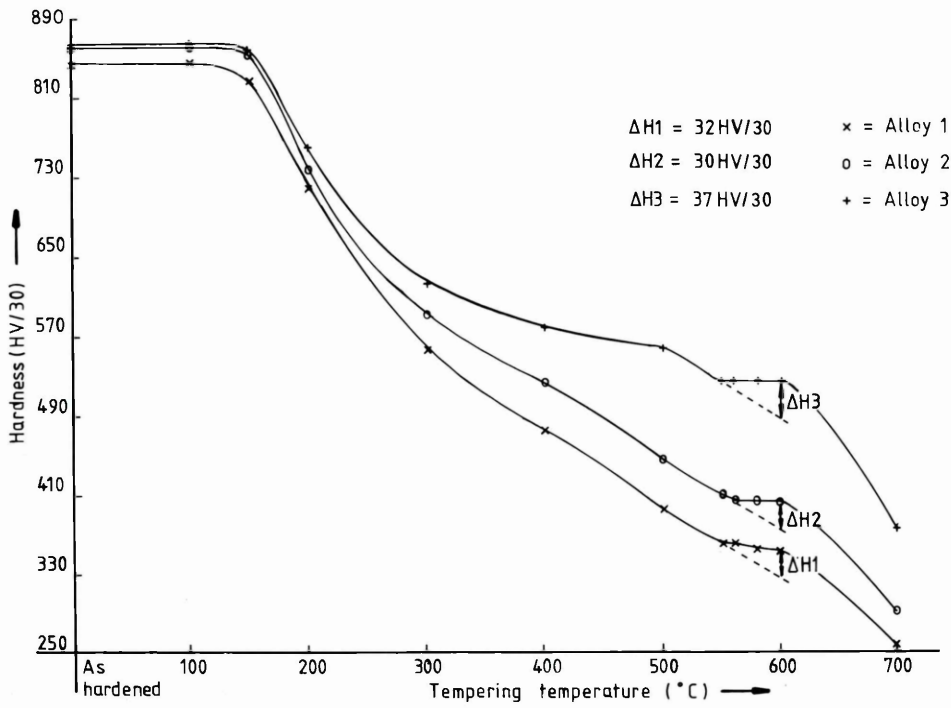
FIG. 98.   Relationship between hardness and tempering temperature for Alloys 1, 2 and 3.   The tempering time in each instance was 1 hour.

FIG. 99.   Effect of tempering temperature on hardness for Alloys 1, 2 and 3.   Hardening had been carried out by austenitisation at 850°C for 20 minutes, followed by water quenching.   The tempering time in each instance was 1 hour.

Top figure axes:
Hardness (Hv/30) vs Tempering temperature (°C)

y-axis: 890, 810, 730, 650, 570, 490, 410, 330, 250
x-axis: As hardened, 100, 200, 300, 400, 500, 600, 700

x = Alloy 1
o = Alloy 2
+ = Alloy 3

Bottom figure axes:
Hardness (Hv/30) vs Tempering Temperature (°C)

y-axis: 880, 800, 720, 640, 560, 480, 400, 320
x-axis: As Hardened, 100, 200, 300, 400, 500, 600, 700

x = Alloy 4 (Si.)
O = Alloy 5 (Mo.)

$\triangle H_4$ = 132 Hv/30
$\triangle H_5$ = 88 Hv/30

$\triangle H_5$
$\triangle H_4$
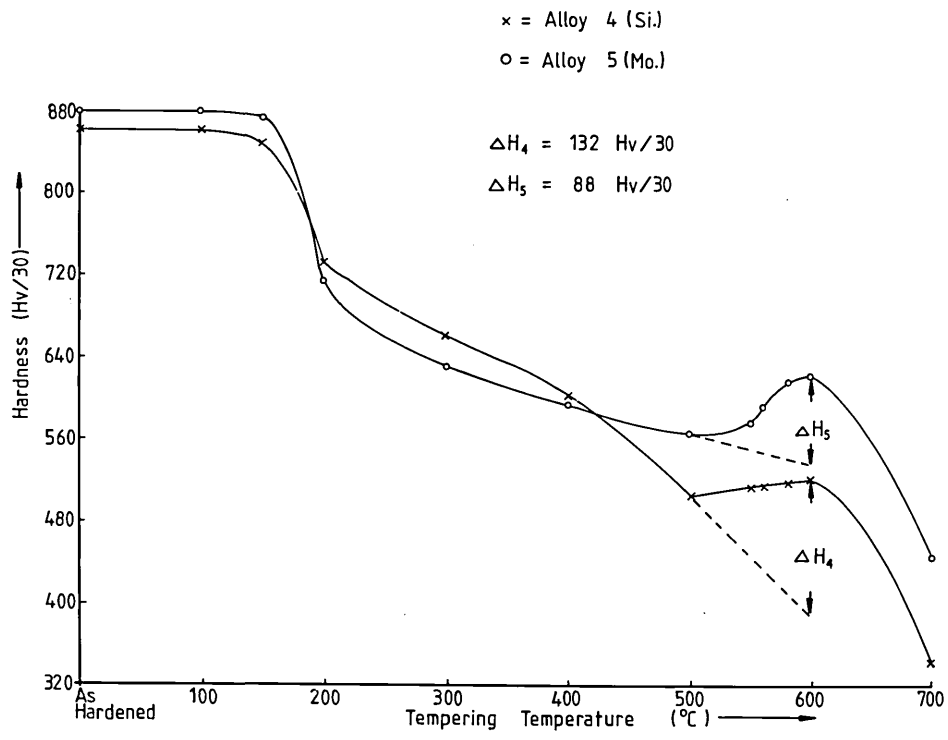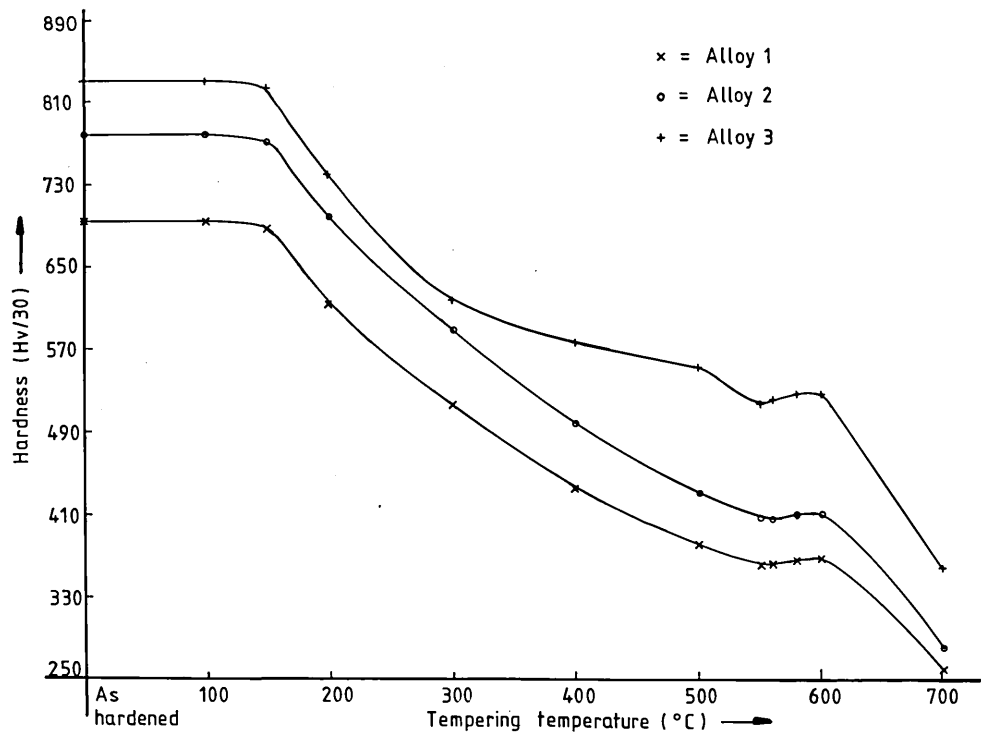
FIG. 100.   Relationship between hardness and tempering temperature for Alloys 1, 2 and 3.   Hardening had been carried out by austenitisation at 1200°C for 20 minutes, followed by water quenching.   The tempering time in each instance was 1 hour.

FIG. 101.   Effect of tempering tempera.   ...ss for Alloys 4(Si) and 5(Mo).   The tempering time in each was 1 hour.
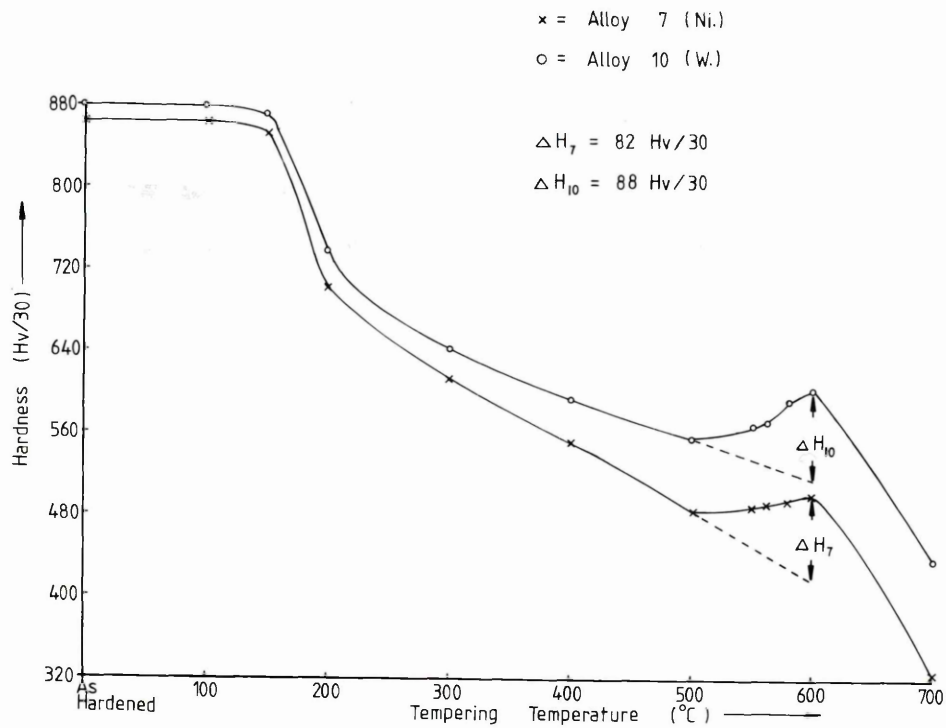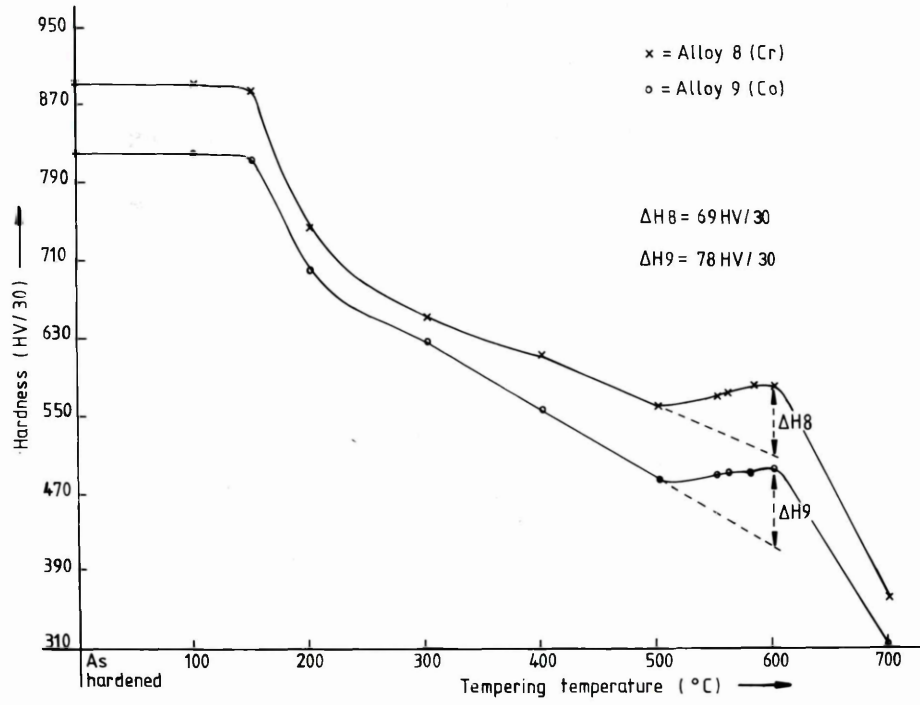
FIG. 102.   Effect of tempering temperature on hardness
for Alloys 8(Cr) and 9(Co).   The tempering time in each
instance was 1 hour.

FIG. 103.   Relationship between hardness and tempering
temperature for Alloys 7(Ni) and 10(W).   The tempering time
in each instance was 1 hour.

x = Alloy 6 (Mn)

ΔH6 = 94 HV / 30

x = Alloy 5 (Mo.)
o = Alloy 9 (Co.)
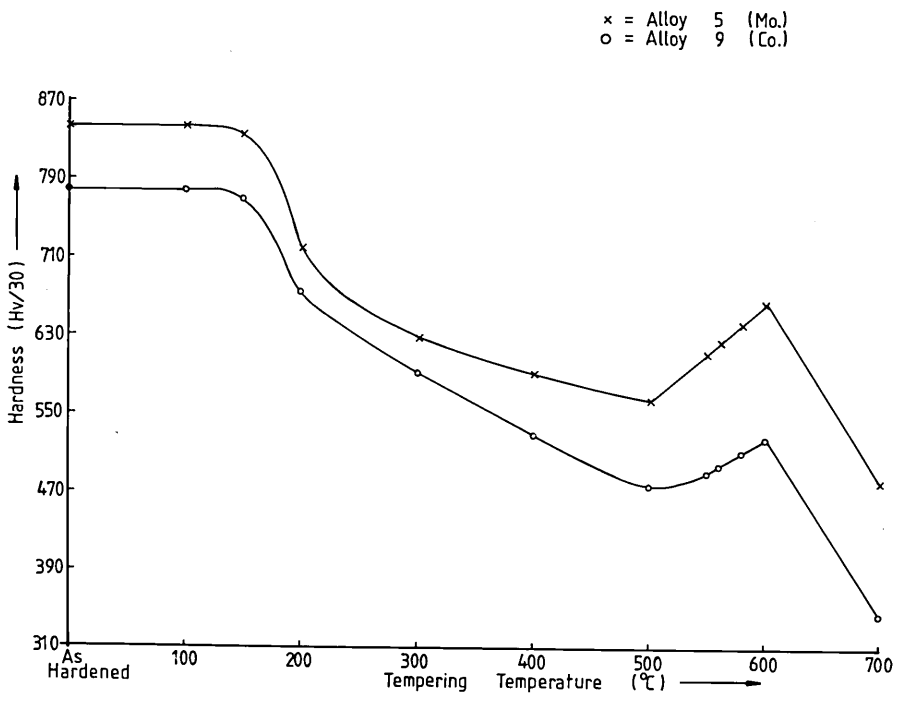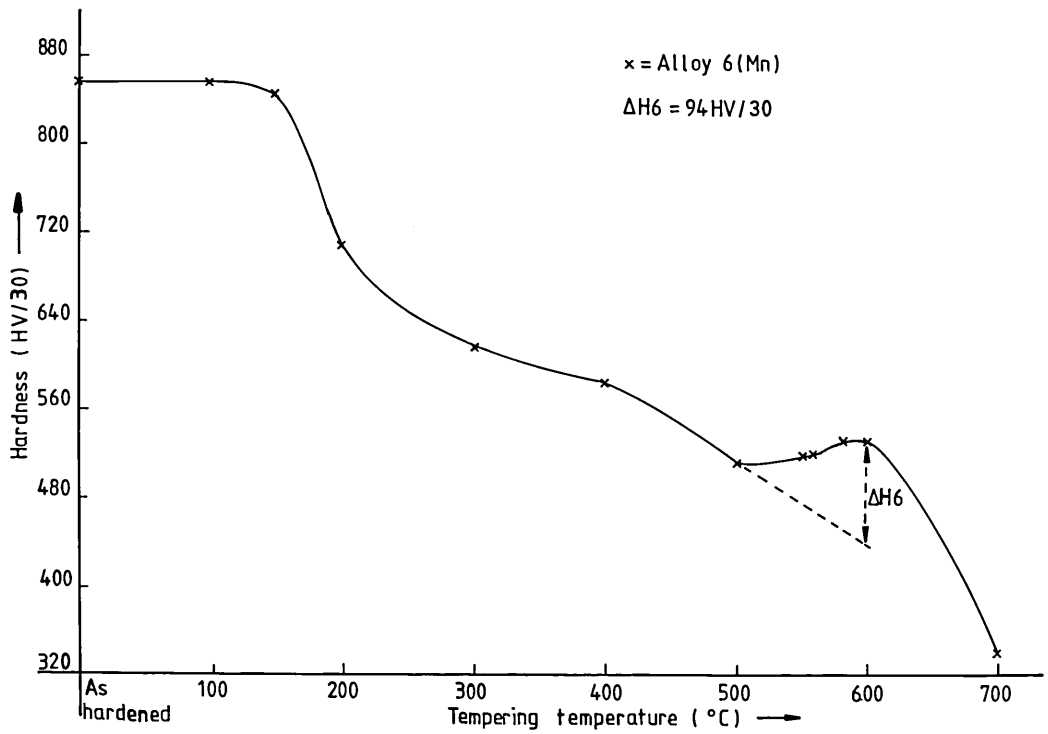
FIG. 104.   Effect of tempering temperature on hardness
for Alloy 6(Mn).   The tempering time in each instance was
1 hour.

FIG. 105.   Relationship between hardness and tempering
temperature for Alloys 5(Mo) and 9(Co).   Hardening had been
carried out by austenitisation at $1200^{o}C$ for 20 minutes, with
subsequent water quenching.   The tempering time in each instance
was 1 hour.
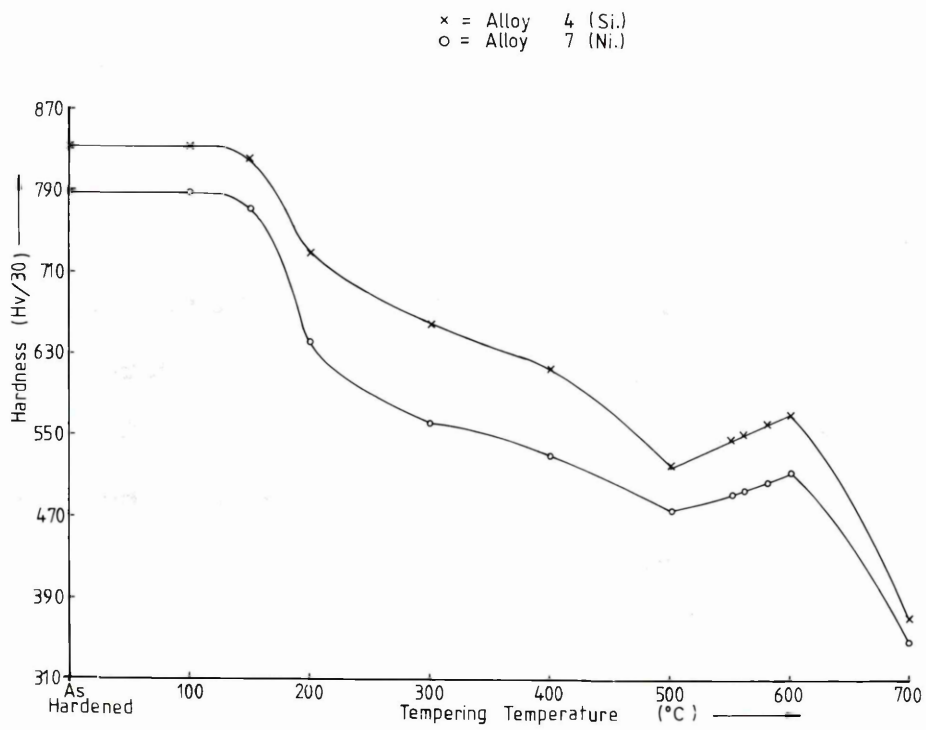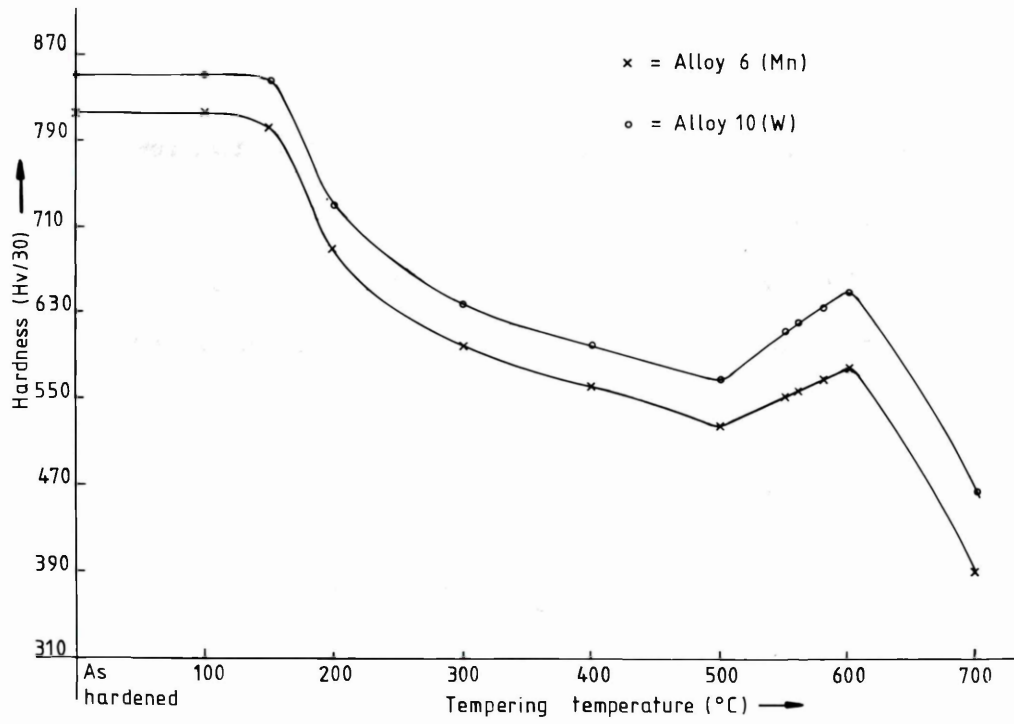
FIG. 106. Effect of tempering temperature on hardness for Alloys 6(Mn) and 10(W). Hardening had been carried out by austenitisation at 1200°C for 20 minutes, followed by water quenching. The tempering time in each instance was 1 hour.

FIG. 107. Relationship between hardness and tempering temperature for Alloys 4(Si) and 7(Ni). Hardening had been carried out by austenitisation at 1200°C for 20 minutes, with subsequent water quenching. The tempering time in each instance was 1 hour.
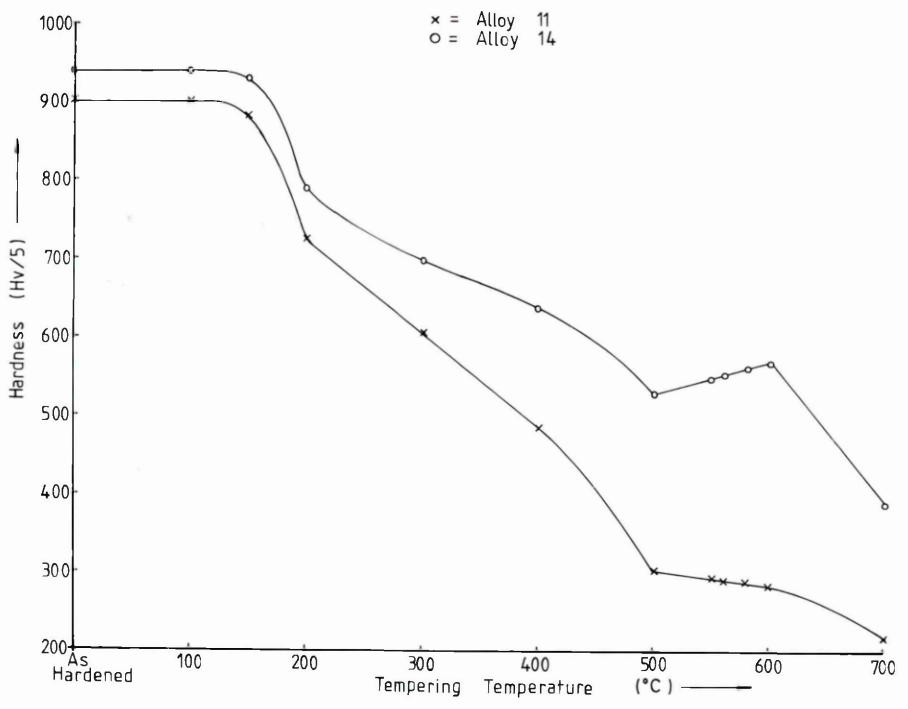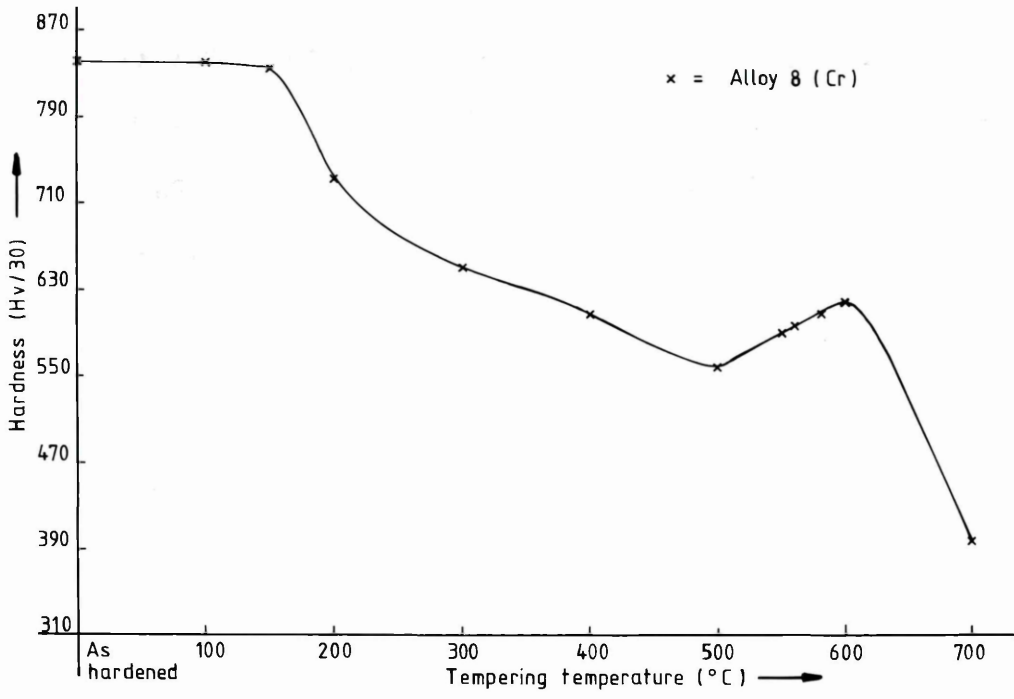
FIG. 108.   Effect of tempering temperature on hardness
for Alloy 8(Cr).   Hardening had been carried out by austeni-
tisation at 1200°C for 20 minutes, followed by water quenching.
The tempering time in each instance was 1 hour.

FIG. 109.   Relationship between hardness and tempering
temperature for Alloys 11 and 14.   Hardness readings were
taken at positions in the carburised cases where the carbon
content was 1.29 wt. %.
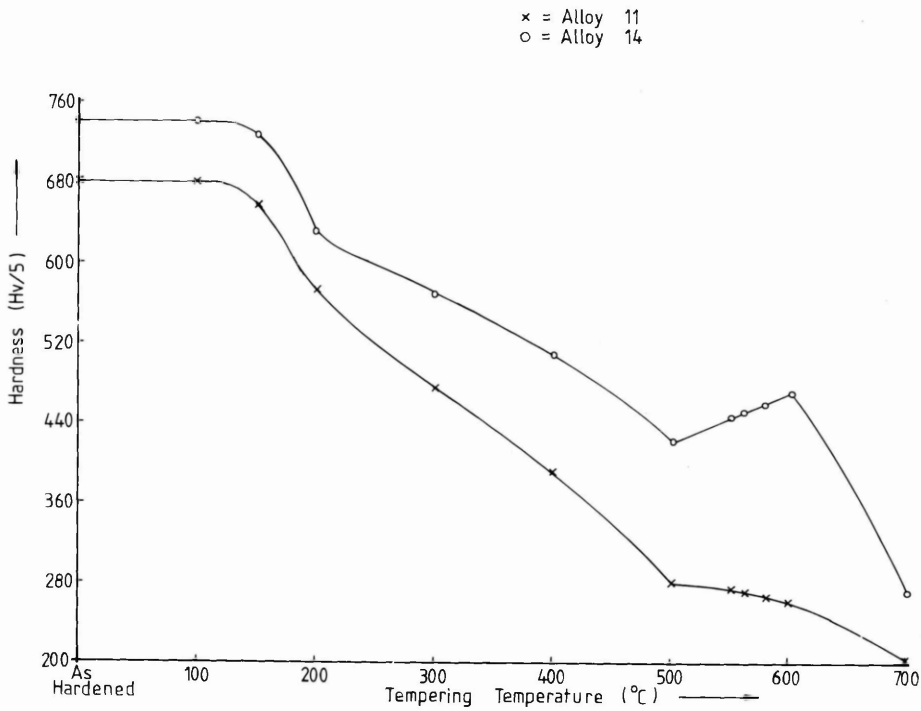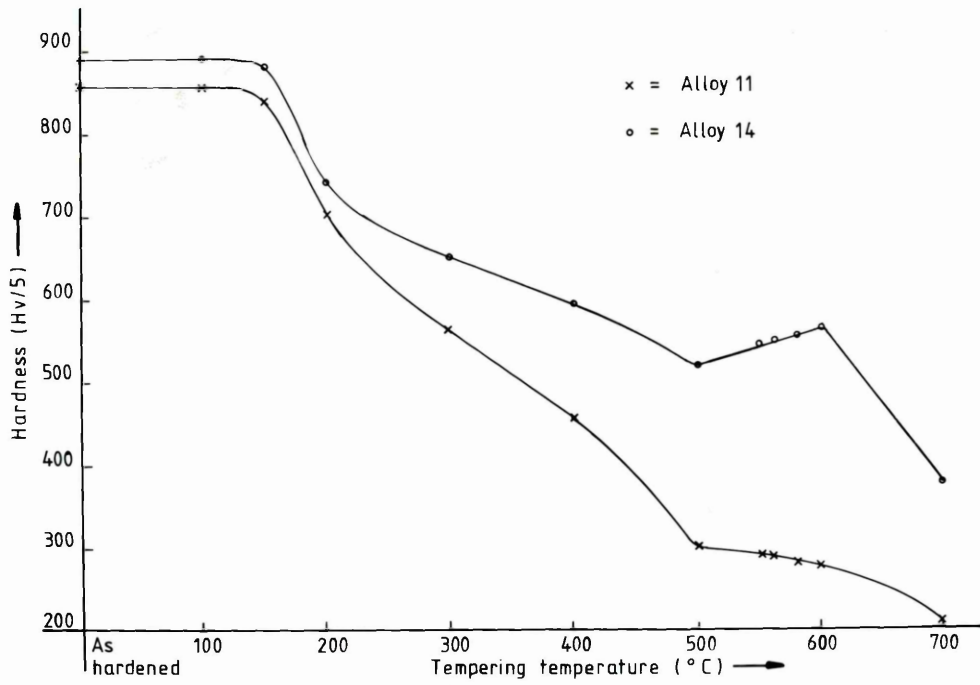
FIG. 110. Effect of tempering temperature on hardness for Alloys 11 and 14. Hardness readings were taken at positions in the carburised cases where the carbon content was 0.80 wt. %.

FIG. 111. Relationship between hardness and tempering temperature for Alloys 11 and 14. Hardness readings were taken at positions in the carburised cases where the carbon content was 0.40 wt. %.

Hardness (Hv/5) vs Tempering temperature (°C)

x = Alloy 11
o = Alloy 14

[Hardness after tempering at 600°C for 1 hour] − [500°C] (Hv/5) vs Carbon content (Wt %)

X = Alloy 11
O = Alloy 12
~ = Alloy 13
Δ = Alloy 14
x = Alloy 15
o = Alloy 16
+ = Alloy 17
∇ = Alloy 18
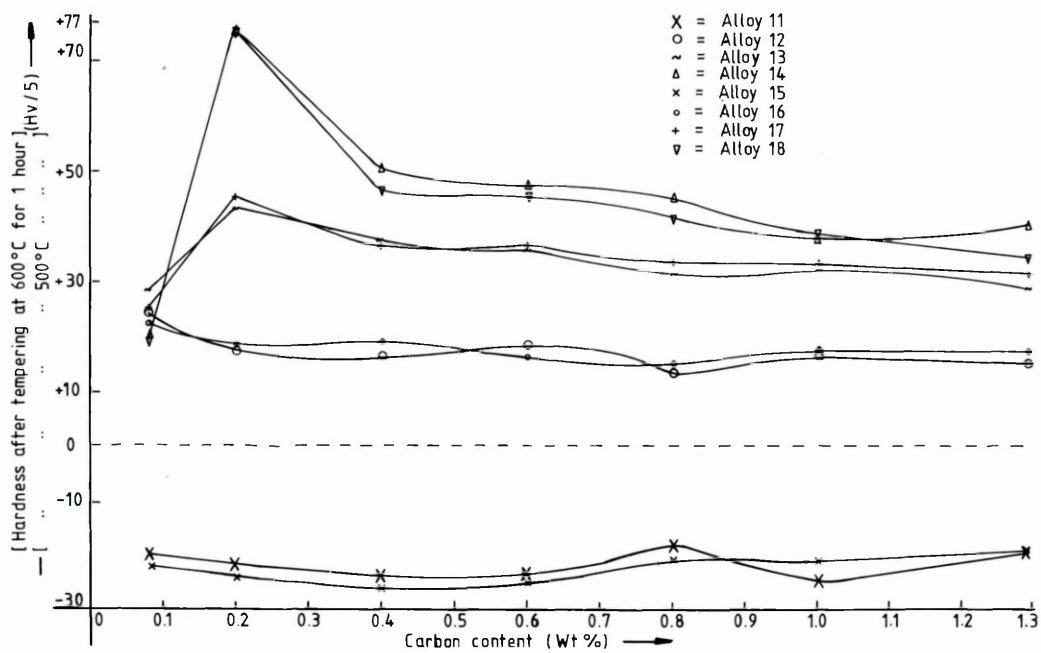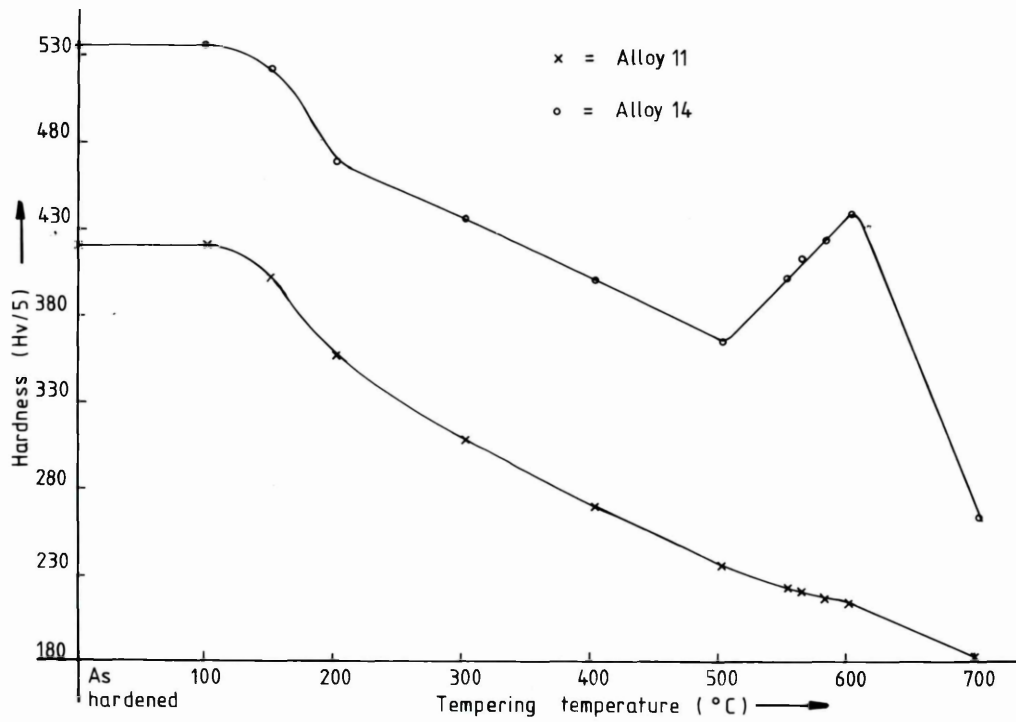
FIG. 112. Effect of tempering temperature on hardness for Alloys 11 and 14. Hardness readings were taken at positions in the carburised cases where the carbon content was 0.20 wt. %.

FIG. 113. Variations in hardness after tempering at $600^{\circ}C$ for 1 hour, as opposed to $500^{\circ}C$ for the same duration, as a function of carbon content for all the carburised steels.
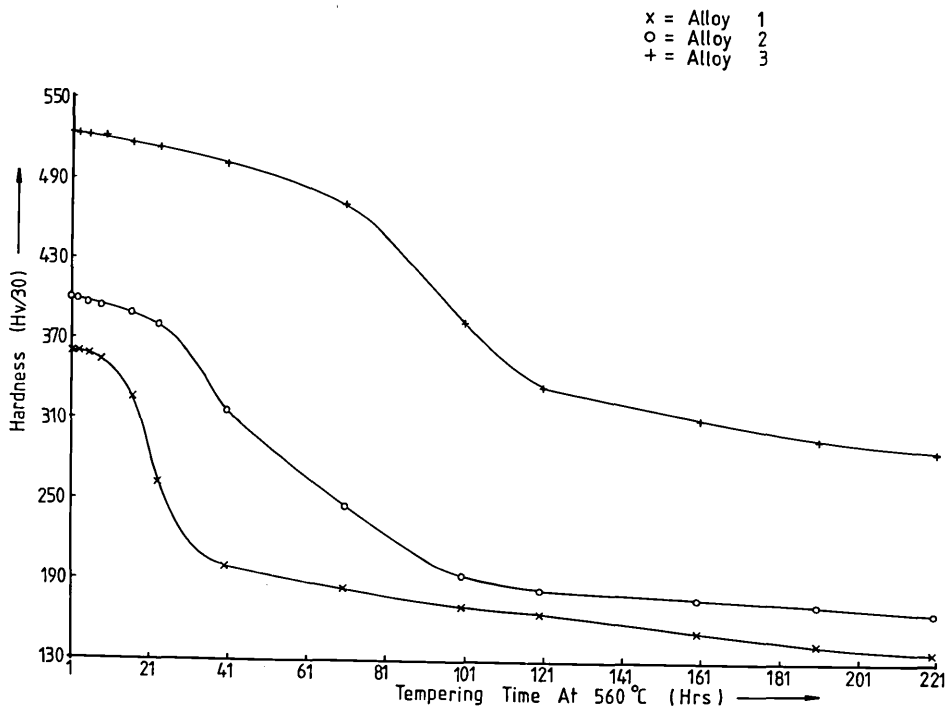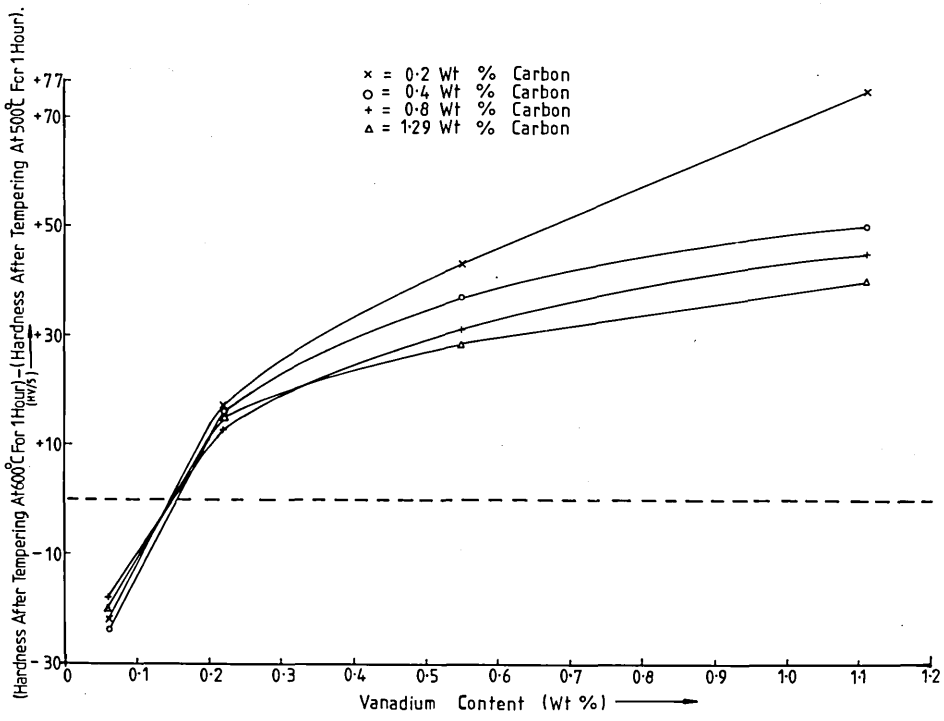
FIG. 114.   Variations in hardness after tempering at
600°C for 1 hour, as opposed to 500°C for the same duration,
as a function of vanadium content for Alloys 11, 12, 13 and 14.

FIG. 115.   Effect of tempering time at 560°C on hardness
for Alloys 1, 2 and 3.
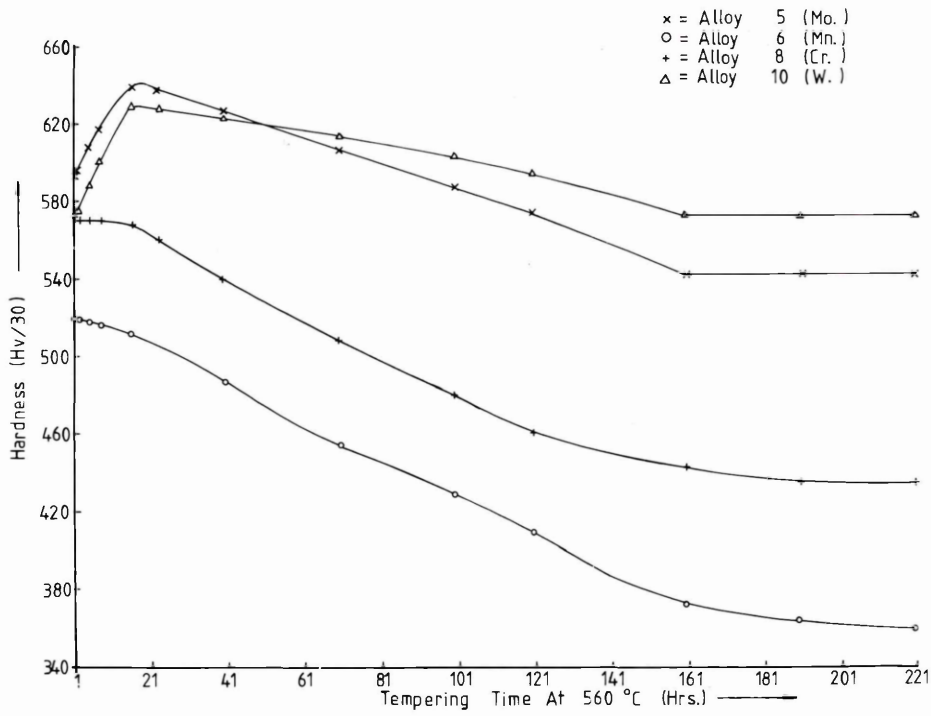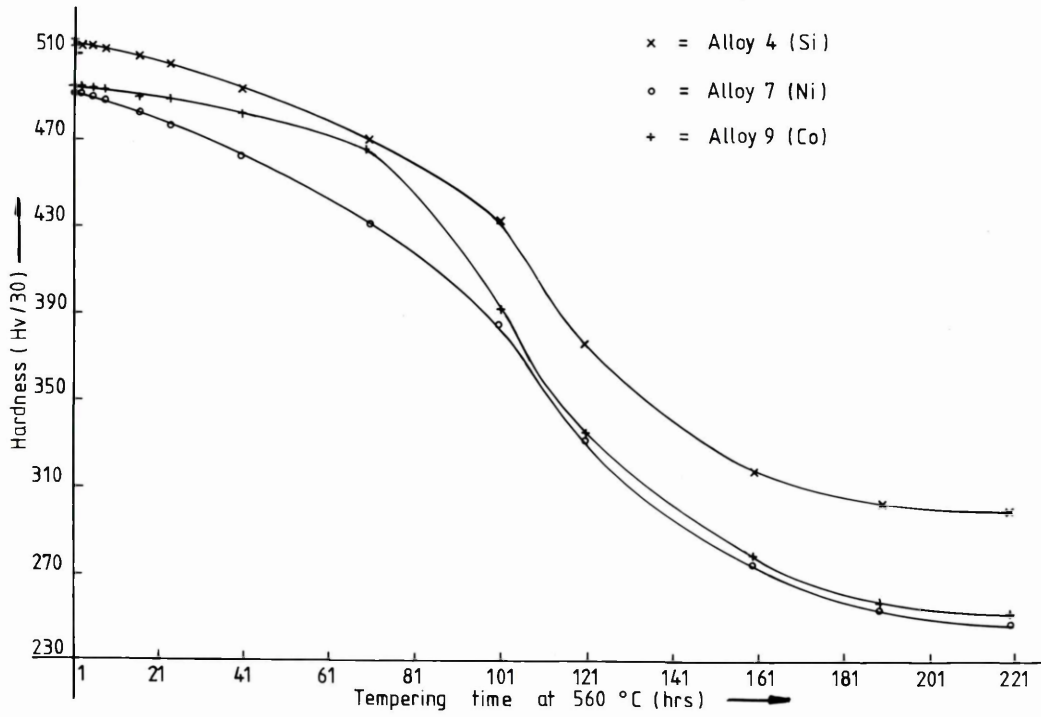
FIG. 116. Relationship between hardness and tempering time at 560°C for Alloys 4(Si), 7(Ni) and 9(Co).

FIG. 117. Effect of tempering time at 560°C on hardness for Alloys 5(Mo), 6(Mn), 8(Cr) and 10(W).

x = Alloy 11 (At a position in the case with a carbon content
of 1.29 wt. %)
o = Alloy 12 (·· ··   ··   ·· ·· ·· ·· ·· ·· ··)
+ = Alloy 13 (·· ··   ··   ·· ·· ·· ·· ··   ··)
Δ = Alloy 14 (·· ··   ··   ·· ·· ·· ·· ··   ··)

Hardness (Hv / 5)

Tempering   time at   560 °C (hrs)

x = Alloy 11 (At A position In The Case With A Carbon Content of 0·80 Wt.%)
o = Alloy 12 ('' ''   ''   '' '' ''   '' '' ''   '' '' '' '')
+ = Alloy 13 ('' ''   ''   '' '' ''   '' '' ''   '' '' '' '')
Δ = Alloy 14 ('' ''   ''   '' '' ''   '' '' ''   '' '' '' '')

Hardness (Hv / 5)

Tempering   Time At 560 °C (Hrs)
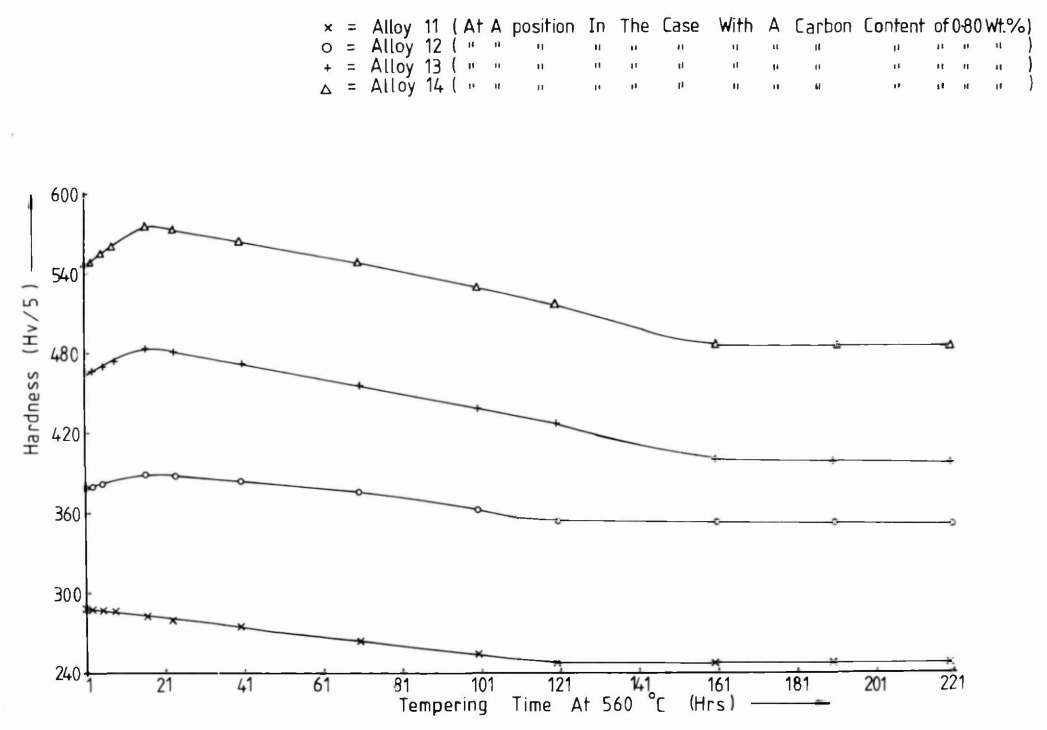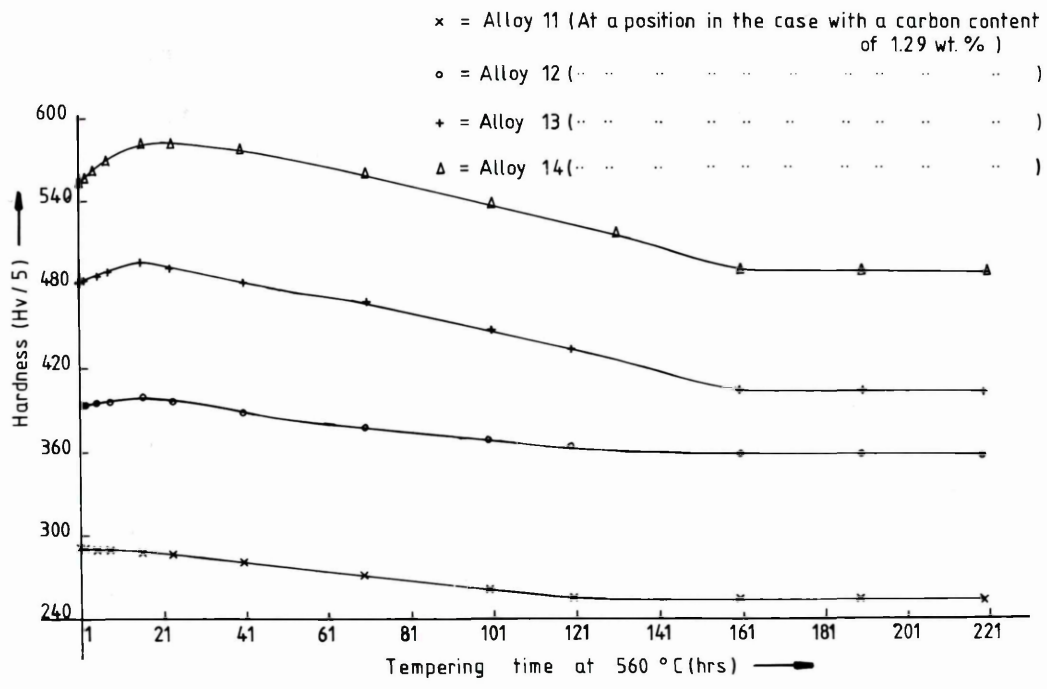
FIG. 118.   Relationship between hardness and tempering time at 560°C for Alloys 11, 12, 13 and 14.   Hardness readings were taken at positions in the carburised cases where the carbon content was 1.29 wt. %.

FIG. 119.   Effect of tempering time at 560°C on hardness for Alloys 11, 12, 13 and 14.   Hardness readings were taken at positions in the carburised cases where the carbon content was 0.80 wt. %.

x = Alloy 11(At a position in the case with a carbon content of 0.40 Wt%)
o = Alloy 12(·· ·· ·· ·· ·· ·· ·· ·· ·· ·· ·· ·· ··)
+ = Alloy 13(·· ·· ·· ·· ·· ·· ·· ·· ·· ·· ·· ·· ··)
∧ = Alloy 14(·· ·· ·· ·· ·· ·· ·· ·· ·· ·· ·· ·· ··)

x = Alloy 11 (At A Position In The Case With A Carbon Content Of 0·20 Wt%)
o = Alloy 12 (·· ·· ·· ·· ·· ·· ·· ·· ·· ·· ·· ··)
+ = Alloy 13 (·· ·· ·· ·· ·· ·· ·· ·· ·· ·· ·· ··)
Δ = Alloy 14 (·· ·· ·· ·· ·· ·· ·· ·· ·· ·· ·· ··)
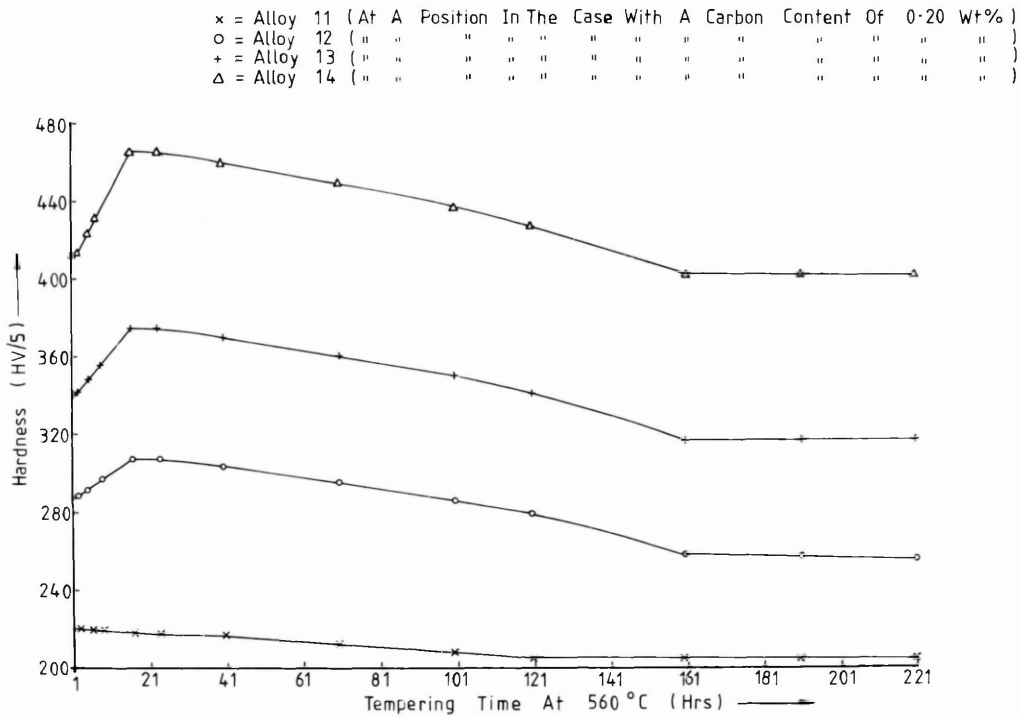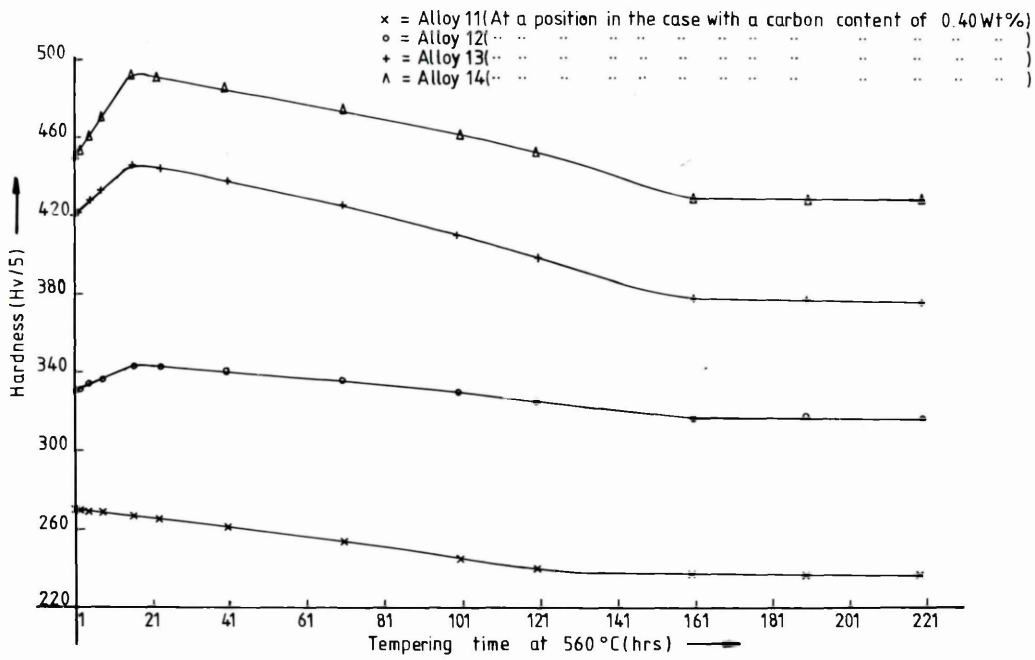
FIG. 120. Relationship between hardness and tempering time at 560°C for Alloys 11, 12, 13 and 14. Hardness readings were taken at positions in the carburised cases where the carbon content was 0.40 wt. %.

FIG. 121. Effect of tempering time at 560°C on hardness for Alloys 11, 12, 13 and 14. Hardness readings were taken at positions in the carburised cases where the carbon content was 0.20 wt. %.

Upper graph:

Y-axis: (Hardness After Tempering For 16 Hours At 560°C) - (Hardness After Tempering For 1 Hour At 560°C). (HV/5)

X-axis: Carbon Content (Wt %)

Legend:
- × = Alloy 11
- ○ = Alloy 12
- + = Alloy 13
- △ = Alloy 14
- —·×·— = Alloy 15
- —○·— = Alloy 16
- —·+·— = Alloy 17
- —·△·— = Alloy 18

Y-axis values: +70, +60, +50, +40, +30, +20, +10, 0, -10

X-axis values: 0, 0.1, 0.2, 0.3, 0.4, 0.5, 0.6, 0.7, 0.8, 0.9, 1.0, 1.1, 1.2, 1.3

Lower graph:

Y-axis: [Hardness after tempering at 560 °C for 16 hours] − [″ ″ ″ ″ 1 hour]   (HV / 5)

X-axis: Vanadium content (Wt %)

Legend:
- × = 0.2 wt % carbon
- ○ = 0.4 ″ ″ ″
- + = 0.8 ″ ″ ″
- △ = 129 ″ ″ ″

Y-axis values: +60, +50, +40, +30, +20, +10, 0, -10

X-axis values: 0, 0.1, 0.2, 0.3, 0.4, 0.5, 0.6, 0.7, 0.8, 0.9, 1.0, 1.1, 1.2
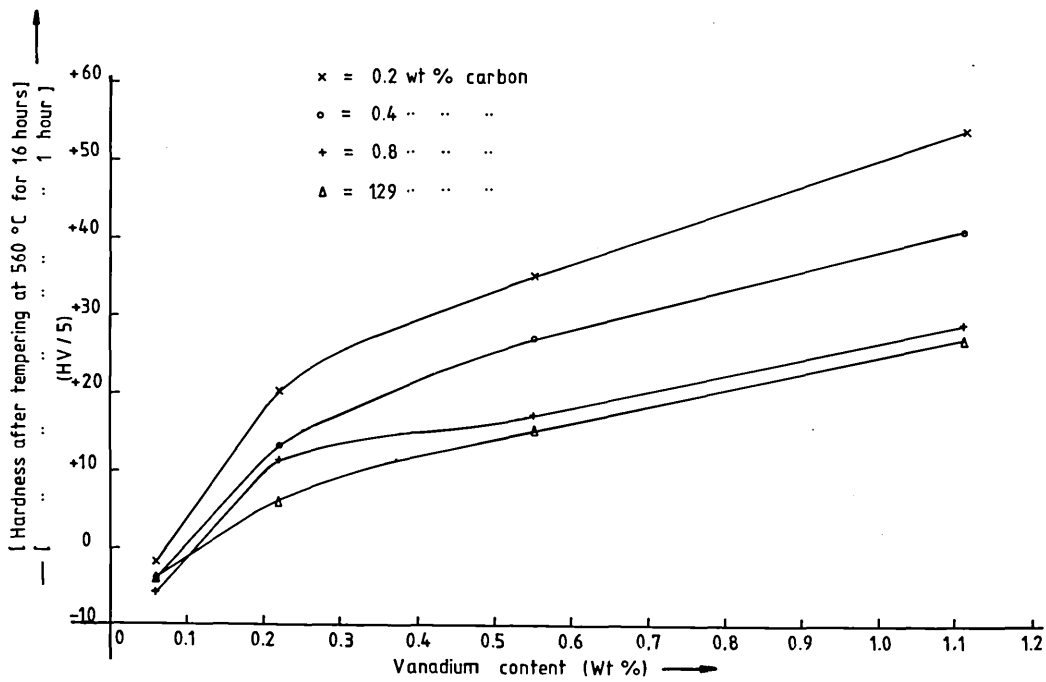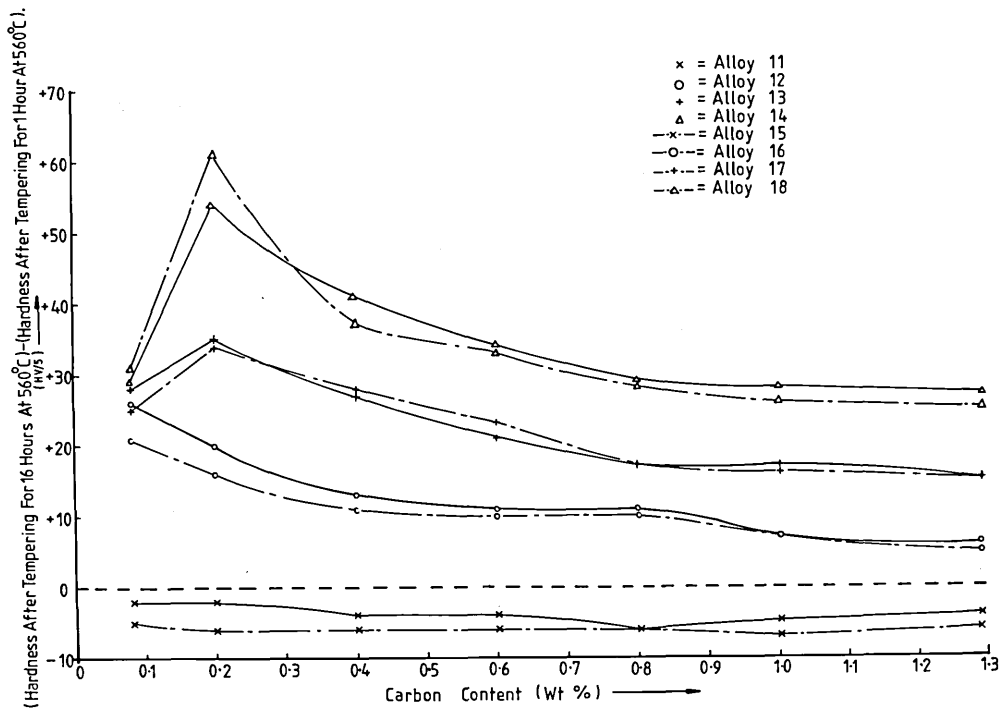
FIG. 122. Variations in hardness after tempering at 560°C for 16 hours, as opposed to 1 hour at the same temperature as a function of carbon content for all the carburised steels.

FIG. 123. Variations in hardness after tempering at 560°C for 16 hours, as opposed to 1 hour at the same temperature, as a function of vanadium content for Alloys 11, 12, 13 and 14.
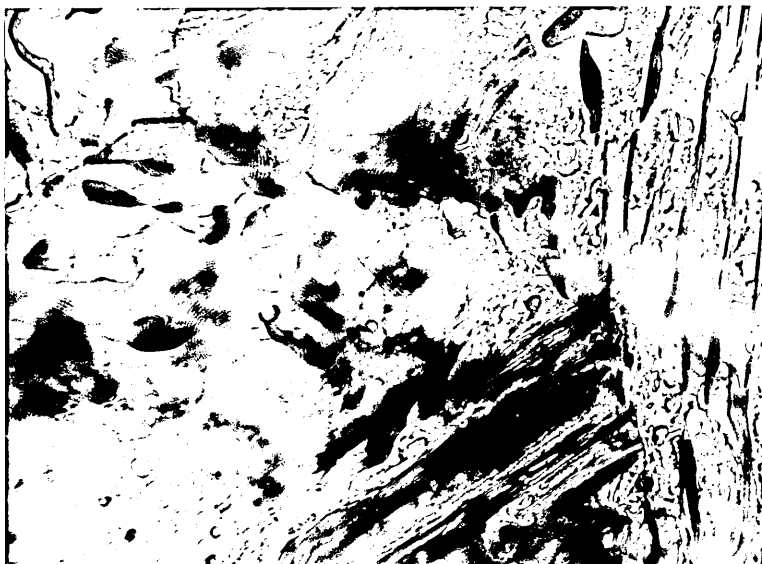
FIG. 124.   Thin foil electron micrograph of Alloy 9(Co)
in the forged condition.   Magnification:- x30,000.

FIG. 125.   Thin foil electron micrograph of Alloy 8(Cr)
in the forged condition.   Magnification:- x30,000.

FIG. 126.   Thin foil electron micrograph of Alloy 3 in
the as-hardened condition.   Austenitisation was carried out
at 1120°C for 20 minutes, with subsequent water quenching.
Magnification:- x30,000.

FIG. 127.   Thin foil electron micrograph of Alloy 4(Si)
in the as-hardened condition.   Austenitisation was carried
out at 1120°C for 20 minutes, with subsequent water quenching.
Magnification:- x30,000.
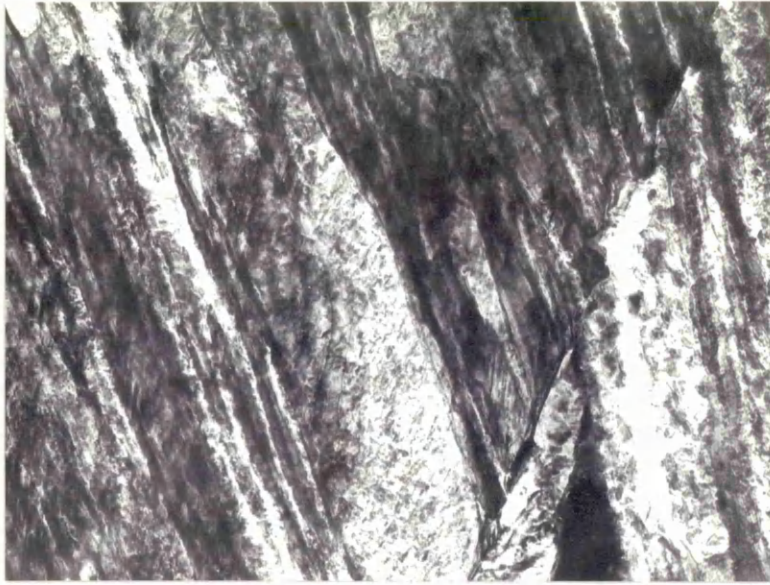
FIG. 128.   Thin foil electron micrograph of Alloy 8(Cr) in the as-hardened condition.   Austenitisation was carried out at $1150^{\circ}C$ for 20 minutes, with subsequent water quenching. Magnification:- x40,000.

FIG. 129.   Thin foil electron micrograph of Alloy 10(W) in the as-hardened condition.   Austenitisation was carried out at $1150^{\circ}C$ for 20 minutes, with subsequent water quenching. Magnification:- x30,000.
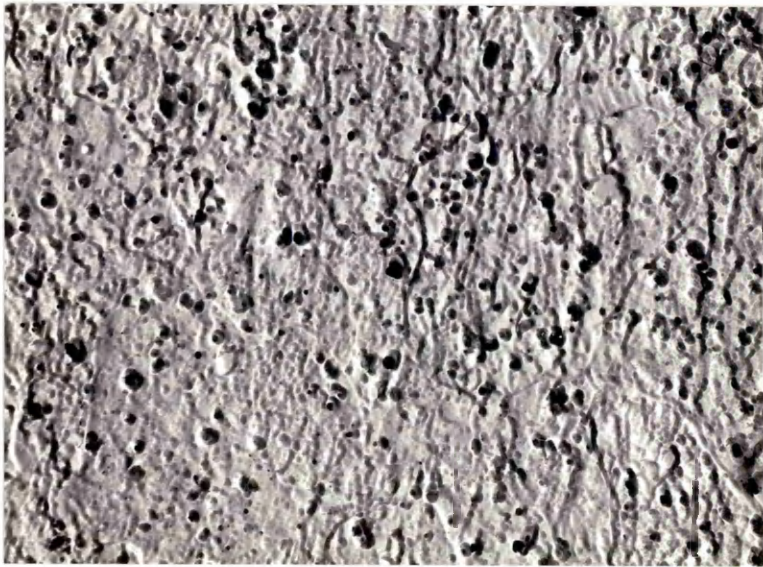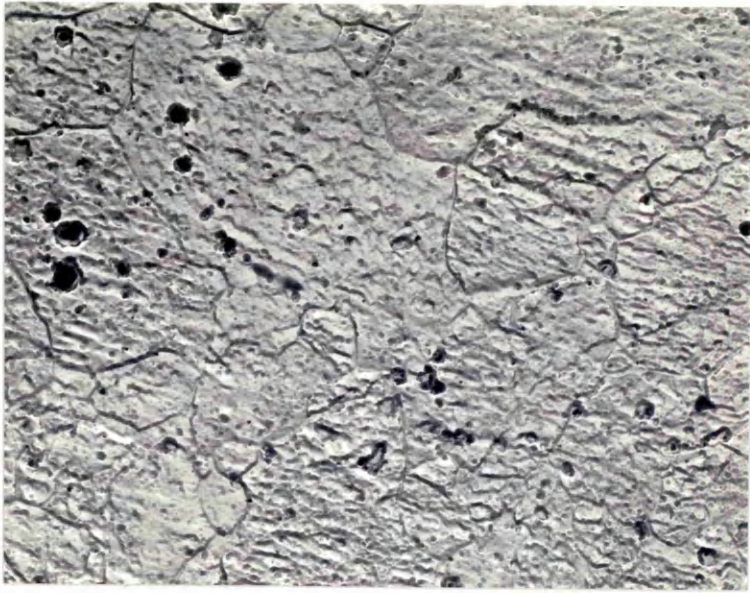
FIG. 130. Carbon replica electron micrograph of Alloy 1 in the hardened and tempered condition. Tempering was carried out at 560°C for 23 hours. Magnification:- x2,500.

FIG. 131. Carbon replica electron micrograph of Alloy 2 in the hardened and tempered condition. Tempering was carried out at 560°C for 70 hours. Magnification:- x2,500.
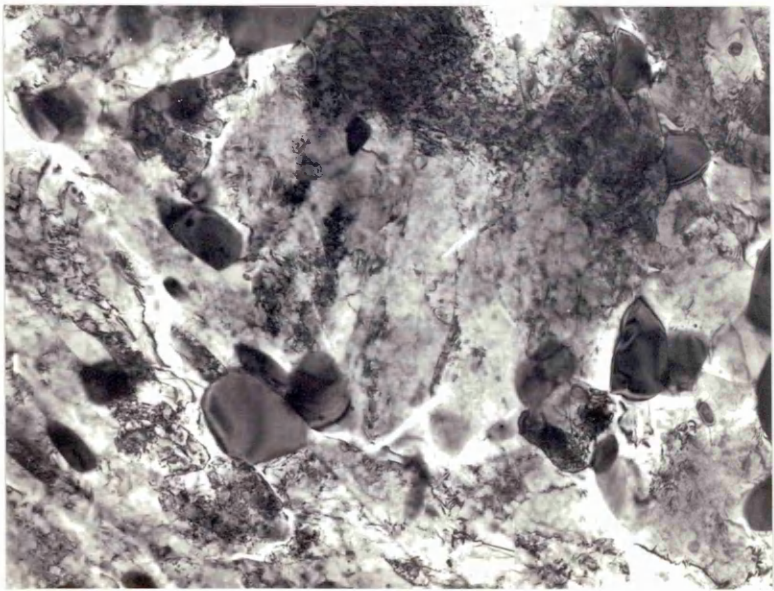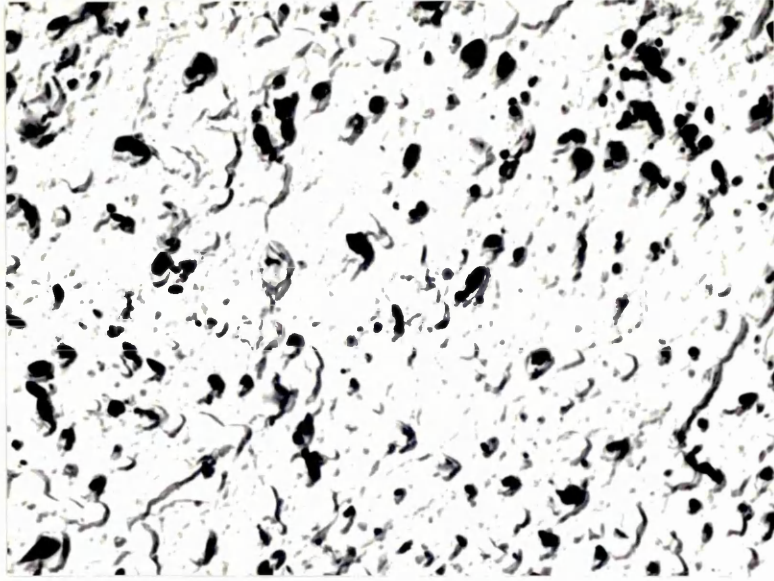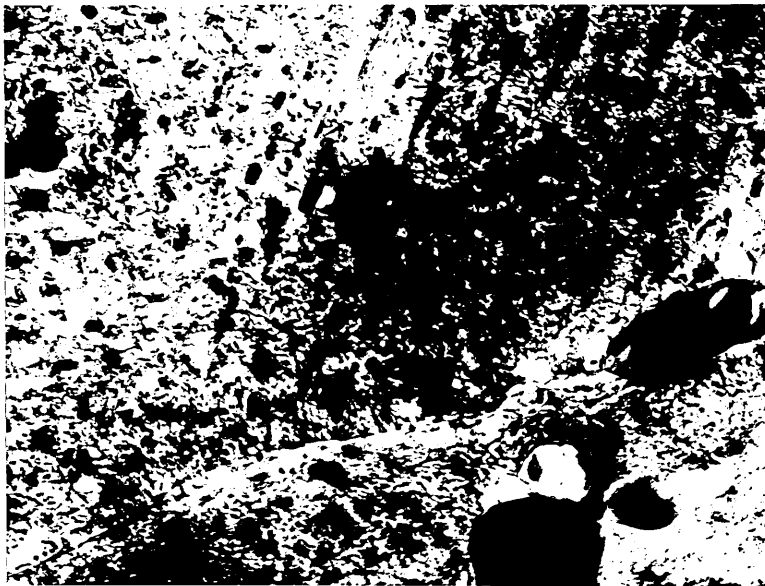
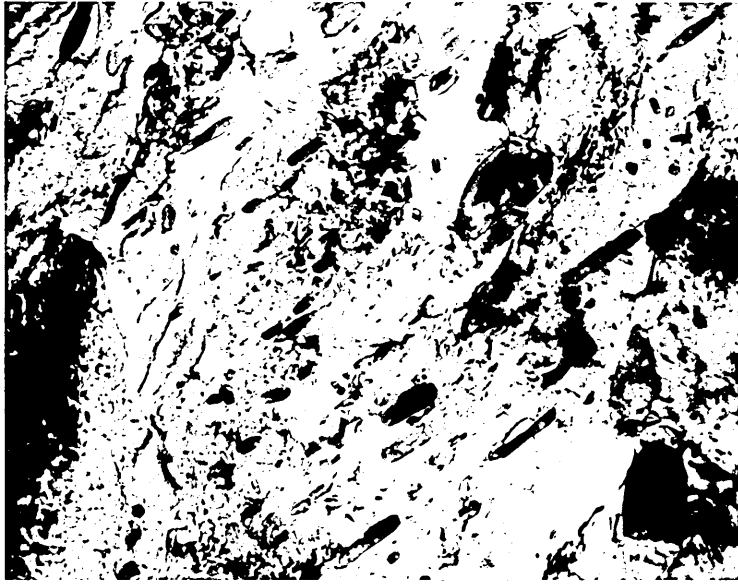FIG. 132.   Carbon replica electron micrograph of Alloy 3 in the hardened and tempered condition.   Tempering was carried out at 560°C for 190 hours.   Magnification:- x4,000.

FIG. 133.   Thin foil electron micrograph of Alloy 1 in the hardened and tempered condition.   Tempering was carried out at 600°C for 16 hours.   Magnification:- x30,000.
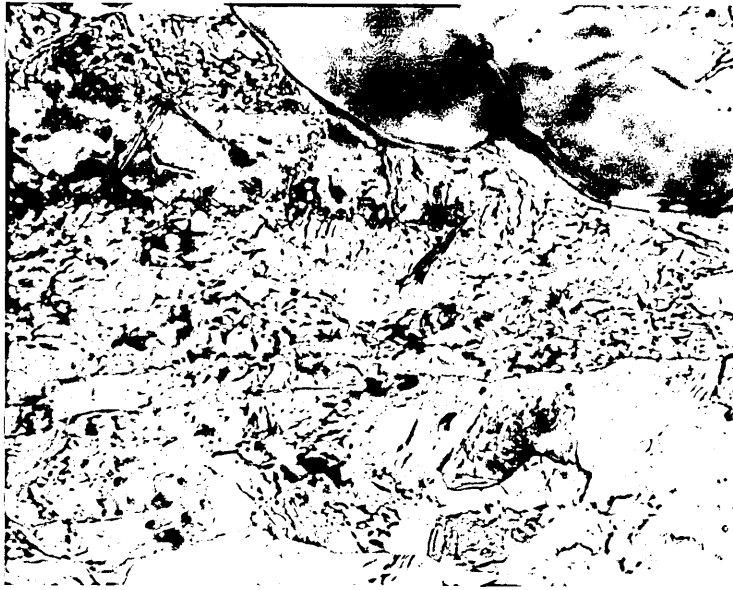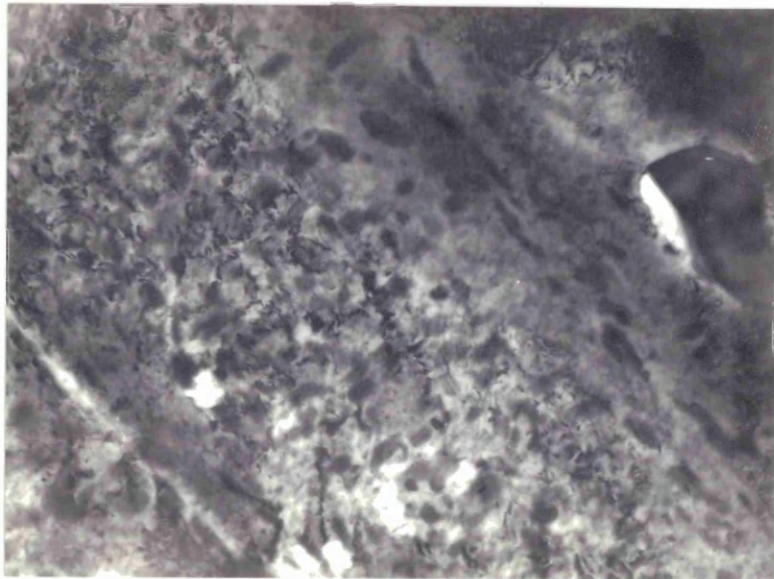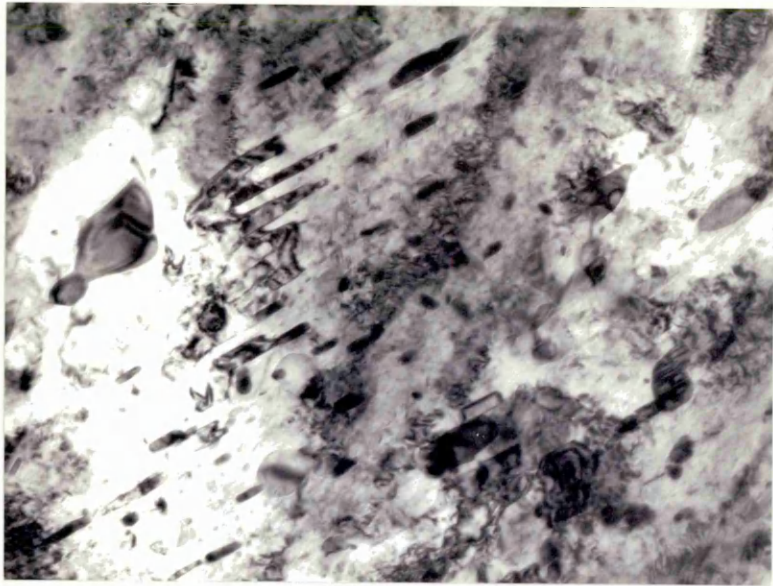
FIG. 134.   Thin foil electron micrograph of Alloy 1
in the hardened and tempered condition.   Tempering was
carried out at 600°C for 16 hours.   Magnification:- x70,000.

FIG. 135.   Thin foil electron micrograph of Alloy 1
in the hardened and tempered condition.   Tempering was carried
out at 600°C for 16 hours.   Magnification:- x60,000.
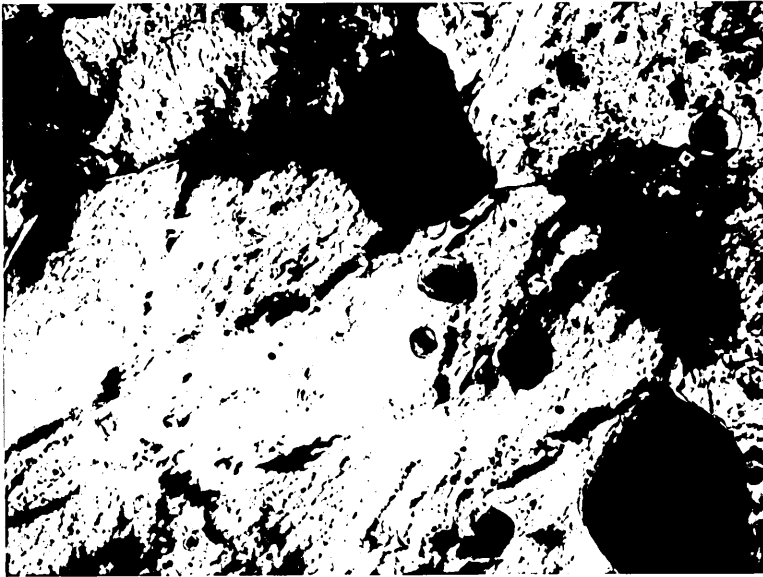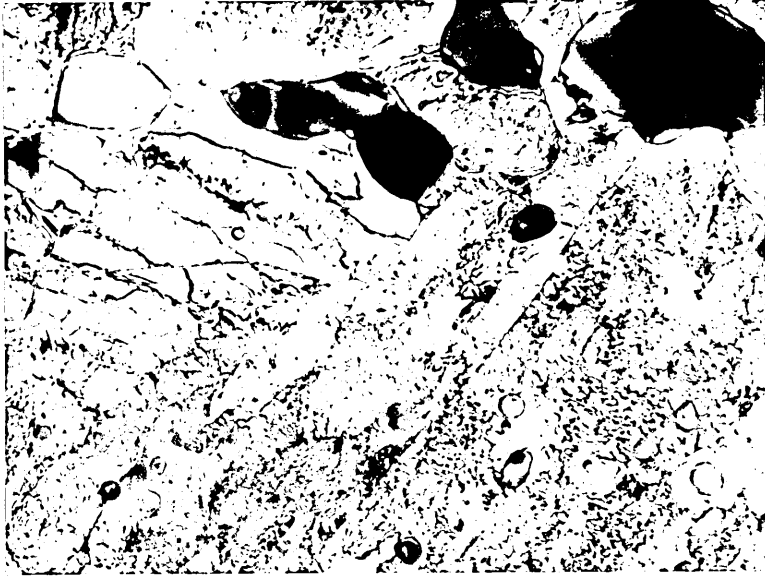
FIG. 136.   Thin foil electron micrograph of Alloy 2 in the hardened and tempered condition.   Tempering was carried out at 600°C for 16 hours.   Magnification:- x50,000.
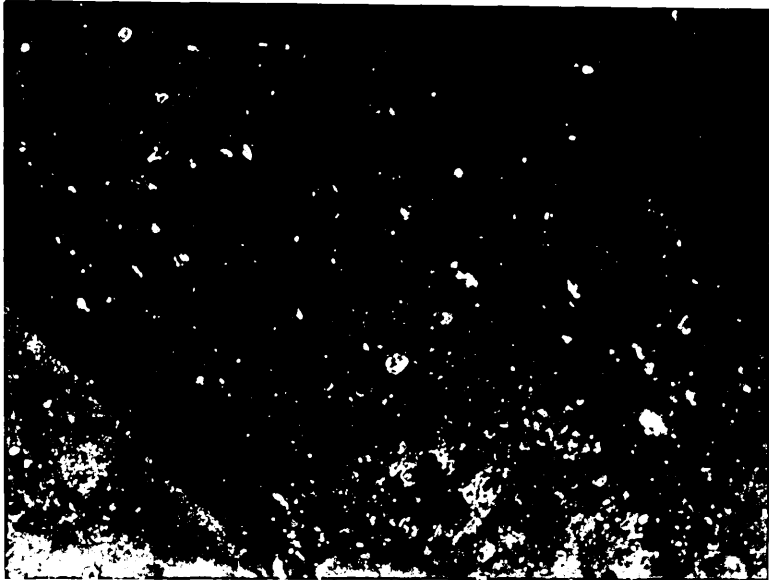
FIG. 137.   Thin foil electron micrograph of Alloy 2 in the hardened and tempered condition.   Tempering was carried out at 600°C for 23 hours.   Magnification:- x60,000.
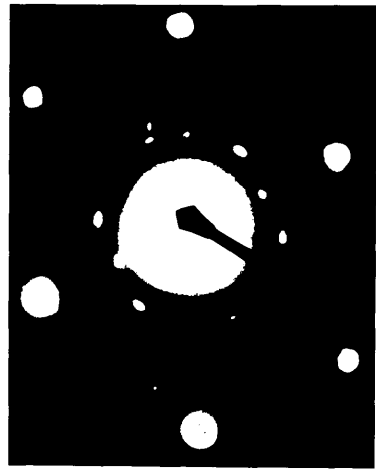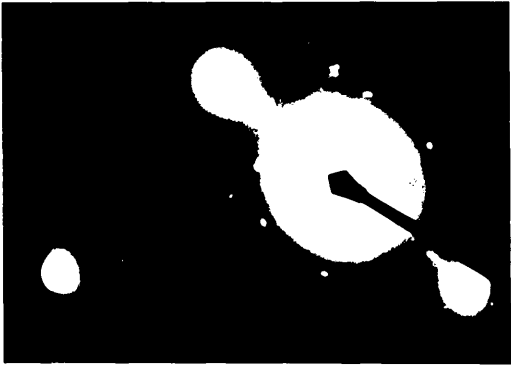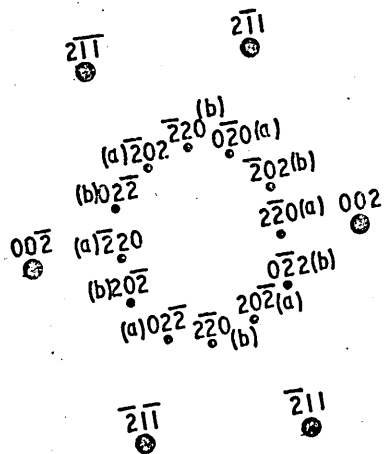
FIG. 138. Diffraction pattern taken from a precipitated V_4C_3 particle, present in Alloy 2 in the hardened and tempered condition. Tempering was carried out at $600^{\circ}C$ for 23 hours. Zone axis of the carbide diffraction pattern is $\left[211\right]$, whilst that of the matrix is $\left[011\right]$.
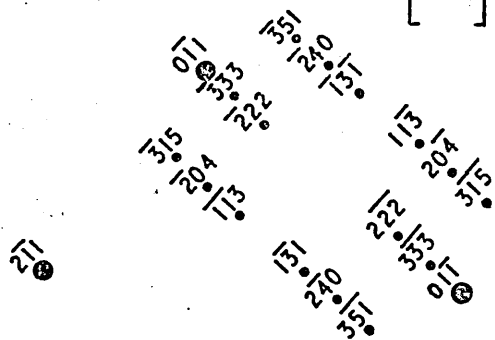
● = Matrix.

• = Precipitated V_4C_3.

● = Matrix.

•(a) = Primary V_4C_3 1.
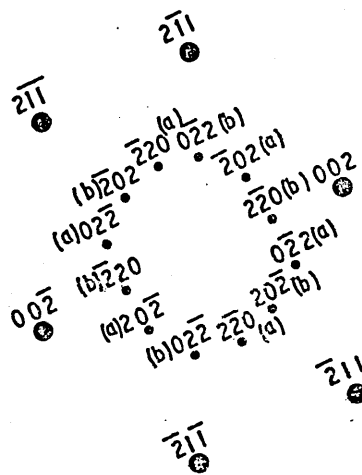
•(b) = Primary V_4C_3 2.

FIG. 139. Double diffraction pattern taken from two primary V_4C_3 particles, present in Alloy 2 in the hardened and tempered condition. Tempering was carried out at $600^{\circ}C$ for 23 hours. Zone axis of each carbide diffraction pattern is $\left[111\right]$, whilst that of the matrix is $\left[120\right]$.
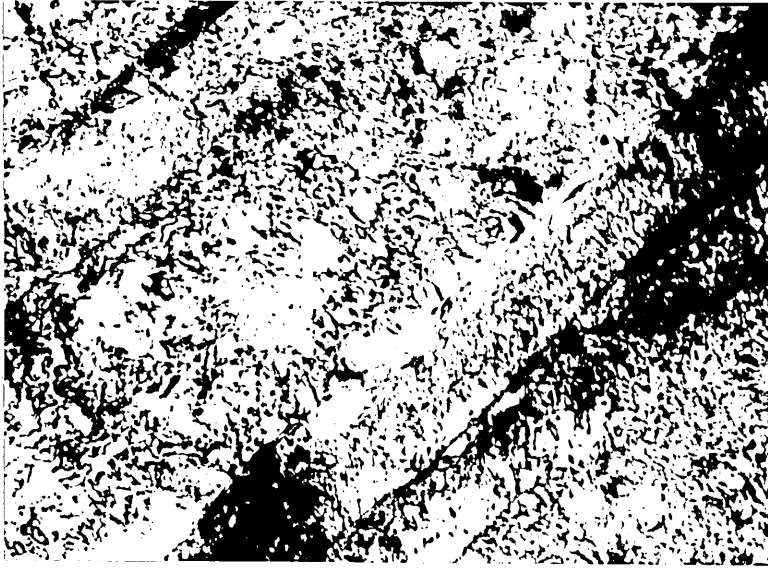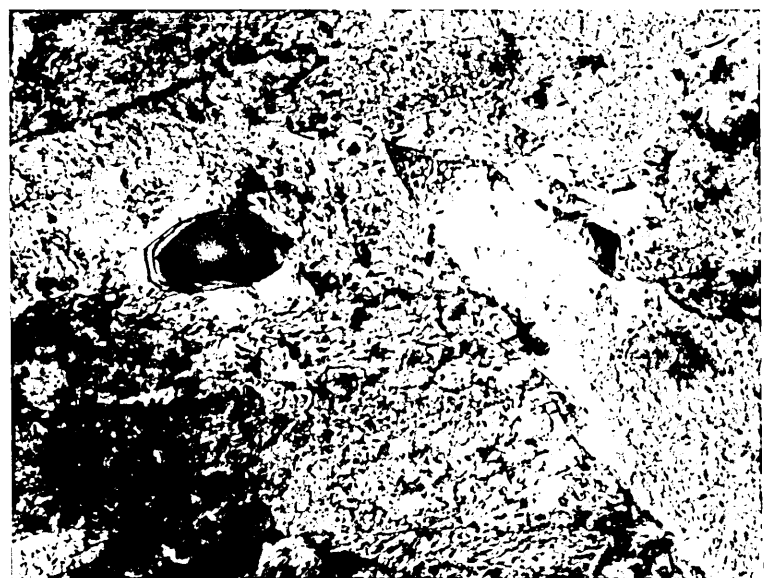
FIG. 140.   Thin foil electron micrograph of Alloy 3 in the hardened and tempered condition.   Tempering was carried out at 600°C for 16 hours.   Magnification:- x80,000.

FIG. 141.   Thin foil electron micrograph of Alloy 3 in the hardened and tempered condition.   Tempering was carried out at 600°C for 23 hours.   Magnification:- x80,000.
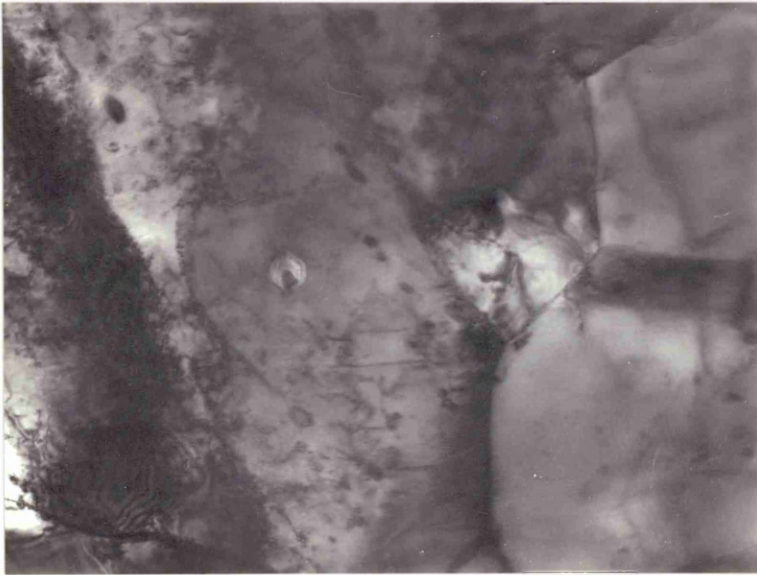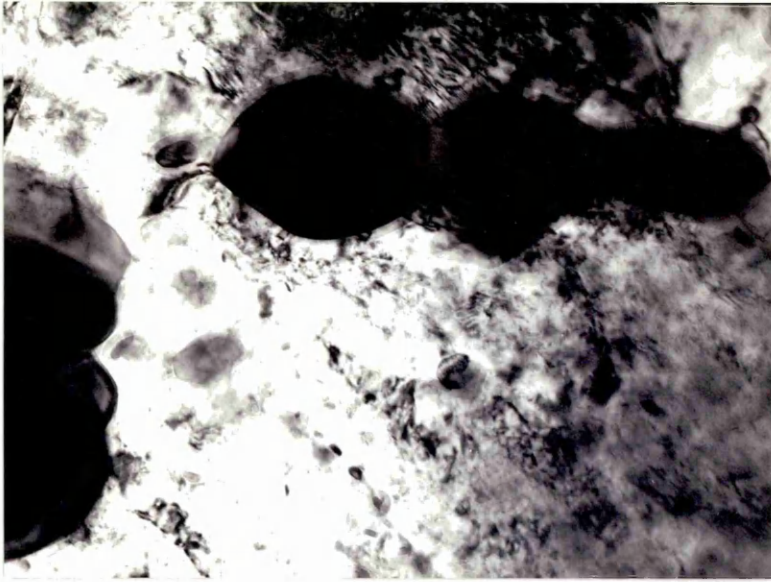
FIG. 142. Thin foil electron micrograph of Alloy 3 in the hardened and tempered condition. Tempering was carried out at 600°C for 40 hours. Magnification:- x100,000.

FIG. 143. Thin foil electron micrograph of Alloy 2 in the hardened and tempered condition. Tempering was carried out at 700°C for 7 hours. Magnification:- x50,000.
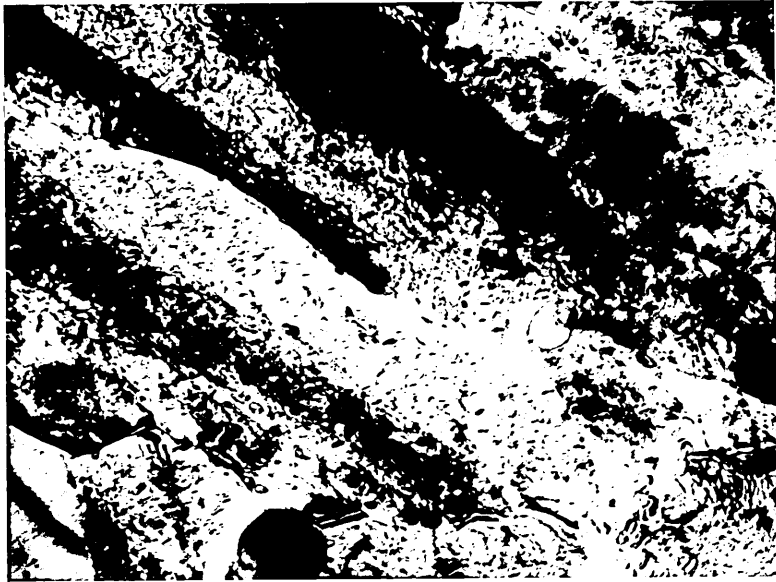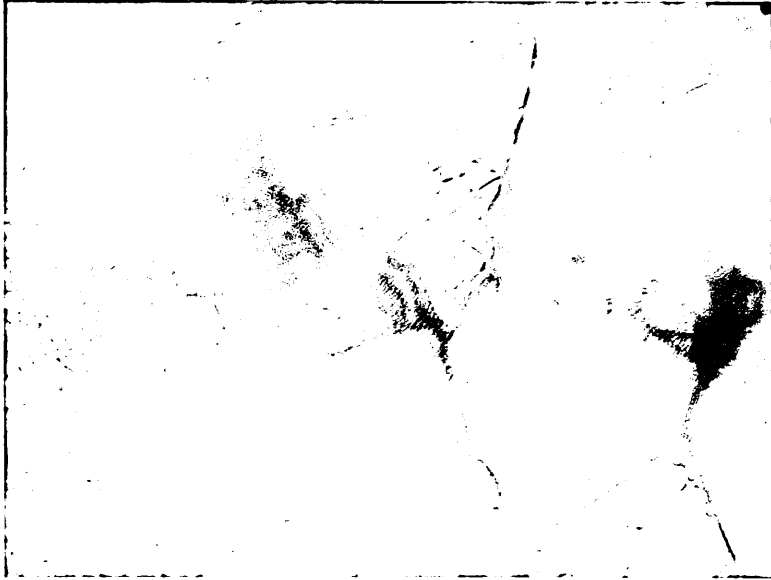
FIG. 144.   Thin foil electron micrograph of Alloy 2 in the hardened and tempered condition.   Tempering was carried out at 700°C for 24 hours.   Magnification:- x60,000.

FIG. 145.   Thin foil electron micrograph of Alloy 6(Mn) in the hardened and tempered condition.   Tempering was carried out at 600°C for 40 hours.   Magnification:- x45,000.
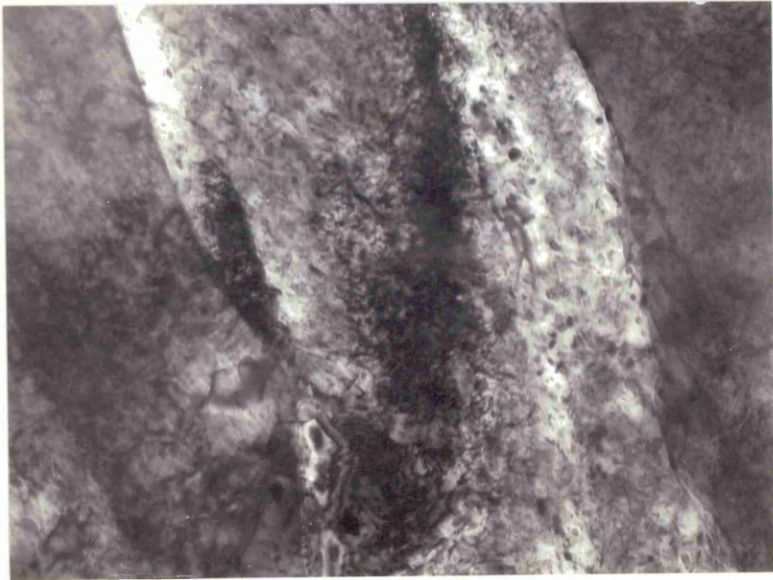
FIG. 146.   Thin foil electron micrograph of Alloy 9(Co) in the hardened and tempered condition.   Tempering was carried out at 600°C for 40 hours.   Magnification:- x45,000.

FIG. 147.   Thin foil electron micrograph of Alloy 7(Ni) in the hardened and tempered condition.   Tempering was carried out at 600°C for 40 hours.   Magnification:- x50,000.
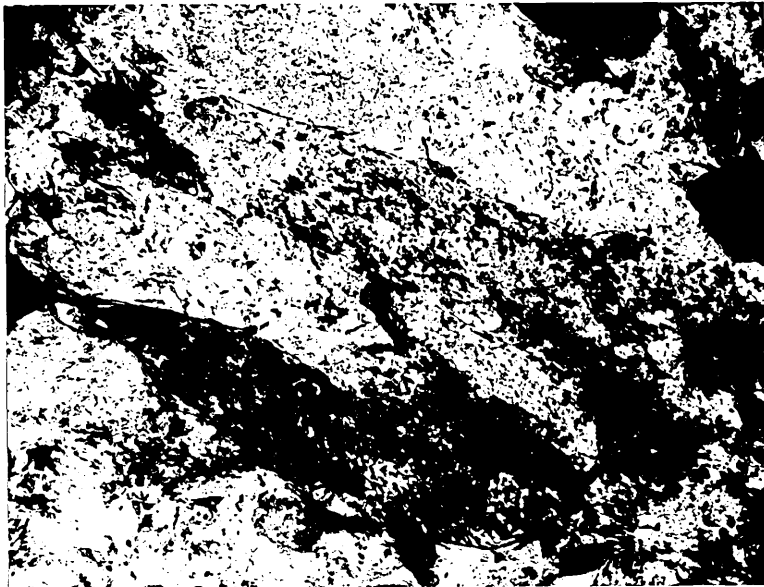
FIG. 148. Diffraction pattern taken from a precipitated V_4C_3 particle, present in Alloy 7(Ni) in the hardened and tempered condition. Tempering was carried out at 600°C for 40 hours. Zone axis of the carbide diffraction pattern is $\left[211\right]$, whilst that of the matrix is $\left[331\right]$.
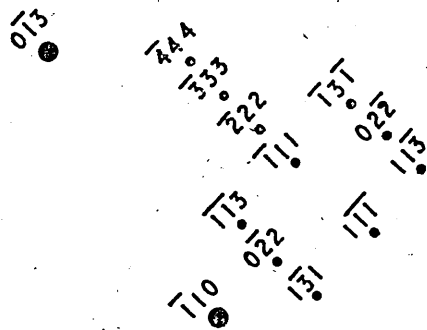
⊕ = Matrix .

• = Precipitated V_4C_3

FIG. 149. Thin foil electron micrograph of Alloy 5(Mo) in the hardened and tempered condition. Tempering was carried out at 600°C for 40 hours. Magnification:- x60,000.

FIG. 150.   Thin foil electron micrograph of Alloy 10(W) in the hardened and tempered condition.   Tempering was carried out at $600^{\circ}C$ for 40 hours.   Magnification:- x50,000.

FIG. 151.   Thin foil electron micrograph of Alloy 8(Cr) in the hardened and tempered condition.   Tempering was carried out at $600^{\circ}C$ for 8 hours.   Magnification:- x40,000.

FIG. 152. Thin foil electron micrograph of Alloy 8(Cr) in the hardened and tempered condition. Tempering was carried out at $600^{\circ}C$ for 8 hours. Magnification:- x50,000.

FIG. 153. Thin foil electron micrograph of Alloy 8(Cr) in the hardened and tempered condition. Tempering was carried out at $600^{\circ}C$ for 8 hours. Magnification:- x50,000.

FIG. 154.   Thin foil electron micrograph of Alloy 8(Cr) in the hardened and tempered condition.   Tempering was carried out at 600°C for 16 hours.   Magnification:- x50,000.

FIG. 155.   Thin foil electron micrograph of Alloy 8(Cr) in the hardened and tempered condition.   Tempering was carried out at 600°C for 16 hours.   Magnification:- x60,000.

FIG. 156. Double diffraction pattern taken from two primary V_4C_3 particles, present in Alloy 8(Cr) in the hardened and tempered condition. Tempering was carried out at 600°C for 16 hours. Zone axis of each carbide diffraction pattern is $\left[111\right]$, whilst that of the matrix is $\left[120\right]$.

$2\bar{1}\bar{1}$ $2\bar{1}\bar{1}$

(a)$\bar{1}20\bar{2}$ $\bar{2}20$(b) $0\bar{2}0$(a)

(b)$02\bar{2}$ $\bar{2}02$(b)

$00\bar{2}$ (a)$\bar{1}\bar{2}0$ $2\bar{2}0$(a) 002

(b)$\bar{2}0\bar{2}$ $0\bar{2}2$(b)

(a)$02\bar{2}$ $2\bar{2}0$(b) $20\bar{2}$(a)

$\bar{2}\bar{1}\bar{1}$ $\bar{2}11$

⊕ = Matrix.

•(a) = Primary V_4C_3 1.

•(b) = Primary V_4C_3 2.

FIG. 157. Dark field electron micrograph taken using a (2$\bar{2}$0) V_4C_3 zone reflection from the diffraction pattern shown in Fig. 156. This dark field is of the corresponding area shown by the bright field in Fig. 155. Magnification:- x60,000.

FIG. 158.   Thin foil electron micrograph of Alloy 8(Cr) in the hardened and tempered condition.   Tempering was carried out at 600°C for 40 hours.   Magnification:- x50,000.

FIG. 159.   Thin foil electron micrograph of Alloy 4(Si) in the hardened and tempered condition.   Hardening was carried out by austenitisation at 1200°C and subsequent water quenching, whilst the tempering treatment was 16 hours at 600°C. Magnification:- x70,000.
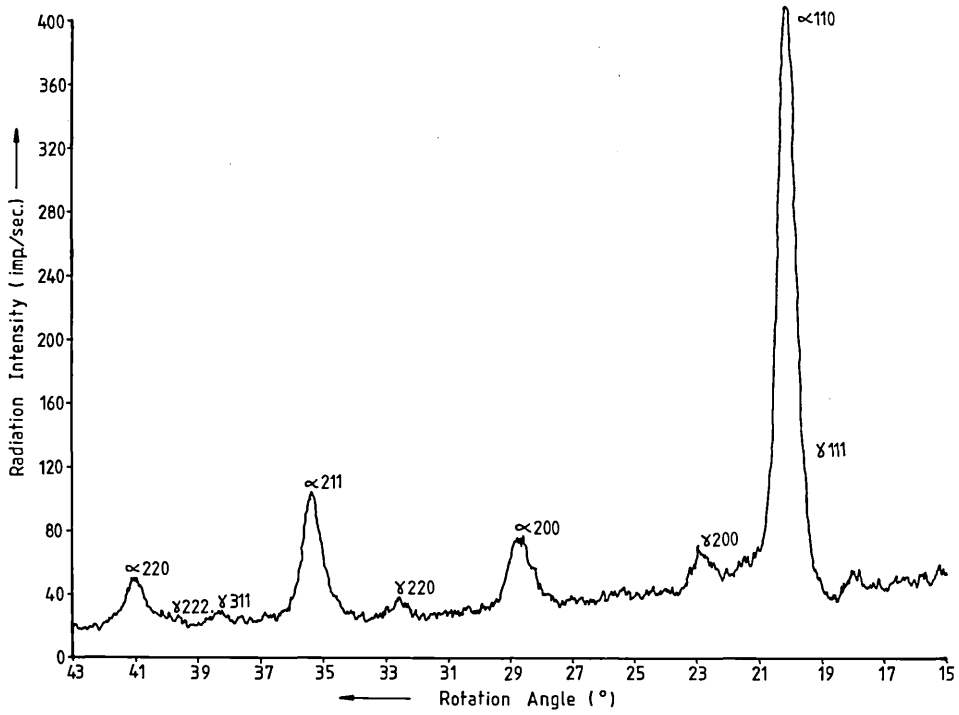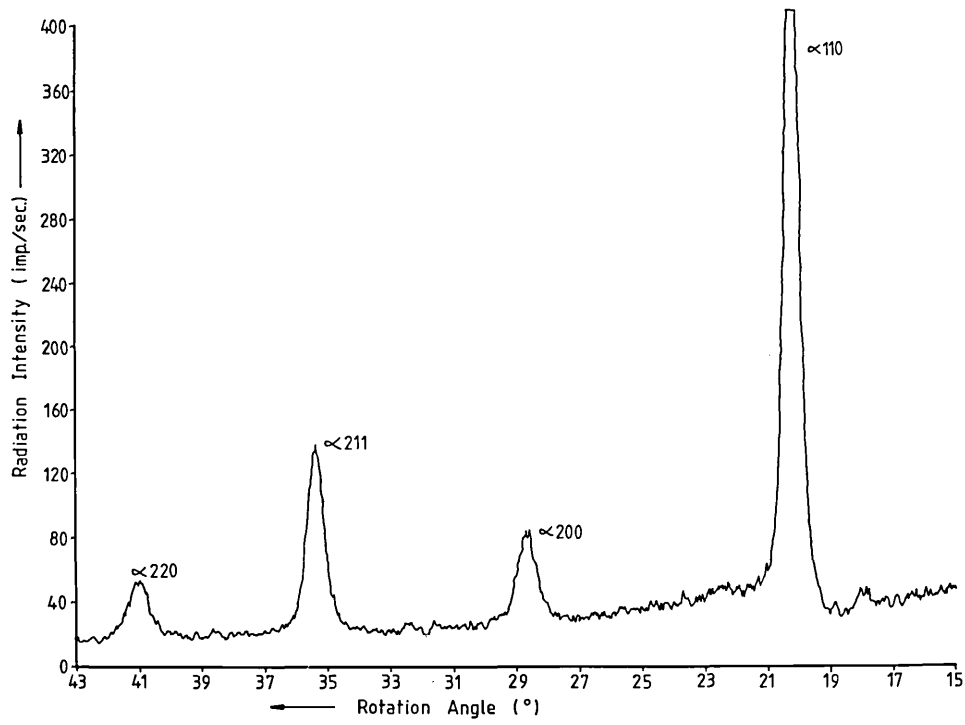
FIG. 160. X-ray diffraction scan for Alloy 8(Cr) in the as-hardened condition. Austenitisation was carried out at 1150°C for 20 minutes, with subsequent water quenching. The radiation employed was molybdenum Kα .

FIG. 161. X-ray diffraction scan for Alloy 7(Ni) in the as-hardened condition. Austenitisation was carried out at 1200°C for 20 minutes, with subsequent water quenching. The radiation employed was molybdenum Kα.
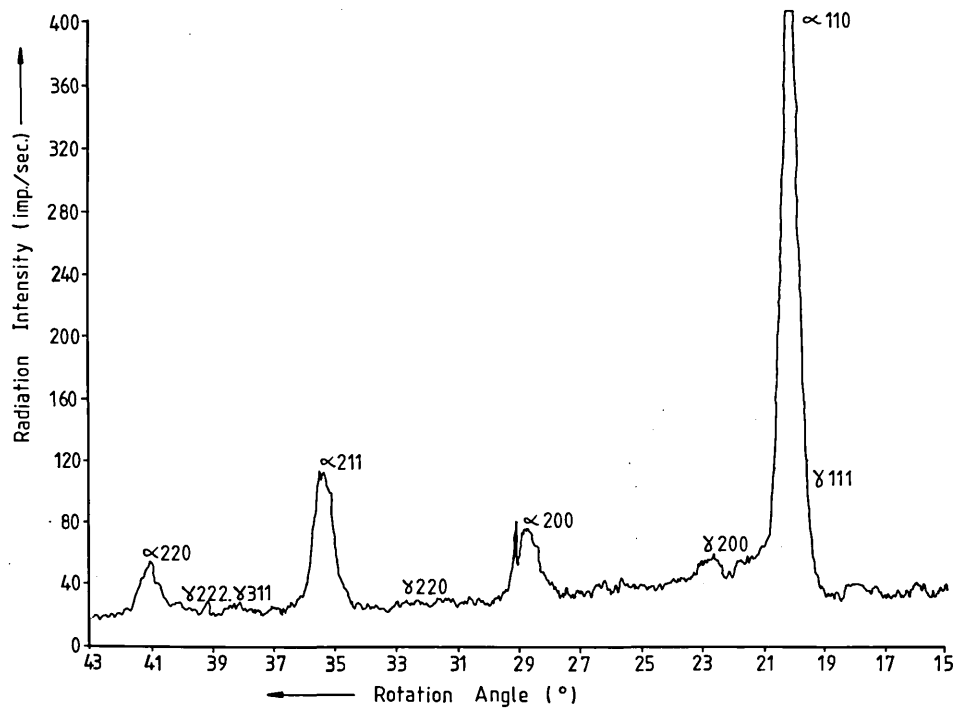
FIG. 162.   X-ray diffraction scan for Alloy 9(Co) in
the as-hardened condition.   Austenitisation was carried out
at 1200°C for 20 minutes, with subsequent water quenching.
The radiation employed was molybdenum Kα.
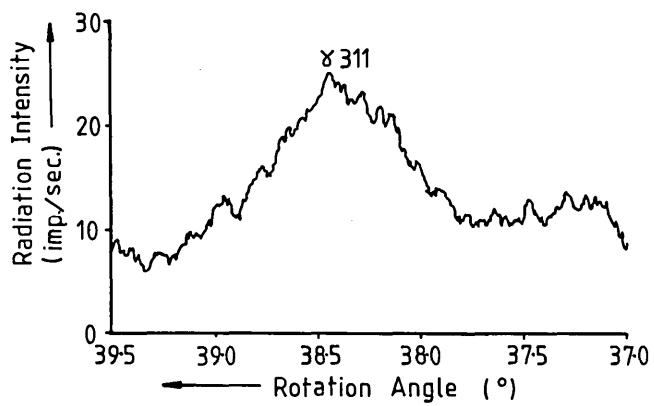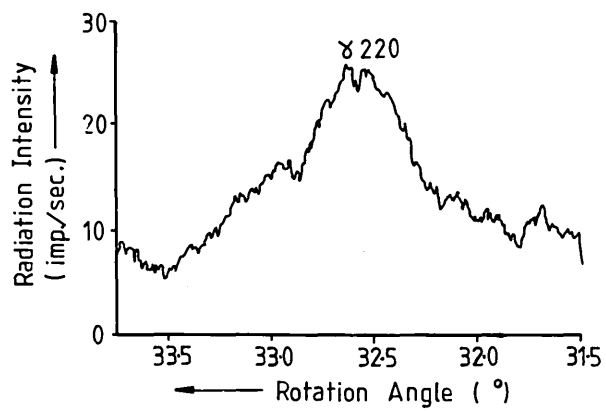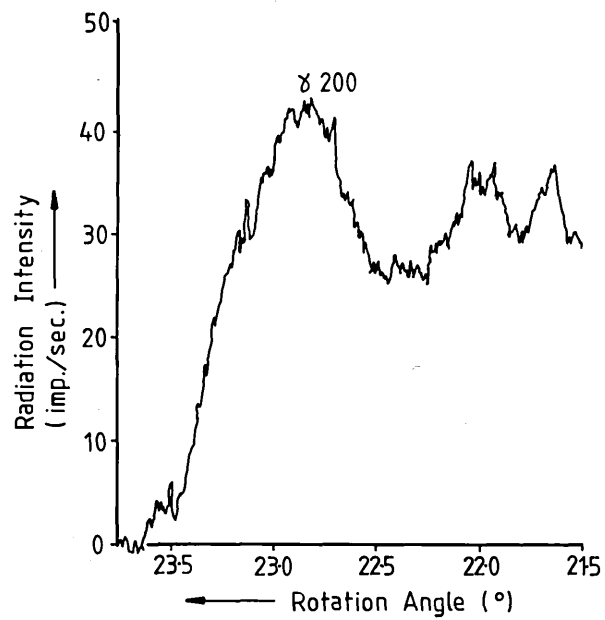
FIG. 163. X-ray diffraction step scan (to achieve greater resolution) through the γ_{200}, γ_{220} and γ_{311} peaks shown for Alloy 7(Ni) by the lower sensitivity scan in FIG. 161.
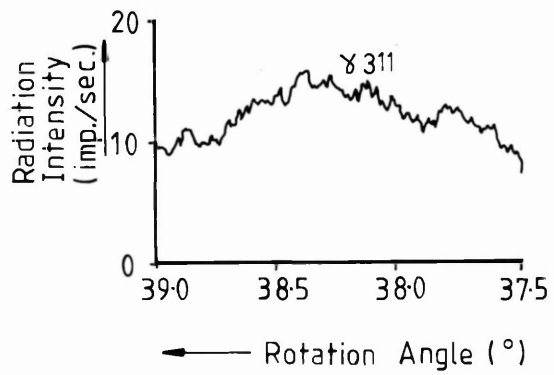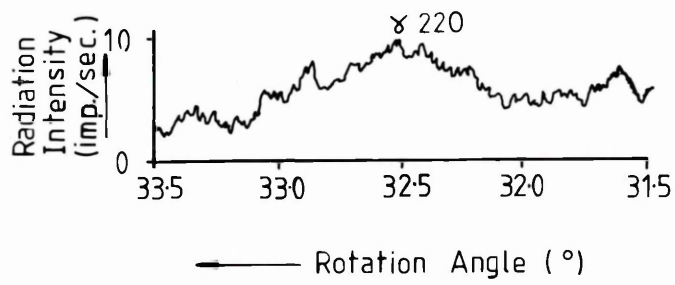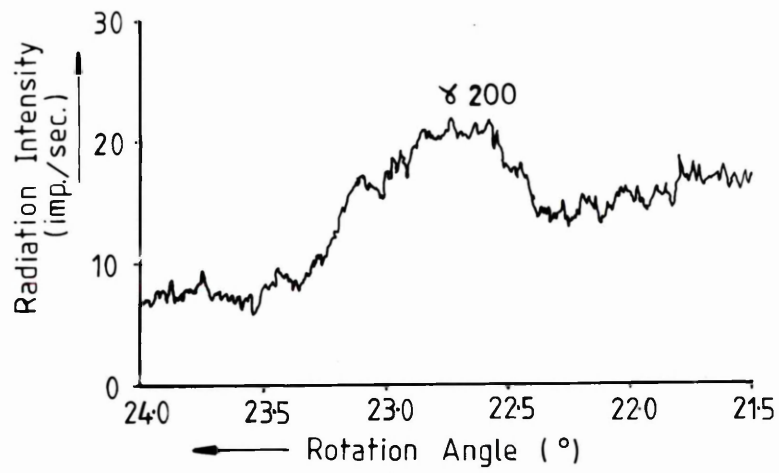
FIG. 164.   X-ray diffraction step scan through the δ_{200}, δ_{220} and γ_{311} peaks shown for Alloy 9(Co) by the lower sensitivity scan in Fig. 162.
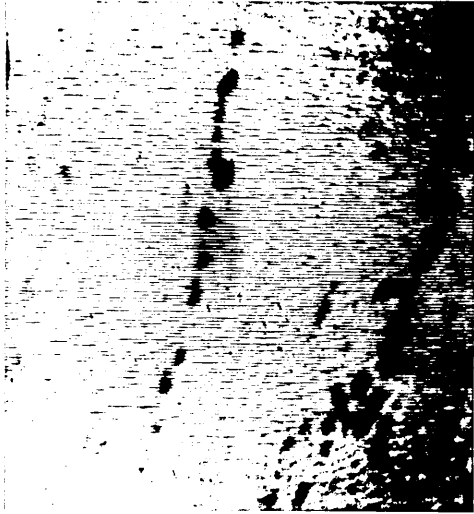
FIG. 165.   Electron image showing stringers of primary V_4C_3 particles present in a martensitic matrix in Alloy 3 in the as-hardened condition.   Austenitisation was carried out at $1200^{\circ}C$ for 20 minutes, with subsequent water quenching. Magnification:- x1100.

FIG. 166.   X-ray image showing the distribution of vanadium over the corresponding field presented in FIG. 165. The analysing crystal used was lithium fluoride.
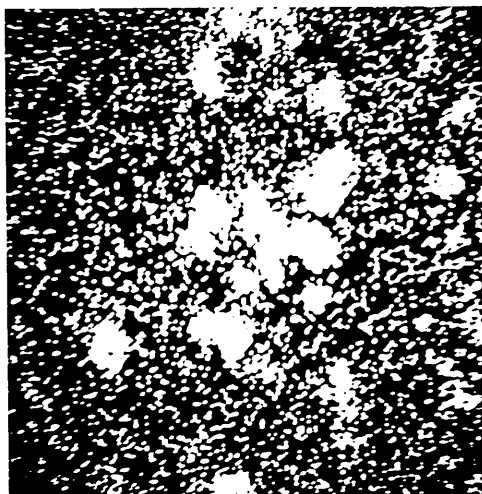
FIG. 167. X-ray image showing the partitioning of vanadium between primary V_4C_3 particles and the martensitic matrix in Alloy 7(Ni) in the as-hardened condition. Austenitisation was carried out at 1200°C for 20 minutes, with subsequent water quenching. The analysing crystal used was lithium fluoride.
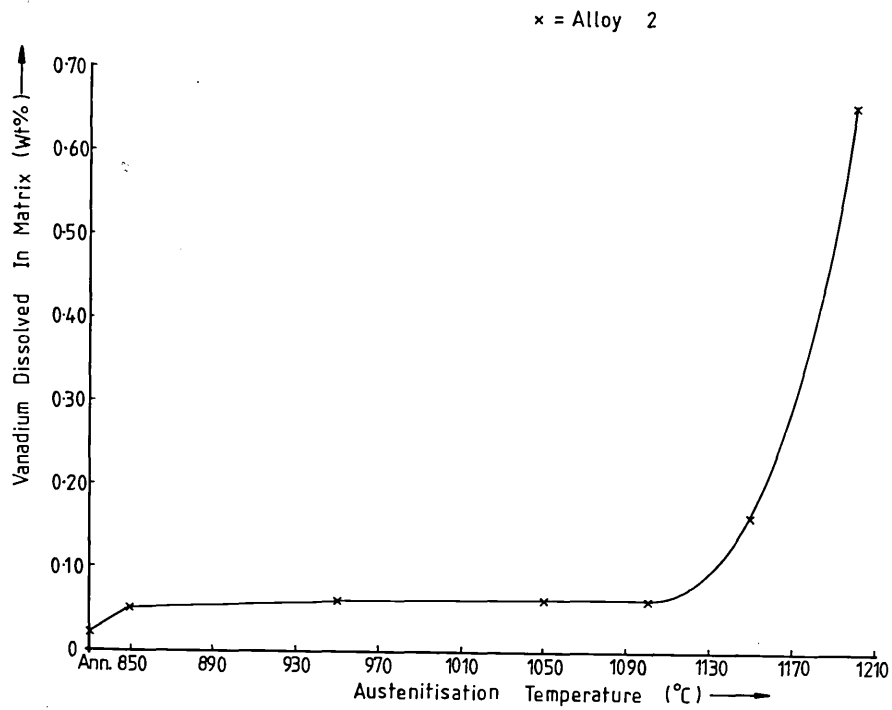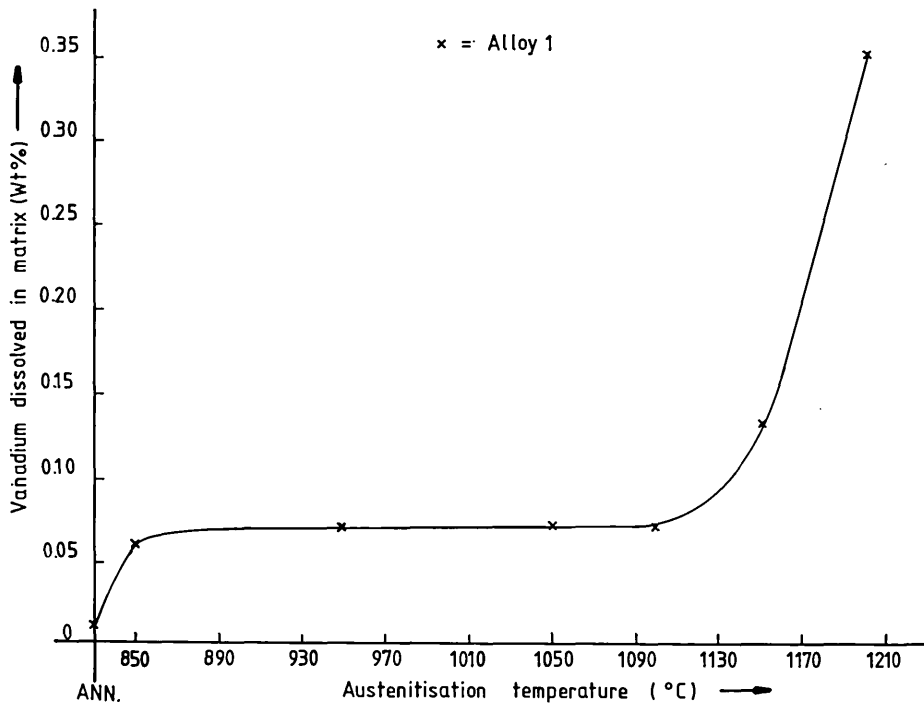
FIG. 168. X-ray image showing the partitioning of vanadium between primary V_4C_3 particles and the martensitic matrix in Alloy 8(Cr) in the as-hardened condition. Austenitisation was carried out at 1200°C for 20 minutes, with subsequent water quenching. The analysing crystal used was lithium fluoride.
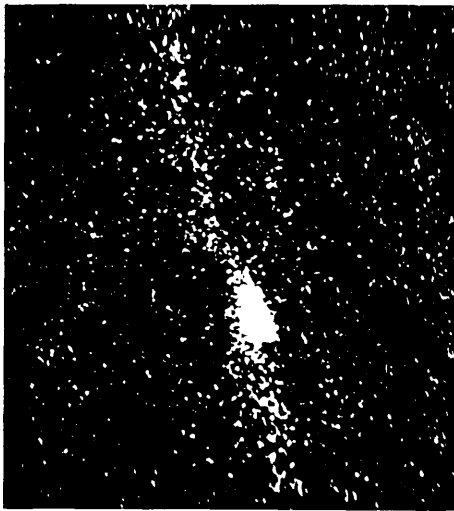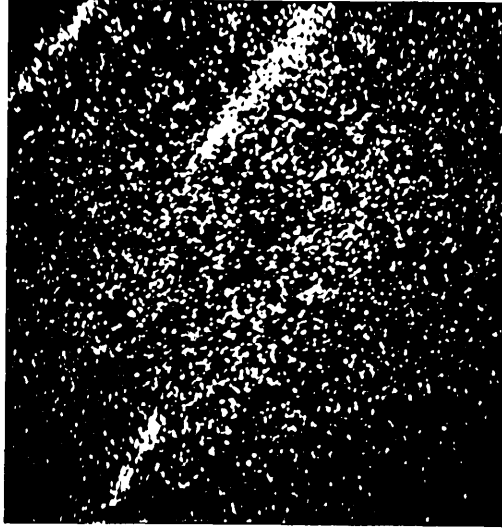
FIG. 169.   X-ray image showing the partitioning of chromium between primary Cr_7C_3 and V_4C_3 particles, and the martensitic matrix in Alloy 8(Cr) in the as-hardened condition. Austenitisation was carried out at $1050^{\circ}C$ for 20 minutes, with subsequent water quenching.   The analysing crystal used was lithium fluoride.

FIG. 170.   X-ray image showing the partitioning of molybdenum between primary Mo_2C particles and the martensitic matrix in Alloy 5(Mo) in the as-hardened condition. Austenitisation was carried out at $1150^{\circ}C$ for 20 minutes, with subsequent water quenching.   The analysing crystal used was P.E.T.

x = Alloy 1

Vanadium dissolved in matrix (Wt%) →

Austenitisation temperature (°C) →

ANN.

x = Alloy 2

Vanadium Dissolved In Matrix (Wt%) →

Austenitisation Temperature (°C) →

Ann.
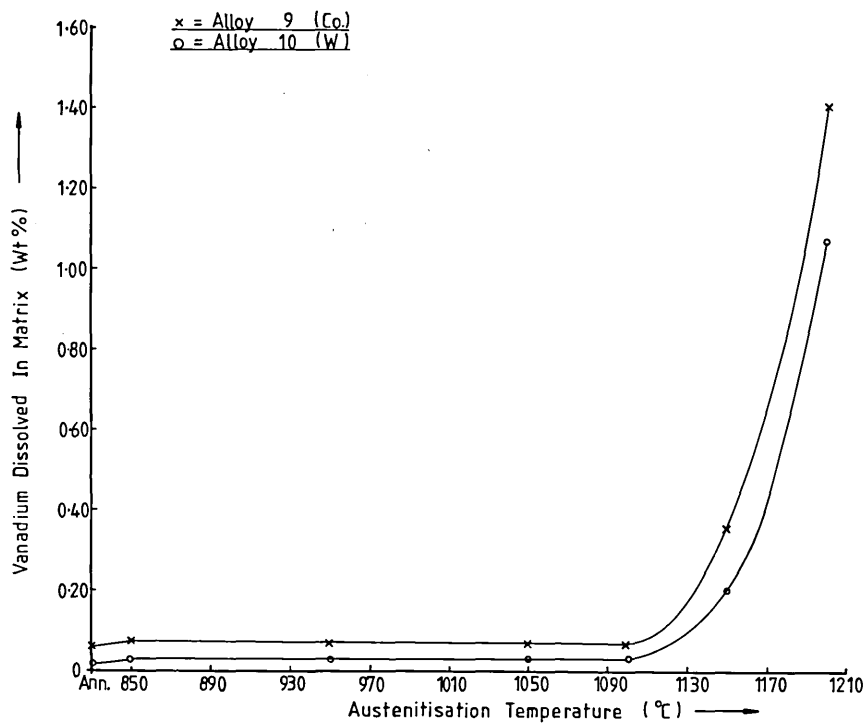
FIG. 171.   Relationship between matrix vanadium content and austenitisation temperature for Alloy 1 in the as-hardened condition.   The soaking time in each case was 20 minutes, with subsequent water quenching.

FIG. 172.   Effect of austenitisation temperature on the matrix vanadium content for Alloy 2 in the as-hardened condition.   The soaking time in each case was 20 minutes, with subsequent water quenching.
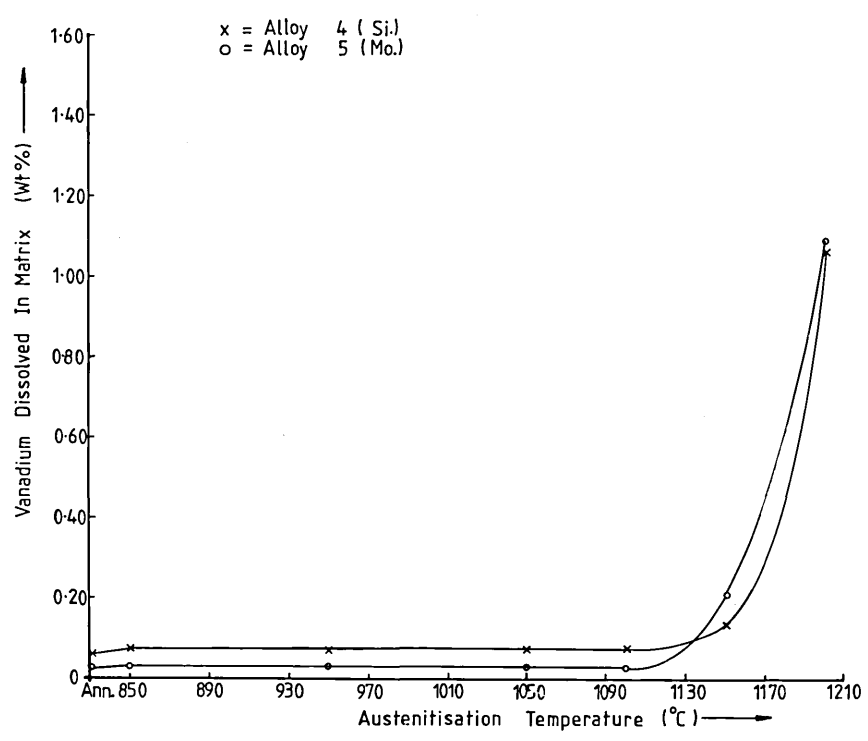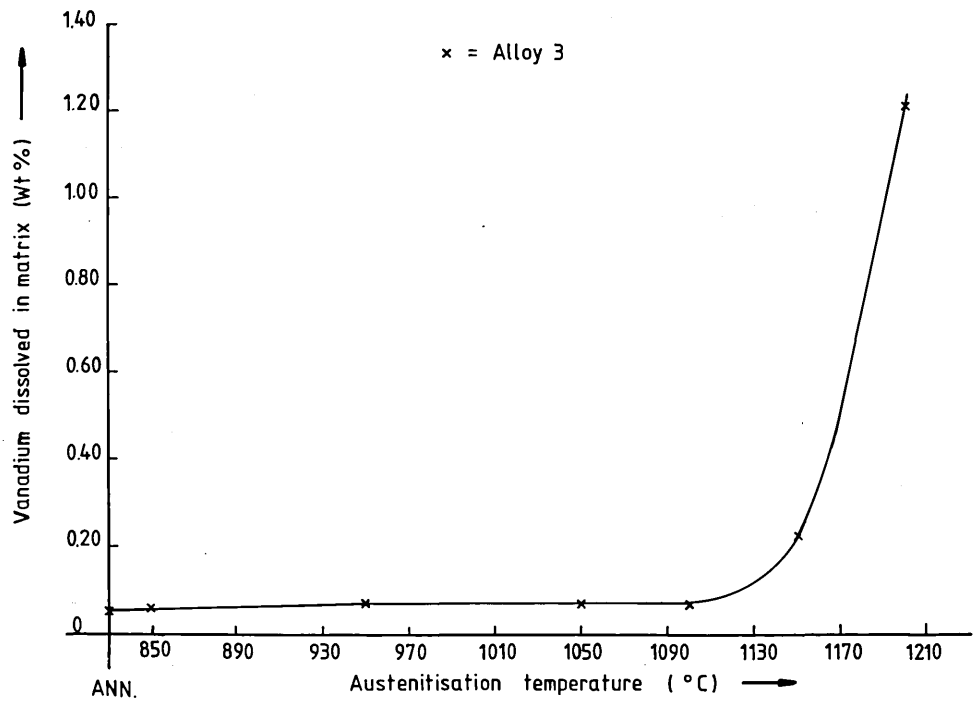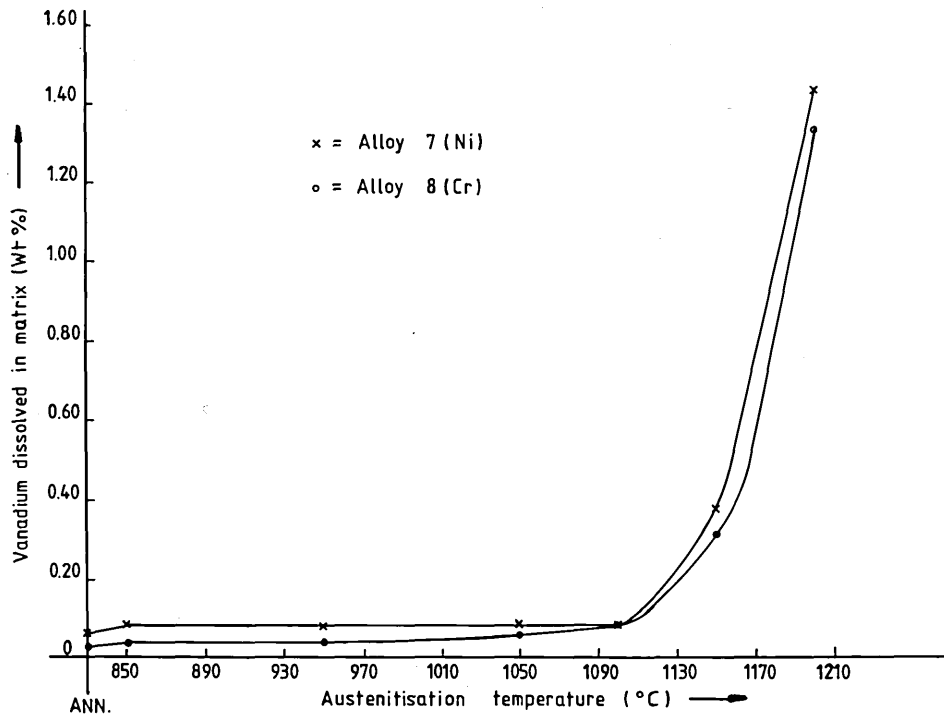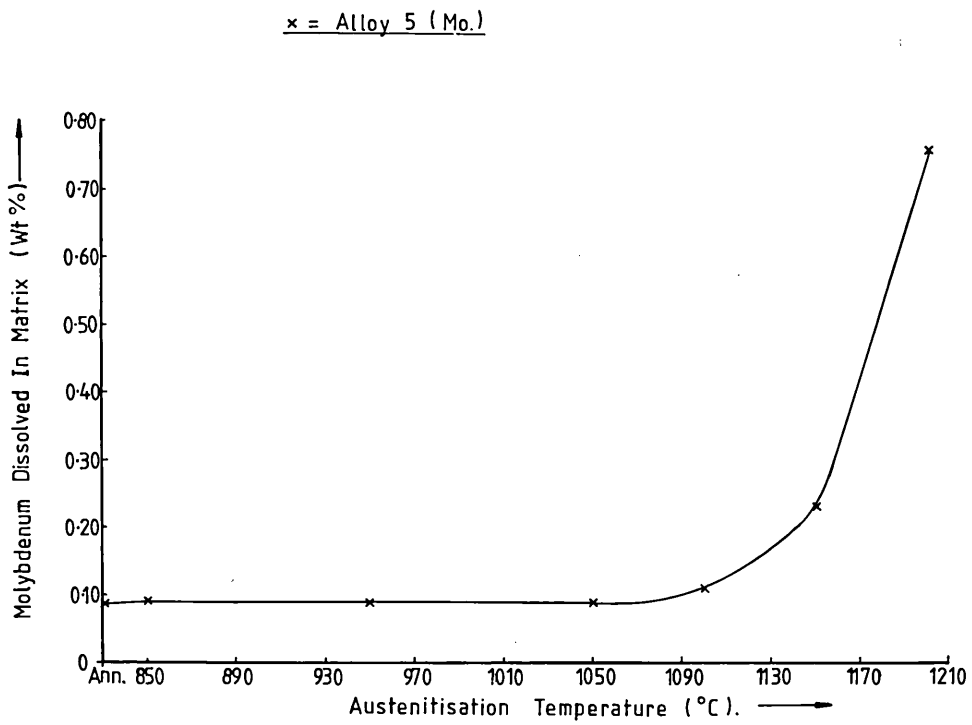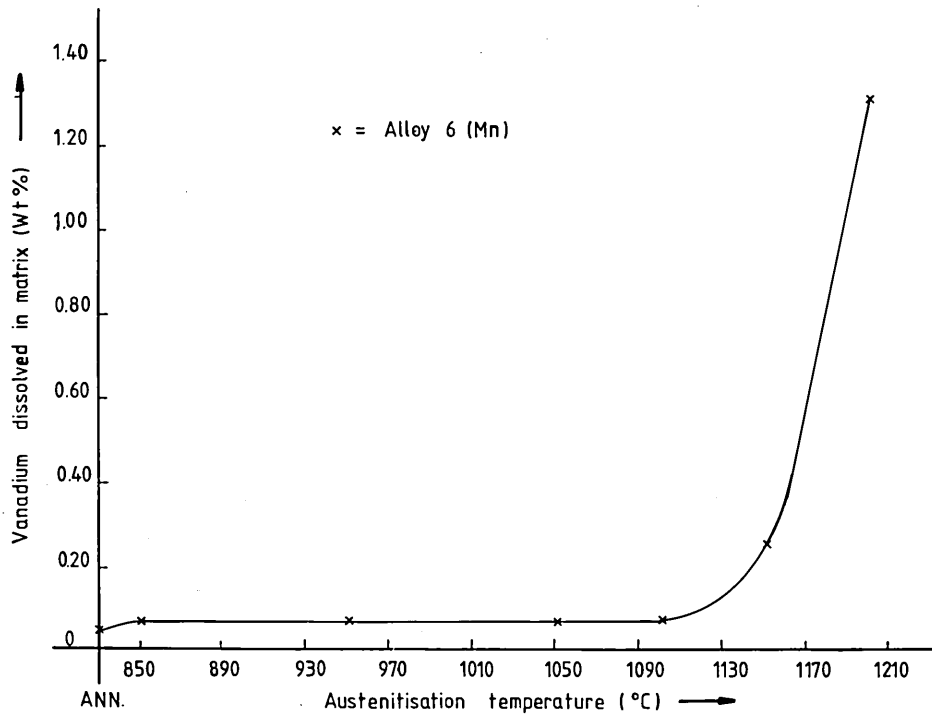
FIG. 173. Relationship between matrix vanadium content and austenitisation temperature for Alloy 3 in the as-hardened condition. The soaking time in each case was 20 minutes, with subsequent water quenching.

FIG. 174. Effect of austenitisation temperature on the matrix vanadium content for Alloys 4(Si) and 5(Mo) in the as-hardened condition. The soaking time in each case was 20 minutes, with subsequent water quenching.

FIG. 175. Relationship between matrix vanadium content and austenitisation temperature for Alloys 7(Ni) and 8(Cr) in the as-hardened condition. The soaking time in each case was 20 minutes, with subsequent water quenching.

FIG. 176. Effect of austenitisation temperature on matrix vanadium content for Alloys 9(Co) and 10(W) in the as-hardened condition. The soaking time in each case was 20 minutes, with subsequent water quenching.

x = Alloy 6 (Mn)

Vanadium dissolved in matrix (Wt %)

ANN.

Austenitisation temperature (°C)

x = Alloy 5 (Mo.)

Molybdenum Dissolved In Matrix (Wt %)

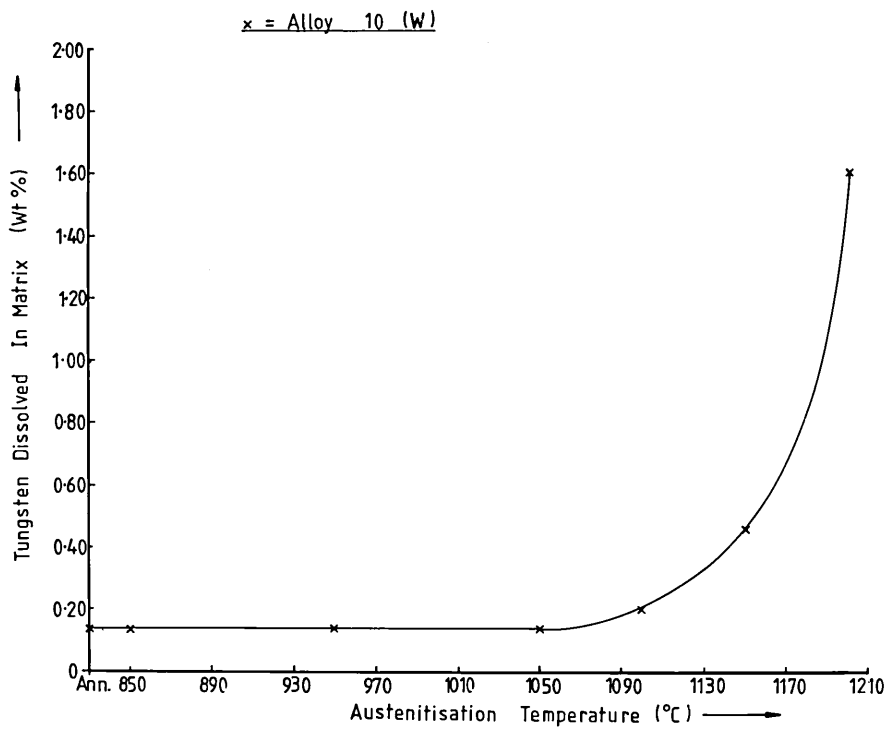Ann.

Austenitisation Temperature (°C).

FIG. 177. Relationship between matrix vanadium content and austenitisation temperature for Alloy 6(Mn) in the as-hardened condition. The soaking time in each case was 20 minutes, with subsequent water quenching.

FIG. 178. Effect of austenitisation temperature on matrix molybdenum content for Alloy 5(Mo) in the as-hardened condition. The soaking time in each case was 20 minutes, with subsequent water quenching.
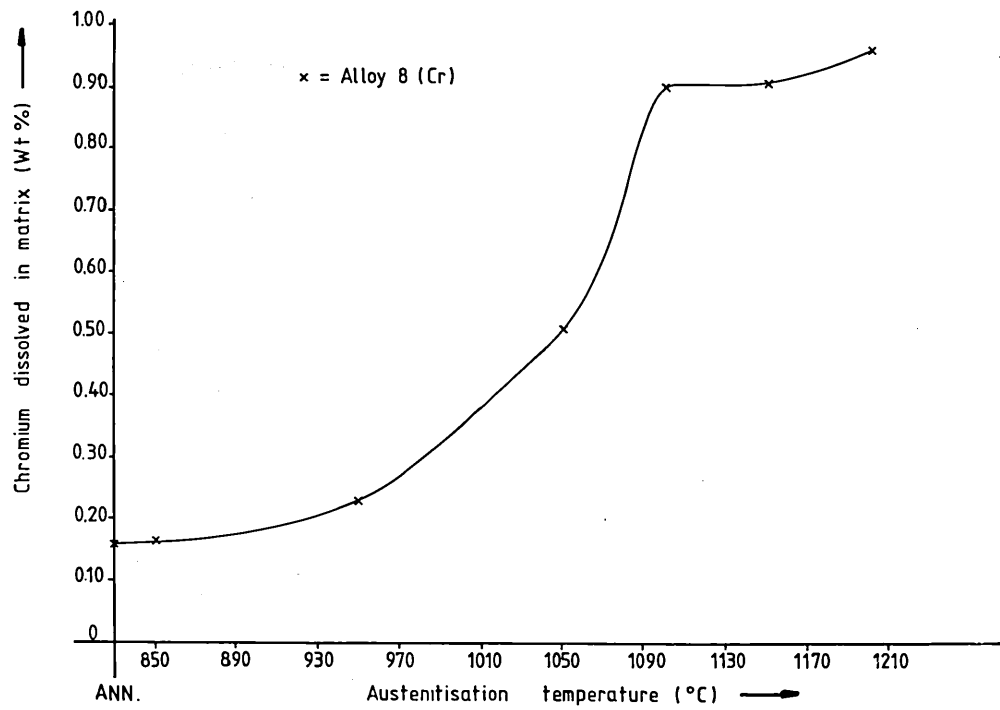
x = Alloy 8 (Cr)

Chromium dissolved in matrix (Wt %)

ANN.

Austenitisation   temperature (°C)

x = Alloy   10   (W)

Tungsten Dissolved In Matrix   (Wt %)

Ann.

Austenitisation   Temperature (°C)

FIG. 179. Relationship between matrix chromium content and austenitisation temperature for Alloy 8(Cr) in the as-hardened condition. The soaking time in each case was 20 minutes, with subsequent water quenching.

FIG. 180. Effect of austenitisation temperature on matrix tungsten content for Alloy 10(W) in the as-hardened condition. The soaking time in each case was 20 minutes, with subsequent water quenching.
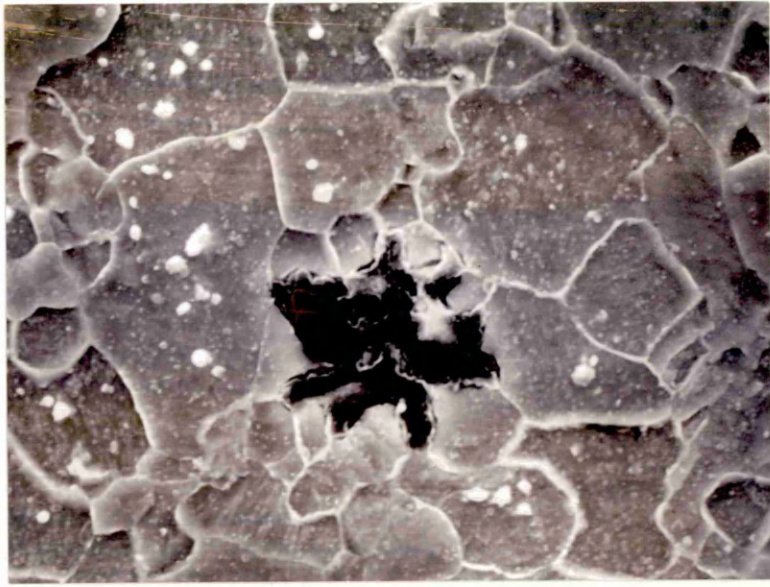
FIG. 181.   Scanning electron micrograph showing a graphite particle present in Alloy 1 in the hardened and tempered condition.   Tempering was carried out at 560°C for 220 hours.   Magnification:- x3500.

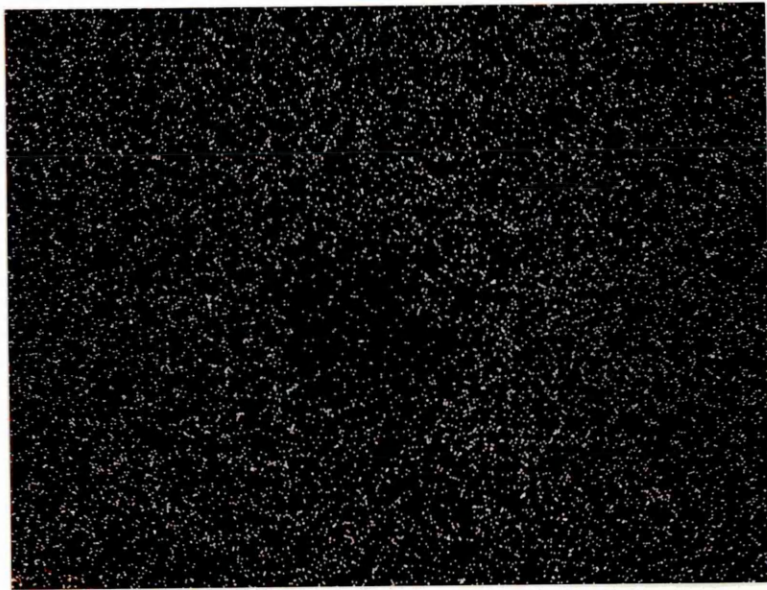FIG. 182.   X-ray image showing the distribution of iron over the corresponding field presented in Fig. 181.

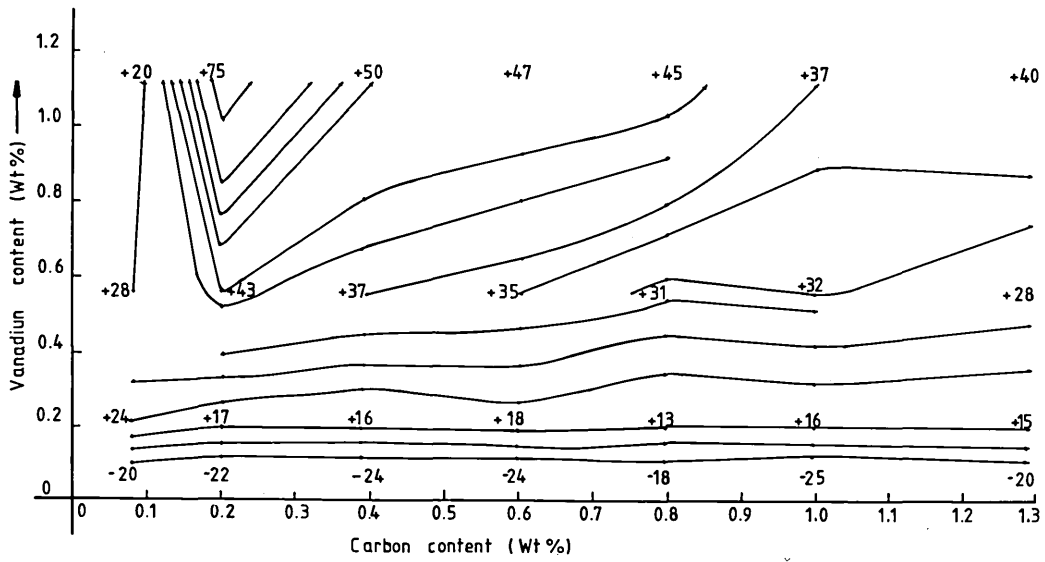FIG. 183.   X-ray image showing the distribution of vanadium over the corresponding field presented in Fig. 181.
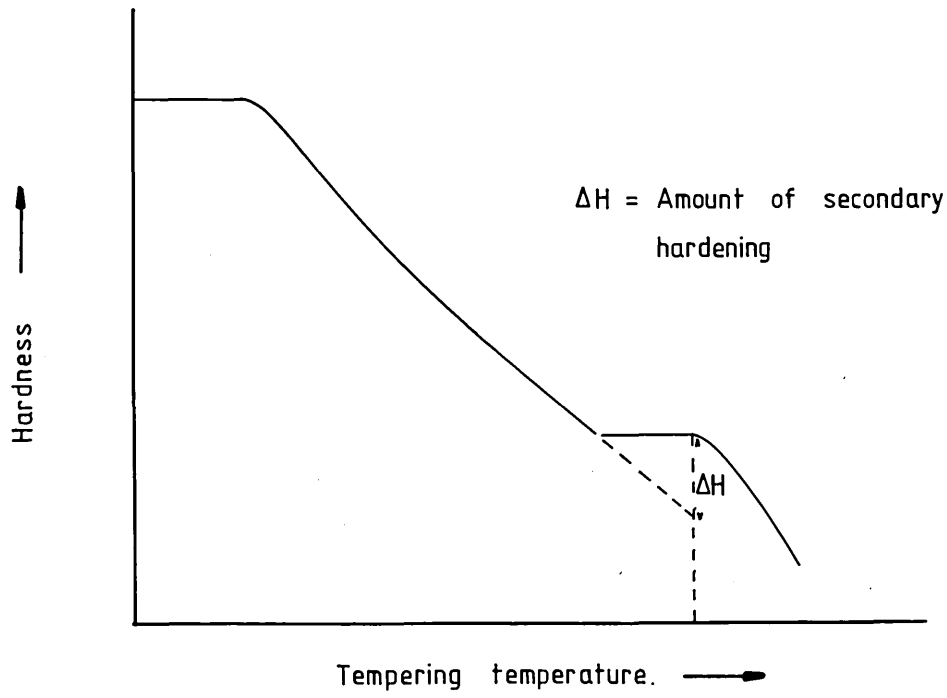
ΔH = Amount of secondary hardening

Hardness →

ΔH

Tempering temperature. →

Vanadium content (Wt %) →

1.2

+20   +75   +50   +47   +45   +37   +40

1.0

0.8

+28   +43   +37   +35   +31   +32   +28

0.6

0.4

+24   +17   +16   + 18   +13   +16   +15

0.2

-20   -22   -24   -24   -18   -25   -20

0

0   0.1   0.2   0.3   0.4   0.5   0.6   0.7   0.8   0.9   1.0   1.1   1.2   1.3

Carbon content (Wt %)

FIG. 184.   Hypothetical diagram showing how the degree
of secondary hardening can be measured for an alloy which
shows a plateau rather than a peak, over the temperature range
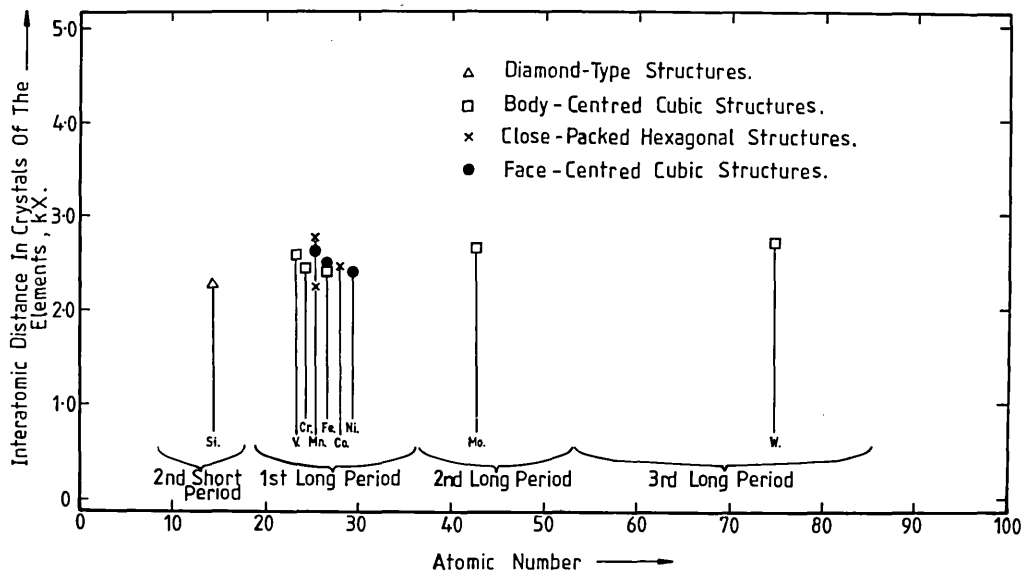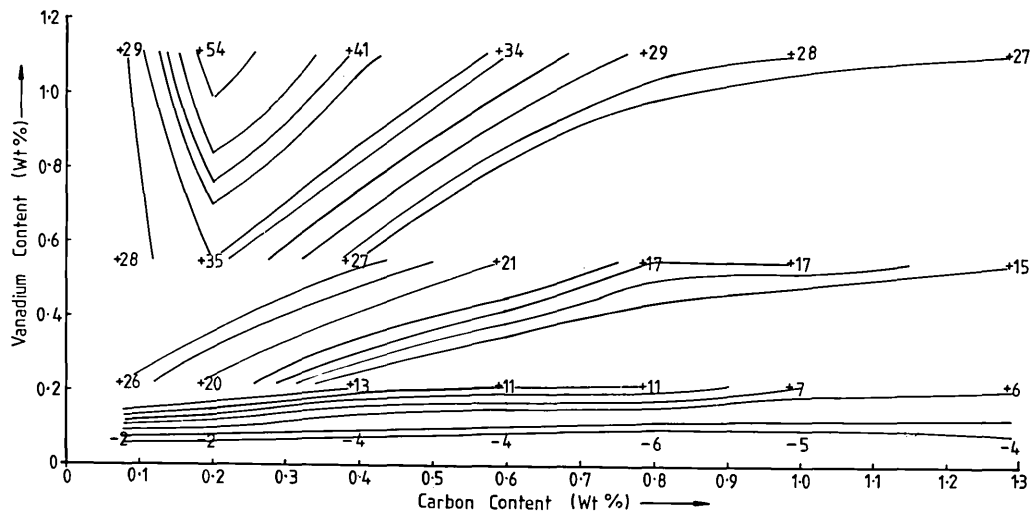for carbide precipitation, in the relationship between hardness
and tempering temperature.

FIG. 185.   Iso-hardness diagram showing vanadium and
carbon contents which give corresponding hardness variations
after tempering at $600^{\circ}C$ for 1 hour, as opposed to $500^{\circ}C$ for
the same duration, for the carburised steels.

Figure 1

Vanadium Content (Wt %) —

1·2
1·0
0·8
0·6
0·4
0·2
0

+29   +54   +41   +34   +29   ±28   +27

+28   +35   +27   +21   +17   +17   +15

+26   +20   +13   +11   +11   +7   +6

−2   −2   −4   −4   −6   −5   −4

0   0·1   0·2   0·3   0·4   0·5   0·6   0·7   0·8   0·9   1·0   1·1   1·2   1·3

Carbon Content (Wt %) ⟶

Figure 2

Interatomic Distance In Crystals Of The Elements, kX. —

5·0
4·0
3·0
2·0
1·0
0

△   Diamond-Type Structures.
□   Body-Centred Cubic Structures.
×   Close-Packed Hexagonal Structures.
●   Face-Centred Cubic Structures.

Si.

Cr. Fe. Ni.
V. Mn. Co.

Mo.

W.

2nd Short Period   1st Long Period   2nd Long Period   3rd Long Period

0   10   20   30   40   50   60   70   80   90   100

Atomic Number ⟶

FIG. 186. Iso-hardness diagram showing vanadium and carbon contents which give corresponding hardness variations after tempering at $560^{\circ}C$ for 16 hours, as opposed to 1 hour at the same temperature, for the carburised steels.

FIG. 187. Interatomic distances in the crystals of the elements, presented as a function of atomic number.
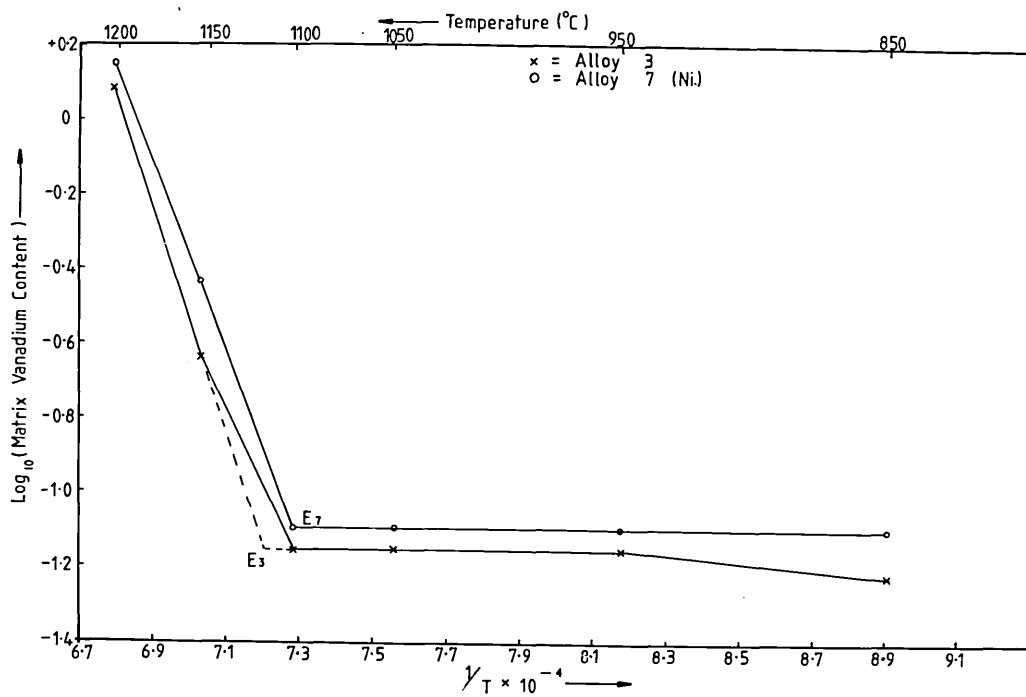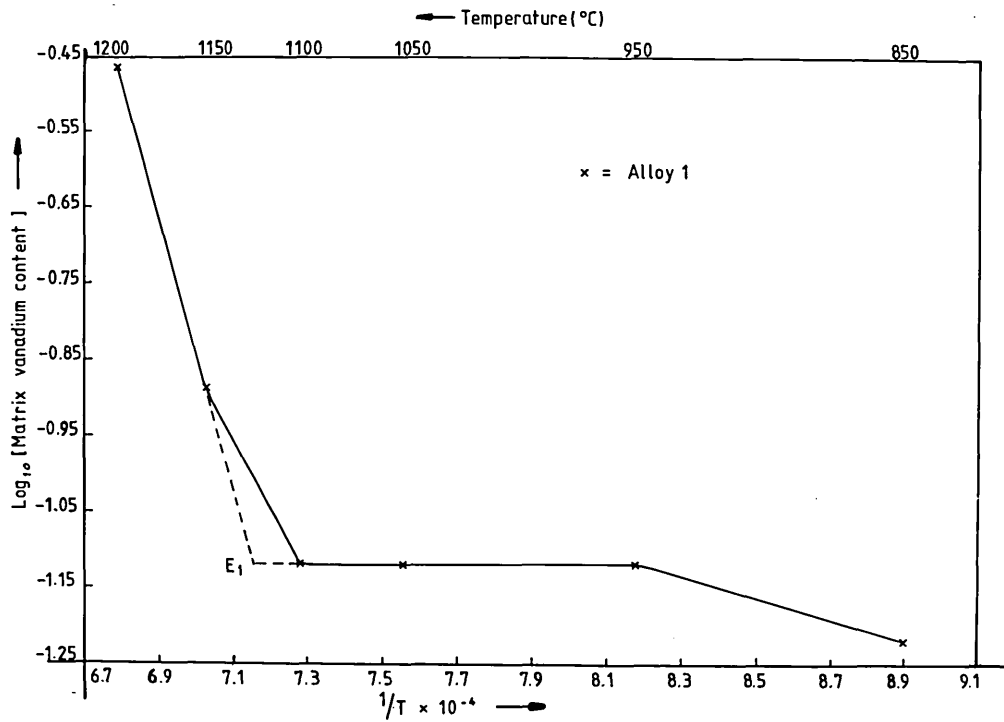
Temperature (°C)

1200 1150 1100 1050 950 850

x = Alloy 1

E₁

$^1/T \times 10^{-4}$

Temperature (°C)

1200 1150 1100 1050 950 850

x = Alloy 3
o = Alloy 7 (Ni.)

E₇

E₃

$^1/T \times 10^{-4}$

FIG. 188. Relationship between $\log_{10}$ [matrix vanadium content] and the reciprocal of the austenitisation temperature for Alloy 1.
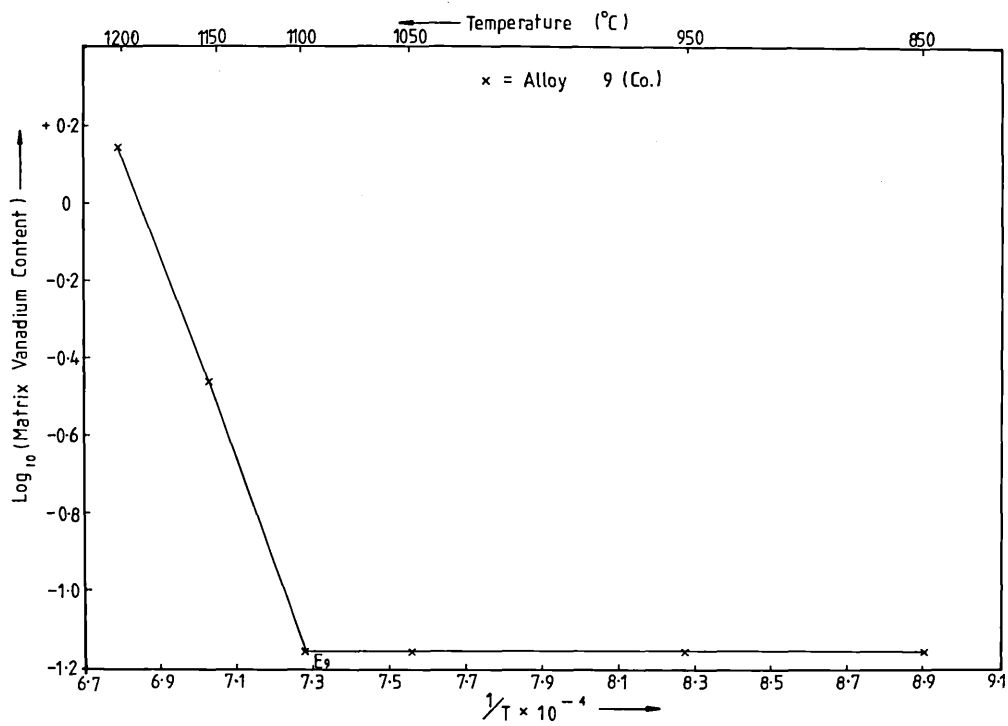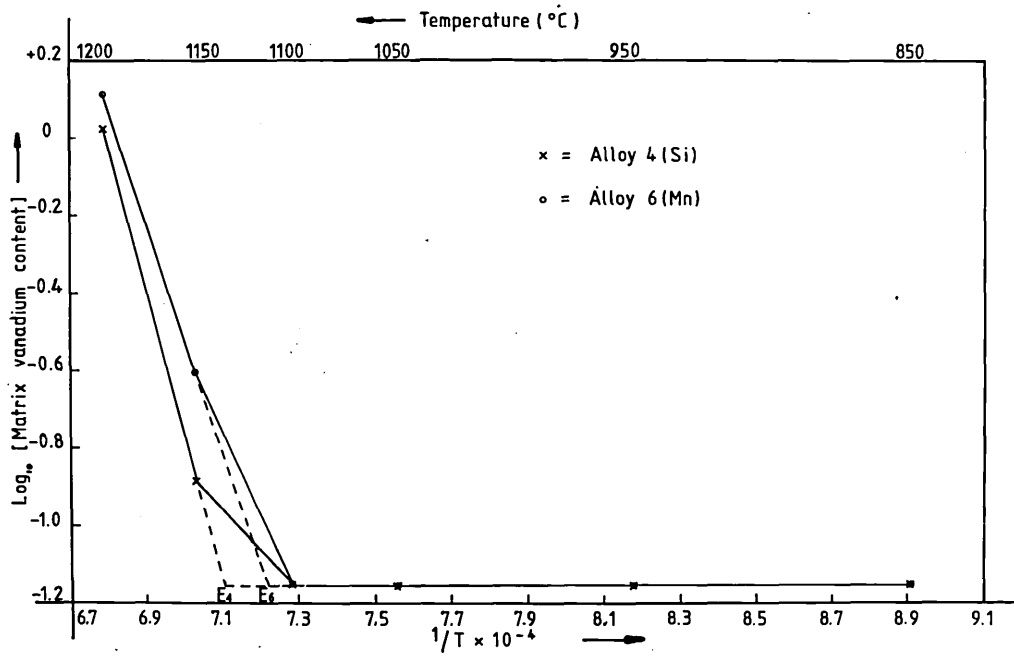
FIG. 189. Relationship between $\log_{10}$ [matrix vanadium content] and the reciprocal of the austenitisation temperature for Alloys 3 and 7(Ni).

FIG. 190.   Relationship between $\log_{10}$ [matrix vanadium content] and the reciprocal of the austenitisation temperature for Alloys 4(Si) and 6(Mn).

FIG. 191.   Relationship between $\log_{10}$ [matrix vanadium content] and the reciprocal of the austenitisation temperature for Alloy 9(Co).
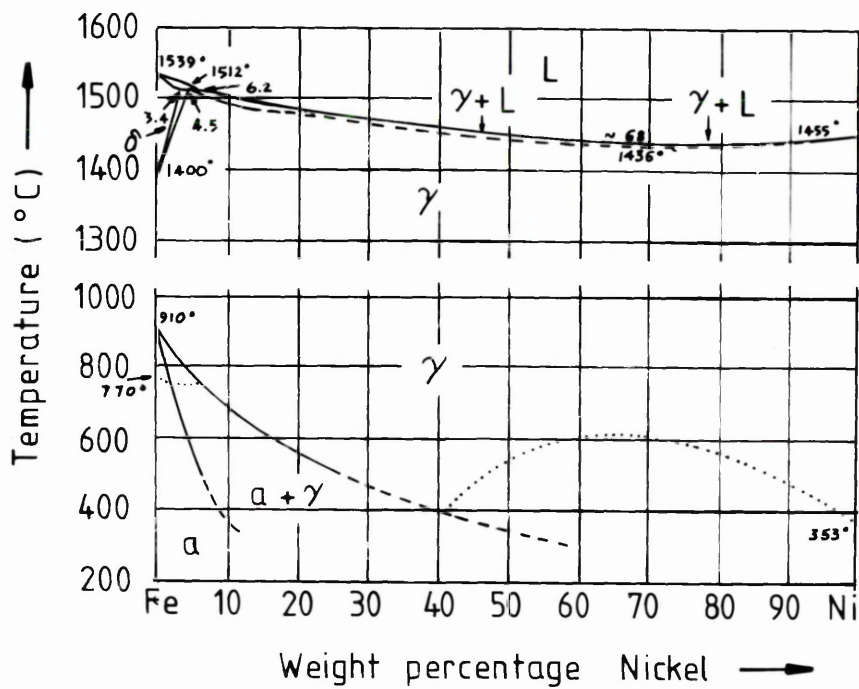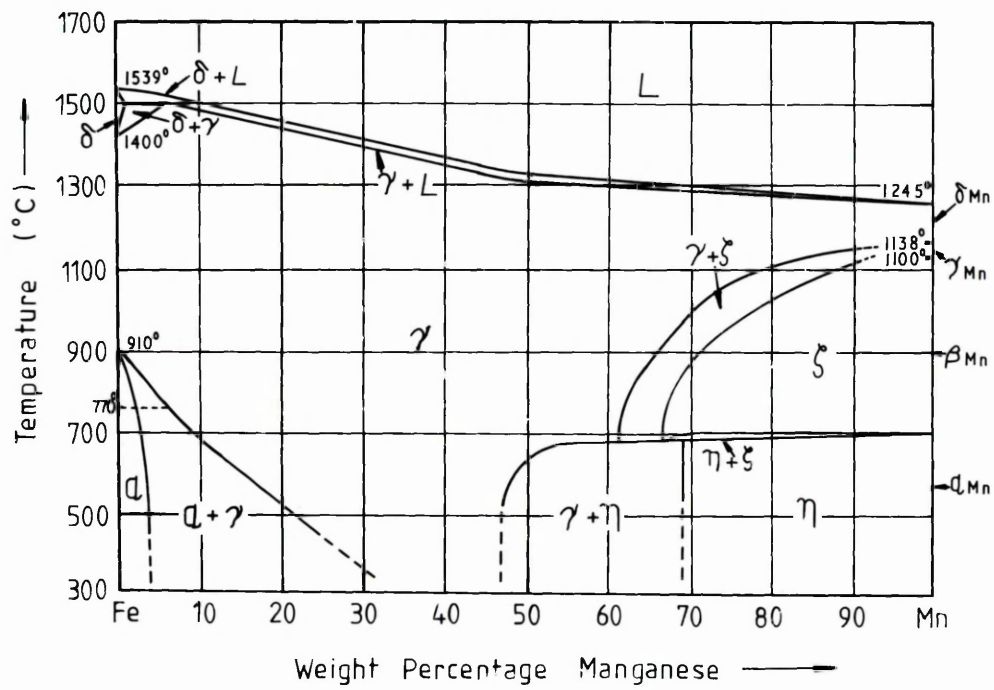
FIG. 192.   Fe – Mn binary equilibrium diagram.

FIG. 193.   Fe – Ni binary equilibrium diagram.
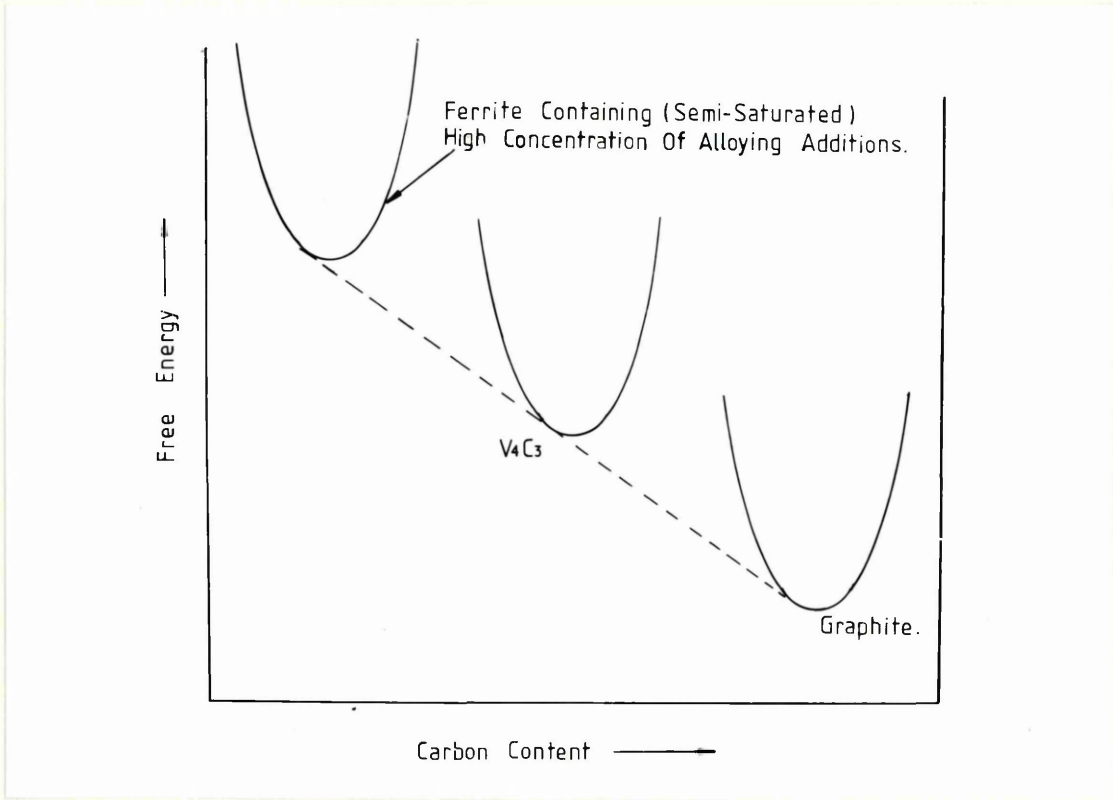
Carbon Content ⟶

FIG. 194. Hypothetical free energy curves at a point in time during tempering when graphite formation is about to commence.

FIG. 195. X-ray map for carbon on a field containing graphite particles, present in Alloy 1 in the hardened and tempered condition. Tempering was carried out at $560^{\circ}C$ for 220 hours. Magnification:- x600.